Volatile Organic Compound Profiling of Mouse Models of Intestinal Inflammation and Colon Carcinogenesis

Thesis submitted in accordance with the requirements of the University of Liverpool for the degree of Doctor in Philosophy

By

Sophie Peterson Reade

March 2016

DECLARATION

I hereby declare that this thesis is a presentation of my original work. Wherever contributions of others are involved, every effort has been made to indicate this clearly, with due reference to the literature.

The work was done under the joint guidance of Professor Chris Probert and Professor Mark Pritchard, both of the Gastroenterology Research Unit, Department of Cellular and Molecular Physiology, Institute of Translational Medicine, at the University of Liverpool.

For Nain and Taid

Dyfal donc a dyr y garreg

ACKNOWLEDGEMENTS

Firstly, I would like to thank the Institute of Translational Medicine at the University of Liverpool for part funding this work, along with the Gastroenterology Research Unit. I would like to thank my supervisors Professor Chris Probert and Professor Mark Pritchard, for their guidance throughout my PhD. I would like to thank Prof Pritchard for his expert advice regarding the feasibility and planning of specific experiments, and for proof-reading this thesis. I would like to thank Prof Probert for introducing me to, and for sharing his profound knowledge into the area of volatile organic compounds, which was new to me four years ago. I count myself extremely lucky to have been supervised, and mentored by someone with both excellent clinical and scientific expertise. The unwavering support provided by Chris and his research group has allowed me to grow as an independent research scientist. For this, I would also like to offer a special thank you to Tanzeela Khalid, Raphael Aggio and Arnaud Mayor. This thesis would not be what it is without their help, inspiration and friendship; we made a great team.

I would also like to say a huge thank you to everyone, both past and present, from the Gastro department, for making my time spent there such a happy time. In particular, thank you to Carrie Duckworth, Jonathan Williams and Dave Berry for their teaching and help in the lab. Thank you to Susan Courtney for being a wonderful friend and always being there with a smile and an ear to listen. I have been lucky to share this experience with two of my best friends, Hannah Simpson and Helen Box; thank you to you both for going on this journey with me and being by my side through the highs and lows.

Last but by no means least, I owe the biggest thank you to the people I love most in this world, my wonderful parents, grandparents, Harri, Lucy, Oliver and of course, my better half, Stevie. There are no words to say how much I have to thank you for, I hope you know how extremely grateful I am for everything you have done, and continue to do; I love you all very much.

ABSTRACT

A non-invasive, inflammatory bowel disease (IBD)-specific biomarker would be clinically useful due to the often inaccurate and unpleasant current diagnostic methods. The duration and extent of IBD increases the risk for colorectal cancer (CRC) therefore non-invasive screening for CRC in patients with long-term IBD may lead to early detection of abnormal changes and improve the chance of survival. To date, human metabolomic studies have shown potential for the identification of a faecal marker of IBD, but are limited by variation from diet, environment and medication. The aim of this work was to report the first study using HS-SPME-GC-MS to detect the VOC faecal metabolome in commonly used mouse models of IBD and CRC. Using an optimized method, the identification of the healthy murine faecal VOC profile resulted in little variation between individual mice with a noted significant effect of gender and age. Comparison of healthy mouse to human found 39 and 62 VOCs respectively with 33% overlap between the two species, thereby demonstrating the more complex gut environment of humans. These studies led to the identification of a VOC profile, characterized by an increase in aldehydes and a decrease in alcohols, as a marker of acute diarrhoea, compared to a significantly different profile for chronic colitis, characterised by the presence of methyl ketones. In addition, VOC profiling is capable of detecting murine-specific metabolic signatures associated with premalignant lesions of the colon, providing rationale for the investigation of new non-invasive methods for early tumour detection. These results were supported by findings questioning the specificity of faecal calproctectin as a marker of IBD due to the increased levels of calprotectin found in both colitis and cancer groups, compared to healthy controls. In conclusion, we have provided evidence that the identification of disease-associated VOC concentration ranges combined with specific marker compounds would potentially increase the likelihood of finding an IBD-specific faecal VOC marker profile. This work has presented rationale for future studies to investigate further the true origin of these marker VOCs by performing both *in vitro* and further *in vivo* work. The investigation of the faecal metabolome of a number of different murine models in combination,

rather than the use of a single mechanistic model may be provide a better reflection of human disease.

PUBLICATIONS ARISING FROM THIS THESIS

Papers

Reade S, Mayor A, Aggio R, Khalid T, Pritchard DM, Ewer AK and Probert CS. Optimisation of Sample Preparation for Direct SPME-GC-MS Analysis of Murine and Human Faecal Volatile Organic Compounds for Metabolomic Studies. J Anal Bioanal Tech. 2014 Mar; 5: 184.

Probert CS, Reade S, Ahmed I. Faecal volatile organic compounds: a novel, cheaper method of diagnosing inflammatory bowel disease? Expert Review Clin. Immunol. 2014 July; 10(9): 1129-1131.

Aggio RBM, Mayor A, Reade S, Probert CS, Ruggiero K. Identifying and quantifying metabolites by scoring peaks of GC-MS data. BMC Bioinformatics 2014 Dec; 15: 374.

Abstracts

Reade S, Sawbridge D, Khalid T, Probert CS. Sniffing disease? Optimisation of sample preparation for volatile organic metabolomic studies. Gut 2013; 62: A221-A222 (Poster, BSG Glasgow 2013).

Sawbridge D, Reade S, Khalid T, Probert CS. Charting the volatile organic metabolome (VOM): A comparison of murine and human faeces. Gut 2013; 62: A134 (Poster, BSG Glasgow 2013).

Reade S, Duckworth C, Khalid T, Mayor A, Aggio R, Pritchard DM, Probert CS. A metabolomic profiling study of a chemically-induced mouse model of intestinal inflammation Gut 2014; 63: A172 (Poster of distinction, BSG Manchester 2014).

Mayor A, Reade S, Aggio R, Khalid T, Probert CS. Paediatric faecal voc analysis: method optimisation Gut 2014; 63: A218 (Poster, BSG Manchester 2014).

Reade S, Simpson H, Aggio RBM, Probert CSJ. Hypervirulent clostridium difficile has a unique odour profile Gut 2015; 64: A158 (Poster, DDF London 2015).

Reade S, Williams JM, Pritchard DM, Probert CSJ. Volatile organic compound (VOC) profiles as indicators of early lesions in murine colon carcinogenesis Gut 2015; 64: A374-A375 (Poster, DDF London 2015).

CONTENTS

LIST OF FIGURES

LIST OF TABLES

LIST OF ABBREVIATIONS

ACF	Aberrant crypt foci
AIEC	Adherent-invasive *Escherichia coli*
ANOVA	Analysis of variance
AOM	Azoxymethane
APC	Adenomatous polyposis coli
CAR-PDMS	Carboxen-polydimethylsiloxane
CD	Crohn's disease
CE-TOFMS	Capillary electrophoresis-time of flight mass spectrometry
CEACAMs	Carcinoembryonic antigen-related cell adhesion molecules
COX-2	Cyclooxygenase-2
CRC	Colorectal cancer
CRP	C-reactive protein
CV	Coefficient of variation
DAI	Disease activity index
DMH	1,2-dimethylhydrazine
DPX	Distrene, Plasticisel, Xylene
DSS	Dextran sulphate sodium
DVB	Divinylbenzene
eGFR	Estimated glomerular filtration rate
ESR	Erythrocyte sedimentation rate
EUA	Examination under anaesthetic
FAP	Familial adenomatous polyposis
FBC	Full blood count
FC	Fold change
FOBT	Faecal occult blood test
FOI	Faecal output index
FOI	Faecal output index
GC-MS	Gas chromatography-mass spectrometry
GF	Germ-free

GI	Gastrointestinal
H&E	Haematoxylin and eosin
HID-AB	High iron diamine-alcian blue
HNPCC	Hereditary non-polyposis colorectal cancer syndrome
HS	Headspace
HS-SPME-GC-MS	Headspace-solid phase microextraction-gas chromatography-masspectrometry
I.P.	Intraperitoneal
IBD	Inflammatory bowel disease
IBS	Irritable bowel syndrome
LPS	Lipopolysaccharide
MDF	Mucin depleted foci
$MgSO_4$	Magnesium sulphate
MT	Masson's Trichrome
NA	
MW	Molecular weight
NFκB2	Nuclear transcription factor kappa B/subunit 2 (p100)
NIST	National Institute of Standards and Technology
NMR	Nuclear magnetic resonance
NO	Nitric oxide
NSAIDs	Non-steroidal anti-inflammatory drugs
PCA	Principle component analysis
PG-PS	Peptidoglycan-polysaccharide
POCTS	Point-of-care tests
ROS	Reactive oxygen species
RT	Retention time
SCFAs	Short-chain fatty acids
SI	Small intestine
SIFT-MS	Selected-ion flow-tube mass spectrometry
SOP	Standard operating procedure
SPF	Specific pathogen free

SPME	Solid phase microextraction
TCA	Tricarboxylic acid
TLR4	Toll-like receptor 4
TMB	Tetramethylbenzidine
TNBS	2,4,6-trinitrobenzene sulphonic acid
TWIMMS	Travelling wave ion mobility mass spectrometry
UC	Ulcerative colitis
UEG	United European Gastroenterology
VOC	Volatile organic compound
WT	Wild-type

Chapter 1

Introduction

1.1 GASTROINTESTINAL DISEASES

Gastrointestinal (GI) diseases are disorders of the alimentary canal, occurring anywhere from the buccal cavity to the anus, affecting people of all ages, from premature babies to the elderly. Some GI diseases are acute and life-threatening (e.g. liver failure or cancer), whereas others are more chronic and less dangerous to life, but are still severely debilitating (e.g. inflammatory bowel disease (IBD)). Recently, there has been an increase in the incidence of most GI diseases (e.g. hepatitis B and C infections, pancreatitis, alcoholic liver disease, Barrett's oesophagus, diverticular disease and colorectal cancer (CRC)), which bring major implications for future healthcare needs [1]. Consequently, the burden of GI disease is heavy for patients, the NHS, and the economy. It is reported that diseases related to the GI tract are the third most common cause of death, the second most common cause of cancer-related death in both male and females, and the second most common cause of hospital admission, after circulatory disorders, in the UK. About one in six admissions to hospital is for a primary diagnosis of GI disease and one in six of the main surgical procedures in general hospitals being performed is on the digestive tract [2].

The human lower GI tract is composed of the small and large intestines with each having a specific role to play in the digestion, secretion and adsorption of nutrients from food. The GI tract also has an extremely important role to play in the immune system; it is the first line of defence against any harmful bacteria and toxins that may enter the gut [3]. IBD is an example of a disease involving a breakdown in the epithelial defences. Furthermore, patients suffering from long-term IBD are at an increased risk of developing CRC, further contributing to the burden of GI disease for patients, their families and the economy.

1.2 INFLAMMATORY BOWEL DISEASE

Human IBD has two major phenotypes, Crohn's disease (CD) and ulcerative colitis (UC) and is characterised by chronic inflammation of the GI tract. UC, otherwise

known as idiopathic proctocolitis, causes inflammation and diffuse ulceration in the colon, whereas CD differs in the location, which may occur anywhere along the GI tract, and the nature of inflammatory changes, which are usually transmural [4]. Clinically, patients diagnosed with UC or CD present with symptoms such as abdominal pain, diarrhoea, rectal bleeding and weight loss. Both diseases affect people of all ages but predominantly arise in the younger population, and due to their remitting and relapsing nature, have a significant impact on their educational, social, professional and family life [5]. Complications of continual disease activity may include intestinal fibrosis, strictures and fistula formation and cancer, especially of the colon; in some patients, IBD can have extra-intestinal symptoms, affecting the joints, eyes and/or skin [6]. There is a need to focus on methods to control the underlying pathology in order to improve the quality of life and treatment for patients. In addition, the diagnosis may be delayed, sometimes by years, as the symptoms may be confused with the more common irritable bowel syndrome (IBS), so attention also needs to be given to a better means of diagnosing IBD.

1.2.1 Epidemiology of IBD

Reportedly, IBD affects an estimated 1.5 million Americans, 2.2 million people within Europe and several hundred thousand more worldwide. Considerable variation in the epidemiology of IBD has been observed around the world with a wide range of estimates both within, and between, geographic regions. IBD is believed to be associated with the industrialization of nations, with its highest incidence rates and prevalence in North America and Europe [7].

1.2.1.1 Incidence and prevalence

The incidence of IBD (both CD and UC) has increased dramatically in economically prosperous countries since the 1950s, in particular in the established high-prevalence populations of IBD in North America and Western Europe **(Figure 1.1)** [8]. Specifically, the annual incidence of UC varied from 0 - 19.2 per 100,000 people

in North America and 0.6 -– 24.3 per 100,000 in Europe, corresponding to a prevalence of 37.5 - 248.6 per 100,000 and 4.9 - 505 per 100,000, respectively [9]. The incidence of CD was similar to that of UC, varying from 0 – 20.2 per 100,000 in North America and 0.3 – 12.7 per 100,000 in Europe. Furthermore, populations previously considered 'low risk', such as Japan, Hong Kong, South Korea and India, have also witnessed an increase in incidence of both UC and CD between 1950 and 2008. It is clear that Westernisation is contributing to the onset of the disease as immigrants into these countries acquire the same endemic risk of developing IBD within a decade or two [10].

The incidence of IBD in the UK, of both UC and CD, continues to rise and is now estimated to affect 1 in 200 people with a total estimated cost to the NHS of £720 million, based on the prevalence and an average cost of £3,000 per year per patient [11]. Recent European data has reported the prevalence to be between 0.5 - 1% of the total population. In the UK, it is estimated that at least 115,000 people have CD and around 146,000 have a diagnosis of UC [12].

1.2.1.2 Sex, age and racial incidence

Incidence in Western populations is similar in men and women, but is influenced by race and ethnicity. It has been reported that the female to male ratio varies from 0.51 to 1.58 for UC and 0.34 to 1.65 for CD, suggesting an IBD diagnosis is not sex specific [13]. In most studies, the peak incidence of IBD is in the second to fourth decade of life. 78% of CD cases are diagnosed between the age of 20 and 29, for UC it is 51.1%, and has remained unchanged over several decades [9]. As a result, IBD appears to affect individuals in the most productive years of life, potentially resulting in long-term problems and costs for patient, healthcare and society.

As previously mentioned, the highest occurrence of both UC and CD is found within North America and Europe. Within Europe, the highest incidence rates are found in Scandinavia and the UK, whilst they remain low in southern eastern European countries [14]. Total incidence rates in northern Europe were 6.3 for CD and 11.4

for UC per 100,000 person years, compared to 3.6 and 8.0 per 100,000 person years, respectively, in southern Europe. These rates suggest a north-west/south-east gradient in IBD incidence in Europe [14]. This is also apparent in the UK, with a North-South gradient demonstrated by a higher incidence in Scotland, compared to England [11].

The risk of IBD is increased 3-fold in the Jewish population compared to the non-Jewish Caucasians populations and is higher, particularly among Ashkenazi, American and European Jewish populations, compared with those residing in Israel [9]. However, the incidence of IBD in Hispanic and Asian people has been shown to be increasing, and studies have shown that individuals emigrating from low prevalent regions (e.g. Asia) to higher prevalent countries (e.g. England) are at increased risk for developing IBD, particularly among first-generation children [9, 15].

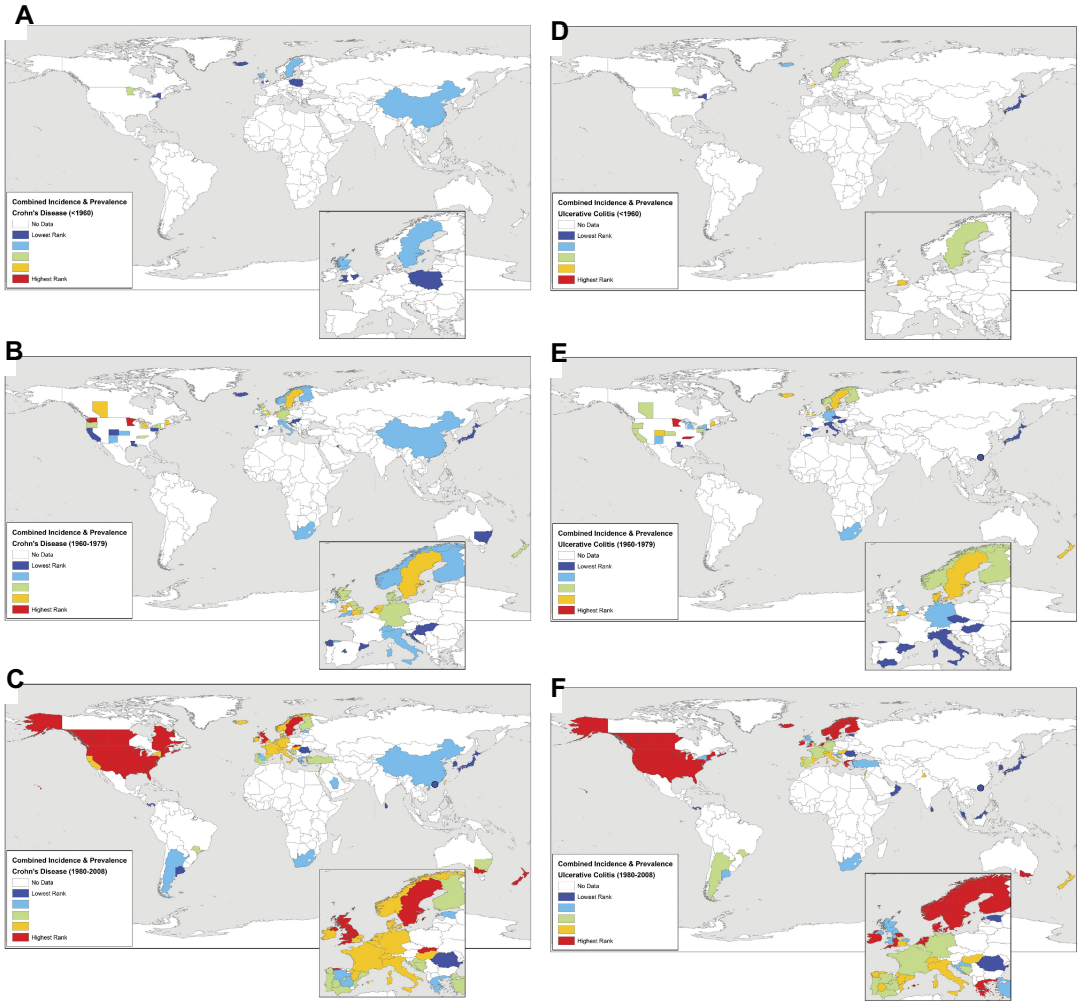

Figure 1.1 The combined incidence and prevalence rates of IBD worldwide, as reported by Molodecky *et al.* in 2012 [9]. Data found as a result from a systematic literature search for CD and UC, respectively, before 1960 (A & D), from 1960 to 1979 (B & E)) and after 1980 (C & F). Incidence and prevalence values were ranked into quintiles representing low (dark and light blue) to intermediate (green) to high (yellow and red) occurrence of disease. Copyright has been granted and figure is used with permission.

1.2.2 Aetiology and pathogenesis of IBD

The aetiology of IBD has been extensively studied in the past few decades; however, the disease pathogenesis is not fully understood. It has been widely hypothesised that the pathogenesis of IBD results from an interaction of environmental factors (e.g. smoking, oral contraceptives, high-fat diet) affecting the intestinal microbiota compared with an inappropriate immune response, often but not only, in a genetically predisposed person **(Figure 1.2)**. Risk alleles include changes in the *NOD2, IL-23R* and *ATG16* genes [16], and more recently, genome-wide association studies and subsequent meta-analyses have been able to identify separate phenotypes between CD and UC. One hundred and sixty three IBD loci have been identified in total with 100 loci contributing to both CD and UC (e.g. *IL23R* and *CD48*), but also some showing specificity for either CD (30 e.g. *ATG16L1, NOD2, and IL6ST*) [17] or UC (23 e.g. *TNFRSF14*, *CARD9,* and *ORMDL3*) [18]. The gut immunological balance is perturbed with a shift towards the pro-inflammatory side, resulting in over-production of pro-inflammatory cytokines (e.g. TNF-α, IL-6), which results in significant tissue damage. Nuclear transcription factor kappa B (*NFκB2*) has been identified as one of the key regulators in the immunological setting [19].

1.2.2.1 Environmental factors implicated in IBD

Environmental influences have become well-established risk factors for IBD; although appendectomy for appendicitis can protect against UC [20]. Recently oral contraceptives and diet have been proposed to increase an individual's risk of developing the disease [21, 22]. Potential environmental factors increasing an individual's chance of developing IBD span the spectrum of life, from mode of childbirth and early-life exposures (including breastfeeding and antibiotic exposure) to exposures later on in adulthood (including smoking, major life stresses, diet and lifestyle) [8]. Data support a risk association between smoking and CD whereas smoking cessation, but not current smoking, is associated with an increased risk of UC [23]. A significantly lower intake of dietary fibre (fruits and vegetables), a higher

intake of saturated fats, depression and impaired sleep, and low vitamin D levels have all been associated with the onset of IBD [8].

1.2.2.2 Role of intestinal microbiota in pathogenesis of IBD

During health, the GI tract is colonized by a broad range of highly diverse microorganisms, which is collectively termed the gut microbiota. The gut microbiota is responsible for the metabolism of exfoliated epithelial cells, dietary carbohydrates and amino acids, and mucus, resulting in the production of metabolites that affect the function of the gut, including intestinal epithelial cell state. Biproducts of digestion also influence host energy balance, immune regulation and homeostasis [24]. These bidirectional communications between the microbiota and the host composed of bacterial and human genes, determine the metabolic profile of the host.

The composition and luminal numbers of dominant microbial species in the human GI tract vary between the gastric, proximal and distal small intestinal and colonic microenvironments. Bacterial counts are very low in the stomach at $0\text{-}10^2$/g compared to 10^{11}/g to 10^{12}/g in the distal luminal contents in the colon [24]. The gut microbiota is primarily composed of four major phyla: Firmicutes (49-76%), Bacteroidetes (16-23%), followed by the less prevalent phyla, Proteobacteria and Actinobacteria [25]. Recent evidence indicates that the intestinal microbiota play a role in initiating, maintaining and determining the phenotype of IBD [26]. It has been well-documented that there are four broad mechanisms explaining the complex relationship between the commensal microbiota and IBD: (i) dysbiosis (i.e. altered balance) of the intestinal microbiota; (ii) induction of intestinal inflammation by presence of pathogens and functional alterations in the bacteria; (iii) host genetic defects in containing commensal microbiota; and (iv) defective host immunoregulation [24].

Intestinal dysbiosis can be defined as an abnormal ratio of beneficial and harmful bacteria species; evidence has suggested that it is the central characteristic of the

gut microbiota in IBD [27]. However, it remains unclear whether this dysbiosis is a cause or consequence of the onset of IBD [28]. A common feature of the gut microbiome in IBD is that overall species diversity is generally reduced in CD and UC. Specifically, there is a reduced abundance of several types of bacteria species, in particular, members of the Firmicutes and Bacteroidetes phyla [29, 30] and an increase in the abundance of others, including the Actinobacteria and Proteobacteria phyla [24]. A study on the faecal microbiota of patients with UC compared to healthy controls looked at clustering of the faecal microbial communities and found the control group samples to cluster separate to 7 clusters consisting of the UC patients was reported. Unclassified bacteria, *Eubacterium*, *Fusobacterium*, *Ruminococcus*, Gammaproteobacteria, *Bacteroides*, and *Lactobacillus* were responsible for these differences. This indicates that these bacteria could be used to distinguish between patients with UC and healthy controls and thus could be potential IBD biomarkers [31].

Adherent-invasive *Escherichia coli* (AIEC) are a potential causative agent in CD [32-34]. Martinez-Medina *et al.* reported that a Western diet (e.g. saturated fats, red meats, lack of fresh fruits) given to mice expressing human carcinoembryonic antigen-related cell adhesion molecules (CEACAMs) resulted in changes to the composition of the intestinal microbiota. This led to alterations in the host barrier function and immunity, thereby creating a microenvironment that facilitated the colonisation of AIEC to the intestinal tract and consequently exacerbated the inflammatory response [32]. Other enteric bacterial pathogens that may exacerbate intestinal inflammation include toxin A-producing *Clostridium difficile* [35] and enterotoxigenic *Bacteroides fragilis* [36].

Studies to date investigating the role of the gut microbiota in IBD have focused on the presence of specific bacteria species rather than the non-bacterial components of the microbiota. Viruses are the most abundant biological entity within the gut and their function in health and GI disease is not well defined. However, it has been demonstrated that virus populations are more diverse and are present at significantly higher levels in patients with CD than in controls, thereby showing

potential as a viral biomarker for CD [37]. Furthermore, recent investigations have also begun to investigate the role of a commensal fungal community on mucosal surfaces, the 'mycobiome'. An overall increase in "opportunistic pathogenic" fungi (*Candida, Trichosporon)* and a decrease in nonpathogenic fungi (*Saccharomyces*) has been found in the presence of gut inflammation, as expected when considering the that inflammation drives changes in the gut bacterial population [38].

With the increasing knowledge of the role of the intestinal microbiota and the growing evidence of the gut mycobiome in the pathogenesis of IBD, the development of novel non-invasive diagnostic tools may be investigated. If the dysbiotic microbiota play a role in disease pathogenesis, interventions that 'normalise it' might be a strategy to treat certain disease processes e.g. faecal transplantation in the treatment of *C. difficile* infection [39]. However, evidence to date suggests that the use of faecal transplantation as a novel treatment for IBD remains variable and further randomized controlled trials are needed to prove the efficacy of this [40].

1.2.2.3 Inappropriate immune response in a genetically predisposed person

A role for genetics in the pathogenesis of IBD was initially derived from familial aggregation studies and twin studies, which suggested an important hereditary component. There are between 2-14% of CD patients that report a family history of the disease with a similar proportion for UC patients (8-14%) [41]. If both parents suffer from IBD, the risk of the offspring developing the disorder before the age of 30 years is estimated to be as high as one-in-three [42]. The familial nature of IBD has been linked with CD-associated genes such as the *NOD2* mutation, described in 2001 [43-45], and the 163 other risk alleles reported, in predominantly white populations [17]. Combined with our improved understanding of the functional consequences of these disease-associated genes, it has become widely accepted that the genetic risk factors do not act in isolation but in synergy with both the external and internal (gut microbiota) environments. The recognised risk genes can be broadly divided into those that influence the maintenance of the integrity of the

epithelial barrier (e.g. *GNA12*), response to oxidative stress (e.g. *PRDX5*), innate immune response and microbial defence (e.g. *NOD2*), restitution and injury repair (e.g. *STAT3*), adaptive immune responses (e.g. *IL10*) and autophagy (e.g. *ATG16*) [8]. These genetic variants in IBD are discussed in more detail in a number of specific reviews [46-48].

The hygiene hypothesis proposes that during early childhood the immune system must be exposed to stimuli such as infectious agents and symbiotic bacteria. Such exposure will allow adequate development of regulatory T cells and natural progression of the immune system to avoid becoming susceptible to autoimmune diseases late on in life [49]. Host genetic defects involved in innate immunity can also contribute to dysbiosis of the gut microbiota in patients with IBD; a number of which can be expected to have an impact on the composition of the intestinal microbiota (e.g. *NOD2, ATG16, NCF4, IRGM*) [24].

1.2.2.4 *NFκB*'s role in intestinal inflammation

The family of *NFκB* proteins control the transcription of DNA and consist of five different members, p65 RelA, c-Rel, RelB, p50/p105 (*NFκB1*) and p52/p100 (*NFκB2*) which are all characterised by a structurally conserved N-terminal 300 amino acid region containing specific domains, responsible for dimerisation, nuclear localisation and DNA-binding [50]. In order to activate this family of proteins, there are two different intracellular pathways, the classical and the alternative activation pathways, resulting in the release of *NFκB* and the translocation to the nucleus to modulate pro-death or pro-survival responses to cellular stresses, such as infection and inflammation [19]. The classical pathway is activated by the presence of microbial products and pro-inflammatory cytokines, specifically TNFα, followed by activation of RelA- or c-Rel complexes. The alternative pathway is triggered by TNF-family cytokines (e.g. CD40 or lymphotoxin β receptor, but not TNFα, resulting in activation of RelB and *NFκB*2 [51], however, the role of the alternative pathway in inflammation is still unclear. The expression and activation of *NFκB* is strongly induced in the inflamed gut of IBD patients [52], with sites of inflammation found to

be associated with the activation of the classical pathway [53]. There is accumulating evidence to suggest that activation of the alternative *NFκB* pathway also plays an important role in the pathogenesis of IBD, and IBD-associated cancer. For instance, Burkitt *et al.* showed that mice lacking the c-Rel subunit were more susceptible to colitis-associated cancer compared to wild-type mice. Mice lacking *NFκB2* were resistant to both colitis and colitis-associated cancer, developing fewer polyps per colon compared to wild-type mice [54].

To summarise, the anti-apoptotic functions of *NFκB* can protect against inflammation, in the case of epithelial cell survival and mucosal barrier integrity, and also maintain the inflammatory response through persistent leukocyte activation [51]. *NFκB*2 is necessary for the development of colitis, whilst c-Rel- and *NFκB1*-mediated signalling regulates epithelial cell turnover following DNA damage.

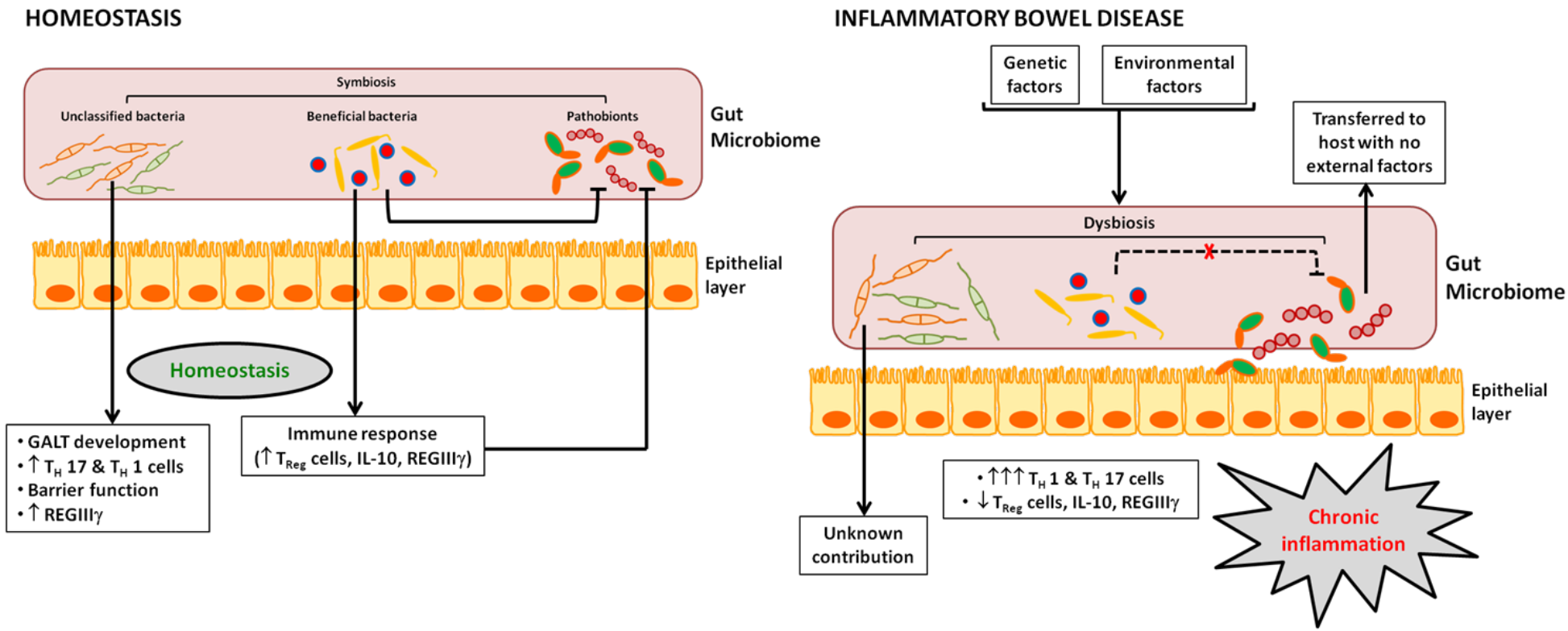

Figure 1.2 Pathogenesis of IBD. A complex interplay between the host immune system and the symbiotic microbiota is necessary for gut homeostasis. Anti-inflammatory activities from the presence of beneficial bacteria species suppress the colitis-inducing pathobionts either directly or through induction of regulatory immune response (left-hand side). In IBD, the combination of genetic and environmental factors result in dysbiosis which in turn leads to a loss of the barrier function and an increase in pathobionts and, consequently, chronic inflammation (right-hand side). It is unknown whether unclassified bacteria have a role in the pathogenesis of IBD (Modified from [55]).

1.2.3 Risk of CRC in IBD

Patients with IBD are at increased risk for developing CRC because of the long duration and extent of colitis and may further increase when combined with a familial history of CRC [56]. IBD is considered the third highest risk factor for CRC, behind familial adenomatous polyposis (FAP) and hereditary non-polyposis colorectal cancer syndrome (HNPCC) [57]. Chronic inflammation is believed to promote carcinogenesis, thereby making it a key risk factor for CRC in patients with IBD. Depending on the study and geographical location, the risk of CRC in patients with UC varies between 0.9 and 8.8 fold with a probability of 2% 10 years after diagnosis, 8% after 20 years and 18% after 30 years [58]. Choi *et al.* performed a forty-year colonoscopic surveillance programme for CRC in UC patients and found the incidence rate to be 4.7 per 1000 patient-years, concluding that colonoscopic surveillance may have a significant role in reducing the risk of CRC in patients with long-standing UC [59]. With CD, there is no statistically significant increase in cancer risk identified when including all patients irrespective of disease extent and duration, but when considering those patients with longstanding colonic CD, the risk of developing CRC is similar to that seen in UC patients [60].

1.2.4 Current diagnostic methods of IBD

The current investigations offered to an individual suspected of having UC or CD involve blood tests, stool tests, endoscopies, imaging (e.g. CT, MRI, ultrasound and bariums), and possibly, examination under anaesthetic (EUA) (Crohn's and Colitis UK, 2013 [61]). Several blood tests can be used to support a diagnosis of IBD, or to monitor the effects of IBD or its treatment. A full blood count (FBC) measures the levels of red, white and platelet blood cells in order to monitor signs of inflammation and detect anaemia. Inflammatory marker tests (e.g. C-reactive protein (CRP) and erythrocyte sedimentation rate (ESR)) are also used to detect inflammation; liver function tests are mainly used to measure serum albumin, low levels of which may occur in inflammatory conditions. Other blood tests that may be helpful in IBD include ferritin, transferrin, vitamin B12 and folic acid levels.

Faecal calprotectin and faecal lactoferrin assays are used to look for signs of intestinal inflammation and endoscopies are used by clinicians to directly examine the intestinal mucosa [61].

Despite the wide range of tests available, the diagnosis and care of IBD remains difficult for clinicians and is commonly based on the presenting symptoms and a range of investigations mentioned previously. Most of these diagnostic methods are invasive, expensive and are considered unpleasant by the patient. The serum markers such as CRP and ESR lack specificity and are increased in other inflammatory diseases [62]. Recently, non-invasive methods of assessing diseases have become the 'holy grail' for research into diagnostics. Examples include faecal calprotectin and lactoferrin are neutrophil proteins that pass into the lumen and enter the faeces when the intestine is inflamed and can be measured directly in the faeces of patients with active IBD [63]. However, although these faecal markers are informative when diagnosing IBD, they have a slow turnaround and are also raised in the presence of faecal blood (e.g. haemorrhoids, polyps or gut infections such as *Clostridium difficile*); so may be unable to distinguish between infectious diseases and IBD [64].

A recent review describes the investigation of faecal volatile organic compounds (VOCs) as a novel, cheaper method of diagnosing IBD [65]. This is also discussed in more detail in **section 1.8.6.**

1.3 COLORECTAL CANCER (CRC)

CRC is a major worldwide health problem because of its high prevalence and mortality rate, which may be attributed to late diagnosis. Regions with the highest incidence rates include Australia, New Zealand, Canada, U.S.A and Europe; China, India and Africa have the lowest incidence rates. Risk factors believed to increase an individual's chance of developing CRC include a family history of bowel cancer, long-term IBD, a high fat diet with low consumption of fibre, smoking and a lack of exercise [66].

1.3.1 Epidemiology of CRC in the UK

National statistics, reported by Cancer Research UK, have reported that CRC is the fourth most common cancer in the UK (2011), accounting for 13% of all new cases of cancer. It is the third most common cancer in both males (14% of cancers in men) and females (11%) separately. Data collected in 2011 found that there were 41,581 new cases of CRC in the UK with male: female ratio of 13:10 (23,171 (56%) in men and 18,410 (44%) in women) [67]. The age-standardised incidence rates are significantly lower in England compared to Wales, Scotland and Northern Ireland, primarily due to a north-south divide across the UK [67]. When looking at CRC incidence by age, an average of 43% of cases were diagnosed in people aged 75 and over, and 95% in those aged >50, indicating that the incidence of CRC is very strongly related to age [67] **(Figure 1.3).** Furthermore, approximately 50% of CRC patients will eventually develop metastatic cancer, with an overall survival rate of five years for 50-60% of patients [68].

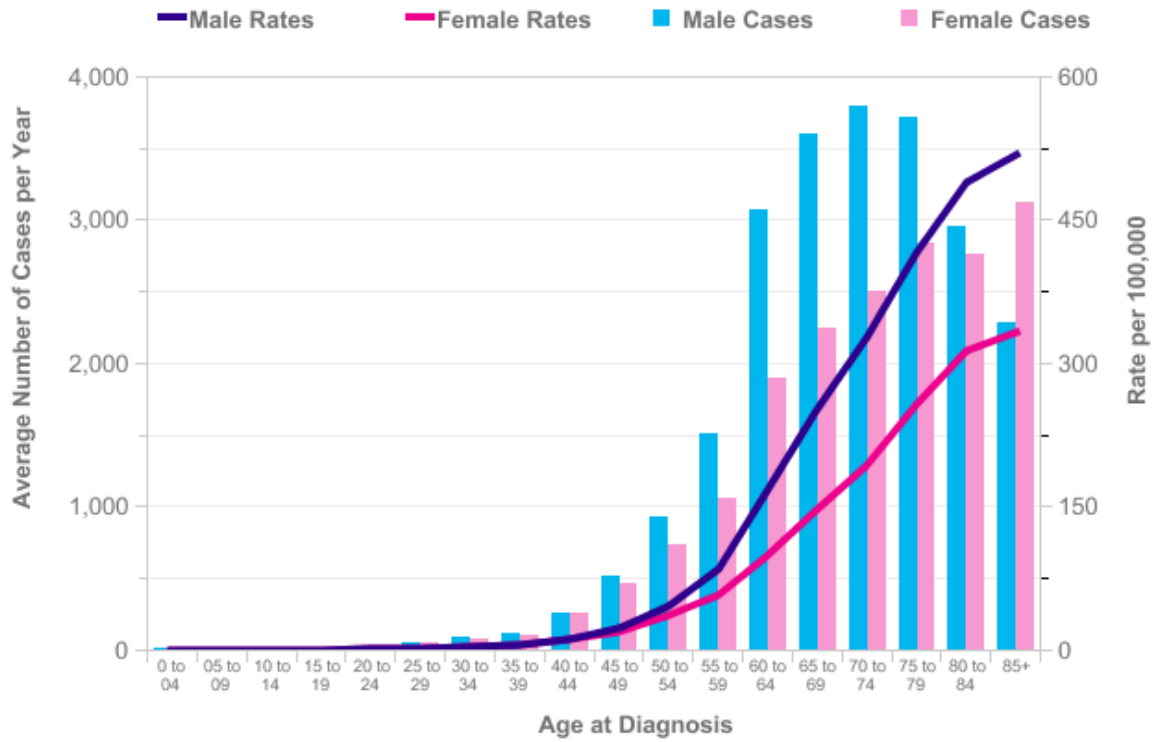

Figure 1.3 CRC incidence statistics, by age. Average number of new CRC cases per year and age-specific incidence rates per 100,000 of the population in the UK, Cancer Research UK, May 2015 [67]. Permission granted for use of figure from CRUK website.

1.3.2 Risk factors for CRC

Several risk factors have been reported to be associated with the incidence of CRC. These risk factors include uncontrollable factors, such as age and an inherited genetic risk, as well as a substantial number of environmental and lifestyle risk factors including diet, obesity, smoking, and heavy alcohol consumption.

1.3.2.1 Age

The probability of developing CRC increases after the age of 40 and rises sharply after the age of 50, with more than 90% of CRC cases occurring in people age 50 or older [66]. However, the incidence of CRC appears to be increasing among younger people with more people aged 20-49 being diagnosed [69], but the explanation for this is unclear [69]. Meanwhile, the United European Gastroenterology (UEG) has called for primary care physicians to be more alert to the symptoms of CRC in young people [69].

1.3.2.2 Personal or family history of CRC or polyps

Neoplastic polyps of the bowel are often benign and are referred to as pre-cancerous lesions or adenomas. Compared with individuals with no personal history of adenomas, those individuals with a history of precursor lesions are at an increased risk of developing CRC [70]. It is estimated that it takes 5 to 10 years for the development of malignancy from benign adenomas [70], therefore the detection and removal of these precursor lesions is vital in order to reduce the risk of CRC.

1.3.2.3 Inherited genetic risk

Sporadic CRC is a term used to define cancers that appear in the absence of a known syndrome or family history. The vast majority of CRC (60-80%) are of the sporadic type [68]. However, approximately 5-10% of CRC are a consequence of

recognised hereditary conditions [66]. Most commonly, these include FAP and HNPCC, also known as Lynch syndrome. HNPCC accounts for about 2-6% of CRCs [71] and is associated with mutations such as the *MLH1* and *MSH2* genes, which are involved in the DNA repair pathway [72]. FAP accounts for less than 1% of all CRCs [66] and is related to mutations in the tumour suppressor gene *APC* [73]. Although relatively low in incidence, almost all individuals with FAP will have developed CRC by age 40 if the colon is not removed [74].

1.3.2.4 Personal history of IBD

As mentioned in **section 1.2.3**, the duration and extent of IBD increase an individual's risk of developing CRC. Therefore, regardless of age and other factors, those individuals with IBD are encouraged to be screened for CRC on a more frequent basis than those without IBD.

1.3.2.5 Lifestyle risk factors

A large proportion of CRC cases may be preventable by recognition of certain lifestyle risk factors. These contributing factors include lack of regular physical activity, low fruit and vegetable intake, a low-fibre and high-fat diet, obesity, alcohol consumption and smoking [75]. It has been reported that obesity and a lack of physical activity account for about a quarter to a third of CRCs. This may be explained by increasing the body's metabolic efficiency and reducing blood pressure and insulin resistance [66]. Smoking is not only associated with lung cancer, but is also extremely harmful to the colon, as tobacco is associated with the formation and growth rate of adenomas [76]. Heavy alcohol consumption acts synergistically with smoking and, combined with a diet low in essential nutrients, make tissues susceptible to carcinogenesis. Diet strongly influences the risk of CRC and is discussed in detail in section 1.3.4.2.4.

1.3.3 IBD-associated CRC

Individuals suffering from long-term IBD are at an increased risk of developing CRC during later life, with UC and CD patients having a 10- and 4- fold increased risk, respectively [77]. UC-associated CRC was first reported by Crohn and Rosenburg in 1925 [78], and CD in 1945 [79]. There is no known genetic basis for the predisposition to CRC in patients with IBD. The mortality rate is higher in this type of CRC than that for sporadic CRC [80]. This risk can be related to the duration and extent of the disease with growing evidence to support the hypothesis that inflammatory cells present from IBD can be actively tumour promoting [81]. A significant correlation has been reported between the colonoscopic and histologic inflammation scores and the risk of colorectal neoplasia [82]. However, the pathogenesis of IBD-related CRC remains poorly understood but influencing risk factors include genetic instability, epigenetic alteration, impaired immune responses by mucosal inflammatory mediators, the presence of oxidative stress, diet and the intestinal microbiota [83].

1.3.4 Pathogenesis of CRC

The primary focus of this thesis is inflammation-associated CRC but to begin to understand its pathogenesis, it is first helpful to appreciate the molecular basis of sporadic CRC.

1.3.4.1 Pathogenesis of sporadic CRC

Sporadic CRC arises from genomic instability, resulting in a loss of chromosomal material, termed aneuploidy, which contributes to the loss of function, or mutation, of key tumour suppressor genes such as *APC* (an early event) and *p53* (a later event) **(Figure 1.4).** This accumulation of mutations drives the transformation of normal colonic epithelium to adenomas to cancer [84]. During the adenoma-carcinoma sequence, further changes occur in the genetic regulation, such as

induction of *K-ras* oncogene. Individuals with FAP often progress to CRC via this pathway [84].

1.3.4.2 Pathogenesis of IBD-associated CRC

CRC in the setting of IBD is believed arise from the progression of no dysplasia to indefinite dysplasia to low-grade to high-grade dysplasia to carcinoma (**Figure 1.4**). Inflammation-associated CRC differs from sporadic CRC in the way that it is not unusual for dysplasia or cancer to be multifocal, rather than sporadic, arising in one or two focal areas of the colon [84]. IBD clearly predisposes individuals to CRC development; the role of, and interactions of, inflammation, diet, oxidative stress and the intestinal microbiota in the pathogenesis of IBD-associated CRC are discussed below.

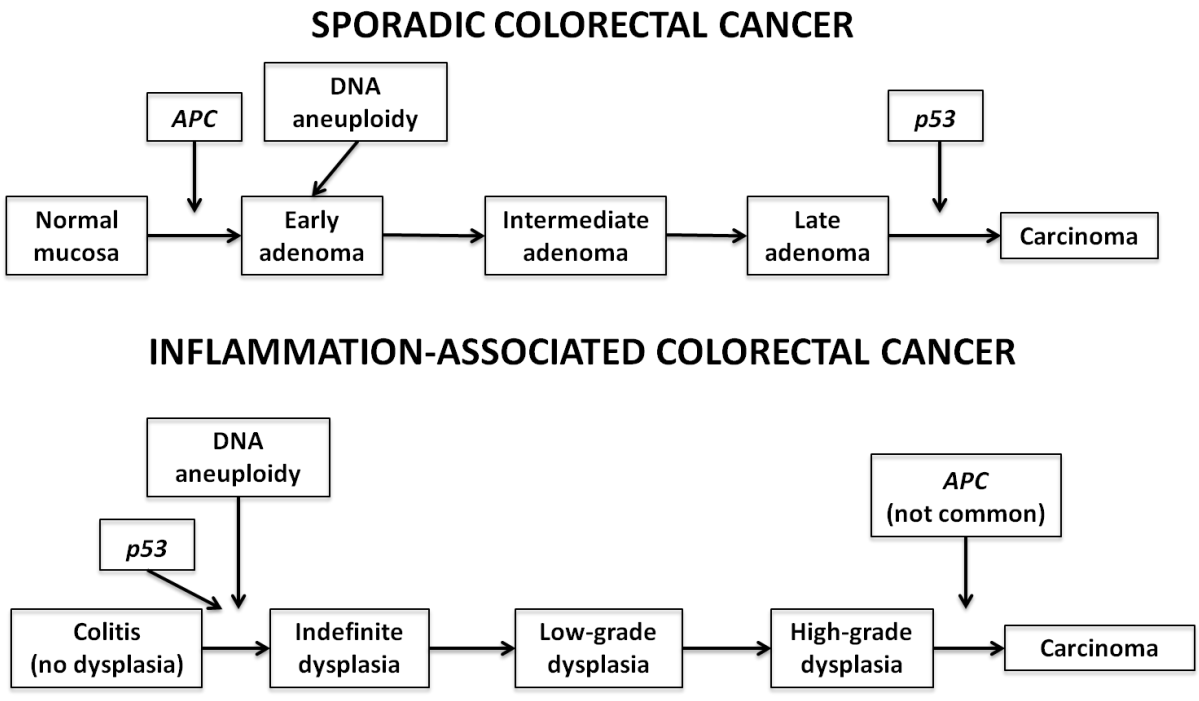

Figure 1.4 The differences in the molecular pathogenesis of sporadic CRC and inflammation-associated CRC. Sporadic CRC is driven by genomic instability resulting in a sporadic adenoma-carcinoma sequence. Inflammation-associated CRC occurs by a progression from no dysplasia to indefinite to low-grade to high-grade dysplasia to carcinoma. Mutations/loss of function in genes: *APC*, adenomatous polyposis coli; *p53*, tumour suppressor protein p53. Adapted from [84].

1.3.4.2.1 Inflammation-dysplasia-carcinoma sequence

Inflammation is an important risk factor for the development of CRC in patients with IBD and the epidemiological data support this assumption [60]. It has been postulated that inflammation results in malignant transformation by enhancing epithelial cell turnover in the colonic mucosa. This is supported by the observation of high rates of mitosis and apoptosis in association with active UC [85]. In addition, it is believed that mutagenic assault and sustained DNA damage appear to drive the whole process. A number of inflammation-associated genes (e.g. cyclooxygenase-2 (*COX-2*), nitric oxide synthase-2 (*NOS2*) and the Fragilis interferon-inducible gene 1-8U) have also been found to be over-expressed in areas of inflamed mucosa [85]. A recent study found Toll-like receptor 4 (TLR4) signalling is over-expressed in both human and murine inflammation-driven CRC and that TLR4-deficient mice were protected from CRC [86]. The authors hypothesised that TLR4 signalling promotes CRC as a result of inflammation by enhancement of COX-2 expression and increased estimated Glomerular Filtration Rate (eGFR).

The detection of these early inflammatory related changes would result in a better prognosis for patients at risk of developing CRC. Aberrant crypt foci (ACF) were originally described in rodents treated with colon-specific carcinogens [87], but have also been identified in humans at high risk of CRC as cancer biomarkers [88, 89]. However, whether ACF are signs of pre-malignancy or not has been questioned [90]. For example, the spontaneous development of ACF in rats was investigated but results suggested that spontaneous ACF rarely progress to colon tumours [91]. In addition, promoters of CRC such as cholic acid, have been reported to decrease the expression of ACF in rats, rather than increase it [92]. More recently, dysplastic foci depleted of mucins (MDF) in the colon of rodents [93] and humans [94] have been described. Similar to colonic tumours, MDF show activation of wnt signalling driven by mutations in the β-catenin gene and *APC*, both key to CRC progression [94, 95].

1.3.4.2.2 Oxidative stress and CRC

Essentially, oxidative stress is an imbalance between the production of free radicals and the ability of the body to counteract their harmful effects [96]. Cellular damage caused by oxidative stress is an important feature of UC; phagocytic leukocytes are increased and result in enhanced production of pro-oxidant molecules [84]. It has been hypothesised that inflammation may be the link between oxidative stress and the development of CRC; wherein the increase in activated leukocytes results in overproduction of reactive oxygen species (ROS) [96]. Inflammatory phagocytic cells (e.g. neutrophils) have an enzyme, nicotinamide adenine dinucleotide phosphate (NADPH) oxidase (NOX), present on their surface where it produces ROS that kill bacteria. The intestinal NOX1 isoform appears over-expressed in CRC tissue, compared to normal colonic mucosa [96, 97]. Furthermore, improved formation of 8-nitroguanine, representative of nitrative damage to nucleobases, has been detected in IBD [60]. Consequently, oxidative stress can pave the way for malignant tumours to develop in inflamed tissue, and ROS and nitric oxide (NO) may contribute to this.

1.3.4.2.3 Inflammation, intestinal microbiota and CRC

The human gut is home to a complex community of bacteria that play a vital part in the overall homeostasis of the host. Currently, the mechanisms by which bacteria contribute to CRC are not fully understood, but evidence suggests a link between the gut microbiota and inflammation in the development of CRC. It is thought that the intake of dietary products interacts with the different species of bacteria present within the gut to promote the chronic inflammation described above and drive the progression of CRC through direct influence of host cell physiology, cellular homeostasis, energy regulation, and/or metabolism of xenobiotics [98] **(Figure 1.5).**

1.3.4.2.4 Diet, intestinal microbiota and CRC

Diets that are high in fat, in particular animal fat, are a key risk factor for CRC. This can be linked to the concept that the typical Western diet is high in fat, favouring the development of a gut microbiota capable of degrading bile salts to potentially carcinogenic compounds, *N*-nitroso compounds [99]. Increased meat consumption is also a major factor to be considered in the development of CRC. Cooking meat at high temperatures results in the production of compounds with carcinogenic properties, namely heterocyclic amines and polycyclic aromatic hydrocarbons [100]. In addition, heme iron from meat has been implicated in the increased risk of CRC [101]. Individuals who have a diet low in fruit and vegetables may be at a higher risk of developing CRC. These intake differences in dietary fibre may therefore be responsible for the geographic differences in the CRC incidence rates. For example, dietary fibre has been proposed to account for the differences in the rates of CRC between Africa and Westernised countries [102]. The increased intake of dietary fibre in Africa may dilute faecal content, increase faecal bulk and reduce transit time. **Figure 1.6** presents the interactions of various components of the diet with the intestinal microbiota during the development of CRC.

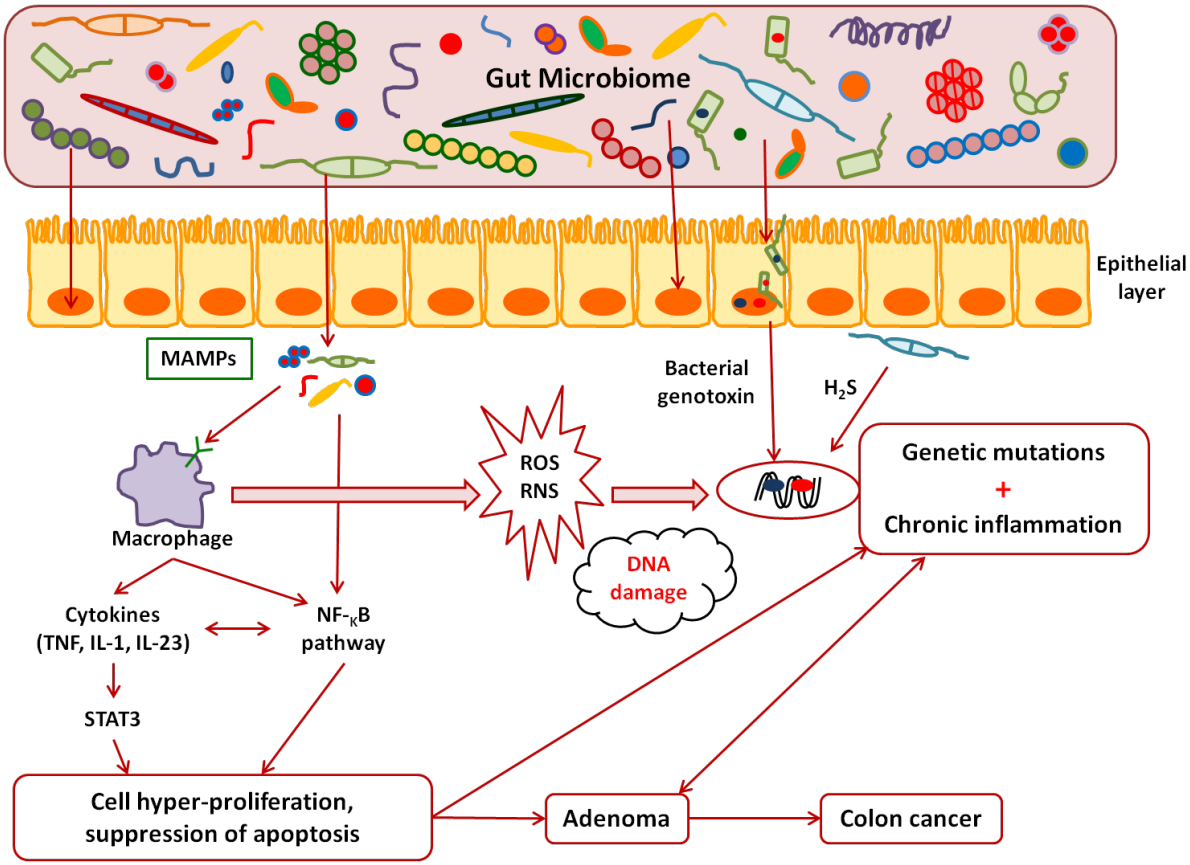

Figure 1.5 Role of the intestinal microbiota in the progression of chronic inflammation to adenoma and CRC. Bacterial dysbiosis causes a breakdown in epithelial barrier function, resulting in bacterial translocation. In turn, this triggers a pro-inflammatory response leading to suppression of apoptosis, cell hyper-proliferation and the production of ROS. Chronic inflammation eventually progresses to adenoma and CRC. Adapted from [98].

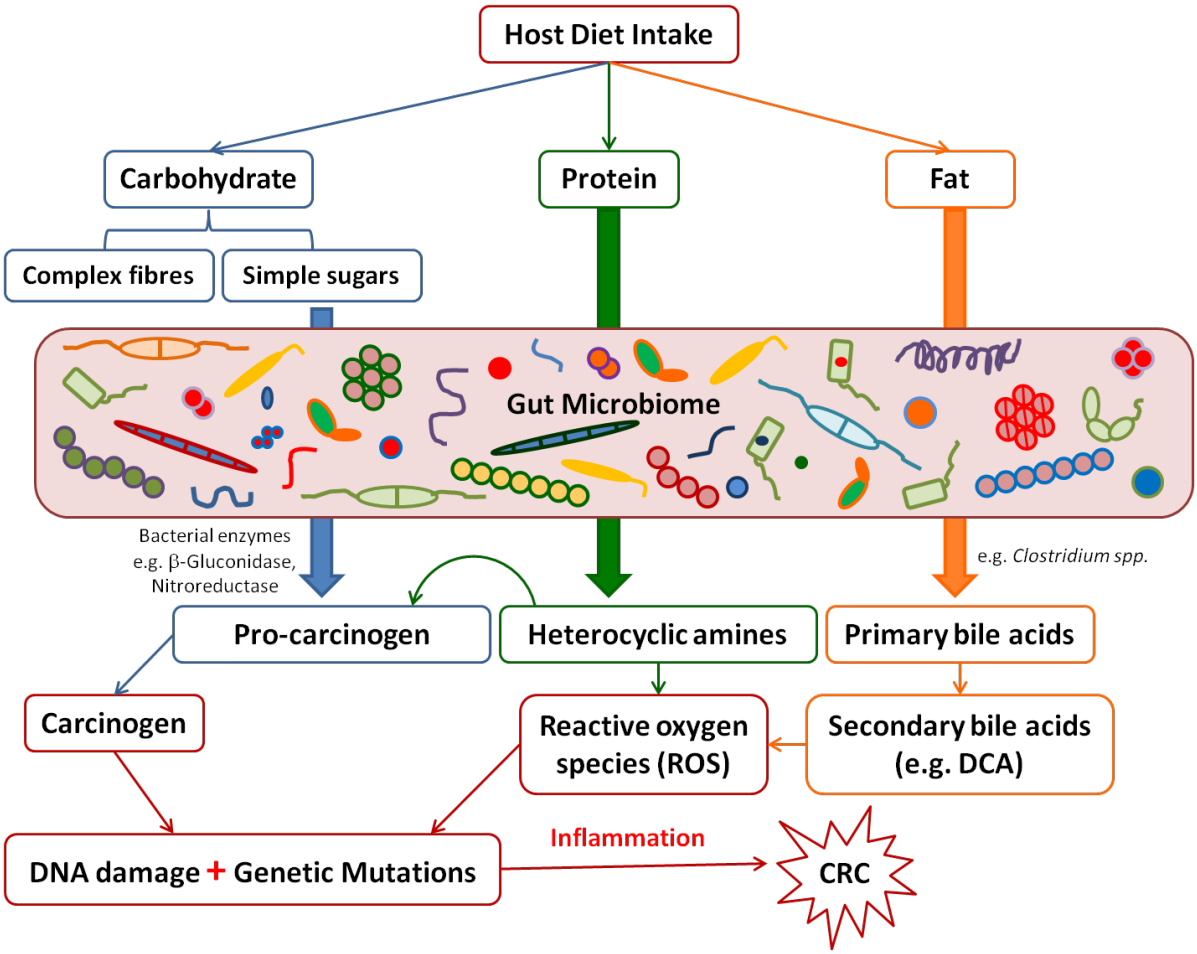

Figure 1.6 The interaction of various components of the diet with the intestinal microbiota in CRC. Carbohydrates, protein and fat are the principal components of diet intake and undergo colonic bacterial digestion. By-products produced are shown here to be involved in CRC via various mechanisms. Adapted from [98].

1.3.5 CRC screening techniques

In general, the purpose of CRC screening is to reduce morbidity and mortality from CRC. Other than cervical cancer, CRC is the only cancer for which population-based screening has shown to improve disease prognosis. The detection of CRC at an earlier stage from a premalignant polyp is associated with better survival, therefore making CRC one of the most preventable cancers [103]. This has been demonstrated by the development of the first staging system for CRC, Dukes' stages of colon cancer, where Dukes and colleagues showed that better patient survival was accompanied by a disease diagnosis at an earlier stage [104].

People in England are currently offered bowel screening at 2-year intervals between the ages of 60-69 to avoid late detection and poor prognosis. This screening involves a faecal occult blood test (FOBT), which is cost-effective but may fail to detect early stage lesions. In March 2015, a new NHS bowel scope screening programme was introduced, offered to men and women aged 55 and involves a flexible sigmoidoscopy [105]. A sigmoidoscopy and a colonoscopy are more sensitive procedures, but extremely invasive and expensive [106]. As a result, scientists and clinicians are working together to find an alternative non-invasive, cheaper method of CRC screening such as disease-specific biomarkers.

1.4 MURINE MODELS OF GI DISEASE

Over the past century, the mouse has developed into the primary mammal for scientific research. Scientists from a wide range of biomedical fields have gravitated to the mouse because of its close genetic and physiological similarities to humans, as well as the ease with which its genome can be manipulated and analysed [107]. Mouse models of disease can be referred to as a 'pure' group of subjects; scientists can control for many resulting interfering factors. This is unlike results produced from human patients who may be influenced by smoking, antibiotics, diet and social environments.

1.4.1 Murine models of colitis

Murine models of experimentally induced IBD are useful tools to investigate the pathogenesis of the disease and to develop novel therapeutics and diagnostic methods to improve the quality of life for patients suffering from IBD. Mouse models of colitis either focus on the more general abnormalities and mechansims of gut inflammation, and those that have a more particular focus. There have been several mouse models of IBD developed, including chemically-induced (e.g. dextran sulphate sodium (DSS)-induced experimental colitis model [108]), bacterial-induced (e.g. *Salmonella* administration [109]), spontaneous (e.g. *SAMP1/4it* [110]), genetically-engineered (e.g. interleukin-10-/- knockout model (*IL-10*) [111]),

transgenic (e.g. $TNF^{\Delta ARE/WT}$ model [112]) and adoptive transfer (e.g. CD45RB high-transfer [109]) **Table 1.1**. Although these models do not represent the complexity of human disease, they are an indispensable tool to decipher the underlying mechanisms of IBD pathogenesis as well as to evaluate potential diagnostics and therapeutics.

Experimental genetically modified transgenic and spontaneous models of colitis are useful in determining disease causation and identifying potential therapeutic targets. The ITF-dnRII transgenic mouse was first described in 2001 [110, 113] to explore the effects of transforming growth factor (*TGFβ1*) on bowel immunity, extracellular matrix protein expression, and carcinogenesis finding that the loss of *TGFβ1* signalling in the intestine does contribute to tissue injury in IBD. The Muc2 colitis [114] and the *MDR1a* colitis [115] models are common examples of spontaneous colitis models with inflammation reportedly associated with increases in intestinal lymphocytes, *TNFα* and *IL-1β* for Muc2 colitis, and driven by Th1 cytokines for the MDR1a colitis. The $IL\text{-}10^{-/-}$ model is one of the earliest models of intestinal inflammation [116, 117] and continues to have great value given the important anti-inflammatory function of this cytokine. Genetic polymorphisms at the IL-10 locus have been reported to increase the risk of both UC [118] and CD [119], and perhaps a familial form of early onset CD [120].

Chemically-induced colitis models are the most commonly [121] used and include acetic acid-induced colitis [122], indomethacin-induced enterocolitis [123], 2,4,6-trinitrobenzene sulphonic acid (TNBS)-induced colitis [124], peptidoglycan-polysaccharide (PG-PS) model [125], lambda-carrageenan-induced rat model [126] and oxazolone-induced colitis [127]. Acetic acid-induced colitis causes epithelial damage accompanied by mucosal and submucosal inflammation in the colon. Indomethacin-induced enterocolitis can either be based on subcutaneous injection or the addition of dissolved indomethacin to the diet, resulting in inflammation in the small intestine and colon of rodents. TNBS- and oxazolone-induced colitis and DSS-induced colitis can either be administered once for acute colitis or by repeated administration for chronic colitis. Although similar to DSS-induced colitis with

clinical and histological features, these models do not show high reproducibility, unlike the DSS model which is used in this thesis, and is discussed in more detail below. It is important to note that no single model of colitis will capture the complexity of human IBD but each model has the potential to provide valuable insights into major aspects of colitis, and together they have led to a generally well-accepted hypothesis for human IBD pathogenesis.

Table 1.1 Animal models of IBD according to the two major human IBD phenotypes, UC or CD (Adapted from [109]).

Animal models of IBD	**Human IBD phenotype**	
	UC	**CD**
Chemically induced	DSS	TNBS/DNBS
	TNBS/DNBS	Indomethacin
	Oxazolone	PG-PS
	Acetic acid	
	Carregeenan	
	Iodoacetamide	
Immunologic	2,4-Dinitrochlorobenzene (DNCB)	
Bacterial induced	*Salmonella* administration	
	Adherent invasive *E.coli*	
	Helicobacter hepaticus [128]	
Spontaneous		C3H/HejBir mice
		SAMP1/4it mice
Genetically engineered	*TGFβ-/-*	*IL-10-/-*
	IL-2-/-	*NOD2-/-*
	MDR1A-/-	*A20-/-*
	GaI2-/-	*IL-23-/-*
	TCRα-/-	*NEMO-/-*
	XBP1-/-	
	NEMO-/-	
Transgenic	*IL-17 Tg*	*STAT4*
	HLA-B27	*HLA-B27*
		DNN Cadherin Tg
Mutation knock in		TNF^{DARE}
Adoptive transfer	CD45RB high-transfer	CD45RB high-transfer

1.4.1.1 Dextran sulphate sodium (DSS)-induced colitis

Oral administration of DSS has been used to induce colitis in experimental animals since 1990 [129] and to date there have been around 1000 papers published using this model [130]. DSS is a water-soluble, negatively charged, sulphated polysaccharide with a highly variable molecular weight, ranging from 5 to 1400 kDa [131]. DSS is administered orally in sterile drinking water at a dose between 1-5% for 5 days, followed by 7 days normal drinking water to induce colitis. This experimental model shares clinical (diarrhoea, bloody stools and weight loss) and histological (crypt erosion, goblet cell depletion, ulceration) features with human UC [108]. It is one of the most commonly used methods to investigate the pathogenesis of IBD; producing a high degree of uniformity and reproducibility of most lesions in the distal colon [132]. The typical features appear by day 5, are maximally expressed by day 8, and show signs of recovery by day 11. Depending on the concentration, the duration and the frequency of DSS administration, the animals may develop acute or chronic colitis. The exact mechanism by which DSS induces intestinal inflammation is unknown, but it likely to be the result of the large DSS molecules interfering with the intestinal barrier function by causing erosion of the epithelial monolayer and stimulation of local inflammation leading to immune cell infiltration, an increase in pro-inflammatory cytokines, such as IL-6 and TNF-α, and consequently, a dysbiosis of the microbiota **(Figure 1.7).**

1.4.1.1.1 Important factors that influence DSS-induced colitis

The reproducible induction of DSS-colitis depends on a number of key factors, such as molecular weight (MW), concentration, duration of exposure, mouse strain, age, gender, body weight and all environmental factors [133]. These factors can be split in to three different groups, those related to:

1. The nature of DSS itself and its mode of administration e.g. MW, concentration, duration, manufacturer and batch of administered DSS.
2. The animal species, animal strain, and gender.
3. Environmental factors such as housing conditions and the intestinal microbiota.

The MW of DSS is highly variable; ranging from 5 kDa to 1400 kDa and depending on the administration of DSS at different MWs, the severity and location of colitis differs. Evidence for this is provided by Kitajima *et al.* who observed the most severe colitis in the middle and distal third of the colon in BALB/c mice treated with DSS of 40 kDa while mice treated with DSS of 5 kDa developed a milder form of colitis mainly in the caecum and upper colon. There were no lesions identified in the colons of mice treated with 500 kDa, which may be due to its high MW preventing the passage of the DSS molecules through the mucosal membrane [134]. Acute (early) colitis is usually induced by continuous administration of 2-5% DSS for short periods whereas chronic (advanced) colitis may be induced by continuous treatment of a lower concentration, or by cyclic administration, of DSS.

The responsiveness of DSS differs among strains shown by a quantitative histological analysis in nine mouse strains, which demonstrated major differences in the severity of DSS-induced colitis with C3H/HeJ being very susceptible and DBA/2J mice being less susceptible [135]. These differences were either attributable to genetic differences in the ability of the mucosa to withstand inflammatory damage, differences in the ability to limit the inflammatory response, or both [108]. This is also demonstrated in BALB/c and C57BL/6 mice, after the withdrawal of DSS, C57BL/6 mice progressed to chronic colitis whereas BALB/c recovered [136]. Differences related to gender have also been investigated with a greater male susceptibility to DSS-induced colonic colitis, not caecal lesions, being reported [135]. DSS-induced breakdown of epithelial barrier function allows the entry of luminal microorganisms into the mucosa causing an inflammatory response, as shown by the reduced susceptibility of germ-free (GF) animals [137] and the improvement in histological parameters in mice treated with antibiotics [138]. Furthermore, DSS is resistant to degradation by intestinal microflora or the effects of different pH conditions and anaerobic incubation [108, 139].

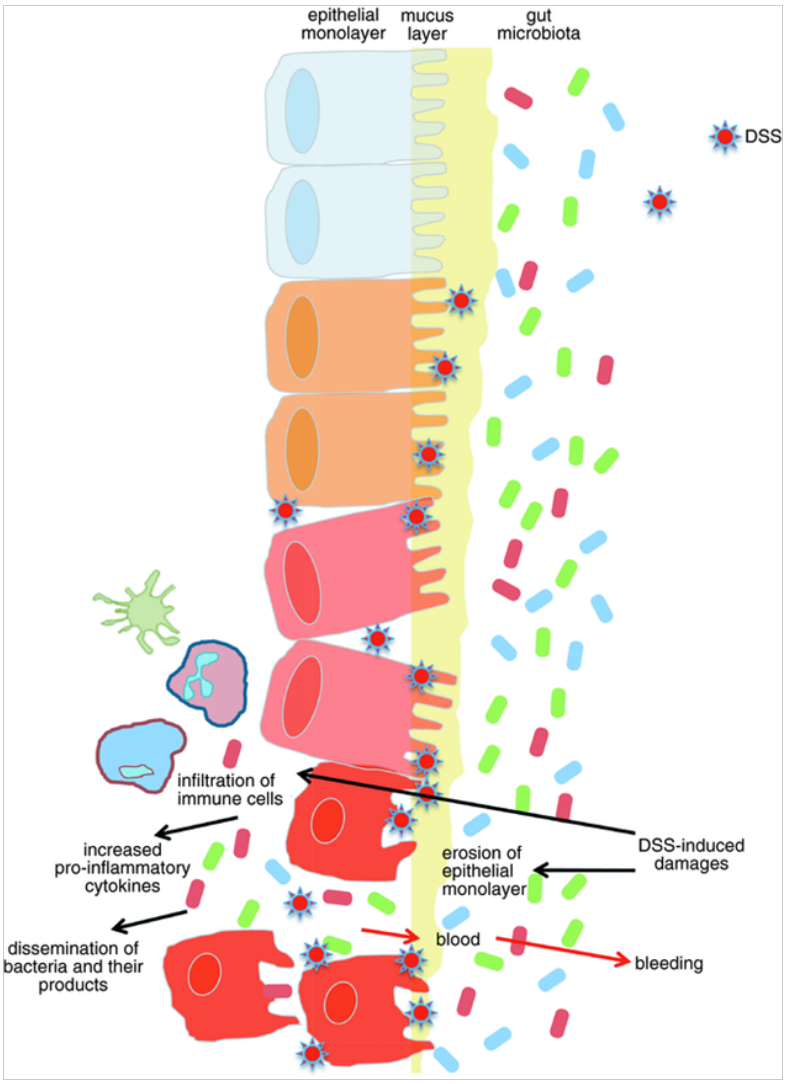

Figure 1.7 Schematic representation of DSS-induced colitis. The mechanism by which DSS is thought to induce colitis in mice is unclear, however is thought to result from a breakdown in barrier function, stimulation of inflammation and dysbiosis. Modified from [133].

1.4.2 Animal models of CRC

Existing data from current animal models of IBD and CRC indicate that inflammation predisposes to CRC [140, 141]. These include genetic, chemical and bacterial CRC studies employing animal models and are discussed in detail in an excellent review [142]. The sporadic and IBD-associated CRC murine models used in this thesis are discussed below; refer to methods chapter **sections 2.2.4** and **2.2.5** for specific protocols used.

1.4.2.1 Sporadic CRC

The carcinogens 1,2-dimethylhydrazine (DMH) and its metabolite, azoxymethane (AOM), are the two most commonly used chemicals to controllably induce and promote CRC in rodents. Both DMH and AOM are DNA alkylating compounds that induce CRC by intraperitoneal (I.P.) injections over several weeks to induce tumours in the distal colon [142]. This model of CRC is similar to HNPCC as the majority of the tumours either display aberrant protein expression for *APC* or involve mutations in the β-catenin gene which both cause an increase in WNT signaling independently, driving tumourigenesis [143], therefore resembling human CRC. AOM has some advantages over DMH including higher potency, reproducibility and greater stability in the dosing solution [144]. It involves a stepwise activation post injection, including a hydroxylation step mediated by cytochrome P450 in the liver, excretion and further metabolism by the microbiota [144] **(Figure 1.8).**

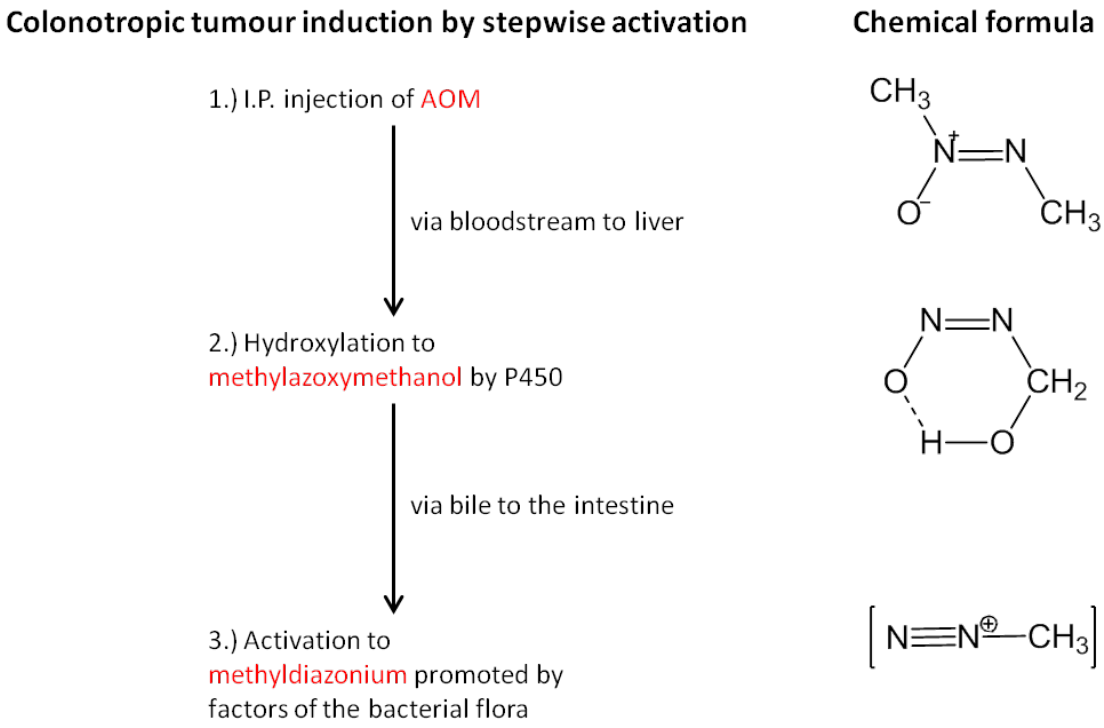

Figure 1.8 Activation of AOM. The AOM murine model of CRC is successful in investigating numerous factors involved in the role of tumour initiation and progression. Adapted from [144].

1.4.2.2 IBD-associated CRC

An alternative option using AOM includes the pro-inflammatory reagent DSS and induces a colitis-associated tumour development. This combination also dramatically shortens the latency time for the development of CRC compared to AOM alone [95] (10 weeks vs 30 weeks, respectively). This model is useful when studying the tumour progression driven by chronic inflammation, as seen in UC or CD patients [144]. The induction of colitis by oral administration of DSS is described in section 2.2.1; a two-stage CRC model combines AOM and DSS and is based on a single injection of AOM and three cycles of DSS [144]. AOM/DSS treatment in mice is a powerful model for the initiation of ACF (early precursor lesions) [145].

1.5 BACTERIAL COMMUNITY OF THE MURINE GI TRACT

In gut microbiota research, mouse models are being increasingly used. Therefore, the comprehensive characterisation of the normal murine GI microbiota is critical to understand and predict alterations in bacterial communities in relation to disease. Gu *et al.* used *16S* rRNA gene sequence based analysis to examine the microbiota along the entire GI tract of healthy C57BL/6 specific pathogen free (SPF) mice [146]. They found that jejunal and ileal samples had the lowest diversity whilst samples from the caecum, colon, and faeces had the highest diversity of bacterial communities. Twenty one different bacterial phyla were identified with the majority of sequences obtained belonging to Bacteroidetes (61.94%) and Firmicutes (30.55%) with the rest distributed among Proteobacteria (5.39%), *Cyanobacteria* (0.63%), Tenericutes (0.165%), Actinobacteria (0.13%), Deferribacteres (0.10%) and unclassified bacteria (0.95%). Higher inter-mouse variations were detected among the gastric and small intestinal samples than among the large intestinal and faecal samples. In addition, clustering of bacterial communities suggested that the large intestine and faeces were distinct from those in the stomach and small intestine.

1.5.1 Gut microbiota in murine models of IBD

One of the earliest studies reporting the induction of colitis by administration of DSS in 1990 also provided evidence for the role of microbiota in experimental colitis. Okayasu *et al.* found a significant increase in members of *Bacteroidaceae* and *Clostridiaceae* spp. Families, in particular species such as *Bacteroides distasonis* and *Clostridium ramonsum,* in the intestines of mice exposed to DSS [129]. More recently, C57BL/6 female mice were administered 4% DSS and resulted in elevated *16S* rRNA gene copy numbers of the mucin-degrading Gram-negative bacterium *Akkermansia muciniphila* and of *Enterobacteriaceae* [147, 148]. The gut microbiota is enriched in colonic polyps in $Apc\Delta^{468}/Il\text{-}10^{-/-}$ mice compared to healthy tissues, in particular, two genera, *Bacteroides* and *Porphyromonas* [149]. The microorganisms reported to be associated with murine models of IBD have been summarized in **Table 1.2.**

A breakthrough in the understanding of the role of microbiota in mouse models of IBD came with observations that treatment with antibiotics or GF breeding is associated with significantly less severe bowel inflammation and cancer [148]. For instance, Dove *et al.* showed that $Apc^{Min/+}$ housed in a GF environment displayed more than a 50% reduction in tumour growth, compared to the same animals housed in SPF [150]. Also, IL-10 deficient mice were resistant to spontaneous colitis when kept in GF environment [151].

Different bacterial species may coordinate the initiation of inflammation, whereas others may have a role in its continual progression [152]. The administration of probiotics, including *Lactobacillus, Bifidobacterium* and *Streptococcus salivarious,* has beneficial effects on both humans, and murine models of IBD [153], but not with colitis-associated CRC mouse models [154].

Table 1.2 Bacterial species reported to be altered in IBD murine models. Modified from [148].

Type of model	Microorganisms	Final effect
DSS-induced colitis	*Bacteroides distasonis, Clostridium ramonsum, Akkermansia muciniphila, Enterobacteriaceae*	Increased numbers correlate with acute and chronic UC [129, 147]
IL-10 deficient spontaneous colitis	*Enterobacteriaceae,* adherent-invasive *E. coli*	Increased numbers correlate with inflammation (*Enterobacteriaceae*) and cancer (*E. coli)* [155, 156]
Colitis in *pcC*Δ^{468}/Il-10$^{-/-}$ hereditary CRC model	*Bacteroides, Porphyromonas* genera	Increased numbers correlate with inflammation and colon polyposis [149]
TNBS-induced colitis	*Enterobacteriaceae, Bacteroides*	Increased numbers correlate with inflammation [157]

1.6 THE SCENT OF DISEASE

Although the analysis of disease-specific odours is a relatively young field of research, the detection of abnormal human smells as an indicator of certain diseases dates back to around 400 BC. The Ancient Greek physician and the father of medicine, Hippocrates, instructed his students to smell the breath of their patients and pour human saliva on hot coals as an effective means of identifying their ailments [158, 159]**.** Later during the 11th century, the Arab physician and philosopher, Avicenna, noted differences in the smell of urine from patients with an illness, compared to those without [160]. Traditional Chinese medicines were able to diagnose diabetes in patients whose urine emitted a smell of a rotten apple [161, 162]. In 1857, Wilhelm Petters discovered acetone in the urine of diabetic patients [163] and Johannes Muller made the first quantitative measurements of acetone in the breath of diabetic patients in 1898 [164]. Robert Koch investigated the presence of foul odours from infected wounds and odours produced from pathogenic bacteria grown in culture for proof of his germ theory, based on experiments with anthrax in the 19th century [165]. In 1923, Omelianski *et al.* supported these findings by reporting on odours from naturally-liberated microbes associated with the accumulation of staling metabolic products such as organic acids and alcohols in cultures of *Mycobacterium tuberculosis* and *Pseudomonas aeruginosa* [166].

The characterisation of abnormal odours associated with diseases has been investigated further since the development of gas chromatography (GC) and mass spectrometry (MS) instruments. Davies and Hayward identified acetylcholine emitted from patients' urine and proposed that it may be a precursor of trimethylamine, a possible early microbial chemical marker of urinary tract infections caused by *Proteus* and *Klebsiella* species [167]. The first half of the 1980s saw the clinical application of the urea breath test applied in gastroenterology for the diagnosis of gastritis associated with *Helicobacter pylori* [168]. Even though many of these practices are centuries old, they provide evidence that early medical practitioners were clearly able to recognise that the presence of human diseases could change the odour of bodily excretions, including breath, blood, urine and faeces.

1.7 METABOLOMICS

Systems biology studies the complex interactions and behaviours of a cell or organism. It has developed into an inter-disciplinary science, combining genomics, transcriptomics, proteomics and metabolomics [169]. The latter represents the outcome of systems biology, such that the varying concentrations of metabolites in a cell are relative to the changes occurring in the genome, transcriptome and proteome. Metabolomics can be defined as the investigation of a group of endpoint metabolites of a physiological or pathophysiological process, aiming to define the chemical fingerprint unique to a specific organism [170]. Therefore, it has the potential to provide answers to some unanswered questions in order to improve the diagnosis, treatment and prevention of diseases. More recently, the detection of abnormal smells as indicators of specific diseases from bodily fluids such as faeces or breath has been termed the Faecal, or Breath, Metabolome. A number of studies have emphasized the role of VOCs in identifying disease-specific metabolome patterns.

1.8 VOLATILE ORGANIC COMPOUNDS (VOCS)

VOCs are, by definition, a large and diverse group of carbon-based chemicals, related by their volatility at room temperature and which include hydrocarbons, alcohols, aldehydes, ketones, esters and organic acids. Most vapours emitted from biological samples (e.g. breath, sweat, blood, urine and faeces) contain odorous VOCs and those that vary between conditions may be used as an indication of cellular metabolism leading to, or indicative, of a diseased state. VOCs can be thought of as intermediates of metabolic pathways such that observed changes in the presence or levels of certain VOCs will indicate the change in a person's phenotype. The method of detection of VOCs is a key step and of paramount importance, therefore considerable effort has been invested in developing and improving the sampling and pre-concentration techniques.

1.8.1 The origin of VOCs

The current understanding of the human VOC spectrum is at an early stage [171]. However, a recent review reported 1,840 VOCs appearing in exhaled breath (872), skin emanations (532), urine (279), saliva (359), human breast milk (256), blood (154) and faeces (381) [172]. Interestingly, only 0.7% were ubiquitous to all the bodily fluids and breath examined: acetylaldehyde, 2-propanone, benzaldehyde, 1-butanol, 2-butanone, hexanal, heptanal, octanal, pentanol, benzene, styrene and toluene. The major sources of VOCs include breath, blood, urine and faeces and can vary with age, diet, sex, disease and physiological status and possible genetic background.

1.8.1.1 Breath

Of the 1,840 compounds identified emitted from bodily fluids of healthy humans, the majority were identified in breath (872) [172]. Of these exhaled breath VOCs, isoprene and acetone were the most prominent [172] and 29 dienes, 27 alkenes and 3 alkynes are related, but not specific, to smoking [173]. Isoprene is formed

along the mevalonic pathway of cholesterol synthesis and it is thought to relate to oxidative damage within the fluid lining of the lung [174, 175]. Acetone is one of the most abundant VOCs in breath and its concentration increases in patients with diabetes mellitus [176]. Other VOCs may be related to food consumption or medication, and their interactions or degradation with the gut microbiota, such as hydrogen or methane [172]. Exhaled breath aliphatic hydrocarbons have been regarded as stable markers of lipid peroxidation and, therefore, may be used to monitor levels of oxidative damage in the body [174].

To name a few examples, breath markers have been found in patients with lung cancer [177], cystic fibrosis [178], lung transplantation [179], and kidney failure [180]. Despite the number of promising results showing diagnostic potential of detection of VOCs from breath, it has not yet been introduced into clinical practice. This is because of the limitations with sampling, pre-concentration and analysis.

1.8.1.2 Urine

A recent review of VOCs from urine from apparently healthy volunteers found nine to be ubiquitous to all samples tested: propanone, 2-butanone, 2-pentanone, 2-heptanone, 3-hexanone, 4-heptanone, 2,5-dimethylfuran, 2-ethyl-5-methylfuran, and toluene [181]. Authors suggested that the source of some or all of these VOCs is likely to be the gut, as some are also found in faeces. In addition, the large number of ketones identified in urine probably arise as products of metabolism by the gut microbiota as ketones were decreased significantly in the urine of GF rats [182]. Alterations in the urine VOC metabolome have been used to detect diseases including urinary tract infections [183], liver disease [184] and bladder, prostate and other cancers [171].

1.8.1.3 Faeces

Patients often report an abnormal odour emitted from their faeces during disease relapse, yet there has been little research performed to investigate the composition

of faecal gases. The human gut microbiota is comprised of numerous species of bacteria, which during health, are thought to contribute to the mucosal integrity, the maintenance of host health and, thus, the protection against invading organisms [185]. This resident microbiota is responsible for the fermentation of undigested foods in the colon, producing putrefactive compounds such as ammonia, aliphatic amines, branched chain fatty acids, indole, phenol and volatile sulphur containing compounds, hence, affecting both the colonic and metabolic health [185, 186]. Faecal VOCs have been implicated in differentiating between certain infectious and non-infectious bowel conditions such as *Clostridium difficile* [187], *Salmonella* [171], *Cholera* [64], *Campylobacter* [188] and irritable bowel syndrome (IBS) [189] and IBD [190].

1.8.1.4 Other

Blood, skin secretions, saliva and milk are examples of other biological sources of VOCs. Although the analysis of blood-derived VOCs is an active area of research and can directly reflect the internal environment of the body, obtaining samples requires trained phlebotomists and may be less tolerated by patients compared to urine or breath. Skin secretions produced a large number of VOCs; however, an individual's odour is very particular and can vary significantly depending on which part of the skin is tested. Currently, there are limited number of studies on the analysis of VOCs in saliva and milk [172].

1.8.2 Chemical composition of VOCs

The chemical analysis of VOCs for the biological sources described above results in a list of compound classes as follows: hydrocarbons, acids, esters, alcohols, aldehydes, ketones, furans and ethers, sulphur containing, nitrogen containing, halogen containing, chloro biphenyls and others [172]. **Figure 1.9** presents the total classes of compounds based on the number of different VOCs identified, not upon their relative concentration, found in each bodily fluid.

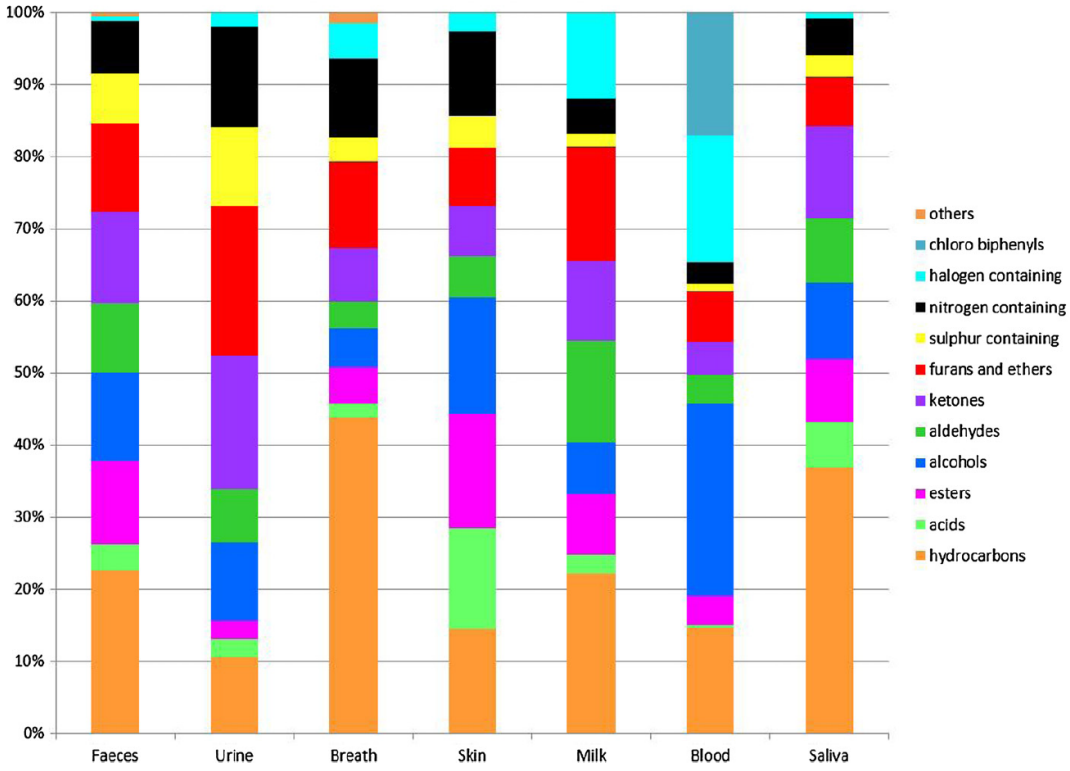

Figure 1.9 Classes of VOCs in human biological material. The relative number of different compound classes that have been detected in faeces, urine, breath, skin, milk, blood and saliva, as reported by Costello *et al.* The total number of VOCs identified in each compound class represented as a percentage of the total VOC profile for each biological matrix. Copyright has been granted from publisher and authors and figure is used with permission [172].

1.8.3 Oxidative stress and VOCs

All organisms need oxygen to live, but high concentrations can be toxic, therefore, organisms have developed protective mechanisms in order to maintain oxygen homeostasis. Energy is obtained via processes involving the four-electron reduction of oxygen to water; also generating dangerous by-products (i.e. free radicals, ROS). The implication of ROS in the pathogenesis of diseases involves the reaction of ROS with cellular components such as lipids, proteins and nucleic acids causing tissue damage [171]. Lipid peroxidation is a chain reaction with initiation, propagation and termination steps. Peroxidation of lipids and other biomolecules by ROS produce measurable VOCs (e.g. ethane, 1-pentane) **(Figure 1.10)**. The non-invasive detection and monitoring of oxidative stress is not only desirable in autoimmune, neurological, inflammatory diseases and cancer, but also during surgery and in

intensive care units. Oxidative stress due to smoking could cause increased lipid peroxidation resulting in diene formation, therefore offering an explanation for the presence of butadiene, a notable carcinogenic compound related to tobacco smoking [191].

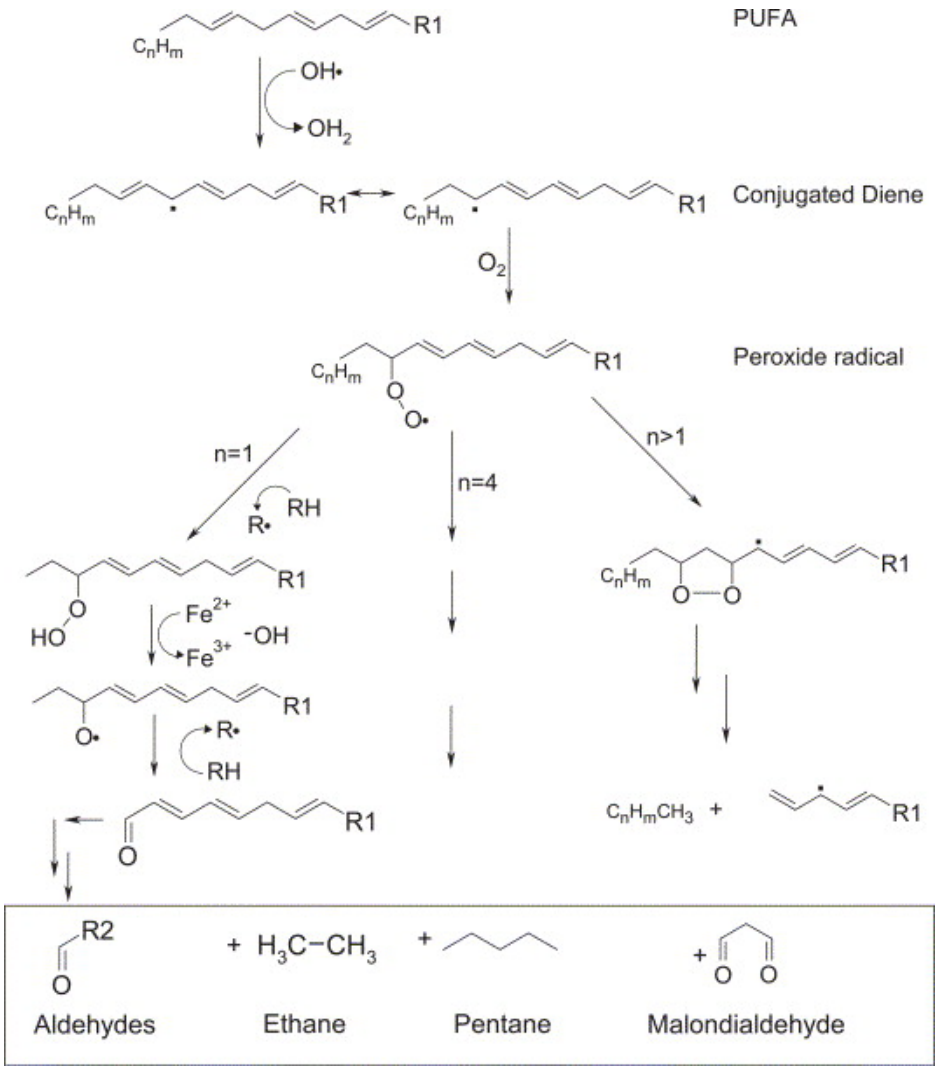

Figure 1.10 Lipid peroxidation. Possible reactions and products of free radical-mediated lipid peroxidation [174]. Copyright has been granted and figure is used with permission.

1.8.4 Microbial VOCs

Microbial VOCs are a group of compounds produced from the metabolism of bacteria and fungi, formed during either primary (e.g. DNA synthesis) or secondary metabolism (e.g. intermediates of primary metabolism). They often have strong

odours and are responsible for the smells including “old cheese”, “dirty socks” or “locker room” [192]; all smells associated with mould and bacterial growth. The investigation of bacterial and cell cultures *in vitro* may open up new possibilities for the clarification of the biochemical background of such VOCs. The resultant VOC profile of biological samples is said to reflect the microbial metabolic activity and may potentially be a specific biomarker of colonic disease [193].

1.8.5 Diet and VOCs

Interactions between the gut microbiota and their host include the microbial breakdown of nutrients, in particular carbohydrates, in order to salvage energy. Short-chain fatty acids (SCFAs) (e.g. acetate, propionate, butyrate) are commonly detected in the faeces of humans and are most likely to arise from the metabolism of undigested carbohydrate by colonic bacteria [188] **(Figure 1.11).** Hydrogen sulphide and methanethiol are generated from sulphur-containing substances in the diet and can be very damaging to the colonic epithelium [194]. Garner *et al.* also reported that the commonly detected VOCs, toluene and xylene, might also have dietary origin; possibly from potatoes [188]. Pro-inflammatory molecules including lipopolysaccharide and peptidoglycan are produced by the gut microbiota and may influence host metabolism. For example, choline obtained from the diet is metabolised to generate bioactive VOCs, which can eventually lead to cardiovascular disease [195]. Detection of the compounds may be indicative of the disease state of an individual.

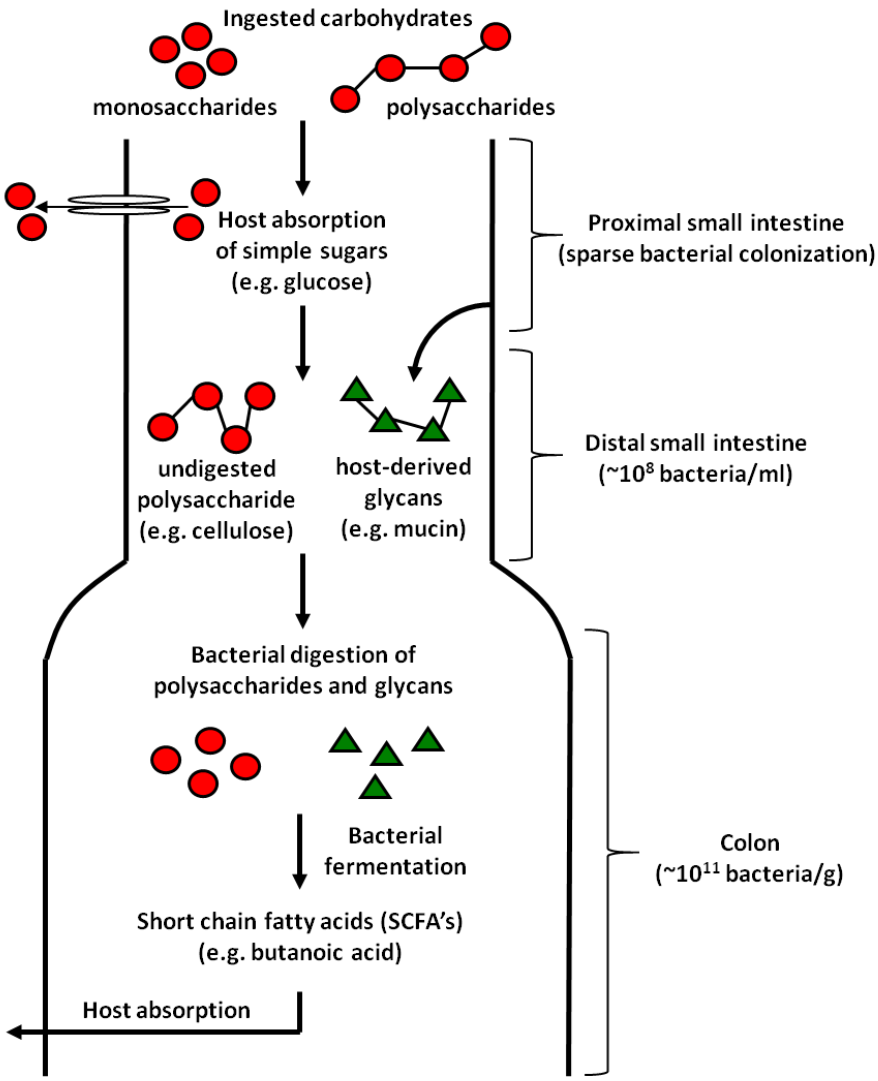

Figure 1.11 Host and microbial contributions to carbohydrate degradation in the intestine. Absorption of simple sugars from the breakdown of ingested carbohydrates via active transport occurs in the small intestine. Undigested matter passes through to the colon where they undergo degradation by resident bacterial communities. By-products of the gut fermentation, including SCFAs are absorbed and utilised by the host. Adapted from [196].

1.8.6 VOCs in human GI disease

Pathological processes, including different bacterial infections, inherited disorders of metabolism and various cancers, can influence odour fingerprints by producing new VOCs or by changing the ratio of VOCs that are produced normally. The human GI tract harbours over 100 trillion bacteria, causing the gut microbiome to be 100 times more abundant than the host genome [197]. Identification of the metabolic

profiles associated with IBD and CRC onset and progression will improve the diagnosis and treatment of these diseases. This may also enable the dissection of the metabolic profiles involved with the metabolism of such bacteria, fungi, genes and proteins within the gut, during health and in the presence of disease. An advantage of acquiring a better understanding of the unique metabolic profile of CRC would be to improve the possibility of a clear distinction between cancer cells and normal cells.

Progress in analytical methods such as gas chromatography-mass spectrometry (GC-MS), or devices that electronically mimic the human olfactory system, termed the 'electronic nose'; have been developed to provide an opportunity to identify VOCs related to diseases in research laboratories [198]. Dogs can also be used as detectors of certain cancers as they have an extraordinary sense of smell with odour detection thresholds as low as parts per trillion. In cases of melanoma, bladder, ovarian and colorectal cancer, dogs can be trained to distinguish patients based on VOCs from patients' urine, tumours or breath samples, more successfully than would be expected by chance alone [199, 200]. The development of the electronic sensors and analytical methods will continue to improve the accuracy and sensitivity of marker VOCs from complex biological samples, allowing disease-specific 'volatile biomarkers' to be used more regularly in clinical practice. There are currently a limited number of studies investigating the murine metabolome of IBD-induced models [112, 125, 201, 202].

1.9 GAS CHROMATOGRAPHY-MASS SPECTROMETRY

Numerous volatile and non-volatile, polar and non-polar metabolites can be measured with GC-MS systems [203]. GC-MS is used in this work for the separation and identification of thermally stable and volatile compounds emitted from samples into the headspace (HS) of sample glass vials. This platform is a combination of two different analytical techniques comprising a gas chromatograph coupled to a mass spectrometer.

Metabolites are introduced into the instrument via injection through a septum into the GC injection port where they travel in a flowing carrier gas (helium) to the GC column. The GC column determines when the compound is eluted, its retention time (RT), depending on the columns length, diameter and phase thickness. The VOCs continue to travel along the column and undergo separation by their relative affinity for the stationary phase of the column based of their chemical properties. The MS is then able to capture, ionize, accelerate, deflect and detect the ionized molecule separately. Each molecule is broken into fragments, which are then detected using their mass-to-charge ratio. GC-MS has been described as a "gold standard" for forensic science due to its high degree of specificity and sensitivity.

1.10 SOLID PHASE MICROEXTRACTION

Solid phase microextraction (SPME) was developed in the 1990s by Professor J Pawliszyn to provide a quick and solvent-less technique for the isolation of analytes in a sample matrix [204]. SPME operates with a stationary-phase-coated fused-silica fibre, contained within a syringe device that provides both protection and easy transport of the fibre phase [205]. For analysis, the syringe is placed into the analyte solution or into the headspace above the sample and the coated fibre is exposed for a fixed amount of time to allow for absorption of compounds. Once the equilibrium is reached, the fibre is retracted into the needle and removed from the sample vial and inserted in the GC injector for desorption of VOCs into the column **(Figure 1.13)**.

1.10.1 Principles of SPME

As previously mentioned, the extraction of VOCs by SPME is based on an equilibrium forming between the fibre and the sample. Extraction of VOCs from the sample headspace onto the fibre coating begins as soon as the fibre is inserted into the sampling vial. This process is completed when the VOC concentration adsorbed has reached its distribution equilibrium between the fibre coating and sample headspace **(Figure 1.12)**. This equilibrium forms between three phases:

1. Fibre coating to sample phase
2. Headspace to sample phase
3. Fibre coating to headspace

The distribution about the three phases after equilibrium can be represented by:

$C_o V_o = C_{h^\infty} V_h + C_{s^\infty} V_s + C_{f^\infty} V_f$

Where:

C_o = initial concentration of the compound in the sample

C_{h^∞}, C_{s^∞} and C_{f^∞} = equilibrium concentrations of the compound in the headspace (*h*), sample (*s*) and fibre coating (*f*), respectively.

V_h, V_s and V_f = volumes of headspace (*h*), sample (*s*) and fibre coating (*f*), respectively.

The time required to reach equilibrium in SPME is driven by diffusion kinetics of the analytes in the phases that are present in the sample vial. An extraction is considered complete when the analyte concentration has reached its distribution equilibrium between the SPME coating and the sample biological matrix.

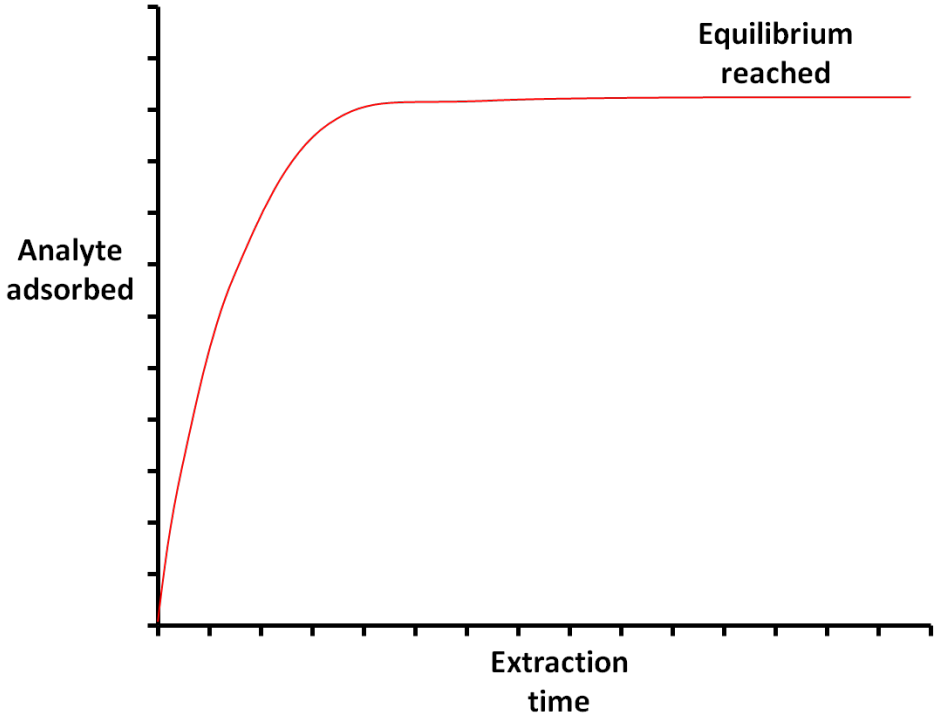

Figure 1.12 Adsorption mechanism for SPME. Distribution equilibrium between the fibre coating and the sample matrix.

1.10.2 HS-SPME-GC-MS platform

The platform used for the extraction and detection of VOCs is accurate and reliable. There are three types of VOC extraction methods that can be utilised with a SPME fibre: direct extraction, HS and membrane-protected SPME. Direct extraction involves the SPME fibre being directly immersed into the sample matrix. Membrane-protected SPME extraction is similar to direct extraction but is protected by a selective membrane (e.g. porous polypropylene). HS sampling with SPME is the preferred method to extract VOCs and was developed in 1993 [206]. This is the method used throughout this work and involves a SPME fibre being exposed to the HS above the sample matrix **(Figure 1.13).** It is reliant on kinetics of mass transport, such that the analytes in the sample matrix undergo a series a transport processes into the gas phase, and then to the fibre coating. Advantages of HS sampling include protection of the fibre from damage by high molecular weight and non-volatile metabolites in the matrix.

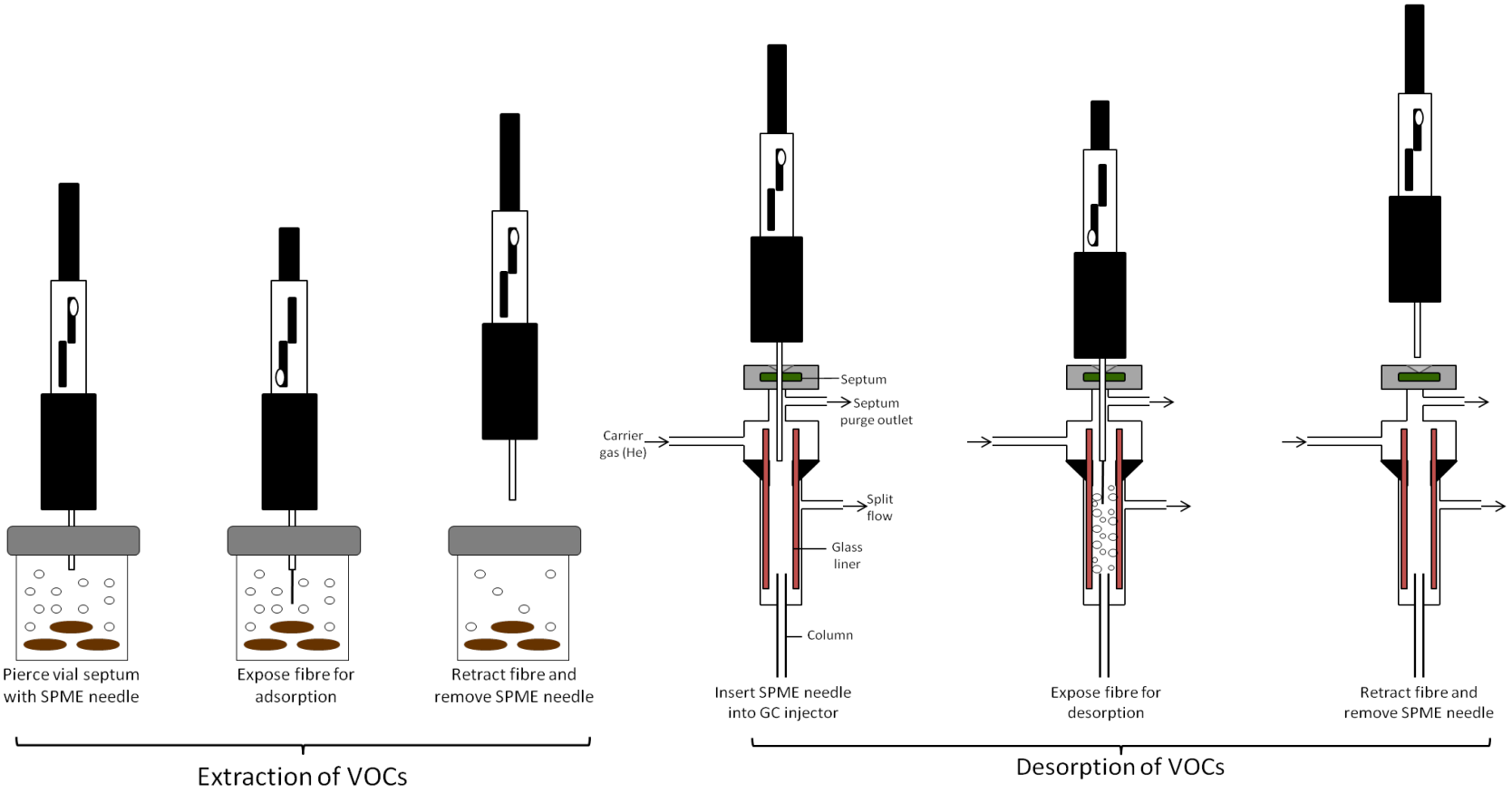

Figure 1.13 Schematic diagram of the headspace SPME apparatus. A SPME needle is inserted into a glass vial via piercing the septum and the SPME fibre is exposed to the headspace of the sample for a fixed amount of time then retracted and device is removed. Desorption of VOCs involves injection of SPME needle into GC injector, exposure of fibre, retraction and removal. Adapted from Steven Smith's thesis, University of the West of England [207].

1.11 SYNOPSIS

The burden of GI disease has dramatically increased during the 20th century, significantly affecting millions of persons worldwide, inducing a considerable economical impact compromising healthcare and an individual's quality of life. This thesis will focus on IBD and IBD-related CRC. The pathogenesis of IBD is poorly understood, but is believed to be a combination of genetics, a disruption to the immune system and an imbalance of the gut microbiota. The duration and anatomic extent of IBD increases the risk for CRC; the mortality is higher in CRC patients in the setting of IBD, compared to those with sporadic CRC. Currently, the diagnosis of IBD is difficult, invasive and not always accurate which may have a profound effect on patient care. Therefore, a non-invasive, IBD-specific biomarker would be clinically useful. The early detection of CRC significantly improves the prognosis and increases the chances of survival beyond five years from diagnosis. Recently, the investigation of the metabolome in IBD patients compared to healthy controls has begun to receive considerable attention and correlations between the faecal VOC metabolome and IBD are emerging. However, human studies are limited by the variation in diet and the unpredictability of the disease. As a result, animal models have been widely used as model organisms in biomedical research to gain insight into the workings of human disease. Here, we report the first study using HS-SPME-GC-MS to detect the VOC faecal metabolome in the commonly used mouse models of IBD and CRC, DSS-induced colitis and AOM-induced CRC.

1.12 HYPOTHESIS

The murine faecal VOC metabolome will significantly differ according to the alteration of gut metabolism by the induction of GI diseases. The identification of these changes by the detection of the faecal VOC profile will enable the investigation into the pathogenesis of such diseases and provide evidence for further investigation of human GI disease.

1.13 AIMS

The aims are to:

1) develop standard operating procedure (SOP) for the detection of VOCs in the HS of faeces from healthy WT C57BL/6 mice using a SPME-GC-MS platform;
2) characterise the normal murine faecal metabolome, considering the effect of gender, age, presence of microbiota, diet and housing conditions;
3) investigate the metabolic differences in the development of:-
    i) Acute colitis
    ii) Chronic colitis
    iii) Inflammation-associated CRC
    iv) Sporadic CRC

Chapter 2

Materials and Methods

2.1 ANIMALS

2.1.1 Wild-type C57BL/6 mice

Inbred, wild-type (WT) C57BL/6 mice were purchased from Charles River Laboratories (Margate, UK), and were acclimatised under standard animal unit conditions specific pathogen free (SPF) for a minimum of 1 week prior to being used in experimental procedures. For the optimisation of sample volume, a cage of four 9-week old males were used, and for SPME method development, four 5-week old male mice, housed individually, were used. For the establishment of the healthy murine metabolome, both male and female mice aged 5 weeks old were used and for all disease induction experiments, adult 9 or 10 week old female mice were used. For all experiments used in chapters 3-8 all animals were housed individually under conventional conditions with food and water *ad libtum* throughout. Animals were kept on a 12:12 hour light-dark cycle. Mice were fed a standard pelleted diet suitable for short term maintenance supplied by Special Diets Services (SDS), Essex, UK.

2.1.2 *NFκB2*-null mice

An *NFκB2*-null strain of mice was generated on the C57BL/6 genetic background and kindly donated to our laboratory by Dr Jorge Caamano of the University of Birmingham. The homozygote *NFκB2*$^{-/-}$ colony was maintained under conventional conditions. Confirmation of this genotype was previously performed by Dr Mike Burkitt of the Department of Gastroenterology, Univeristy of Liverpool by PCR. Dr Jonathan Williams of the Department of Gastroenterology, University of Liverpool conducted all experiments involving *NFκB2*-null mice used in this thesis, with the assistance of the author, and faecal samples were donated for analysis by GC-MS.

2.1.3 Germ-free mice

The GF colonies, C3H/HeN and *Junbo* mice and their non-GF SPF strain equivalent were bred MRC Harwell, Oxford. The *Junbo* colony is maintained on a C3H/HeN

background and are otherwise healthy animals, but with a hearing defect [208]. Faecal samples were kindly provided by Ms Julie Roberts of MRC Harwell, Oxford from healthy GF and non-GF mice from a mixture of male and female mice of 6-7 weeks old and were fed a standard diet of chow.

2.2 ANIMAL PROCEDURES

Experiments were conducted with UK Home Office approval under a project licence as specified by the Animals (Scientific Procedures) Act 1986. All experiments were performed by the author, as a UK Home Office personal licensee, and conducted within an SPF animal unit with barrier precautions in place to maintain the microbiological status of the animals housed within it, at the University of Liverpool. All experiments were conducted during the daytime starting between 9-11am.

2.2.1 Induction of colitis using dextran sulphate sodium (DSS)

2.2.1.1 Optimal dosing of DSS

The optimal dose of DSS to induce colitis in the C57BL/6 strain was investigated using doses between 2 and 5% (M.W = 36,000-50,000; Catalogue number: 160110; Lot number: 5237K; MP Biomedicals, LLC, UK). These pilot studies were designed to determine the DSS dosing regimen to induce an acute colitis with a maximum weight loss of 20-25% before euthanasia administration, in accordance with the project license and Institutional Animal Care and Use Committee (IACUC) recommendations. In order to determine the optimal dose of DSS concentrations of 2, 3, 4, 4.5 and 5% DSS were used. Ideally, a maximum weight loss of 20-25% would signify an acute form of intestinal damage.

C57BL/6 female mice were given DSS in their drinking water at concentrations of 2, 3, 4 and 5% for 5 days, followed by 4 days of normal water to induce acute colitis. Concentrations of 2 and 3% DSS did not cause weight loss or show any clinical signs

of colitis (*n*=2 per dose). The concentration of DSS was consequently increased to 4%, resulting in a very mild colitis with an average weight loss of 9.5 ± 1.3% at day 6 with slightly loose stools and no visible signs of rectal bleeding (mean ± SD, *n*=2). Subsequently, 4.5 and 5% DSS were too severe with a significant weight loss and mice were unable to recover. Therefore, the experiment was terminated early, at day 7 **(Figure 2.1A).** Histological analysis of H&E-stained distal colonic sections confirmed these clinical findings **(Figure 2.1B).**

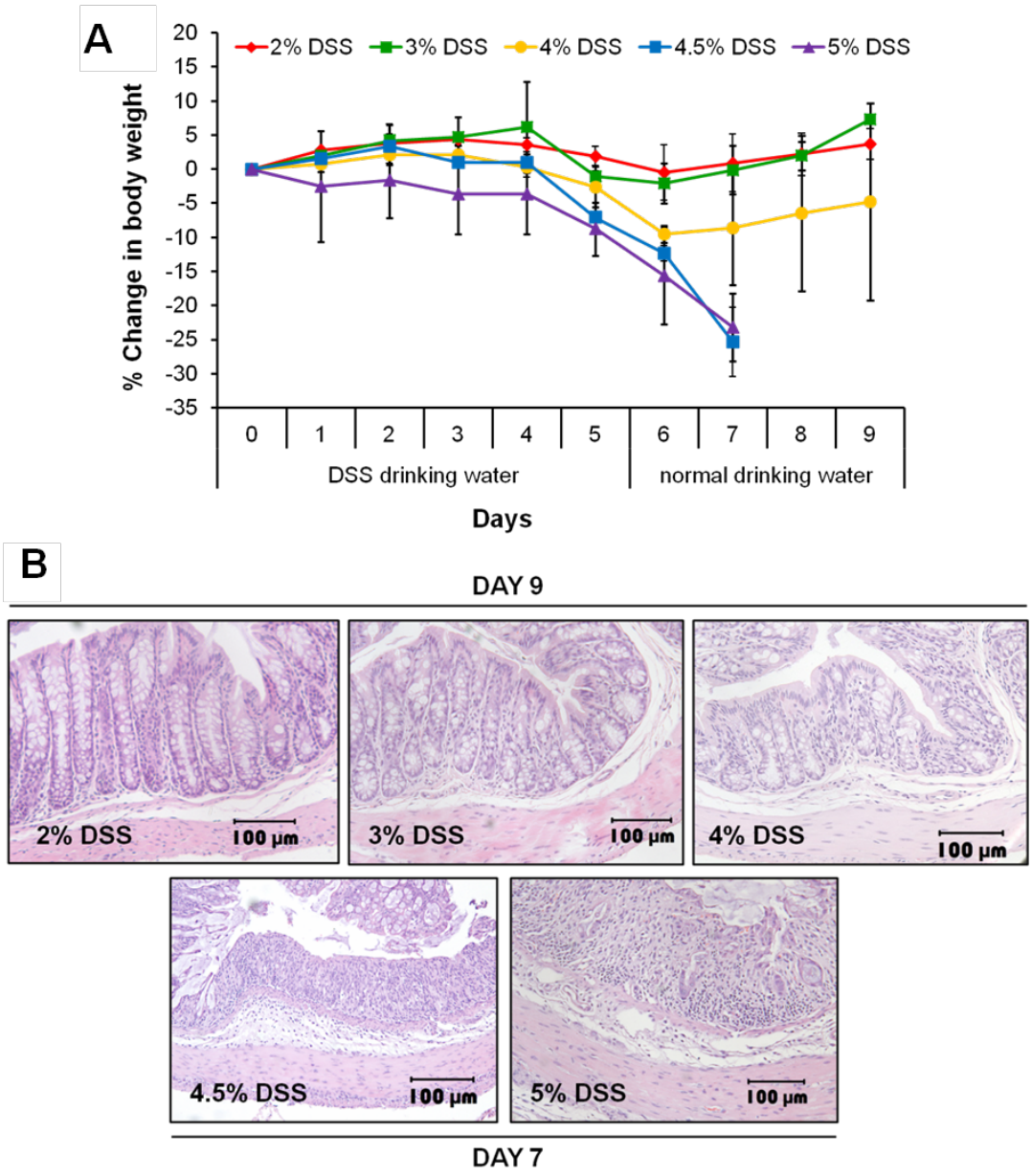

Figure 2.1 Optimal dosing of DSS-induced intestinal inflammation in mice. (A) The change in the body weight of mice was measured daily with a maximum weight loss of 20% reached according to ethical guidelines of protocol. Values are represented

as mean ± SD. (B) H&E stained colonic sections from mice culled at day 9 (top) and day 7 (bottom) after DSS treatment.

2.2.1.2 Preliminary investigations of the metabolism of DSS

Preliminary investigations were performed to determine the effect of DSS on the murine intestines. Analysis by HS-SPME-GC-MS was performed of isolated colonic epithelial cells incubated with and without DSS, and also the analysis of colonic tissue from mice treated with and without DSS. Results included chromatograms with no peaks, indicating the lack of VOCs emitted from these matrices and leading to the conclusion that future studies involving detection of VOCs from faecal samples are likely to originate from the presence of the intestinal microbiota.

Furthermore, it has been reported that DSS remains as an intact sulphated macromolecule through the murine intestine and is not broken down [ref 107]. Analysis of DSS powder and DSS drinking water by HS-SPME-GC-MS produced chromatograms with no peaks therefore also indicating that future studies involving the detection fo VOCs from faecal samples are unlikely to originate from the DSS molecules.

2.2.1.3 Acute DSS-induced colitis

C57BL/6 female mice were administered 4.25% DSS (wt/vol) in their drinking water for 5 days followed by 6 days of normal water, in order to induce acute colitis **(Figure 2.2).** Clinical parameters of body weight loss, stool consistency and the presence of rectal bleeding were assessed daily. Mice were sacrificed at experimental days 0 (*n*=11), 5 (*n*=11), 8 (*n*=11) and 11 (*n*=8); colonic, caecal, small intestine contents and mid-large bowel and distal small bowel tissues sections were taken from each mouse and stored at -20°C prior to analysis by GC-MS. The entire small and large intestine tissues were taken for histological analysis. Samples collected from mice euthanized at day 0 were treated as untreated control to be compared with days 5, 8 and 11.

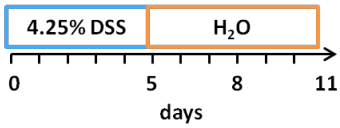

Figure 2.2 Timeline of DSS-induced acute colitis. C57BL/6 mice were administered 4.25% DSS in their drinking water for 5 days. The typical disease features appear by day 5, are maximally expressed by 8 and present with signs of recovery by day 11 (*n*=11 sacrificed at day 0, 5, 8 and 11).

2.2.1.4 Further DSS dose optimisation

The induction of acute colitis using 4.25% DSS was repeated 3 times, each experiment increasing the number of mice used. The third and final experiment resulted in a variable acute colitis across the animals, with a couple of mice having very severe colitis at day 8. Although the majority of mice were able to recover by day 11, it was concluded that this dose was too high for future experiments and further optimising was required. Concentrations of 4, 3.75, 3.25 and 3% DSS were administered to groups of 3 mice each following the same timeline shown in **Figure 2.2**. A maximum weight loss of 15-20% was considered necessary. The lowest concentration of 3% resulted in a weight loss of 16±2% (mean±SD) **(Figure 2.3).** The animal unit used to perform these experiments in was newly opened as this work began. We have speculated that over the space of 12 months, since the opening of the unit, the increase in sensitivity to DSS was due to stabilisation of the barrier to microbes and environment within the unit.

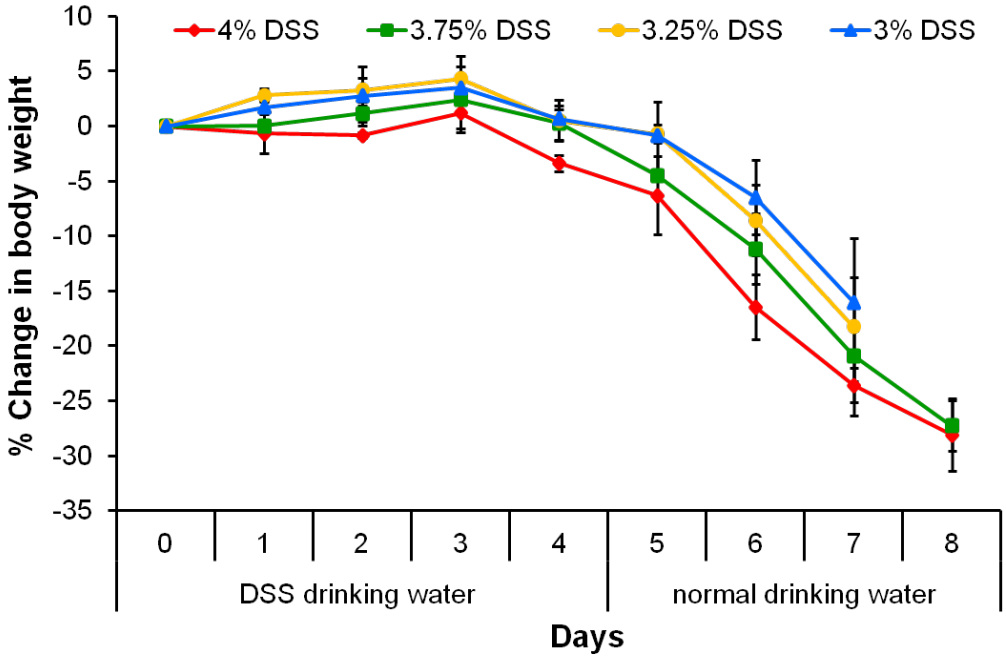

Figure 2.3 Optimal dosing of DSS. Due to the onset of a moderate/severe colitis during the latest 4.25% acute colitis experiment, lower doses of 4, 3.75, 3.25 and 3% were used to determine an acute form of colitis with a maximum weight loss of 15-20%. Values are represented as mean ± SD (*n*=3/concentration of DSS).

2.2.1.5 Induction of acute colitis by DSS in *NFκB2*$^{-/-}$ mice

An additional experiment took place using male *NFκB2*-null mice and was led by Dr Jonathan Williams, assisted by the author of this thesis. The induction of acute colitis was performed with mice receiving 2% DSS. Four groups of mice were included: *NFκB2*$^{-/-}$ DSS treated (*n*=6), *NFκB2*$^{-/-}$ untreated control (*n*=4), C57BL/6 DSS treated (*n*=6), and C57BL/6 untreated controls (*n*=4).

2.2.1.6 Chronic DSS-induced colitis

In order to induce a chronic form of colitis, cyclic DSS administration was used, the concentration required should be considerably lower than that for the acute colitis. Mice were administered 0.75% DSS (wt/vol) in their drinking water for 5 days, followed by 7 days of normal water. This cycle was repeated three times to induce chronic colitis [108]; the DSS concentration increased slightly to 1% for cycles two and three and to 1.25% for cycle four **(Figure 2.4).** The control group of mice

remained on normal drinking water throughout the course of the experiment (*n*=6 control; *n*=6 treated). Clinical parameters of body weight loss, stool consistency and the presence of rectal bleeding were assessed daily, as with the acute colitis experiment. Faecal samples were collected on experimental days 5, 8 and 11 of each cycle from each individual cage. Colonic, caecal, small intestine contents and mid-large bowel and distal small bowel tissue sections were taken from each mouse and stored at -20°C prior to analysis by GC-MS. The entire small and large intestine tissues were taken for histological analysis.

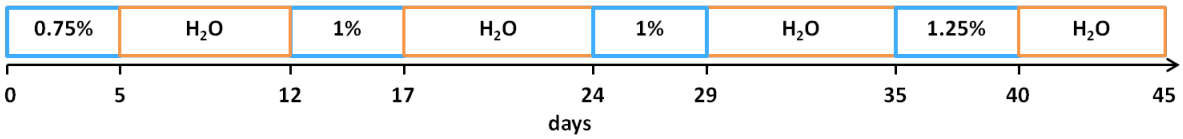

Figure 2.4 Timeline of DSS-induced chronic colitis. Chronic colitis was induced in C57BL/6 mice by 4 cycles of 0.75-1.25% DSS for 5 days followed by 7 days of normal water (*n*=6 control; *n*=6 treated).

2.2.2 Induction of osmotic diarrhoea using $MgSO_4$

Diarrhoea was induced by oral administration of anhydrous magnesium sulphate ($MgSO_4$) at the dose of 2g/kg to each mouse with a control group receiving one dose of distilled water (*n*=3 control; *n*=5 treated) [209]. Animals were fasted overnight before the experiment. Following the administration of the $MgSO_4$, the animals were placed on filter paper, which was changed every hour. Both the amount and consistency of the faeces were assessed each hour for 6 hours. Faecal samples were collected every hour and at termination of the experiment. These faecal samples were used as controls against the DSS colitis samples to identify compounds differentiated from colitis that are produced as a result of an inflammatory response.

2.2.3 Induction of colorectal cancer using azoxymethane (AOM)

The induction of colonic tumours in C57BL/6 female mice using AOM had never been performed before in the SPF animal unit at the University at Liverpool. The

experiment was therefore based on the Nature protocol of cancer induction using AOM [144]. The C57BL/6 mice have a lower susceptibility to this cancer model [210] compared to other strains so the concentration of AOM was increased from 10mg/kg to 12.5mg/kg. To begin, a stock solution of AOM was prepared in distilled water at 12.5mg/ml, aliquoted in glass tubes and stored at -20°C. Immediately before use, stock solution aliquots, as required, were thawed and further diluted 1:10 in sterile isotonic saline to obtain a working solution of final concentration of 1.25mg/ml. On day 1 of the experiment, mice were weighed and injected i.p. with AOM working solution (12.5mg/kg body weight, i.e. 125µl working solution per 10g mouse body weight) for the treated group or sterile isotonic saline for the control group. For spontaneous tumour progression, this process was repeated at the start of weeks 2, 3, 4, 5 and 6 to give a total of 6 injections/mouse **(Figure 2.5).** Faecal samples were collected once a week from each mouse through the course of the experiment. At week 30, animals were killed via cervical dislocation for tumour load analysis. The entire small and large intestine tissues were taken for histological analysis. Initially, the experiment was performed using a control and AOM-treated group (*n*=4/group) in order to see the outcome of using 12.5mg/kg of AOM. It was successful (for results, refer to **section 7.5.1**) and was repeated using *n*=6 mice in each group.

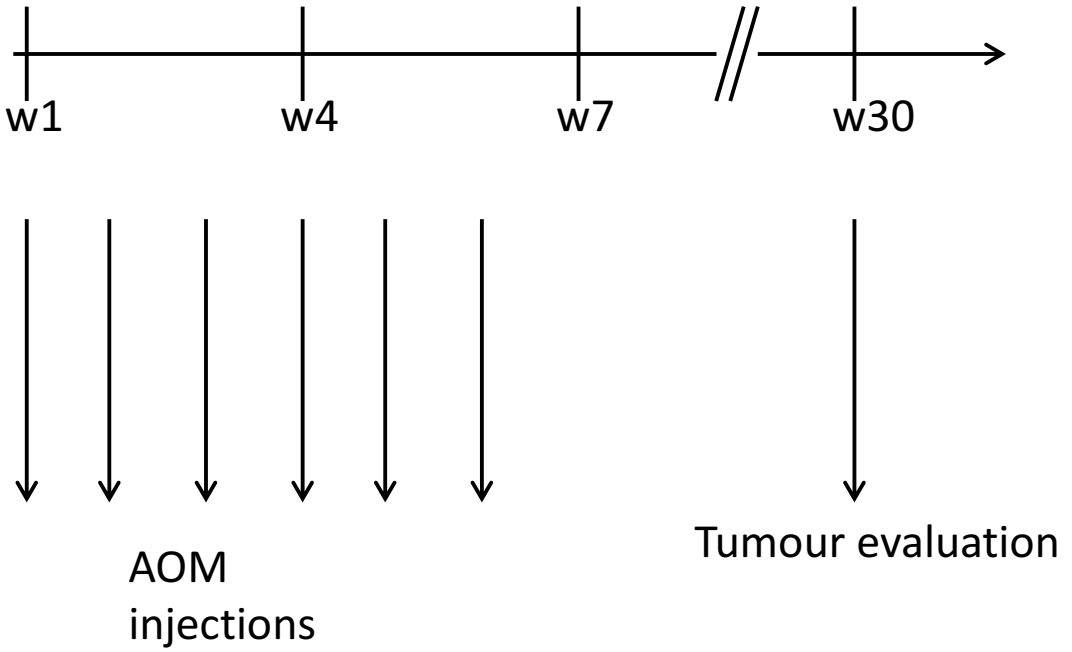

Figure 2.5 AOM-induced CRC development. Scheme for the experimental course of AOM-induced CRC with spontaneous tumour progression by 6 weekly injection of 12.5mg/kg AOM; w = week.

2.2.4 Induction of inflammation-associated colorectal cancer using AOM/DSS

Based on the findings observed in both the chronic DSS-induced colitis and the AOM-induced CRC experiments (**sections 2.2.1.6 and 2.2.3**, respectively), C57BL/6 female mice were dosed with one injection of 12.5mg/kg AOM and received 4 cycles of 1.5% DSS for the induction of inflammation-associated CRC. The AOM was prepared as described in section 2.2.3 and the treated group received one i.p. injection at 12.5mg/kg body weight (*n*=6) on day 1 with the control group receiving one injection of sterile isotonic saline (*n*=6). Five days following AOM injection, 1.5% DSS was administered in the drinking water for 5 days followed by 16 days of ordinary water; the control group remained on ordinary water throughout the experiment. This DSS cycle was repeated twice and animals were sacrificed 12 days after the final cycle, as described by Greten *et al.* 2004 [211] **(Figure 2.6).**

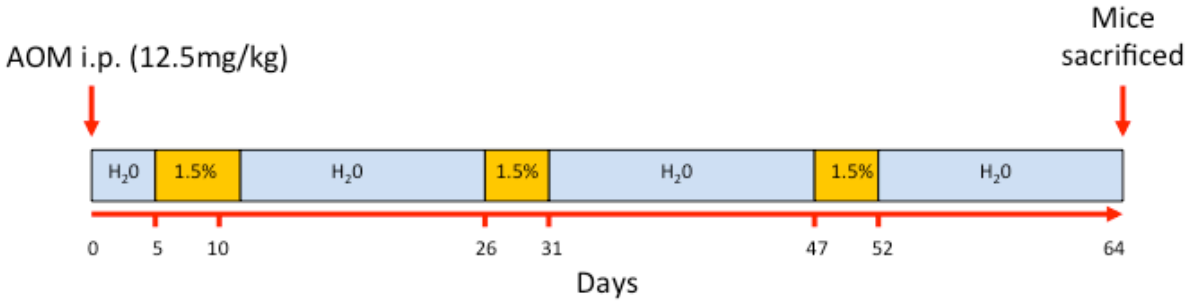

Figure 2.6 Timeline of AOM/DSS-induced inflammation-associated CRC. C57BL/6 mice received one injection of 12.5mg/kg AOM followed by 3 cycles of 1.5% DSS.

2.3 TISSUE DISSECTION AND PREPARATION

All animals were sacrificed via schedule 1 and standard dissection techniques were used to excise the small intestine and the colon. Faecal matter was carefully removed from the small intestine, caecum and colon with curved tweezers onto a glass slide. The faecal content was immediately transferred to labelled glass vials and frozen at -20°C within one hour of collection. A 0.5 cm tissue section from the distal small intestine and mid-colon were also stored the same as the faecal contents. The remaining excised intestines were rinsed with PBS and immersed in 4% formalin solution overnight to preserves tissues from degradation. Tissues were then stored in 70% ethanol prior to gut bundling.

2.3.1 Gut bundling, processing, embedding and cutting of tissues

The fixed colon tissue was divided into proximal and distal colon, before bundling, whereas the entire small intestine tissue was bundled in one piece. Both were cut into roughly 1 cm sections and placed, with care, into loops of about 3 cm micropore surgical tape, creating bundles by squeezing the tape around the tissue. Each bundle was then cut into roughly 0.6 cm lengths with any excess tape and tissue cut off using a Swann-Morton size 22 scalpel blade (VWR international Ltd, Lutterworth, UK). All bundles were placed in histology cassettes and stored in 70% ethanol prior to tissue processing overnight, before being embedded in paraffin wax the morning after. During the embedding step, bundles were orientated vertically in order to obtain transverse sections during tissue cutting. Once the wax

had set, the hardened blocks are ready to be sectioned. Vertical sectioning perpendicular to the surface of the tissue is the usual method. A steel knife is mounted in a microtome and used to cut 10 µm thick tissue sections which are then carefully transferred to a 60°C water bath and mounted on a glass microscope slide.

2.3.2 The 'Swiss roll' technique for the analysis of colon tumours

This technique was used for the preparation of colonic tissue from animal models of CRC [212]. After excision of the small and large intestine, the large bowel was cut at the caecum to separate from small intestine; both were flushed and rinsed with PBS. Tissues were then fixed in 4% formalin for maximum of 1 hour before performing the 'swiss roll' technique. The entire length of the colon was carefully slit open with scissors from the distal end and any remaining faeces were removed. Mucosal side exposed, the colon was carefully rolled around a wooden cotton bud and secured with a needle **(Figure 2.7)** before undergoing fixation in 4% formalin solution for 24 hours.

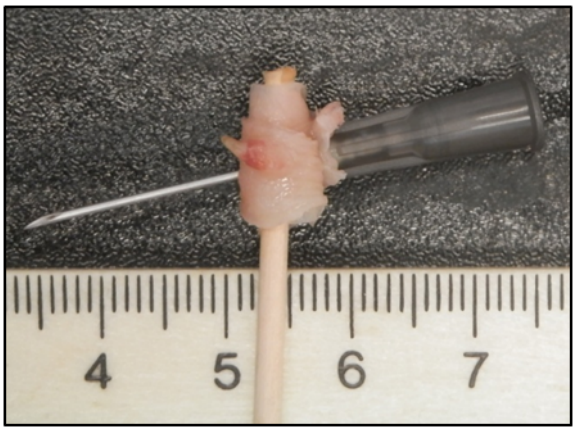

Figure 2.7 CRC tissue preparation. Photograph of a swiss roll preparation of large intestine treated with AOM±DSS.

2.3.3 Haematoxylin and eosin (H&E) staining

The transverse tissue sections of 4 µm thick attached to glass microscope slides were dried at 37°C for 24 hours or 60°C for 1 hour. Slides were then immediately de-paraffinized in xylene for 10 minutes and subsequently rehydrated by passing

through a series of decreasing ethanol concentrations to distilled water (100%, 90%, 70%, H_2O). The nuclei of the tissues undergo regressive staining by immersing in haematoxylin (Sigma-Aldrich Co, Dorset, UK) for 3 minutes and then washed in running tap water until the water turned clear (5-10 minutes). The tissue sections were then placed in eosin (Sigma-Aldrich Co, Dorset, UK) for 4 minutes to regressively stain the cytoplasm. Any excess eosin was removed by washing under running water for roughly 1 minute. Sections were then dehydrated by dipping the slides briefly in 70%, 90% then 100% ethanol (<30 seconds each). Finally, after clearing in xylene for about 10 minutes, the slides were carefully mounted with Distrene, Plasticisel, Xylene (DPX) and a cover slip and left to dry for 24 hours. The transverse sections of tissues were then examined under a light microscope.

2.3.4 Masson's Trichrome stain

Masson's Trichrome (MT) is used to distinguish collagen from muscle tissue, an indicator of fibrosis. Distal colon tissue sections of 4 µm thick attached to glass microscope slides were dried at 37°C for 24 hours or 60°C for 1 hour. Slides were then immediately de-paraffinized in xylene for 10 minutes and subsequently rehydrated by passing through a series of decreasing ethanol concentrations to distilled water (100%, 90%, 70%, H_2O). All tissues were formalin fixed and prior to staining, were re-fixed in Bouin's solution for 1 hour at 56°C to improve staining quality. Slides were then rinsed under running tap water for 10 mins to remove the yellow colour before undergoing staining with Weigert's iron haematoxylin working solution for 10 mins (Weigert's haematoxylin A and B at a 1:1 ratio). Slides were then rinsed for a second time in running warm water for 10 minutes, quickly washed in distilled water and stained in Biebrich scarlet-acid fuchsin solution for 10-15 minutes. After another rinse in distilled water, slides were differentiated in phosphomolybdic-phosphotungstic acid solution for 10-15 minutes or until collagen was no longer red. Sections were transferred directly (without rinse) to aniline blue solution and stained for 5-10 minutes before being rinsed briefly in distilled water and differentiated in 1% acetic acid solution for 2-5 minutes. Slides were then washed in distilled water for a final time and dehydrated very quickly through 95%

and 100% ethanol, cleared in xylene and mounted with resinous mounting medium, DPX. Results should show collagen stained blue, nuclei stained black and muscle, cytoplasm, keratin stained red.

2.3.5 High iron diamine (HID) and Alcian blue (AB) stain

MDF are foci of crypts depleted of mucins in a background of normal crypts using the HID-AB technique [213], which allows differentiation between sialomucin and sulfomucin production. Firstly, the HID solution was prepared in a Coplin jar by dissolving the two diamine salts, N,N-dimethyl-meta-phenylenediamine-dihydrochloride (120mg) and N,N-dimethyl-para-phenylenediamine-dihydrochloride (20mg), in 50ml distilled water and adding freshly prepared 60% ferric chloride solution (1.4ml). Distal colon tissue sections of 4 µm thick attached to glass microscope slides were dried at 37°C for 24 hours or 60°C for 1 hour. Slides were then immediately de-paraffinized in xylene for 10 minutes and subsequently rehydrated by passing through a series of decreasing ethanol concentrations to distilled water (100%, 90%, 70%, H_2O). Sections were then taken to distilled water for 5 minutes and treated in HID solution for 18-24 hours at room temperature. Next, slides were washed well in running tap water for 5-10 minutes and stained in 1% AB in 3% acetic acid (pH 2.5) for 5 minutes. Finally, sections were rinsed in tap water and dehydrated, cleared and mounted, as described previously. Expected results are to see sulphated mucins stained brown/black and carboxylated mucins stained blue.

2.4 PHYSIOLOGICAL AND HISTOLOGICAL SCORING METHODS

There were various methods applied to quantify and confirm the physiological responses following different treatments. All scoring procedures were performed by the author who was blinded to the treatment of the samples being scored. The author received training for these different scoring methods from a certified veterinary pathologist, Dr Jonathan Williams.

2.4.1 Disease activity index scoring in DSS-induced acute/chronic colitis

Daily clinical assessment of body weight, stool consistency, presence of rectal bleeding, and general appearance and well-being of the DSS-treated mice was performed. Each animal was given a disease activity index (DAI) score, according to **Table 2.1**, providing a comprehensive functional measure similar to the clinical symptoms observed in human IBD. The DAI was scored using a validated method described previously [201, 214].

Table 2.1 Disease activity index (DAI) scoring.

Score	Weight loss (%)	Stool consistency	Occult/gross
0	None	normal	normal
1	1-5	-	-
2	5-10	loose stools	Hemoccult +
3	10-15	-	-
4	>15	diarrhoea	gross bleeding

DAI = (combined score of weight loss, stool consistency and bleeding)/3. Normal stool = well-formed pellets; loose stools = pasty stools that do not stick to the anus; and diarrhoea = liquid stools that stick to the anus **[201, 214]**.

2.4.2 Histological scoring of colitis severity

Following fixation in 4% formalin and embedding in paraffin, sections were stained with H&E as described previously. In order to quantify inflammatory changes following DSS administration, a histological scoring system was applied as described [215]. The histological colitis severity score (range from 0 to 6) was determined as shown in **Table 2.2.**

Table 2.2 Histological scoring of colitis severity.

Score	Cell infiltration	Tissue damage
0	None	None
1	Focally increased numbers of inflammatory cells in the lamina propria	Discrete epithelial lesions
2	Confluence of inflammatory cells extending into the submucoa	Mucosal erosions
3	Transmural extension of the infiltrate	Extensive mucosal damage and/or extension through deeper structures of the bowel wall

The combined histological colitis severity score, ranging from 0 to 6, is the sum of the two equally weighted sub-scores (cell infiltration and tissue damage).

2.4.3 Histological fibrosis scoring method

Following fixation in 4% formalin and embedding in paraffin, sections were stained with MT stain as described previously. In order to quantify the amount of fibrosis present following DSS administration, a histological scoring system was applied as described by Ding *et al*. 2012 [216].

Table 2.3 Histological fibrosis scoring method.

Category	Score	Description
Collagen (fibrosis)	0	No increase
	1	Increased in the submucosa
	2	Increased in the mucosa
	3	Increased in the muscularis mucosa; thickening/dis-organisation of the muscularis mucosa
	4	Increased in the muscularis propria
	5	Gross disorganisation of the muscularis propria
Percent involvement	1	1-25% of section
	2	26-50% of section
	3	51-75% of section
	4	76-100% of section

The fibrosis score for each animal is the sum of the collagen score and the percent involvement.

2.4.4 Faecal output scoring in $MgSO_4$-induced diarrhoea

On the basis of consistency of stool, a numerical score was assigned as follow: 1 = normal stool, 2 = semi-solid, 3 = watery stool. The faecal output index (FOI) was defined as the sum of the consistency scores of all the motions passed within the observation period of 3 hours. A mouse passing a stool of score 2 at least once was counted as suffering from diarrhoea [217].

2.4.5 Measurement of colon tumour number and size

At the end of the AOM±DSS experiments, described previously in **sections 2.2.3 and 2.2.4**, mice were sacrificed and the whole colon was carefully dissected and flushed with PBS. The colon was cut open longitudinally and gently washed with PBS to remove any remaining faecal content. The opened colon was carefully inspected

macroscopically for the presence and location of polyps. The size and the number of polyps, if any, were then carefully measured. The swiss roll technique (**section 2.3.2**) was then used to prepare tissues for histological analysis.

2.4.6 Identification of Mucin-depleted foci (MDF)

Mucin production was analysed by staining distal colonic sections with HID-AB. MDF were identified as focal lesions by the following criteria:

i. Absence or very small production of mucins
ii. Distortion of the opening of the lumen compared with normal surrounding crypts
iii. Elevation of the lesion above the surface of the colon
iv. Multiplicity (i.e. the number of crypts forming each focus) higher than 3 crypts

To be defined as an MDF a focus has to fulfil the first criterion and at least two of the other criteria [218].

2.5 CALPROTECTIN MOUSE ELISA

All murine faecal samples were stored at -20°C post-GC-MS run until used for the quantitative determination of calprotectin via the "sandwich" S100A8/S100A9 (calprotectin) ELISA technique using a 96-well plate (Biohit Healthcare, Cheshire, UK (suppliers), Immunodiagnostik, Germany (manufacturers)). All ELISA reagents and samples were brought to room temperature prior to the start of the assay. Each sample was extracted 1:50 in extraction buffer (100mg stool + 5ml extraction buffer), and centrifuged for 5 minutes at 13000g.

To begin, each well used was washed 5 times with 250µl of diluted wash buffer, firmly tapping the inverted plate on absorbent paper after the final washing step. This was followed by adding 100µl of calprotectin standards (of concentrations 0, 0.25, 0.98, 3.9, 15.6 ng/ml), samples and controls in duplicate to wells coated with high affinity monoclonal anti-S100A8/S100A9 antibodies. The plate was covered

tightly with foil and left to incubate for 1 hour at 37°C to allow for any S100A8/S100A9 present in the samples to bind to the immobilized antibodies. Contents of each well were then aspirated and the plate was washed 5 times with 250µl of diluted washing buffer, firmly tapping the inverted plate on absorbent paper after the final washing step. In a next incubation step, a monoclonal anti-S100A8/S100A9 antibody is added at 100µl/well, covered with foil and left for 1 hour at 37°C. The contents were then aspirated and the washing step was repeated a third time. Then a peroxidase labelled anti-mouse conjugate is added at 100µl/well, covered with foil and left for 1 hour at 37°C. This allows the following complex to form: capture antibodies – S100A8/S100A9 – detection antibody – peroxidase conjugate. After aspirating the contents, washing with 250µl/well of washing buffer and tapping the plate on absorbent paper, 100µl/ well of tetramethylbenzidine (TMB) was added as a substrate for peroxidise. The plate was incubated for 5-15 minutes at room temperature in the dark and observed for a colour change (blue to yellow). Finally, an acidic stop solution was added to terminate the reaction. The intensity of colour change is sensitive so care was taken to ensure the reaction was stopped upon good differentiation. Absorption was determined immediately with an ELISA reader at 450 nm and a dose response curve of the absorbance (optical density, OD at 450 nm) vs. concentration was generated using the value obtained from the standards **(Figure 2.9).** S100A8/S100A9 (calprotectin) present in faecal samples was determined directly from this curve.

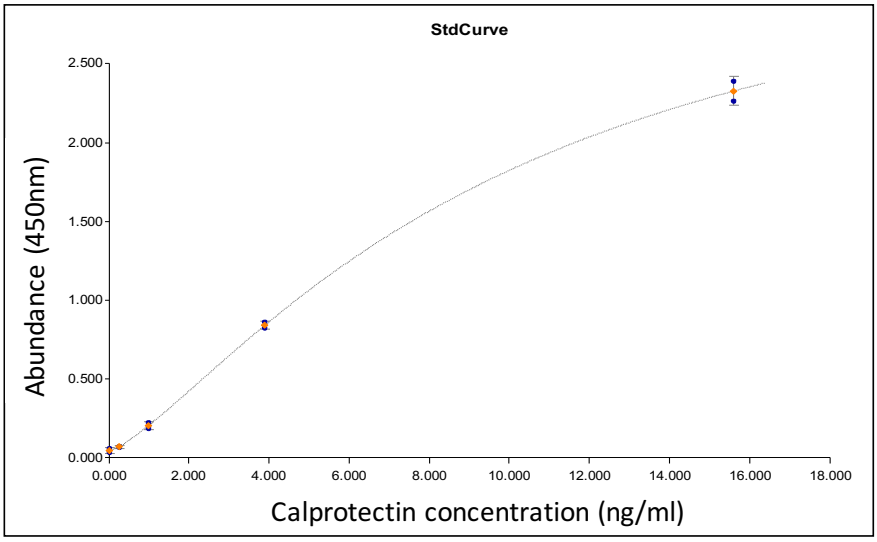

Figure 2.8 Calprotectin ELISA. Standard curve for the measurement of calprotectin concentration (ng/ml) by ELISA.

2.6 VOLATILE ORGANIC COMPOUND (VOC) ANALYSIS

2.6.1 Solid phase microextraction (SPME) coupled to gas chromatography-mass spectrometry (GC-MS)

A PerkinElmer Clarus 500 GC-MS quadrupole benchtop system (Beaconsfield, UK) was used in combination with a Combi PAL auto-sampler (CTC Analytics, Switzerland) for the analysis of all samples. The GC column used was a Zebron ZB-624 with inner diameter 0.25mm, length 60m, film thickness 1.4µm (Phenomenex, Macclesfield, UK). The carrier gas used was helium of 99.996% purity (BOC, Sheffield, UK). The SPME fibres used were carboxen-polydimethylsiloxane (CAR-PDMS) 85µm and divinylbenzene (DVB)-CAR-PDMS 50/30µm (1cm) (Sigma-Aldrich, Dorset, UK). Both fibres were pre-conditioned before use, in accordance with the manufacturer's manual. Vials with magnetic caps of 2 ml (Crawford Scientific, Lanarkshire, UK) and 10 ml (Sigma-Aldrich, Dorset, UK) volume were used. The fibre desorption conditions were 5 minutes at 220°C. The initial temperature of the GC oven was set at 40°C and held for 1 minute before increasing to 220°C at a rate of 5°C/min and held for 4 min with a total run time of 41 min. A solvent delay was set for the first 6 min and the MS was operated in electron impact ionization EI+ mode,

scanning from ion mass fragments 10 to 300 *m/z* with an inter-scan delay of 0.1 sec and a resolution of 1000 at FWHM (Full Width at Half Maximum). The helium gas flow rate was set at 1 ml/min. The sensitivity of the instrument was determined with 2-pentanone only and will vary for other compounds. The limit of detection, as being 3 times the signal/noise ratio, of the method for 2-pentanone with DVB-CAR-PDMS is 16 ppm and with CAR-PDMS is 40 ppm.

2.6.2 Method development for HS-SPME-GC-MS analysis of murine faecal samples

Substantial quantification of VOCs using HS-SPME in complex mixtures with unknown composition is difficult. The reason is that the recovery rate of any individual compound using the SPME fibre is unknown and also that in complex VOC mixtures the compounds will compete against each other. The 'weaker' VOCs will be discriminated by 'stronger' VOCs and this discrimination depends on the VOC composition within the complex mixture present in the headspace of samples such as faecal samples. As a result, 'semi-quantification' with SPME is the best that can be achieved. Furthermore, an internal standard will not help because the recovery rate of the standard compound is also unknown. Therefore, in order to achieve 'semi-quantitative' results, standardisation of the VOC extraction protocol is required and is typical of a non-targeted approach [219].

2.6.2.1 Sample volume

Samples (mean ± SEM) of 3 (40.0 ± 14.1 mg), 5 (76.7 ± 25.0 mg), 10 (133.3 ± 7.0 mg) and 20 (233.0 ± 25.0 mg) pellets of mice faeces were collected in 10 ml glass vials from one cage of four inbred wild-type male C57BL/6 9-week old mice, once a week for 3 weeks and stored at -20°C. Each sample size, in triplicate, was pre-incubated at 60°C for 30 minutes before VOC extraction using a CAR-PDMS SPME fibre at 60°C for 20 minutes prior to desorption into the GC oven. Only VOCs identified in every sample were then used for comparing the VOC abundances according to the sample size used. All data were processed according to the 'Data

processing' section of this chapter with a one-way ANOVA with Tukey's HSD followed by Bonferroni, applied to test for differences between the different sample sizes.

The number of VOCs identified and their abundances were evaluated according to different sample sizes. Samples of 3 pellets showed a significantly lower number of VOCs than 20 pellets (p<0.05), with no significant differences in the number of VOCs between 10 and 20 pellets (p=0.87). Six compounds (pentanal, pentane, propanal, hexanal, 2,3-butanedione and benzaldehyde) were consistently present in every sample with the compounds pentane and pentanal detected at significantly lower abundances in 3 and 5 pellets compared to 10 and 20 pellets.

An increase in sample size led to an increase in both the number of VOCs detected and their abundances, therefore reaching a limit of VOCs identified; a result of fibre overload. Samples of >20 pellets were not included as no significant difference was found between samples of 10 and 20 pellets and it was found experimentally difficult to collect >20 pellets from individual mice. Therefore, it was predicted that any number of faecal pellets higher than 20 pellets would also produce a non-significant result. Samples of 10 pellets were used for all future experiments **(Figure 2.9A&B).**

2.6.2.2 Vial size

For each vial volume of 2 and 10 ml, samples of 10 pellets (n=4), were pre-incubated at 60°C for 30 minutes before VOC extraction using a CAR-PDMS SPME fibre at 60°C for 20 minutes prior to desorption into the GC oven. All data were processed according to 'Data processing' section of this chapter with a Student's t-test applied to test for differences between different vial sizes.

The number of VOCs identified and their abundances were evaluated according to different vial volumes used for SPME-GC-MS analysis. Vials of 2 ml showed a slightly higher number of VOCs identified than 10 ml; however, there were no significant

differences in VOC abundances between vial size (p>0.05). This difference may be explained by the fact that if the volume of headspace surrounding the sample decreases, the concentration of compounds increases, leading to better coverage of the VOC profile in the samples. Therefore, 2 ml vials were used for all later samples **(Figure 2.9C).**

2.6.2.3 VOC extraction time and temperature

Extraction time: samples of 10 pellets were pre-incubated at 60°C for 30 minutes before VOC extraction using a CAR-PDMS SPME fibre at 60°C for 10 (n=3), 20 (n=3) or 30 minutes (n=3) prior to desorption into the GC oven.

Extraction temperature: samples of 10 pellets were pre-incubated at 60°C for 30 minutes before VOC extraction using a CAR-PDMS SPME fibre at 50 (n=3), 60 (n=3) or 70°C (n=3) for 20 minutes prior to desorption into the GC oven. All data were processed according to 'Data processing' section of this chapter with a one-way ANOVA with Tukey's HSD followed by Bonferroni correction, applied to test for differences between the different extraction times and temperatures tested.

Although there was no significant difference in the number of VOCs reported by the exposure times tested, 20 minutes produced the highest number of VOCs (p=0.5). The exposure temperatures of 60, and 70°C showed a significantly higher number of VOCs than 50°C (p=0.03). Although there was no significant differences between 60 and 70°C (p=0.33), the exposure temperature of 60°C produced the highest number of VOCs. Therefore, the extraction time and temperature of 20 minutes and 60°C was used for all later experiments.

Typically, the SPME extraction process is considered complete when the analyte concentration has reached distribution equilibrium between the sample matrix and the fibre coating. Prior to the distribution equilibrium being reached, the extraction process is considered in pre-equilibrium state. These results show that an increase

in extraction time and temperature result in higher numbers of VOCs identified. However, extraction times higher than 20 minutes and extraction temperatures higher than 60°C showed no improvement. This indicates that in the pre-equilibrium state, a small change in extraction time and temperature may result in a large change in the amount of analyte being absorbed. However, once the distribution gets close to the equilibrium, there are either no changes or only small changes in the amount of analyte absorbed. Therefore, the extraction time and temperature are not critical once equilibrium is nearly reached **(Figure 2.9D&E).**

2.6.2.4 SPME fibre coating

Samples of 10 pellets were pre-incubated at 60°C for 30 minutes before VOC extraction using a CAR-PDMS (*n*=5) or a DVB-CAR-PDMS (*n*=5) SPME fibre at 60°C for 20 minutes prior to desorption into the GC oven. All data were processed according to 'Data processing' section of this chapter with a Student's t-test applied to test for differences between different SPME fibres.

Use of the DVB-CAR-PDMS fibre led to the identification of a significantly higher number of VOCs compared to the CAR-PDMS fibre (p=0.04). Seven compounds were exclusively associated with the DVB-CAR-PDMS, while two compounds were associated with the CAR-PDMS. Therefore, when possible, the use of different SPME fibres is ideal to extract a greater diversity of compounds, which is in agreement with previous work from Dixon and collaborators [220]. However, due to the significantly higher number of identified VOCs between fibres for murine samples, a DVB-CAR-PDMS fibre was primarily used for the analysis of later samples **(Figure 2.9F).** Every 200 runs, the SPME fibre was replaced and care was taken to avoid damaging fibre, as advised by Perkin Elmer GC-MS technicians (maximum runs of 100-200 depending on lab conditions).

2.6.2.5 Optimised method

Based on results presented in section 2.6.2, an optimised SPME-GC-MS method for analysing murine samples includes samples of 10 to 20 pellets, stored in 2 ml glass vials, incubated for 30 min at 60°C and extracted by DVB-CAR-PDMS for 20 min [221].

Furthermore, all samples were frozen at -80°C within 1 hour of collection and were run at random to avoid the effect of a sequential pattern influencing the VOC profiles. Samples were run through the GC-MS in blocks of 1-4 weeks depending on the quantity of samples in the sample set. This was put in place to avoid contamination from other sample matrices. Further optimisation also led to introducing a 'blank' run every 6 samples to avoid carryover of sampling.

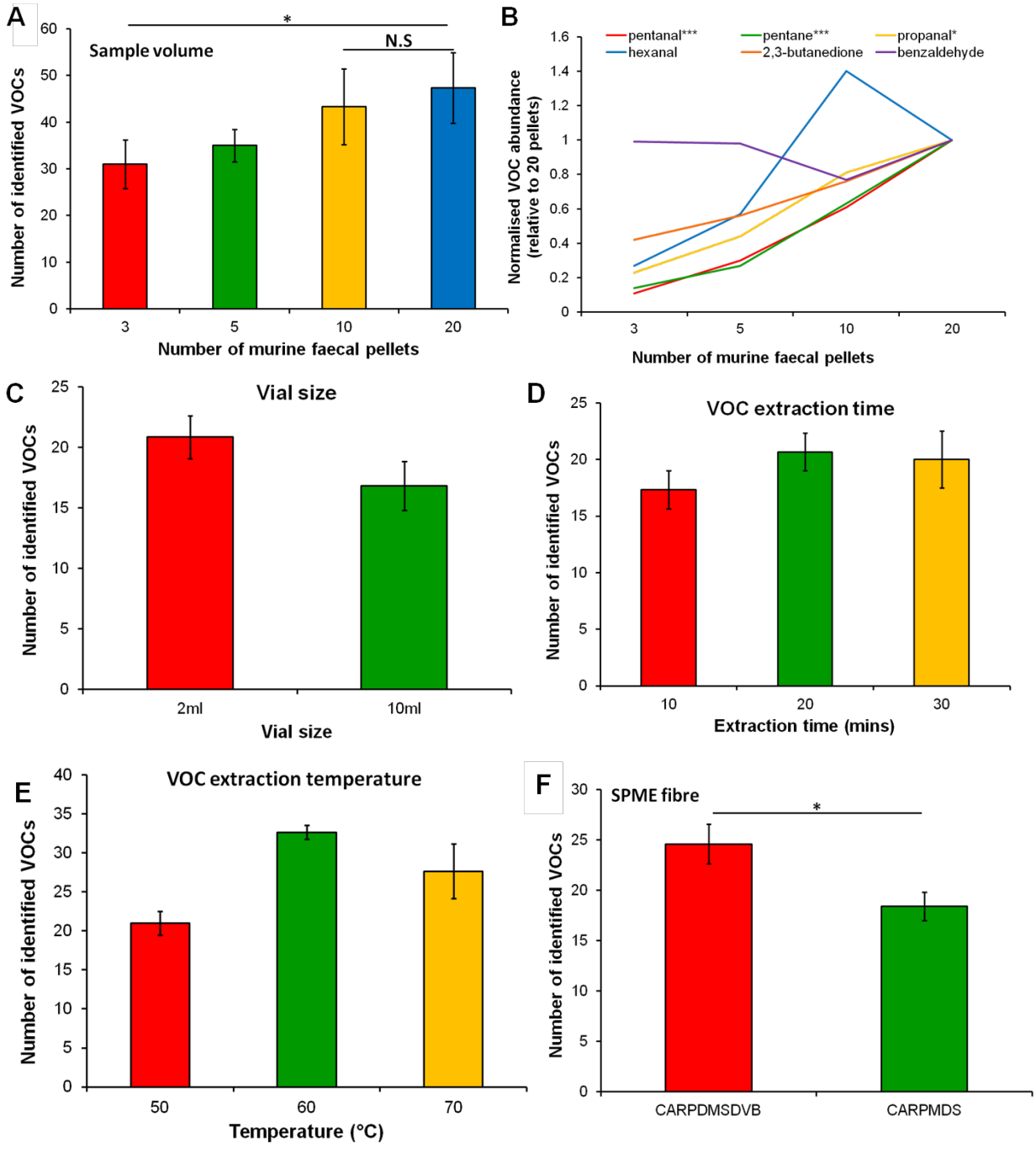

Figure 2.9 Optimised SPME-GC-MS method for murine faecal VOC analysis. (A-B) The number and abundance of VOCs identified in murine faecal samples of 3, 5, 10 and 20 pellets, with VOC abundances normalized to their abundances in samples of 20 pellets (*n*=3/group). (C-F) The number of VOCs identified in samples of 10 pellets according to vial size (C) (*n*=4/vial size), extraction time (*n*=3/time) (D), extraction temperature (*n*=3/temperature) (E) and SPME fibre coating (*n*=3/coating) (F). ANOVA with Tukey's HSD followed by Bonferroni; *p<0.05, **p<0.01, ***p<0.001.

2.7 DATA PROCESSING AND ANALYSIS

2.7.1 Turbomass

The GC-MS instrument used for all experiments in this study is used in conjunction with the PerkinElmer Turbomass GC-MS software. All raw data is generated by this software on a PC to view all chromatograms before being transferred to personal PCs for further data analysis. Turbomass is responsible for maintaining the GC-MS and can be used for data acquisition, analysis, and representation of GC-MS data.

2.7.2 AMDIS, NIST, R

All GC-MS data were processed using the Automated Mass Spectral Deconvolution System using default settings (AMDIS – version 2.71, 2012) in conjunction with the NIST mass spectral library (version 2.0, 2011) and the R package Metab [222]. VOCs were identified using an in-house library built with AMDIS in combination to the NIST library.

2.7.3 Data pre-processing

An in-house library was built using faecal samples collected as part of a baseline murine study (**Chapter 3**). For each dataset, hereafter, at least 50% of chromatograms were randomly chosen for long hand AMDIS analysis, adding any unidentified compounds to the library.

To begin with, raw data in the form of a chromatogram, generated from the GC-MS was converted to the Net.CDF data format using the data bridge tool (Turbomass software). Chromatograms were then analysed against the murine-specific in-house library prior to batch report generation of complete datasets using AMDIS and the in-house compound library. Using Metab [222], an excel report is created using the AMDIS batch report, Net.CDF data and the in-house library. This consists of a list of all compounds present in all samples with the corresponding corrected peak

abundances using a Time Window of 0.5 minutes. Metab selects the most probable metabolite associated to each retention time, by correcting the base peak value calculated by AMDIS. It considers the number of question marks reported by AMDIS and the difference between expected and observed retention times, using the ion mass fragments in the library and the raw data to report the corrected peak abundances in a single spreadsheet [222]. **Appendix 1** includes a comparison of Metab vs. manual, long-hand analysis to demonstrate the robustness of this method.

2.8 STATISTICAL ANALYSIS

All univariate statistics were performed using SPSS and/or R. All multivariate statistics were performed using R version 3.0.2. Due to the large amount of missing data having a significant effect of results, NA values were replaced with 1 prior to any quantitative statistical analysis being performed [223]. All raw data were log transformed prior to any statistical analysis in order to normalise the metabolomics data [224]. Many compounds of low frequency are likely to reflect individual characteristics and, therefore, were not readily selected for further statistical analysis. Compounds present in less than 30% of at least one condition were removed prior to further analysis when determining differences between health and disease. A Student's t-test (two groups) or a one-way analysis of variance (ANOVA) (more than two groups) followed by Tukey's HSD post-hoc test were applied to test quantitative differences between data classes. In order to test for qualitative differences, the presence or absence of each compound was "1" to denote the presence of the compound and "0" to denote its absence in that sample. The presence/absence data were then tested for differences between data classes by applying a Chi-squared test. Final p-values were adjusted for multiple comparisons using Bonferroni correction. P-values < 0.05 were considered as significant. A principle component analysis (PCA) was used to show similarities within data classes. The purpose of a PCA is to represent as much of the variation as possible within the first two components with each point representing a different sample with the different shapes signifying the different time points. A heatmap

and dendrogram were produced using hierarchical cluster analysis with the complete linkage method to find similar clusters, which is a visualising tool for classifying different phenotypes. A heatmap is a graphical method of displaying the concentration of each compound by using colour to represent the numerical values. The clustering algorithm (complete-linkage, default) grouped related rows and/or columns together by similarity, represented by a dendrogram. The PCA, heatmap and dendrogram were produced in R. Time series analysis (two-way repeated measures ANOVA) was performed using the online metabolomics software, MetAtt [225].

Chapter 3

Healthy Murine Faecal VOC Metabolome

3.1 INTRODUCTION

The variability of the metabolome in healthy human cohorts is large. Its biochemical origin is not completely understood because of limiting factors, such as diet, age, sex and medication. Murine models of disease are used in biomedical research to address almost every aspect of human health and disease, including disease pathogenesis, diagnosis and treatment. The composition of the gut microbiota has received considerable attention as a significant factor influencing the health of the host and contributing to the development of experimental inflammatory disease in animal models. Identifying and reducing gut microbiota variation within laboratory animals will control disease parameters and provide more consistent and equivalent models.

Metabolomics is the characterisation of metabolites generated by an organism in a specified physiological and environmental context. Identification of the metabolome could enable a better understanding of the metabolism of our gut microbial communities and, consequently, the role it has to play in health and disease [226]. The sensitivity of metabolomics and other "–omics" technologies relies on the ability to identify the subtle differences occurring as a direct result of pathological stimuli from numerous variables, therefore representing the many fluctuating physiological and/or biochemical processes. It is essential, therefore, that "normal" is defined with regard to an organism's integrated physiological profile, considering the effects of both environmental and genetic factors such as gender, age, strain, and diet to effectively differentiate such variation from that caused by disease.

Rogers *et al.* revealed that the faecal microbiota of healthy mice is dominated by the phyla Bacteroidetes and Firmicutes. Marked variation in the relative abundance of phyla between different housing rooms and between individual genetically-identical animals was also observed. They went on to hypothesise that there would be differences when comparing the metabolome of faeces from healthy mice whose faecal microbiota were distinct. ^{1}H nuclear magnetic resonance (NMR)

spectroscopy was performed on faecal extracts from the same samples used previously for microbiota sequencing, resulting in clear metabolomic differences between the murine faecal samples based on the composition of the bacteria present [227].

Gender-dependent metabolic variation was investigated using ^{1}H NMR of urine from Han Wistar rats. Discriminating molecules, such as trimethylamine-*N*-oxide, *N*,*N*'-dimethylglycine and *m*-hydroxyphenylpropionic acid were all excreted in higher concentrations in samples from female mice [228]. More recently, the urine metabolomic profiles of male and female IL-10 KO mice were examined. The results demonstrated that both IL-10 deficient and WT mice exhibited gender-related changes over time. Specific patterns imperative in the development of intestinal inflammation could be identified which were significant for the gender- and age-specific differences in IBD development [202]. Unlike urine which has been relatively well-characterised, the effect of gender and temporal variation on the murine faecal metabolite profile has not been assessed thoroughly.

HS gases from both the urine and faecal pellets of wild and laboratory mice are known to be rich in VOCs [229]. It has previously been reported that the analysis of VOCs produced from fresh and aged pellets by GC-MS resulted in the identification of many compounds, with ketones, alcohols and carboxylic acids being the most common. Goodrich *et al.* assessed the effects of VOCs on the behaviour of mice. It was found that the introduction of volatiles from faecal pellets from one mouse into the territory of another altered the site at which the resident mouse deposited its faeces. In addition, transferring the faecal pellets of one mouse into the environment of another improved the success of a social encounter between the two mice [230].

Here, we use our optimised HS-SPME-GC-MS method (**Chapter 2**) to establish a baseline faecal VOC profile for healthy WT male and female C57BL/6 mice, which will aid the analysis of later studies included in this thesis.

3.2 HYPOTHESIS

The hypotheses were:

- The healthy murine faecal VOC metabolome will be similar between individual mice of the same age and gender.
- There will be significant differences between the VOC profiles emitted from the faecal pellet between mice of different gender and age.
- The composition of VOCs emitted from faeces will differ according to location of the lower GI tract.

3.3 AIMS

1. Detect and identify VOCs present in the headspace of faeces from healthy WT C57BL/6 mice using a SPME-GC-MS platform.
2. Establish similarities or differences in the abundance and presence of specific VOCs according to the age and/or gender of mice, or the location of faeces in the lower GI tract.
3. Investigate the composition of VOC emitted from faeces of GF mice.

3.4 METHODS

3.4.1 Experimental design

3.4.1.1 Baseline murine study

A detailed description of the methods can be found in **Chapter 2**. Briefly, a longitudinal experiment was performed to determine similarities or differences in abundance of specific VOCs emitted from the faeces of mice, taking into account the effects of gender and age. Six male and 6 female WT C57BL/6 mice were purchased and housed individually for a total of 8 weeks (5-12 w) with faecal samples (10 pellets) collected from each cage once per week for the course of the entire experiment. Bedding was replaced with autoclaved blotting paper 24 hours

preceding the faecal pellet collection and replaced immediately following collection. All samples were stored at -20°C until needed. Mice were sacrificed and the faecal content collected. Aliquots of food and bedding (*n*=3) were also collected and analysed via the same method used for the analysis of VOCs from faecal samples.

3.4.1.2 Germ-free study

Briefly, faecal samples from the GF colonies, C3H/HeN and *Junbo* mice (*n*=6 in total; *n*=3/strain) and non-GF SPF (*n*=6) strain, were provided by MRC Harwell, Oxford. The VOC profile of the faecal pellet from GF mice was compared with their non-GF SPF equivalent and with the VOC profile from the WT C57BL/6 SPF (age-matched) at the University of Liverpool.

3.4.2 HS-SPME-GC-MS sample preparation and analysis

Where possible, 10 pellets or 130mg (maximum volume) of stool were collected and stored in 2ml glass vials at -20°C. Prior to VOC extraction, samples were pre-incubated for 30 mins at 60°C before headspace extraction using the SPME with a CAR/PDMS/DVB fibre for 20 mins prior to desorption into the GC oven [221]. For GC-MS conditions, please refer to **section 2.6.1.**

3.4.3 Data processing and statistical analysis

Chromatograms were processed using the AMDIS in conjunction with the NIST mass spectral library (version 2.0, 2011). VOCs were identified and added to a murine-specific VOC library. A batch report was generated in AMDIS and a spreadsheet created using the R package, Metab [222], consisting of a list of all compounds present in all samples with the corresponding peak abundances using a time window of 0.5 minutes. Compounds identified in at least 30% of samples, in at least one condition, were used for statistical analysis; this was applied to all datasets.

All statistics were performed using SPSS, R version 3.0.2 and/or Microsoft Excel. Missing data have a significant effect on results and so NA values were replaced with 1 prior to any statistical analysis [223]. A Student's t-test or an ANOVA followed by Tukey's HSD test were applied to test differences between data classes. A PCA was used to illustrate variation both within and between data classes. Final *p*-values were adjusted for multiple comparisons using Bonferroni correction. P-values < 0.05 were considered to be significant.

3.5 RESULTS

3.5.1 Biological variation in VOCs from C57BL/6 mice

Inspection of overlaid gas chromatograms from faecal pellets from both female (*n*=6) and male (*n*=6) C57BL/6 WT mice at each week showed the reproducibility and limited biological variation between individual mice **(Figures 3.2-3.9)**. This was not unexpected; C57BL/6 mice are nearly identical to each other, in genotype, as a result of long term in-breeding. Closer inspection of **Figures 3.2-3.9** revealed a shift in RT of peaks at 12.5 and 19.5 minutes. The peak at 12.5 mins was identified as acetic acid and was ubiquitous to all samples of both genders at every time point tested. At weeks 3, 5, 6 and 7, acetic acid is identified at a RT of 0.3 minutes later (12.8 mins) in a number of female mice and at weeks 1, 5, 6 and 7 in a number of male mice. The peak at 19.5 mins was identified as butanoic acid, also present in every sample tested. At weeks 3 and 5, for female mice, and weeks 1 and 6, for male mice, there appeared to be a RT shift of 0.2 minutes (19.7 mins) in a number of mice. In order to confirm that this, the mass spectrum was compared between samples at each RT shift occurrence **(Figure 3.1). Figure 3.1A** shows an example of this RT shift for acetic acid; upon examination of the mass spectrum pattern, the identity of acetic acid in all 6 female mice tested at week 3 was confirmed. Similarly, **Figure 3.1B** presents the RT shift in male mice at week 6 for butanoic acid, also confirming the identification as found using the NIST library. This was the case in both genders at each time point mentioned above. As this RT shift is <0.5 mins and uncommon, it was concluded to be a result of the samples being run over a period

of time and the GC-MS conditions may have varied slightly. Processing of the raw data for all 8 time points yielded two VOC master lists of 90 and 103 VOCs for female and male mice, respectively **(Table 3.2).** There were 83 VOCs shared between female and male mice, with 7 VOCs found exclusively in female mice and 20 in male mice.

To show the uniformity and reproducibility of the WT mouse strain, it was important to be able to show a low level of intra-mouse variability with regard to their VOC faecal profile. Using each master list, **Table 3.1** shows the number of VOCs specific to each time point and the percentage of which were identified in 50% of samples. Across the 8 weeks sampled, between 56.7 to 77.3% of VOCs were identified in at least 50% of samples from female mice, with week 5 having the lowest and week 6 having the highest number, showing the reproducibility of identified compounds between samples of individual female mice. Overall, there was a slightly lower percentage of VOCs identified in at least 50% of samples from male mice across all 8 weeks sampled, from 54.1% at week 3 to 70.2% at week 6. In both genders, week 6 (age 10 weeks old) data showed the largest percentage of total VOCs identified in at least 50% of samples.

To further investigate the biological variation between faecal samples from individual C57BL/6 female and male mice, the SD of the abundance of all VOCs was examined. Of the VOCs present in 50% of samples at each week, more than 50% were within ±3SD of the mean abundance for females and slightly lower for males (>40%), showing that a large number of VOCs varied very little between individual mice of both genders, at each time point **(Table 3.1).**

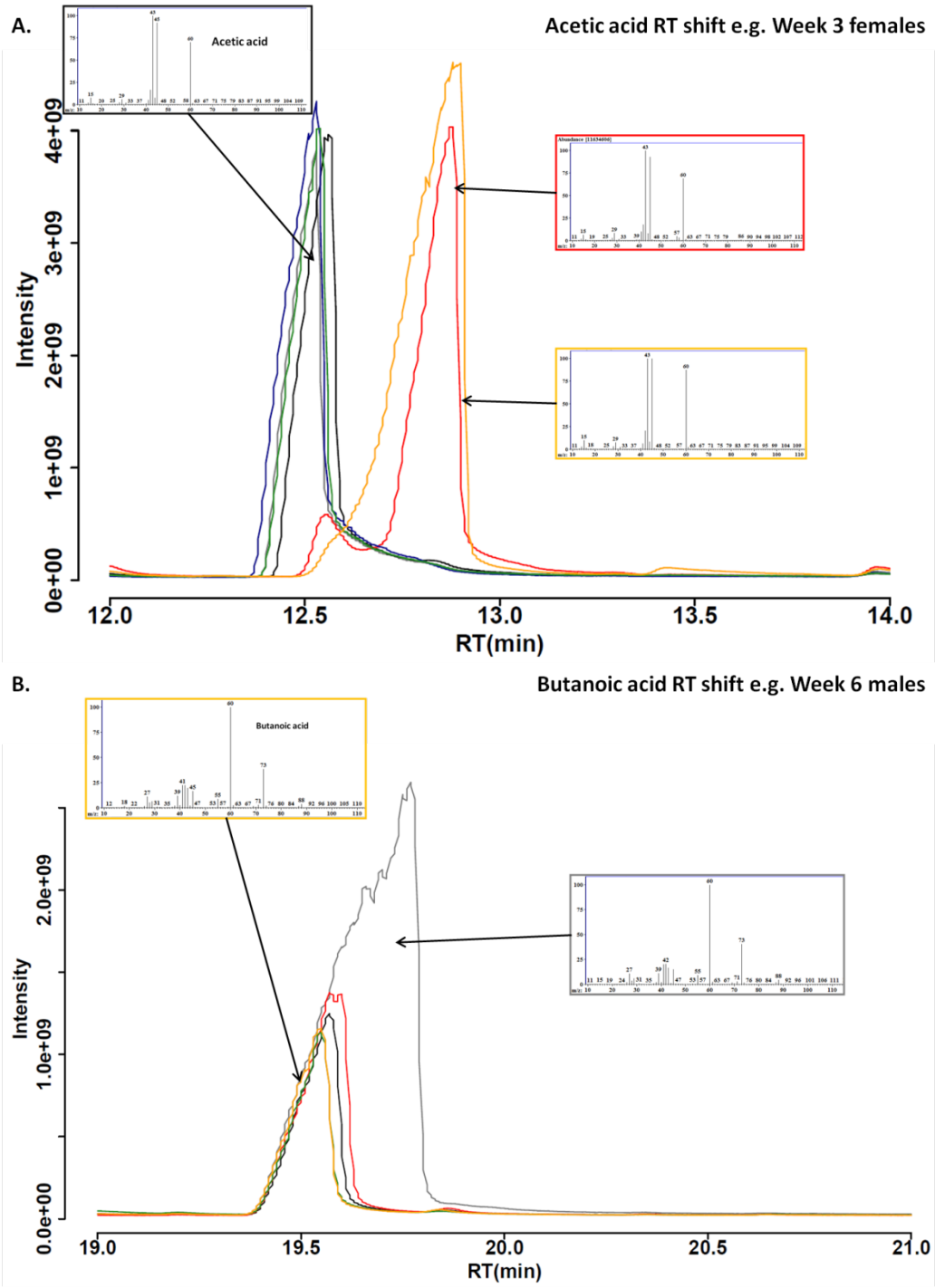

Figure 3.1 Comparison of MS pattern of acetic acid and butanoic acid between individual mice at specific time points. There was a shift in RT of compounds acetic acid (A.) and butanoic acid (B.) at 12.5 and 19.5 minutes, respectively. The MS pattern confirms there was a shift but that the peaks identified were the same compound for both cases.

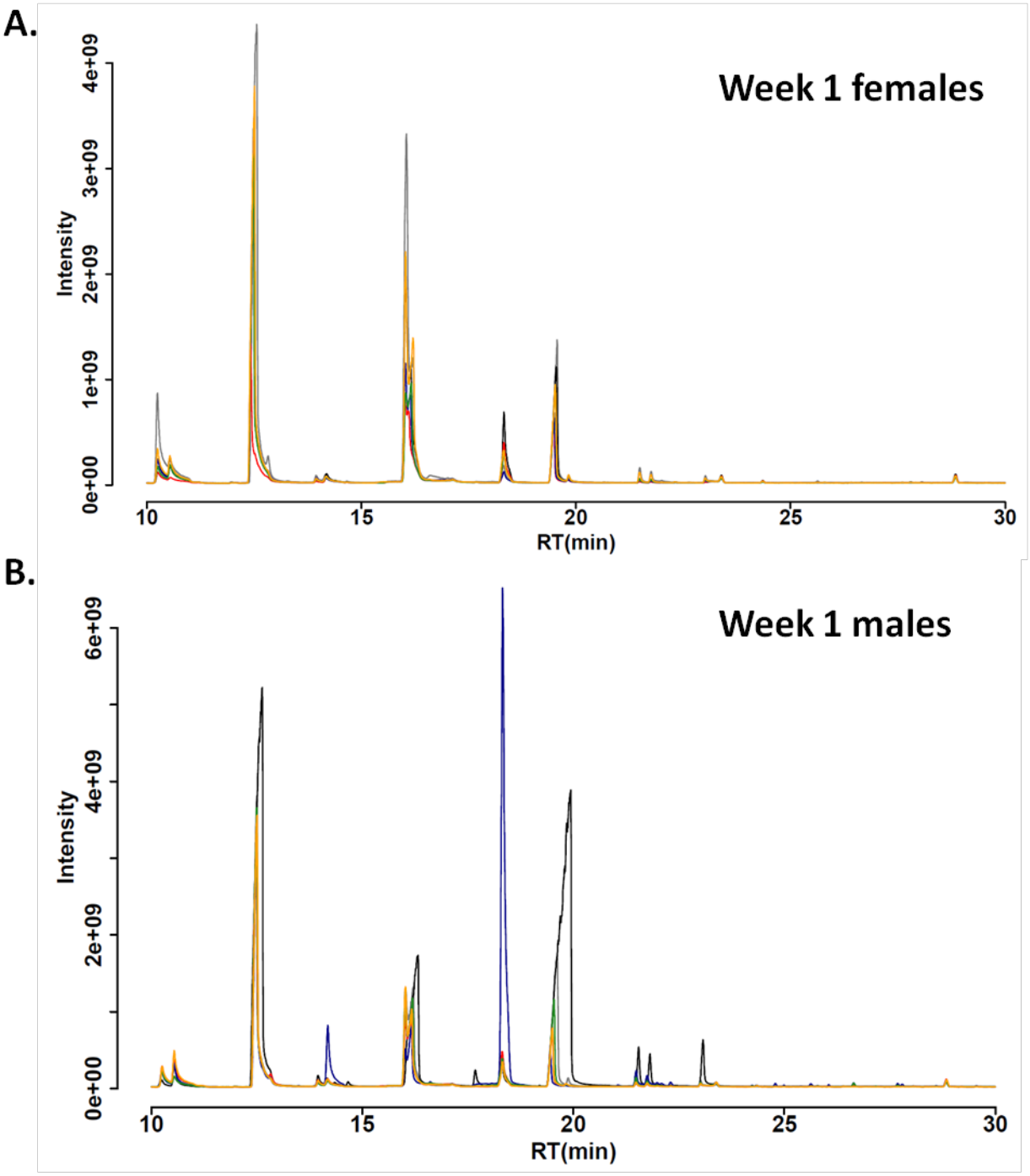

Figure 3.2 Overlay of gas chromatograms from female (*n*=6) (A.) and male (*n*=6) (B.) C57BL/6 murine faecal samples collected at experimental week 1 when mice were 5 weeks old. Samples were collected from all animals once a week and all samples were run through the GC-MS, method previously described. Peak intensity versus RT from 10 to 30 minutes (RT = retention time).

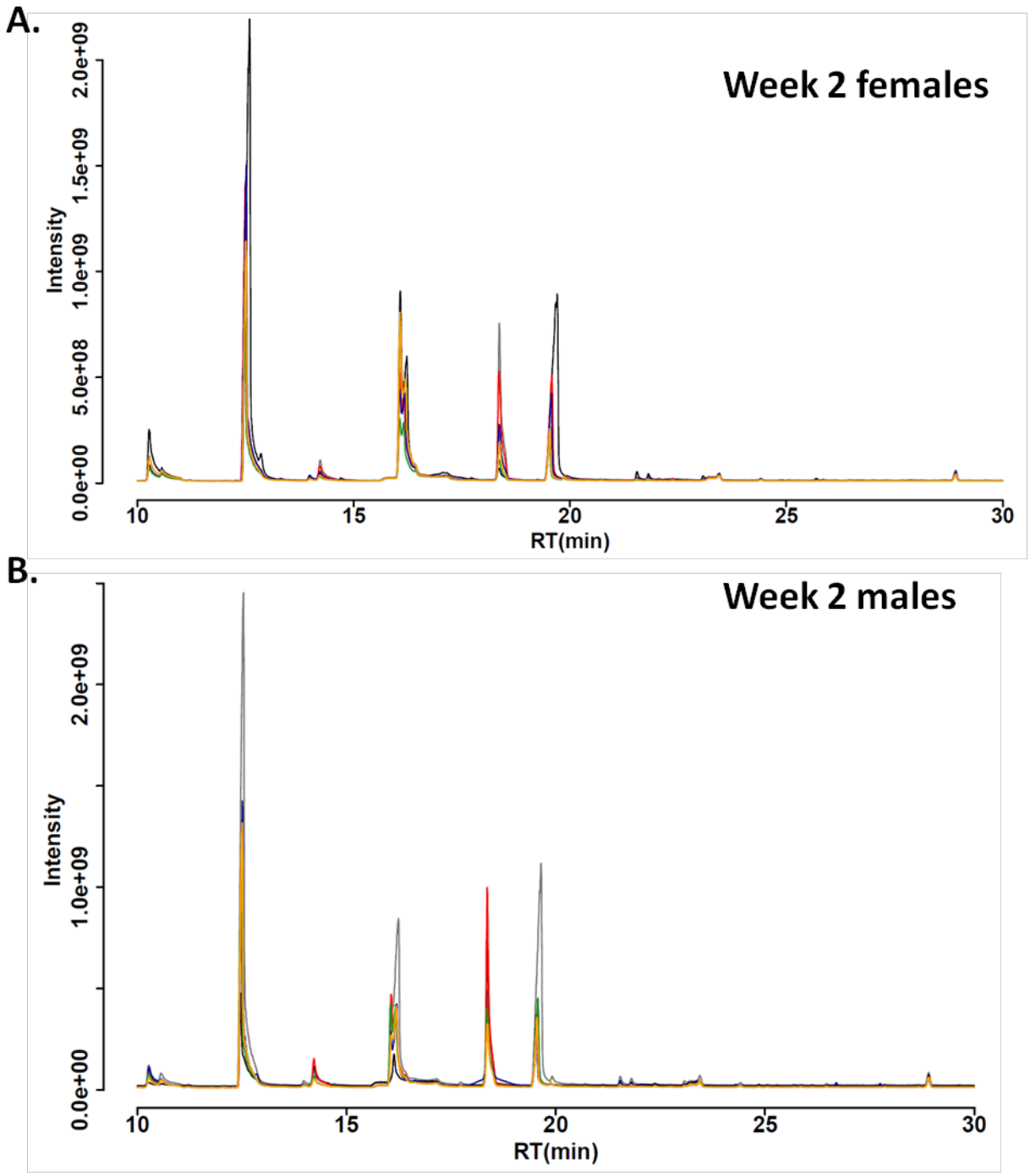

Figure 3.3 Overlay of gas chromatograms female (*n*=6) (A.) and male (*n*=6) (B.) C57BL/6 murine faecal samples collected at experimental week 2 when mice were 6 weeks old. Samples were collected from all animals once a week and all samples were run through the GC-MS, method previously described. Peak intensity versus RT from 10 to 30 minutes (RT = retention time).

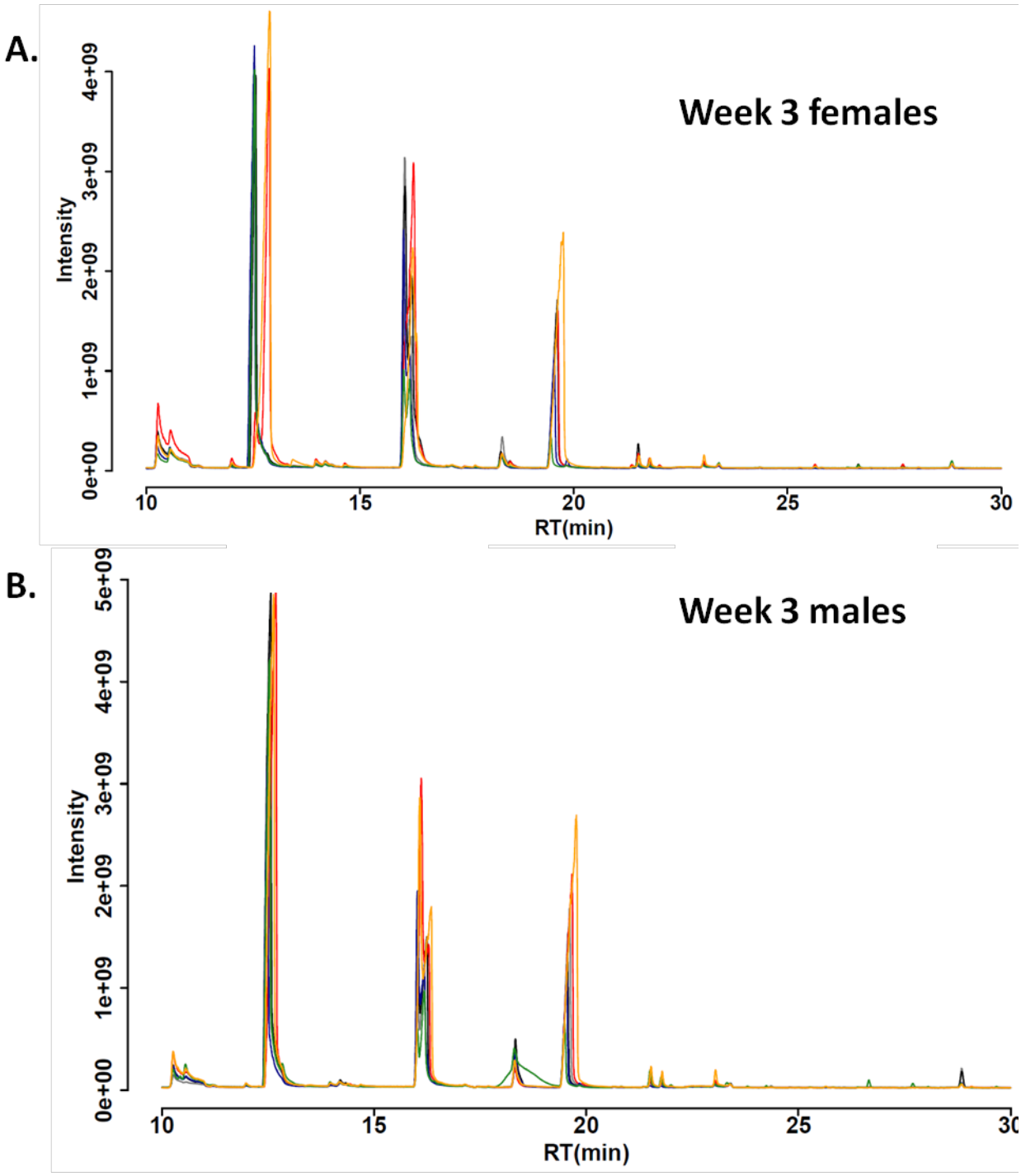

Figure 3.4 Overlay of gas chromatograms from female (*n*=6) (A.) and male (*n*=6) (B.) C57BL/6 murine faecal samples collected at experimental week 3 when mice were 7 weeks old. Samples were collected from all animals once a week and all samples were run through the GC-MS, method previously described. . Peak intensity versus RT from 10 to 30 minutes (RT = retention time).

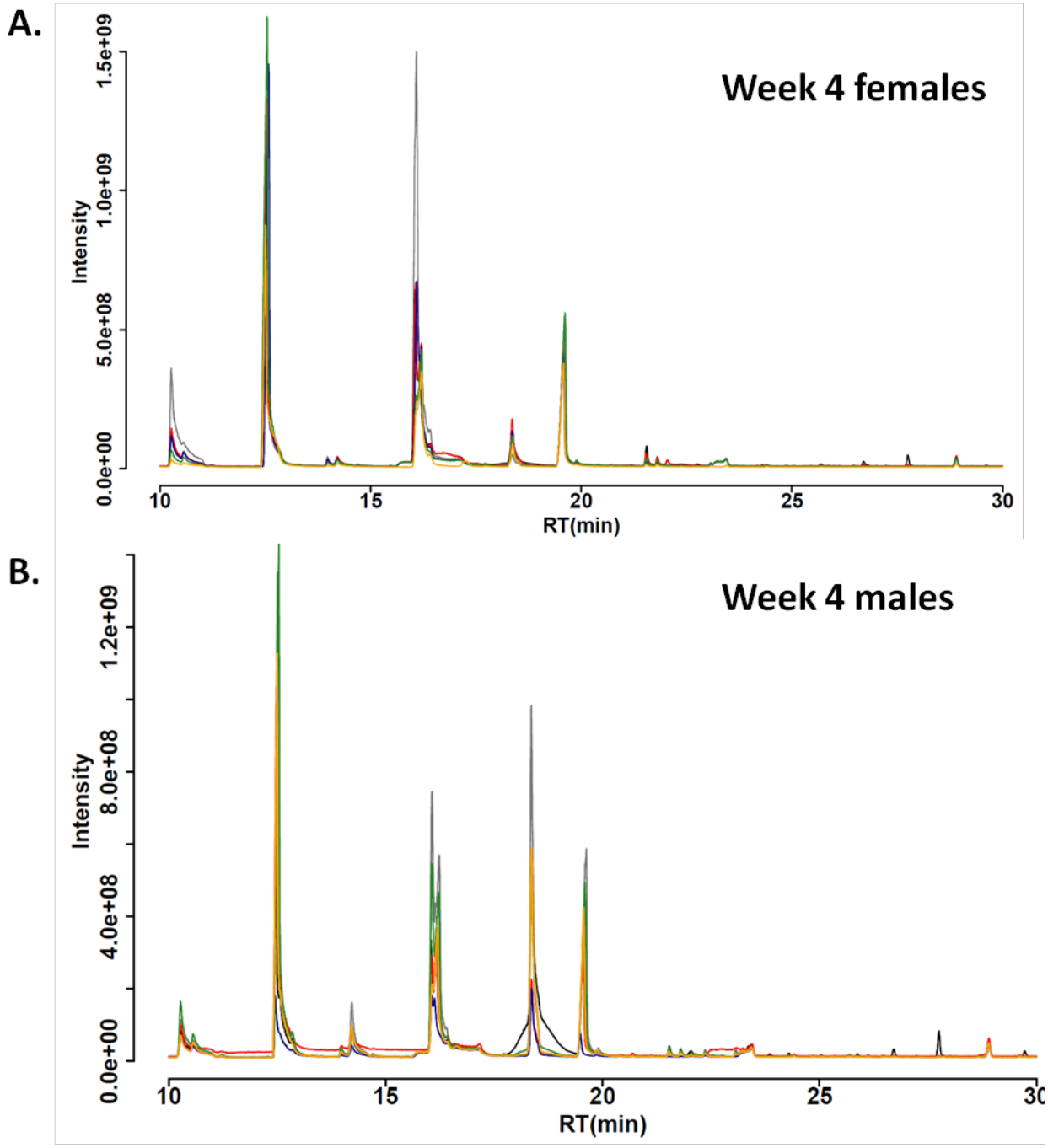

Figure 3.5 Overlay of gas chromatograms from female (*n*=6) (A.) and male (*n*=6) (B.) C57BL/6 murine faecal samples collected at experimental week 4 when mice were 8 weeks old. Samples were collected from all animals once a week and all samples were run through the GC-MS, method previously described. Peak intensity versus RT from 10 to 30 minutes (RT = retention time).

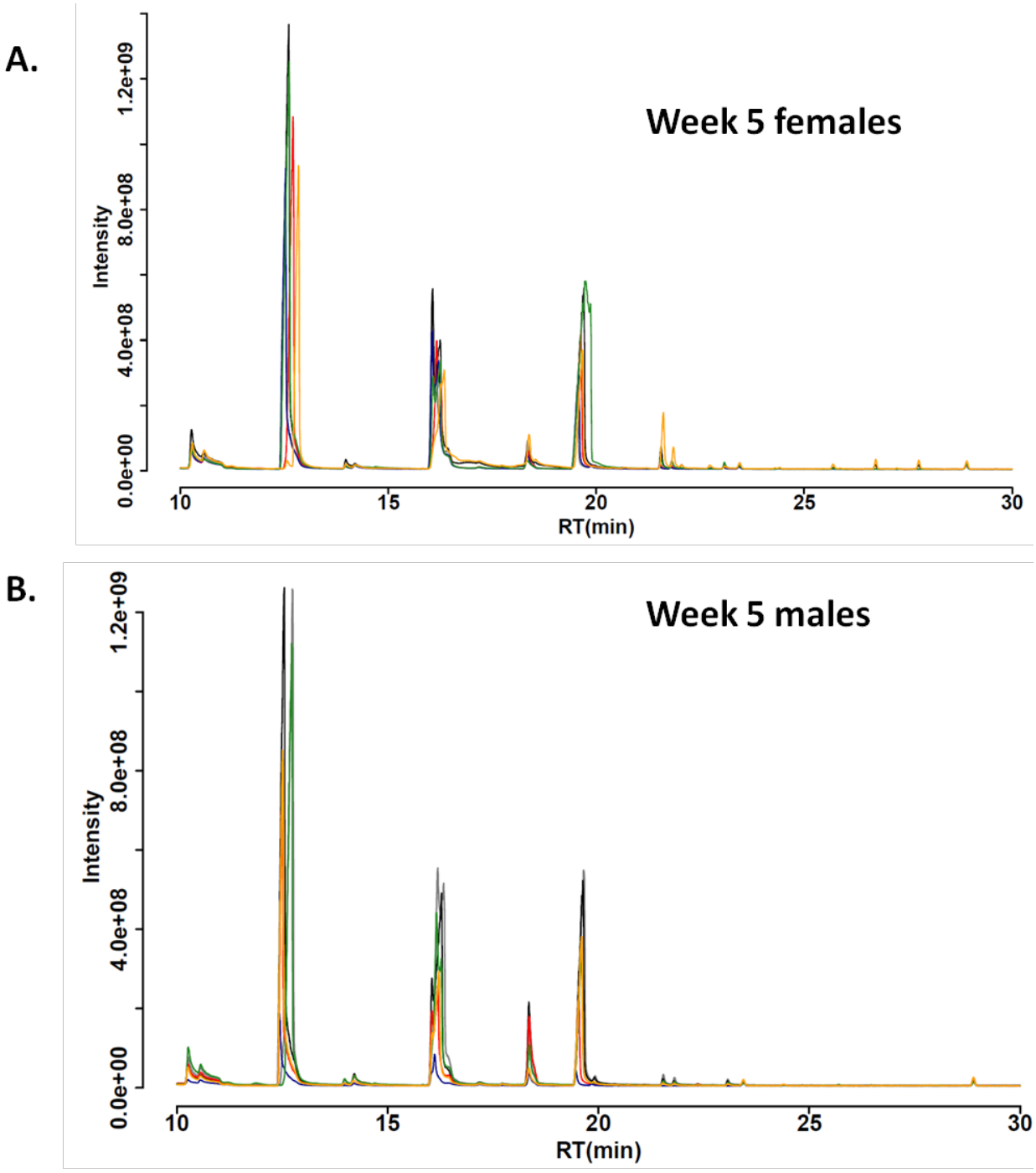

Figure 3.6 Overlay of gas chromatograms from female (*n*=6) (A.) and male (*n*=6) (B.) C57BL/6 murine faecal samples collected at experimental week 5 when mice were 9 weeks old. Samples were collected from all animals once a week and all samples were run through the GC-MS, method previously described. Peak intensity versus RT from 10 to 30 minutes (RT = retention time).

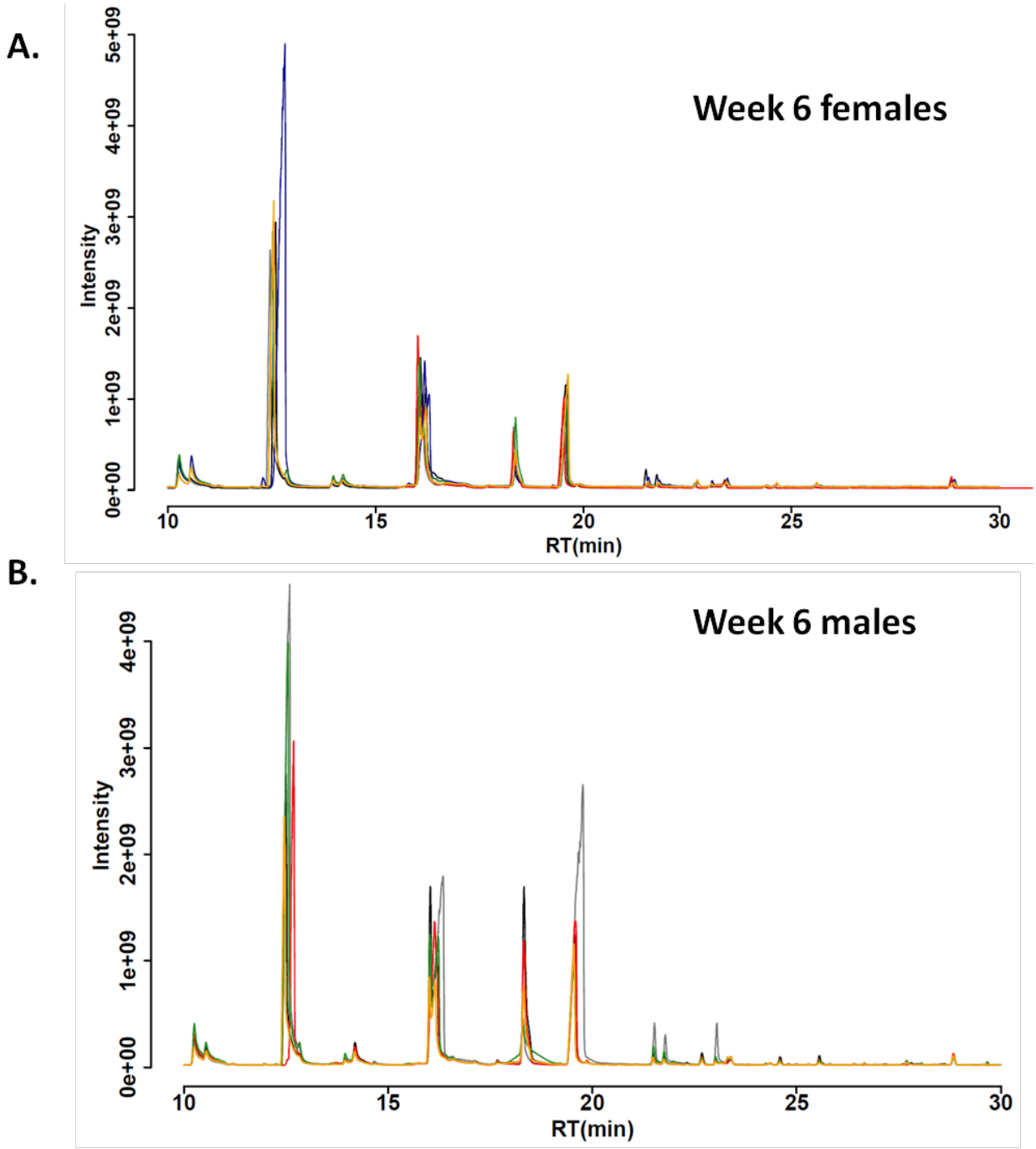

Figure 3.7 Overlay of gas chromatograms from female (*n*=6) (A.) and male (*n*=6) (B.) C57BL/6 murine faecal samples collected at experimental week 6 when mice were 10 weeks old. Samples were collected from all animals once a week and all samples were run through the GC-MS, method previously described. Peak intensity versus RT from 10 to 30 minutes (RT = retention time).

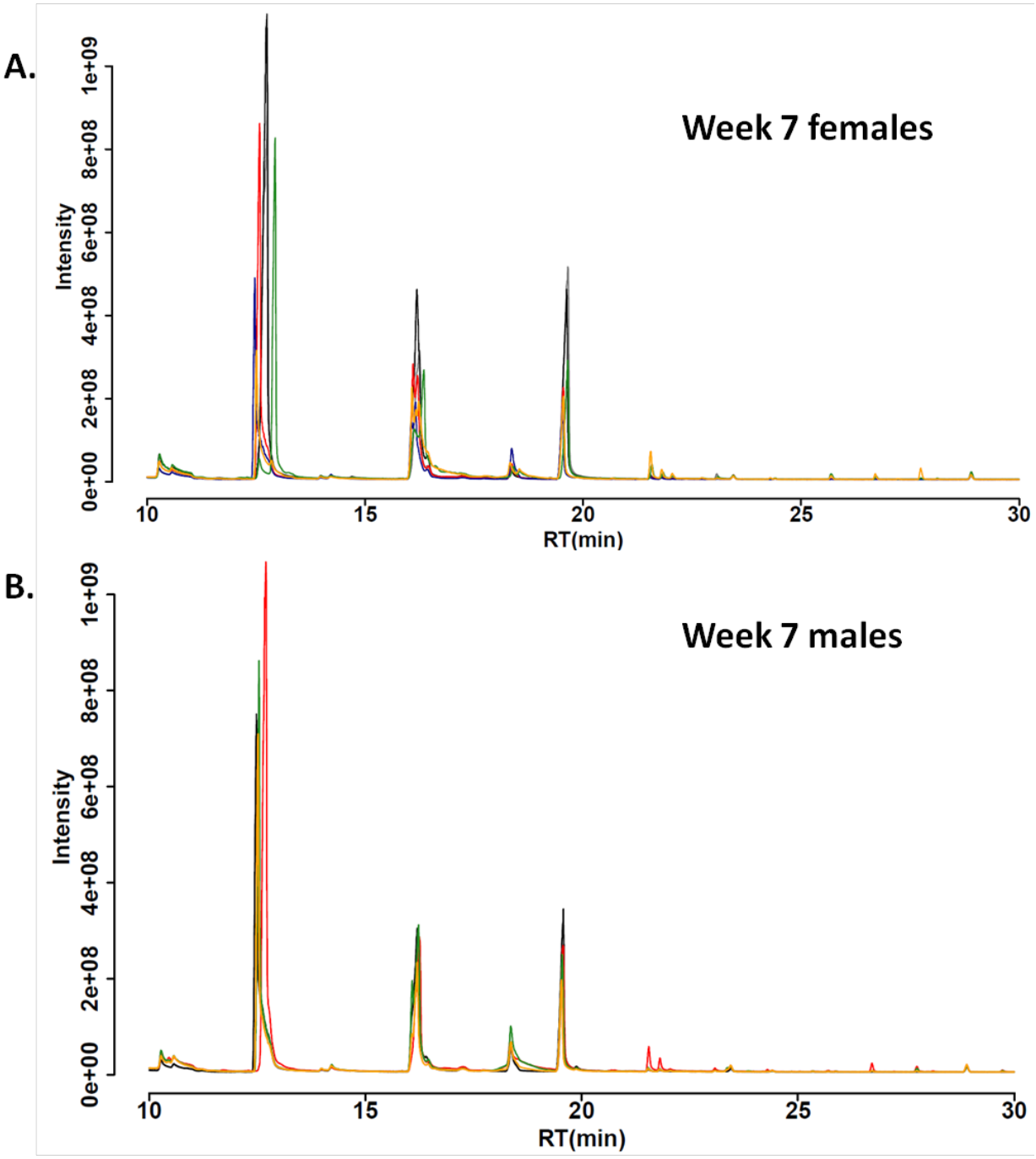

Figure 3.8 Overlay of gas chromatograms from female (*n*=6) (A.) and male (*n*=6) (B.) C57BL/6 murine faecal samples collected at experimental week 7 when mice were 11 weeks old. Samples were collected from all animals once a week and all samples were run through the GC-MS, method previously described. Peak intensity versus RT from 10 to 30 minutes (RT = retention time).

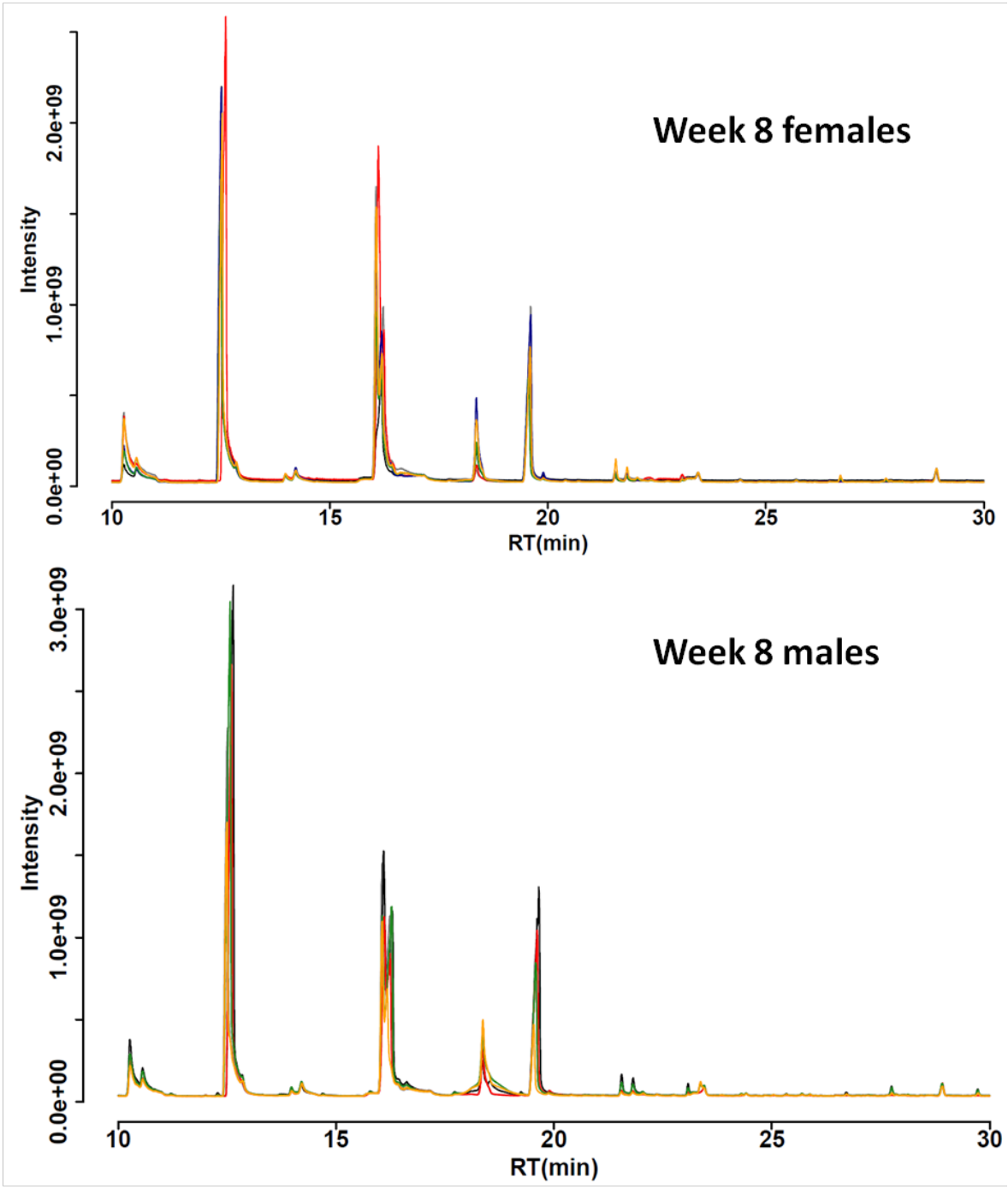

Figure 3.9 Overlay of gas chromatograms from female (*n*=6) (A.) and male (*n*=6) (B.) C57BL/6 murine faecal samples collected at experimental week 8 when mice were 12 weeks old. Samples were collected from all animals once a week and all samples were run through the GC-MS, method previously described. Peak intensity versus RT from 10 to 30 minutes (RT = retention time).

Table 3.1 Percentage of VOCs identified in 50% of samples at each time point for both female and male C57BL/6 mice and a percentage of which fall within ±3 SD of the mean abundance (*n*=6/gender).

	Females		
Weeks	**Total number of VOCs identified**	**Number of VOCs present in 50% of samples (% of total VOCs)**	**% of these VOCs within ±3SD of the mean abundance**
1	68	48 (70.6%)	66.7
2	62	39 (62.9%)	69.2
3	80	53 (66.3%)	77.4
4	59	37 (62.7%)	56.8
5	60	34 (56.7%)	58.8
6	75	58 (77.3%)	58.6
7	47	29 (61.7%)	65.5
8	70	44 (62.9%)	56.8
	Males		
Weeks	**Total number of VOCs identified**	**Number of VOCs present in 50% of samples (% of total VOCs)**	**% of these VOCs within ±3SD of the mean abundance**
1	88	50 (56.8%)	72.0
2	78	43 (55.1%)	61.7
3	85	46 (54.1%)	71.7
4	79	48 (60.8%)	68.8
5	49	32 (65.3%)	65.6
6	94	66 (70.2%)	74.2
7	44	26 (59.1%)	42.3
8	85	55 (64.7%)	43.6

Table 3.2 Master list of VOCs identified in HS gas of faecal samples from healthy male and female C57BL/6 mice across 8 experimental weeks from age 5 weeks to 12 weeks old (*n*=6/gender). Data presented as the percentage occurrence at each week and ordered according to 13 chemical classes; alcohols, acids, esters, aldehydes, alkanes, alkenes, alicyclic compounds, benzenoid compounds, heterocyclic compounds, ketones, nitrogen-, sulphur-containing and unidentified VOCs (w1 = week 1, etc).

	% occurrence at each week															
	Females								Males							
RT_compound	w1	w2	w3	w4	w5	w6	w7	w8	w1	w2	w3	w4	w5	w6	w7	w8
6.61_ethanol	100	100	100	100	100	100	83	100	100	100	100	100	100	100	100	100
7.61_isopropanol	100	100	100	100	100	100	100	100	83	100	100	100	100	100	100	100
9.57_1-propanol	100	0	100	0	17	100	0	50	100	67	100	17	0	100	0	100
10.77_2-butanol	33	0	17	0	0	50	0	17	17	0	17	0	0	80	0	100
11.19_2-methyl-3-buten-2-ol	0	0	0	0	0	0	0	0	17	33	0	33	0	60	0	20
11.90_1-propanol, 2-methyl-	100	0	100	0	0	100	0	33	50	0	100	0	0	100	0	80
13.44_1-butanol	0	0	33	0	0	0	0	0	0	0	0	0	0	40	0	0
16.08_3-buten-1-ol, 3-methyl-	0	0	33	0	0	17	17	0	0	0	0	0	0	0	0	0
14.00_1-penten-3-ol	0	0	0	0	0	0	0	0	0	0	67	0	0	0	0	0
17.45_1-pentanol	0	0	100	0	0	0	0	0	0	0	67	0	0	0	0	0
21.19_1-hexanol	0	0	83	0	0	0	0	0	0	0	100	0	0	0	0	0
25.12_1-octen-3-ol	0	0	83	0	0	0	0	0	0	0	33	0	0	0	0	0
28.14_phenol	17	17	67	0	33	67	17	17	83	17	33	17	17	60	20	40
12.51_acetic acid	100	100	100	100	100	100	100	100	100	100	100	100	100	100	100	100
16.29_propanoic acid	100	100	100	100	100	100	100	100	100	100	100	100	100	100	100	100
18.26_2-methyl-propanoic acid	83	67	100	83	83	50	67	67	83	33	83	33	67	60	60	100
19.62_butanoic acid	100	100	100	100	100	100	100	100	100	100	100	100	100	100	100	100
19.84_2,2-dimethyl-propanoic acid	83	83	67	83	50	83	17	83	100	100	67	100	83	60	60	80
21.51_3-methyl-butanoic acid	100	100	100	100	100	100	100	100	100	100	100	100	83	100	100	100
21.73_2-methyl-butanoic acid	100	100	100	100	100	100	100	100	100	100	100	83	83	100	80	100
23.14_pentanoic acid	100	67	100	100	100	100	83	100	100	100	100	67	83	100	60	100
26.38_hexanoic acid	83	33	50	0	0	50	0	67	100	33	50	50	0	60	0	20
34.02_propanoic acid, 2,2-dimethyl-, sodium salt	0	0	50	17	17	0	33	17	0	0	33	0	17	20	40	0
7.94_methyl acetate	33	17	67	17	0	50	0	50	50	0	67	17	0	60	0	60

Table 3.2 continued.

	% occurrence at each week															
	Females								Males							
RT_compound	w1	w2	w3	w4	w5	w6	w7	w8	w1	w2	w3	w4	w5	w6	w7	w8
10.53_ethyl Acetate	33	17	0	17	33	17	0	17	17	50	0	17	17	40	0	0
10.74_acetic acid ethenyl ester	17	50	67	50	17	50	17	33	0	50	33	33	17	0	20	20
11.21_methyl propionate	67	17	17	0	0	50	0	33	50	33	50	17	0	80	0	80
12.22_isopropyl acetate	0	17	33	67	17	67	50	17	0	0	17	17	0	80	20	60
14.69_methyl butyrate	83	17	33	50	17	100	33	67	100	67	50	33	50	100	0	100
17.72_ethyl butyrate	50	67	83	83	67	100	17	67	33	100	50	83	83	100	0	100
19.08_butanoic acid, 1-methylethyl ester	0	17	33	33	17	67	17	0	17	0	33	17	0	100	0	80
28.90_butyric acid, p-fluorophenyl ester	0	0	33	0	0	0	0	0	0	0	0	0	0	0	0	0
5.12_acetylaldehyde	33	83	50	67	67	33	50	33	17	50	17	33	50	0	0	20
7.11_2-propenal	17	33	50	0	0	0	0	17	17	0	67	17	0	40	0	20
7.21_propanal	100	100	100	100	100	100	67	100	100	100	100	100	100	100	100	100
9.01_2-methyl-propanal	100	100	100	100	100	100	100	100	100	100	100	100	83	100	100	100
10.16_butanal	50	33	0	0	0	33	0	0	67	33	17	33	0	80	0	40
12.49_3-methyl-butanal	67	33	33	50	17	83	50	50	83	33	17	50	17	80	0	40
12.81_2-methyl-butanal	100	83	33	100	67	67	83	100	100	67	50	83	33	100	40	80
14.20_pentanal	83	100	83	100	67	100	100	100	100	100	100	100	100	100	100	100
18.43_hexanal	100	100	50	100	83	83	100	100	100	100	83	100	100	100	100	100
18.51_2-butenal, 3-methyl-	0	0	50	33	33	17	33	33	0	0	0	0	0	0	0	0
20.96_2-hexanal	0	0	0	0	0	0	0	0	0	33	0	50	0	80	0	40
21.97_2-methyl-pentanal	0	0	0	0	0	0	0	0	33	0	17	17	17	0	0	0
22.33_heptanal	100	67	33	83	0	100	0	67	100	100	17	100	50	100	0	100
24.89_2-heptanal	17	33	0	0	0	17	0	33	50	83	17	50	0	80	0	60
26.08_octanal	0	33	0	0	0	33	0	0	67	33	17	67	0	60	0	0
27.67_5-ethylcyclopent-1-enecarboxaldehyde	0	33	0	0	0	17	0	0	17	50	33	33	0	60	0	0
28.62_2-octenal	0	0	0	0	0	0	0	0	17	17	0	50	0	40	0	0
29.57_nonanal	67	17	0	83	0	67	0	67	100	17	0	100	0	100	0	40
5.92_butane, 2-methyl-	17	33	33	17	50	50	0	17	0	50	0	50	33	0	0	40

Table 3.2 continued.

	% occurrence at each week															
	Females								Males							
RT_compound	w1	w2	w3	w4	w5	w6	w7	w8	w1	w2	w3	w4	w5	w6	w7	w8
6.42_pentane	83	83	17	67	17	83	17	67	83	100	33	100	83	60	20	40
12.63_hexane, 3-methyl-	0	0	0	0	0	0	0	0	17	17	0	33	0	20	0	0
16.64_octane	0	0	0	0	0	0	0	0	17	33	0	33	0	20	0	0
22.77_a-pinene	0	0	0	0	0	100	0	17	0	17	0	0	0	100	0	80
24.38_2,2,4,6,6-pentamethyl-heptane	100	100	83	100	83	100	67	100	83	100	17	100	33	80	60	100
27.01_6,8-dioxabicyclo[3.2.1]octane, 7-ethyl-5-methyl-, (1R-exo)-	0	0	0	0	0	0	0	0	33	0	0	17	0	20	0	20
27.68_undecane, 2,8-dimethyl-	50	0	17	0	0	50	0	0	33	17	0	0	0	40	0	40
27.84_heptane, 3,3-dimethyl-	67	0	0	0	0	50	0	17	50	0	0	0	0	80	0	60
28.93_diiodomethane	50	33	33	33	17	83	67	33	67	67	67	67	50	60	60	80
30.96_dodecane	100	50	67	0	0	83	0	67	83	33	33	0	0	100	0	100
16.58_toluene	0	33	0	33	83	0	0	0	0	33	17	33	50	0	40	0
22.67_bicyclo[3.1.0]hex-2-ene, 2-methyl-5-(1-methylethyl)-	33	33	0	0	17	0	0	17	0	0	0	50	0	0	0	20
27.53_7-exo-ethyl-5-methyl-6,8-dioxabicyclo[3.2.1]oct-3-ene	0	0	67	33	33	33	33	50	33	17	67	33	0	80	60	100
8.32_cyclopentane	83	50	100	50	67	83	0	83	50	100	100	33	100	100	60	60
17.94_oxirane, 2-methyl-2-(1-methylethyl)-	0	0	0	0	0	0	0	0	33	0	0	0	0	40	0	0
22.16_pentyl-oxirane	0	0	0	0	0	0	0	0	17	17	0	33	0	20	0	0
20.22_ethylbenzene	50	50	50	50	83	67	33	67	33	100	17	100	17	40	0	60
20.53_1,3-xylene	67	50	67	17	17	83	0	50	50	50	100	50	17	80	0	40
20.56_N-benzyloxy-2-carbomethoxyaziridine	0	0	0	0	0	0	0	0	0	17	0	0	0	40	0	40
25.73_benzaldehyde	83	67	100	83	67	83	50	83	100	67	100	100	67	80	0	100
33.74_benzene, 1, 3-bis(1,1-dimethylethyl)-	100	100	100	33	100	100	67	100	100	83	100	67	83	100	80	100
6.92_furan	0	0	0	0	0	0	0	0	17	0	17	0	0	20	0	40
10.32_furan, 3-methyl-	0	0	0	0	0	0	0	0	17	0	17	0	0	60	0	0
13.51_2-ethyl-furan	50	0	0	0	0	17	0	0	33	17	0	0	0	0	0	20
21.07_2-n-butyl furan	0	0	0	0	0	0	0	0	17	33	0	0	0	0	0	0
24.93_2-pentyl-furan	50	50	17	33	0	67	0	33	100	83	33	100	0	100	0	60
7.41_acetone	100	100	100	100	100	100	100	100	100	100	100	100	100	100	100	100

Table 3.2 continued.

	% occurrence at each week															
	Females								Males							
RT_compound	w1	w2	w3	w4	w5	w6	w7	w8	w1	w2	w3	w4	w5	w6	w7	w8
10.28_2,3-butanedione	100	100	100	100	100	100	100	100	100	100	100	100	100	100	100	100
10.56_2-butanone	100	100	100	100	100	100	100	100	100	100	100	100	100	100	100	100
13.98_2-pentanone	100	100	100	100	100	100	100	100	100	83	83	100	83	100	100	100
14.16_2,3-pentanedione	100	67	83	100	100	100	0	100	67	50	67	67	83	80	60	80
14.65_2-propanone, 1-hydroxy-	33	0	83	0	0	33	0	17	17	0	100	0	0	40	0	40
16.13_3-hydroxy-2-butanone	100	100	100	100	100	100	100	83	100	83	100	100	100	100	100	100
16.46_3-penten-2-one	0	0	0	0	17	0	33	0	33	17	17	50	0	60	0	40
16.98_1-propanone, 1-cyclopropyl-	17	17	50	0	0	17	0	17	0	0	0	0	0	0	0	0
18.10_methyl isobutyl ketone	0	0	33	0	0	17	0	0	33	0	0	0	0	0	0	20
19.73_2-hydroxy-3-pentanone	0	0	0	0	0	0	0	0	0	0	0	0	0	20	0	40
23.99_3-hepten-2-one	0	0	33	17	17	0	0	0	0	0	0	0	0	0	0	0
24.10_3-heptanone, 6-methyl-	0	0	33	17	33	0	33	33	33	17	17	50	0	60	20	60
25.79_2(5H)-furanone	67	50	83	0	33	0	0	0	100	67	33	0	0	20	0	20
22.11_2-heptanone	50	50	67	33	33	100	50	100	83	33	33	50	0	100	0	80
26.79_2(3H)-furanone, dihydro-5-methyl-	0	0	33	0	0	0	0	0	33	17	33	0	0	40	0	20
27.97_3-octen-2-one	0	0	0	0	0	0	0	0	0	0	0	17	0	40	0	0
28.15_1,3-difluoro-2-propanone	33	0	33	17	0	17	17	33	17	0	33	0	0	20	0	60
29.09_5-azacytosine	17	0	50	0	0	0	0	0	0	0	33	0	0	0	0	0
5.59_trimethylamine	0	0	0	0	0	0	0	0	17	17	17	17	0	40	40	40
7.82_thiourea	17	17	50	33	33	50	0	50	83	0	17	33	0	20	0	20
7.90_acetonitrile	50	100	67	83	67	67	0	67	50	100	83	83	67	60	0	60
10.40_nitromethane	0	0	0	0	0	0	0	0	17	17	33	17	0	60	40	60
14.33_hydrogen azide	0	0	33	0	0	17	0	0	0	0	0	0	0	0	0	0
22.56_pyrazine, 2,5-dimethyl-	0	0	17	17	33	0	33	17	50	17	17	0	0	0	0	20
23.37_2-acetyl-1-pyrroline	0	0	0	0	0	0	0	0	0	17	17	17	0	60	40	60
24.80_1,3,5-triazine	0	33	0	0	17	50	0	17	0	33	33	0	50	20	20	20
38.66_indole	33	50	67	50	50	100	50	83	100	50	83	50	33	80	20	80

Table 3.2 continued.

	% occurrence at each week															
	Females								Males							
RT_compound	w1	w2	w3	w4	w5	w6	w7	w8	w1	w2	w3	w4	w5	w6	w7	w8
26.66_dimethyl sulfone	33	17	100	33	50	83	50	83	83	50	83	83	0	100	80	100
23.27_unidentified	67	83	50	67	67	83	0	83	33	67	100	67	17	60	20	100
25.63_unidentified	33	0	17	0	17	0	0	17	17	0	67	0	17	0	20	20
25.82_unidentified	0	0	0	0	0	0	0	0	33	17	17	67	0	60	0	60
29.71_unidentified	0	0	0	0	0	0	0	0	17	17	17	50	0	100	40	60

3.5.2 Chemical composition of murine faecal pellets

Faecal pellets from C57BL/6 mice were rich in compounds at RTs between 10-30 mins with fewer VOCs identified before 10 or after 30 mins **(Figures 3.2 – 3.9).** Inevitably, some compounds can belong to more than one chemical class therefore the VOCs present in **Table 3.2** were sorted according to the following list of compound categories **(Table 3.3).**

Table 3.3 The number of VOCs grouped into each chemical class identified in at least 30% of samples from at least 1 time point from healthy C57BL/6 mice.

Chemical class of compounds	Number of VOCs
1: Alcohols	13
2: Acids	10
3: Esters	9
4: Aldehydes	18
5: Alkanes	11
6: Alkenes	3
7: Alicyclic compounds	3
8: Benzenoid compounds	5
9: Heterocyclic compounds	5
10: Ketones	19
11: Nitrogen-containing compounds	9
12: Sulphur-containing compounds	1
13: Unidentified compounds	4

The most common group of compounds identified in the headspace of faecal pellets from C57BL/6 mice were ketones with 19 in total. Acetone, 2, 3-butanedione, 2-butanone, 2-pentanone and 3-hydroxy-2-butanone were identified in >80% of samples from male and female mice at every time point. There were 18 aldehydes identified with propanal, 2-methylpropanal, 3-methylbutanal, 2-methylbutanal, pentenal and hexanal being common to every week in >60% of samples from males and females. The next most frequently identified chemical classes were alcohols, alkanes and acids. There were only 2 out of the 13 alcohols (ethanol, isopropanol) present at every time point for both genders and 3 out of 11 alkanes. Eight out of the 10 acids identified were present in >60% of samples for males and females at every time point.

3.5.3 Composition of mouse feed

Mice were fed a standard pelleted diet suitable for short term maintenance supplied by Special Diets Services (SDS), Essex, UK. Ingredients include wheat, wheatfeed, barley, de-hulled extracted toasted soya, maize, macro minerals, soya oil, potato protein, hydrolised wheat gluten, full fat soya, maize gluten meal, vitamins, micro minerals and amino acids. Aliquots of feed were run in triplicate to determine the VOCs present in it and were compared with the VOC profiles produced from analysis of murine faeces. Acetic acid, 3-methylbutanal, hexanal, 1-propanol and isopropanol were the VOCs emitted from the food at the highest abundance. A master-list of VOCs found in this food is included in **Table 3.4.** This masterlist was produced to allow the author to make note of any common VOCs throughout all future studies that may be present within the mouse chow.

Table 3.4 List of VOCs found in the chow fed to all mice housed in Liverpool

6.42_pentane
6.61_ethanol
6.92_furan
7.11_2-propenal
7.21_propanal
7.41_acetone
7.49_dimethyl sulfide
7.61_isopropanol
7.94_methyl acetate
8.12_pentane, 2-methyl-
8.61_3-methyl-pentane
9.01_2-methyl-propanal
9.07_hexane
9.57_1-propanol
9.89_2,2-dimethylpentane
10.16_butanal
10.28_2,3-butanedione
10.31_cyclopentane, methyl-
10.32_furan, 3-methyl-
10.56_2-butanone
10.77_2-butanol
11.19_2-methyl-3-buten-2-ol
11.64_cyclohexane
11.90_1-propanol, 2-methyl-
12.49_3-methyl-butanal
12.51_acetic acid
12.63_hexane, 3-methyl-
12.70_heptane
12.81_2-methyl-butanal
13.51_2-ethyl-furan
14.00_1-penten-3-ol
14.20_pentanal
15.94_dimethyl disulfide
16.05_cyclobutanone, 2,2,3-trimethyl-
16.06_1-butanol, 3-methyl-
16.29_propanoic acid
16.46_3-penten-2-one
16.58_toluene
16.64_octane
17.45_1-pentanol
18.10_methyl isobutyl ketone
18.43_hexanal
19.42_hydroxymethyl 2-hydroxy-2-methylpropionate
19.62_butanoic acid
19.84_2,2-dimethyl-propanoic acid
20.53_1,3-xylene
20.56_N-benzyloxy-2-carbomethoxyaziridine
20.96_2-hexanal
21.07_2-n-butyl furan
21.19_1-hexanol
21.51_3-methyl-butanoic acid
21.73_2-methyl-butanoic acid
22.11_2-heptanone
22.33_heptanal
22.67_bicyclo[3.1.0]hex-2-ene, 2-methyl-5-(1-methylethyl)-
22.77_a-pinene
23.14_pentanoic acid
23.27_unknown
23.62_3-(methylthio)-propanal
24.36_pentane, 2, 2, 3-trimethyl
24.38_2,2,4,6,6-pentamethyl-heptane
24.89_2-heptanal
24.93_2-pentyl-furan
25.12_1-octen-3-ol
25.34_dimethyltrisulphide
25.54_butyrolactone
25.63_(1H)pyrrole-3-carbonitrile, 2-methyl-
25.63_unknown
25.73_benzaldehyde
26.08_octanal
26.38_hexanoic acid
26.79_2(3H)-furanone, dihydro-5-methyl-
27.67_5-ethylcyclopent-1-enecarboxaldehyde
28.14_phenol
28.62_2-octenal, (E)
28.66_benzeneacetaldehyde
29.57_nonanal
30.27_2(3H)-furanone, 5-ethyldihydro-
30.96_dodecane
31.81_2-nonenal
33.74_benzene, 1, 3-bis(1,1-dimethylethyl)-

3.5.4 Significant effect of age and gender on the presence of VOCs

A two-way, repeated measures ANOVA was performed on the average number of VOCs identified across time for male and female C57BL/6 mice. There was a significant main effect of time, F (7, 35) = 23.12, p<0.001. This means if other dependent variables (gender) are ignored, the average number of VOCs identified is different across time. There was also a significant main effect of gender, F (1, 5) = 36.68, p<0.01. This effects means if time is ignored, the number of VOCs were different between males and females. In addition, there was a significant interaction between the two variables, time and gender, F (7, 35) = 4.21, p<0.01. This means that the number of VOCs identified for both male and female mice were different for the different time points **(Figure 3.10).** There was a lower number of VOCs identified at weeks 5 and 7, compared to all other weeks, and the moving average was plotted to smooth out these small fluctuations in the data.

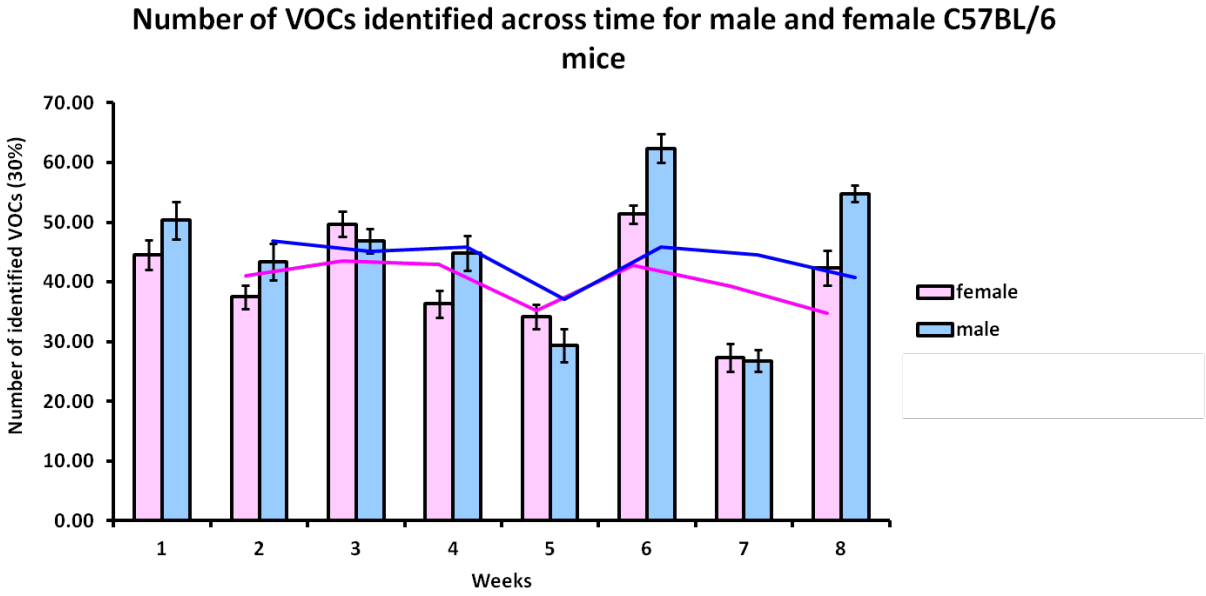

Figure 3.10 Number of VOCs identified in the HS of murine faecal samples collected during 8 consecutive weeks in both female (n=6) and male (n=6) C57BL/6 mice (data expressed as mean±SEM). The pink line is the rolling average for female mice and the blue line is the rolling average for male mice, both showing the trend of number of VOCs over time for both genders.

3.5.5 The effect of gender on murine faecal volatile metabolomic profiles

The effect of gender on the HS faecal pellet VOC metabolomic profile was then investigated in healthy WT C57BL/6 mice. A PCA derived from compound concentrations in murine faecal pellets collected weekly for 8 weeks revealed separation between male and female mice at most time points, with the exception of weeks 2 and 5 **(Figure 3.11).** The largest degree of separation between males and females appeared at weeks 1, 4, 6 and 8. Therefore, at ages 5, 8, 10 and 12 weeks old, respectively, the faecal metabolome of male and female mice appear to be the most different.

In order to investigate which individual VOCs contributed to this separation, the PCA biplot was examined for each time point and univariate statistical tests were performed. There were 7, 1, 4, 6, 3, 5, 5 and 4 compounds found to significantly vary between male and female mice at weeks 1, 2, 3, 4, 5, 6, 7 and 8, respectively (Student's *t*-test, $p<0.05$). The majority of these significant compounds were either increased in males at each time point compared to females, or absent in females. The compounds included 2-pentanone, 3-methylbutanoic acid, phenol, indole and thiourea at week 1; propanoic acid at week 3; pentanal, hexanal, 2-pentylfuran and propanal at week 4; pentane and propanal at week 5; pentanoic acid and 2-heptanal at week 6; propanoic acid, acetone and isopropanol at week 7 and 2-butanol and propanal at week 8. There was one compound unique to males (octanal) at week 1 and week 4 and one unique to females (2(5H)-furanone) at week 1 and week 3. 1-propanol was unique to males at week 2 and week 6 and 1-penten-3-ol at week 3. One compound was found exclusively in males at week 6 (1-hexanal) and week 8 (butanoic acid, 1-methylethyl ester) and two in females at week 7 (3-penten-2-one and 3-methyl-2-butenal).

There are a number of compounds responsible for the separation between males and females at each time point, thus creating a unique profile for male versus female C57BL/6 mice between the ages of 5 to 12 weeks old.

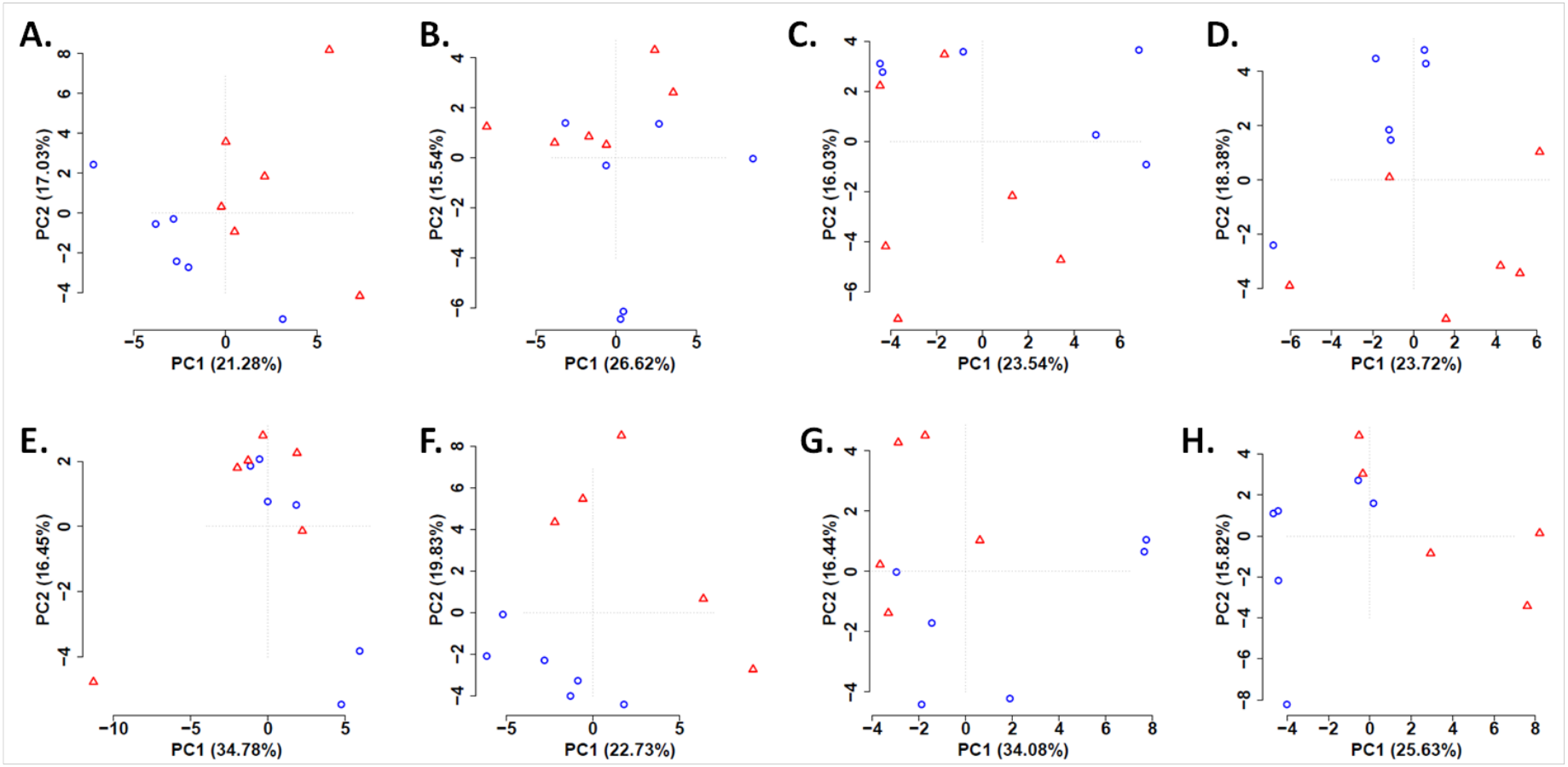

Figure 3.11 A PCA for the VOC metabolomic profiles of male and female C57BL/6 mice at each experimental week tested, weeks 1-8 (A-H, respectively). All PCAs were performed on compounds present in at least 30% of one gender with missing data substituted with the value 1 and data were log transformed (circles = female (*n*=6), triangles = male (*n*=6)).

3.5.6 The effect of age on murine faecal volatile metabolomic profiles

The C57BL/6 faecal VOC profile can separate males from females at certain time points and the longitudinal VOC profiles for males and females were examined individually. A one-way ANOVA was performed on the time series data for males and females, in order to identify those compounds that significantly varied according to time.

This analysis identified 29 and 25 compounds which significantly varied over time for males and females, respectively (ANOVA with Bonferroni multiple comparison correction, $p<0.05$). A PCA of these significantly different compounds showed a tight clustering pattern at all 8 time points for both male **(Figure 3.12)** and female **(Figure 3.13)** mice, which appeared very similar between males and females. Similarities between the two were evident with week 3 (green) having complete separation from the rest of the data points. Weeks 1, 6 and 8 (blue, black and pink) appeared to overlap for both genders, as do weeks 2 and 4 (red and orange). It was observed earlier that weeks 5 and 7 had the lowest number of compounds identified for males and females **(Figure 3.10),** it seems these two weeks are most alike.

The ten most significant compounds that were found to vary over time for male C57BL/6 mice were 1-hexanol, pinene, 2-butanone, 1-propanol, nonanal, 2-methyl-1-propanol, ethanol, heptanal, 2, 3-butandione and propanoic acid ($p<0.001$). For females, the ten most significantly different compounds were 1-pentanol, isopropanol, pinene, 2-methyl-1-propanol, 1-propanol, 1-octen-3-ol, 1-hexanol, 2-butanone, propanoic acid and acetic acid ($p<0.001$). Six of these were shared for male and female. It was concluded that the VOC metabolomic profile from faecal pellets of C57BL/6 changes according to time, but the time-dependent metabolites appear to be similar in male and female mice.

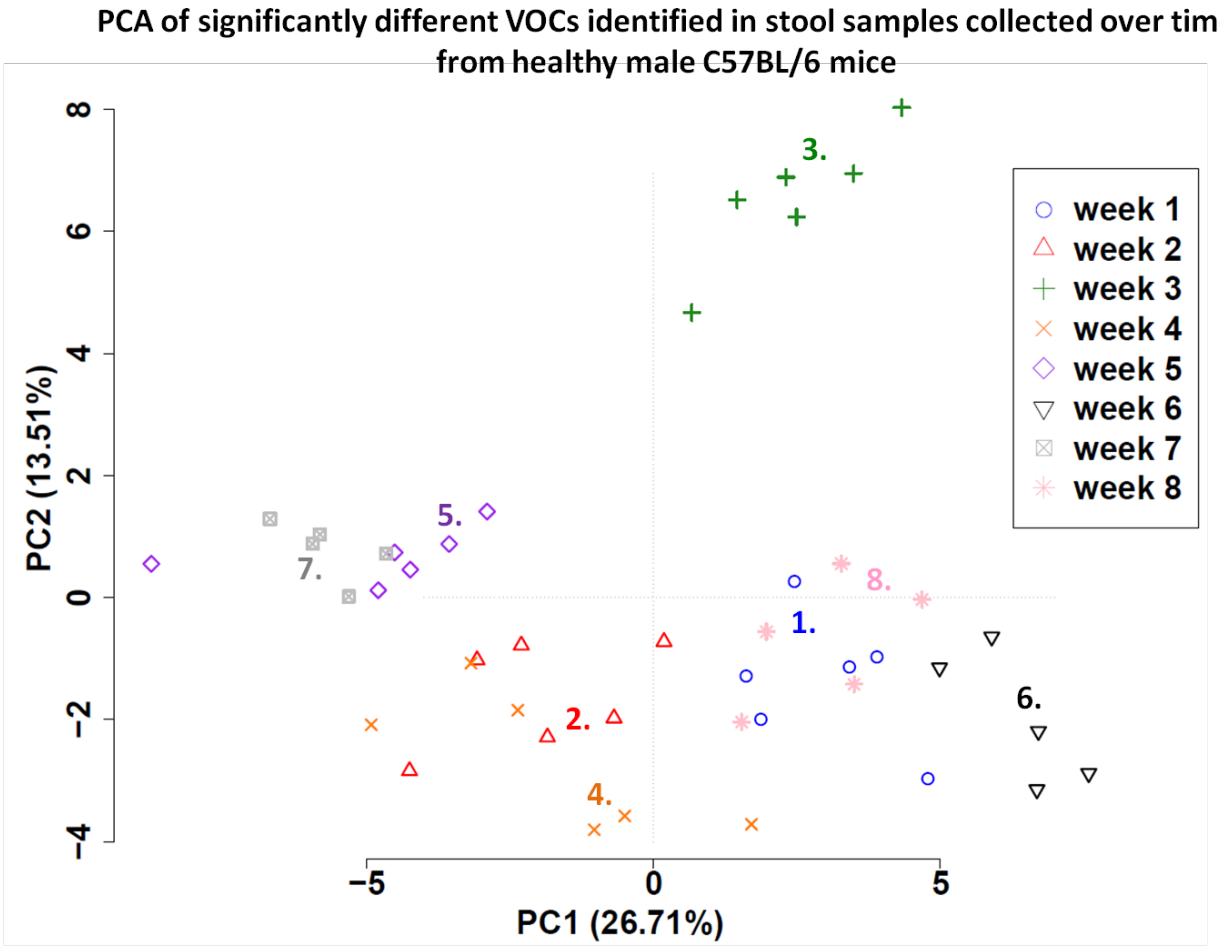

Figure 3.12 A PCA for the faecal samples from healthy male C57BL/6 mice (*n*=6) collected over time from the age of 5 to 12 weeks old. The first PC (26.71%) has been plotted against the second PC (13.51%). The PCA was performed using the 54 VOCs that were found to be significantly different over time (missing data substituted with the value 1, data were log transformed, *n*=12/groups, ANOVA followed by Tukey's HSD Bonferroni correction ($p<0.05$)).

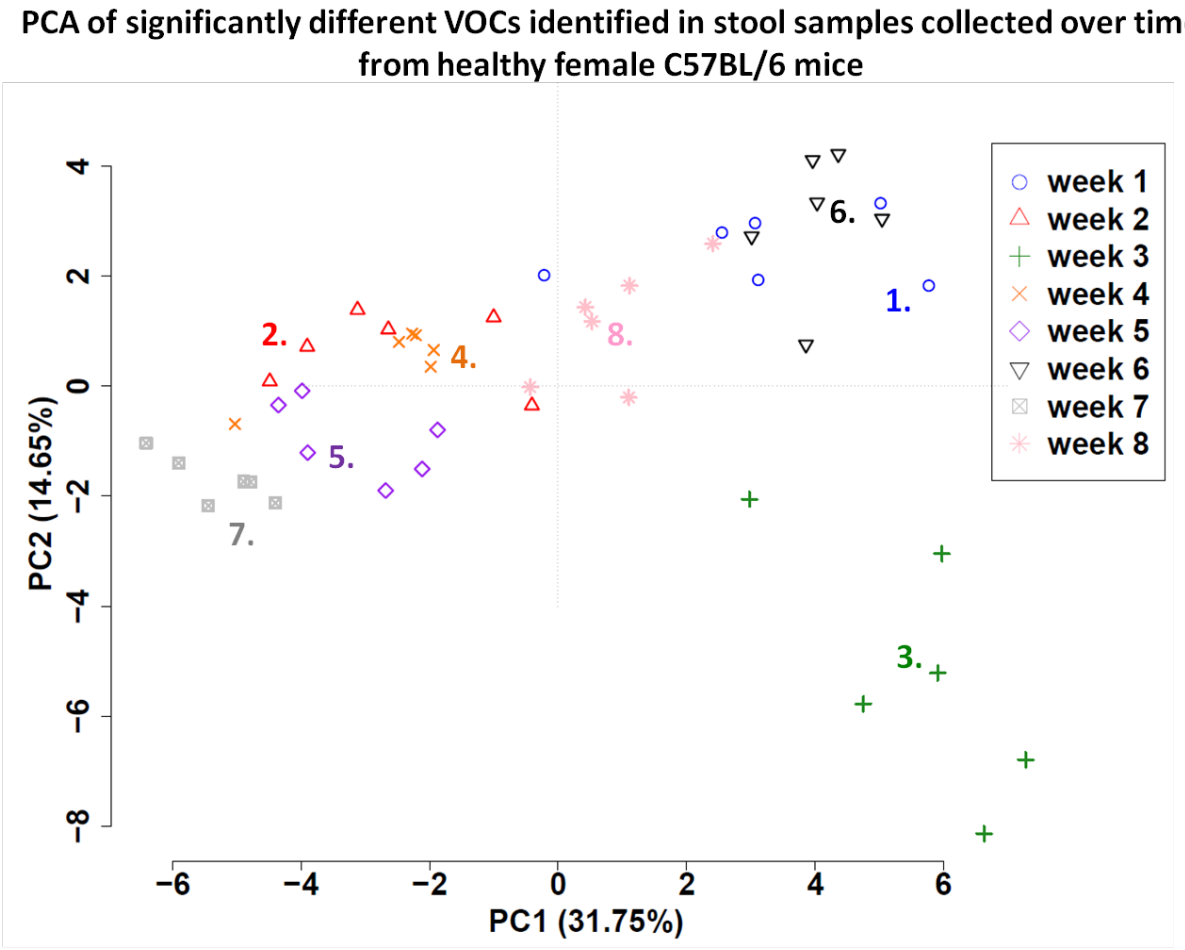

Figure 3.13 A PCA for the faecal samples from healthy female C57BL/6 mice (*n*=6) collected over time from the age of 5 to 12 weeks old. The first PC (31.75%) has been plotted against the second PC (14.65%). The PCA was performed using the 54 VOCs that were found to be significantly different over time (missing data substituted with the value 1, data were log transformed, *n*=12/groups, ANOVA followed by Tukey's HSD Bonferroni correction ($p<0.05$)).

3.5.7 Significantly different VOC profiles according to location of GI tract

Faecal content was collected at the end of the experiment (week 8) from the proximal (ascending) and distal (descending) colon and the small intestine (SI) and was compared to the faecal pellet collected earlier the same day from each mouse. Due to the very minor differences identified earlier between male and female mice, data was not separated according to gender for this comparison.

The number of compounds identified was compared. A significantly lower number of VOCs were identified in the SI content (26.2±1.5) compared to the faecal pellet (44.1±2.0), distal colon content (41.0±2.9) and the proximal colon content (45.9±2.0) (mean±SEM; ANOVA followed by Tukey's HSD, $p<0.001$) **(Figure 3.14A).** The chemical composition of VOCs emitted from all four groups of faecal matter appeared relatively similar. Ester compounds were responsible for 8.7, 13.4 and 14.5% of total VOC composition in the faecal pellet, distal and proximal colon, respectively. However, no esters were identified in the small intestine content. This could explain the significant reduction in the number of VOCs identified in the SI content. One alicyclic compound, cyclopentane, was identified in the faecal pellet (72% of samples) and the proximal colon content (18% of samples) but it was absent in the small intestine content and the distal colon content. Similarly, there were no sulphur-containing compounds found in the distal colon content **(Figure 3.14B).**

A total of 86 compounds were identified across all four groups (present in at least 30% of samples in at least one group). To further investigate differences in these VOC profiles, the abundances of these 86 VOCs were compared, resulting in 74 significantly different VOCs (ANOVA, $p<0.05$). A PCA plot using these 74 VOCs shows the differences between the VOC constituents identified and their abundances in the HS of samples taken from different locations of the small and large bowel. The clustering of similar samples is evident showing reproducibility between individual C57BL/6 mice. The PCA shows that the faecal content collected from the proximal (green) and distal colon (red) overlap; therefore they have the most similar VOC

profiles in this comparison. There is a clear separation between the pellet (blue) and the small intestine content (orange) from each other and the combined colon content groups. There was an increase in the levels of most esters in the distal colon content combined with other compounds such as 2-nonanone, phenol, 3-pent-2-one, butanal and furan, 3-methyl being responsible for the separation between the faecal pellet samples and the distal and proximal colon content, where they were most abundant. Dimethyl sulfone, 2,2-dimethyl propanoic acid and 2-butanol were most abundant in the pellet with pyrrole influencing the separation of the small intestine samples **(Figure 3.15).** Understanding these apparent differences will be useful when analyzing samples from murine models of the GI disease.

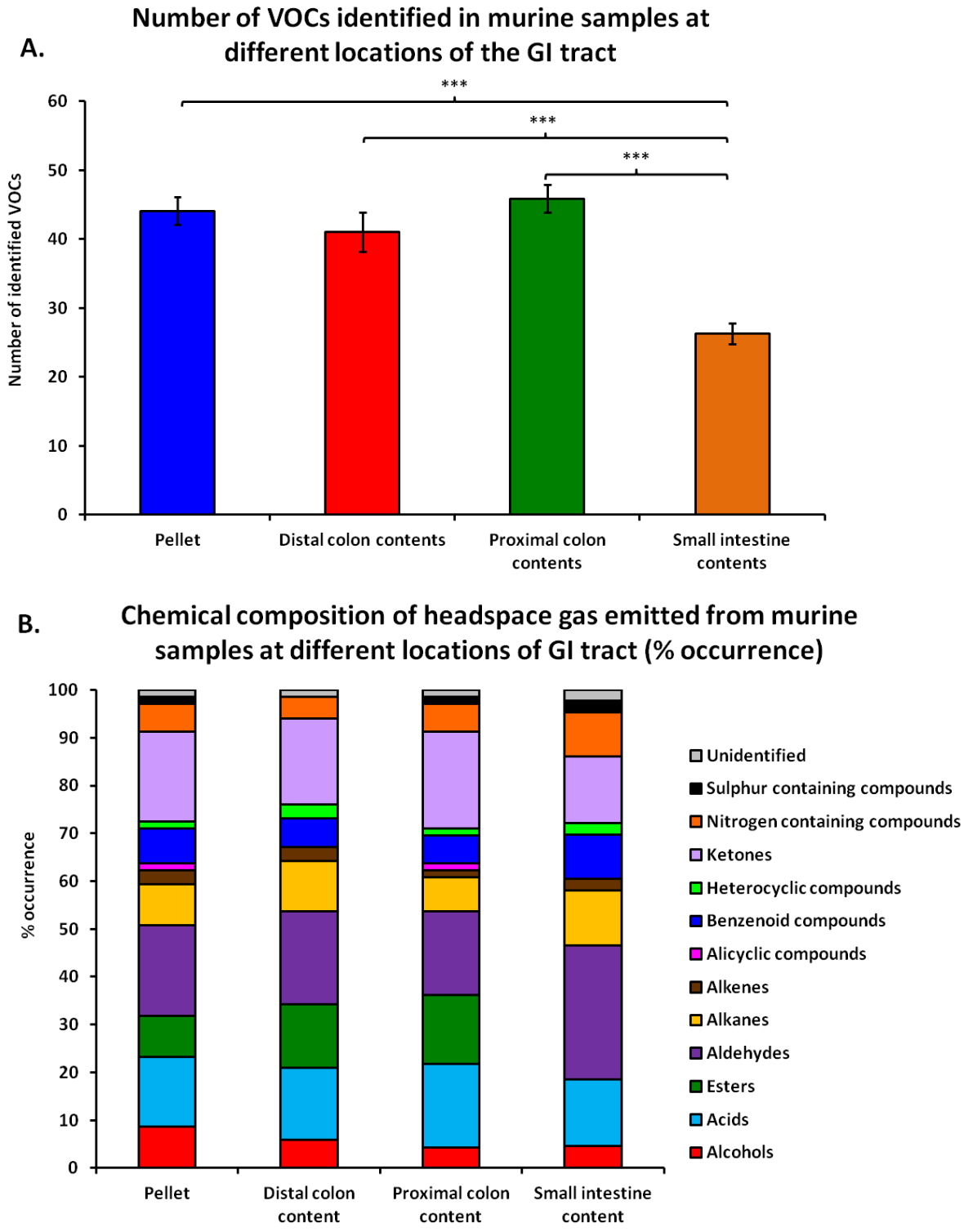

Figure 3.14 The faecal pellet was compared to the faecal content taken from the distal and proximal colon and the small intestine. There was a significant difference between the number of compounds identified when comparing the pellet, distal and proximal colon content to the small intestine content (A.) (Data expressed as mean±SEM, *n*=12/group, ANOVA followed by Tukey's HSD test ***p<0.001). The chemical composition of VOCs across the different groups appears similar with an absence of esters identified in the small intestine content (B).

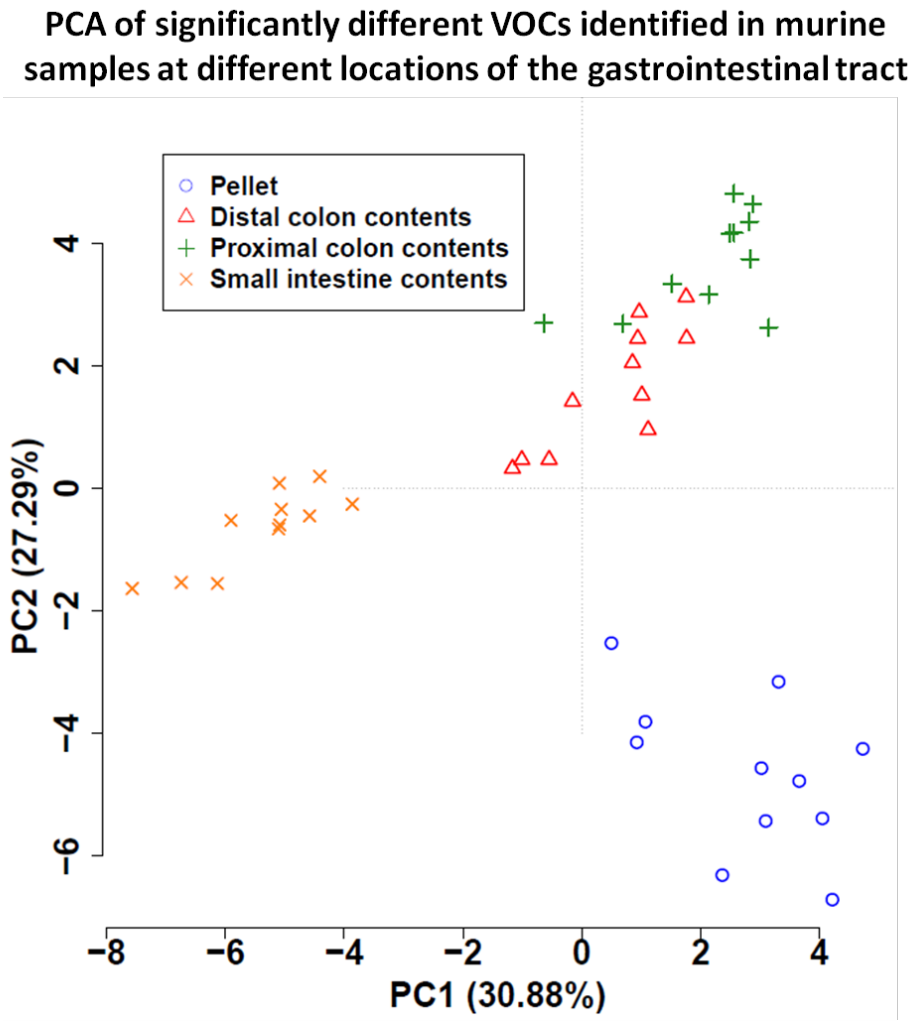

Figure 3.15 A PCA for the faecal samples from healthy female and male C57BL/6 mice sampled at the different regions of the GI tract: cage pellet, distal colon contents, proximal colon contents and small intestine contents. The first PC (30.88%) has been plotted against the second PC (27.29%). The PCA was performed using the 74 VOCs that were found to be significantly different across the four groups (data were log transformed, *n*=12/groups, ANOVA followed by Tukey's HSD ($p<0.05$)).

3.5.8 Impact of a germ-free VOC metabolome

In this study, the impact of the intestinal microbiota on the VOC faecal metabolome of laboratory mice from MRC Harwell, Oxford was investigated using SPME coupled to GC-MS. Specifically, the impact of the host VOC on the faecal metabolome was investigated. Samples collected from GF animals were from a mixture of C3H/HeN and *Junbo* (on a C3H/HeN background) male and female mice. GF and their non-GF strain matched SPF animal groups were of the same age and fed the same diet. Analysis of the headspace gas emitted from faecal pellets of GF and non-GF equivalent mice (SPF housed) identified 54.3±1.3 and 77.0±1.9 compounds, respectively (mean±SEM); thus, there were significantly more VOCs identified in SPF non-GF mice, compared to GF mice (Student's *t*-test, $p<0.001$) **(Figure 3.16).**

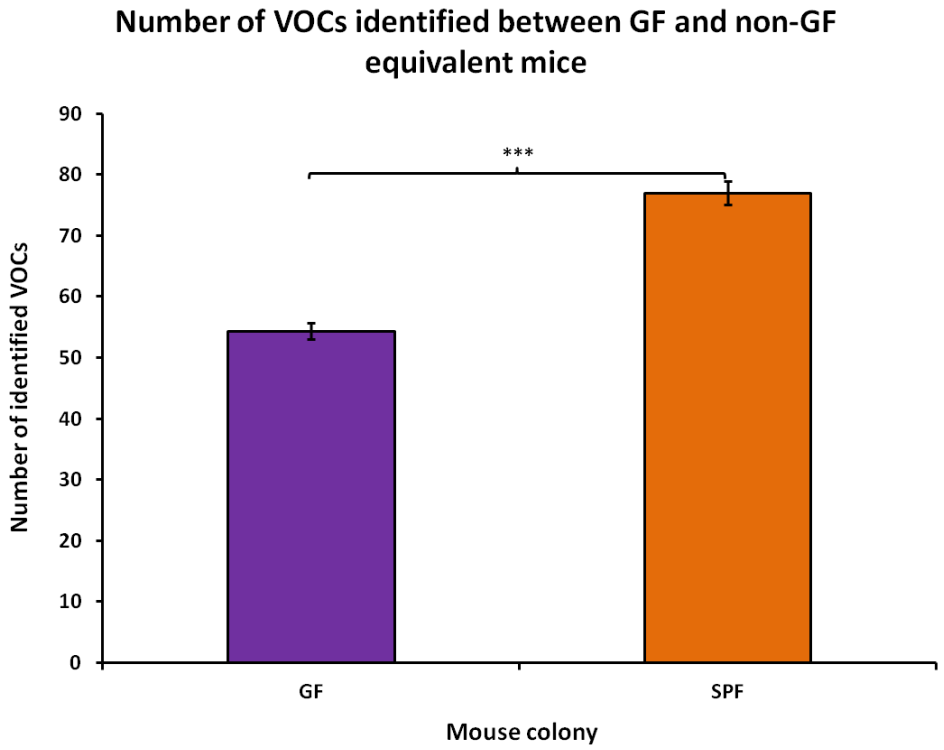

Figure 3.16 Number of VOCs identified in the HS of murine faecal samples collected from a mixture of *Junbo* and C3H/HeN GF mice (*n*=6), and non-GF SPF equivalent (*n*=6), provided by MRC Harwell, Oxford (data expressed at mean±SEM, Student's *t*-test ***$p<0.001$).

The quantitative differences between the two groups were then explored; there were 64 significantly different VOCs (Student's *t*-test with Bonferroni multiple comparison correction, $p<0.05$). Of these 64 VOCs, 35 were absent in GF faecal samples and were found exclusively in the faecal samples of the non-GF equivalent mice, of which the majority were acid and ester compounds. There were 12 VOCs unique to GF faecal samples including 8 alkanes. The abundance of 5 compounds was significantly greater in GF compared to non-GF, of which 3 were aldehydes. In contrast, 7 out of the 12 VOCs which were significantly less abundant, in the GF compared to non-GF samples, were ketones. A PCA showed a remarkable difference observed in the VOCs emitted from the faecal pellet between GF and non-GF mice **(Figure 3.17).**

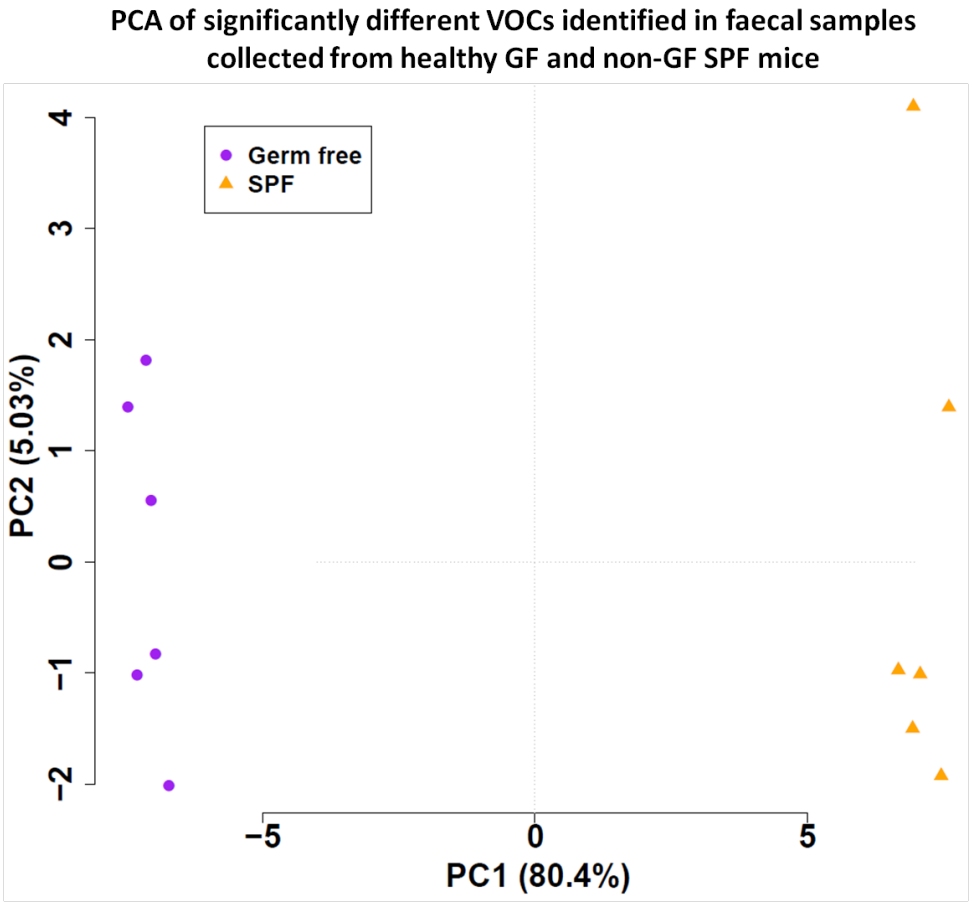

Figure 3.17 A PCA for the faecal samples from healthy GF C3H/HeN and *Junbo* mice compared to non-GF SPF C3H/HeN (n=6/group), collected from MRC Harwell, Oxford. The first PC (80.4%) has been plotted against the second PC (5.03%). The PCA was performed using the 64 VOCs that were found to be significantly different between GF and SPF mice (data were log transformed, Student's *t*-test followed by Bonferroni correction ($p<0.05$)).

The faecal samples used for the investigation of the impact of a GF VOC metabolome were housed in a different geographical location and of a different strain to the samples from mice used for the work in this thesis. The chow fed to the C3H/HeN SPF and GF mice from MRC Harwell was also supplied from SDS and contained the same ingredients as the chow fed to the SPF mice at Liverpool. Therefore, the VOC metabolome of GF and their non-GF SPF equivalent were compared to that of the mice housed in SPF conditions at University of Liverpool. The VOC faecal metabolome was significantly different between healthy GF and non-GF SPF of two different strains and locations **(Figure 3.18).** Butyl- and propyl-acid and ester compounds were significantly different between the faecal pellets of mice from MRC Harwell SPF conditions compared to Liverpool. Butanal, 2-methyl-, 2-heptanone, propanal, 2-methyl-, 2-pentanone and heptanal were a selection of the compounds that were significantly different between GF mice and the healthy SPF C57BL/6 mice housed at Liverpool (ANOVA followed by Tukey's HSD test, $p<0.01$).

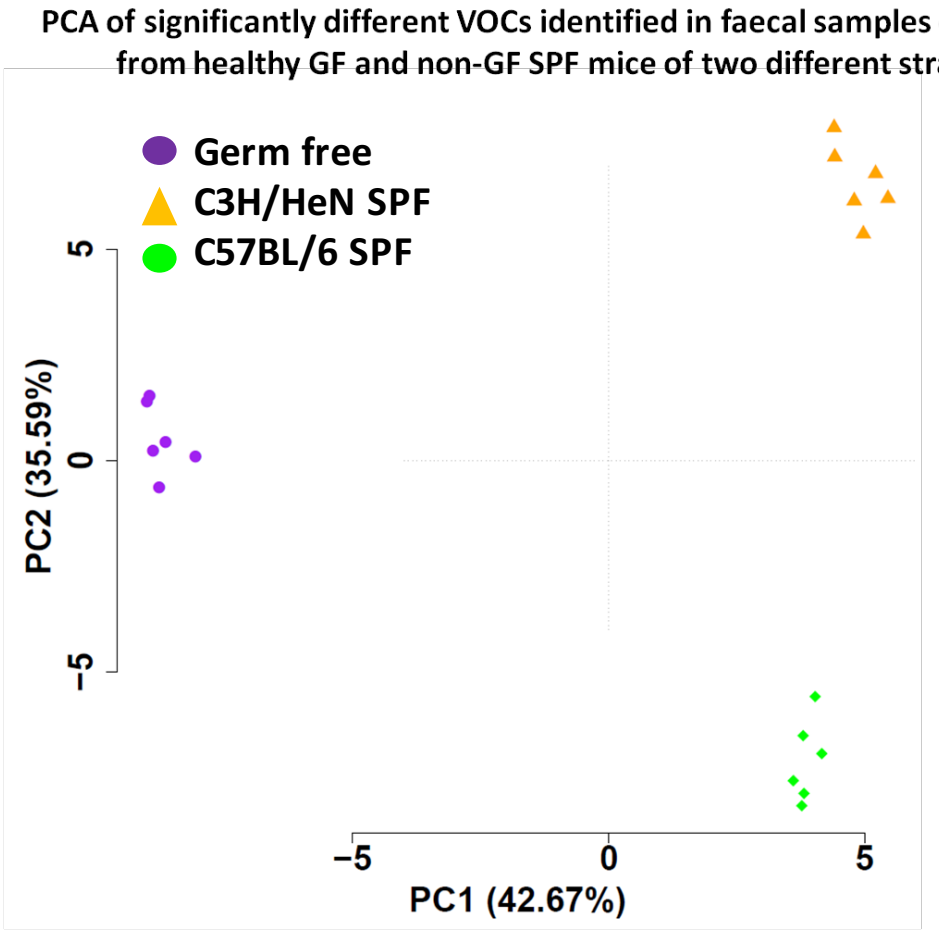

Figure 3.18 A PCA for the faecal samples from healthy GF mice from Oxford, compared to non-GF SPF from Oxford (C3H/HeN), and Liverpool (C57BL/6) (*n*=6/group). The first PC (42.67%) has been plotted against the second PC (35.59%). The PCA was performed using the 66 VOCs that were found to be significantly different over time (data were log transformed, ANOVA followed by Bonferroni correction ($p<0.05$)).

3.6 SUMMARY OF RESULTS

1. Investigation of the healthy murine faecal VOC profile using HS-SPME-GC-MS found little biological variation between individual WT C57BL/6 mice.

2. Analysis of chromatograms produced from female and male mice weekly from 5 to 12 weeks identified 90 and 103 VOCs in total, respectively. There was a variety of different compound classes identified with ketones, aldehydes and alcohols being the most commonly observed compounds.

3. There was a significant effect of age and gender on the average number of VOCs identified in the HS of faecal pellets collected from WT C57BL/6 mice. For the age range tested, there are clear differences between male and female mice when comparing the abundance of all significantly different VOCs.

4. There were 29 and 25 VOCs that varied significantly over time for male and female mice, respectively.

5. The faecal VOC profile varied significantly between the different regions of the murine lower GI tract, and the faecal pellet.

6. The VOC profile from the faecal pellet of GF mice was compared to their non-GF strain equivalent, resulting in significant differences in the number of VOCs identified and the abundance of a large number of specific VOCs.

7. Preliminary data may suggest that there is an effect of geographical location and genetic background on the faecal VOC profile of mice but further investigation is required to separate these differences.

3.7 DISCUSSION

This study has investigated the faecal VOC metabolome of healthy C57BL/6 mice by detecting VOCs in the HS gas using SPME-GC-MS. The gas chromatograms produced from the faecal pellets were abundant in compounds at RT 10-30 minutes. Very little were detected before 10 minutes; those after 30 mins appeared to originate from the food remains in the faecal pellets. More than 50% of compounds identified in 50% of samples tested longitudinally over a period of 8 weeks varied very little between individual mice. However, upon examining the coefficient of variation (CV), also known as the relative standard deviation, between individual mice, it was above the statistically acceptable range of 30% [231]. In order to have a low CV between individual samples, it would require at least 10 biological replicates. However, this is beyond the scope of this study as we aimed to establish the VOC metabolome, taking into consideration the ethical guidelines underpinning the humane use of animals in scientific research, the three Rs (replace, reduce and refine) [228, 232].

Stable establishment of the microbial groups requires cooperation in food networks, such as cross-feeding where metabolites from one organism act as a substrate for another [233]. In the intestinal environment, one of the most important roles of microbial activity is the fermentation of dietary or host-derived components, including the conversion of non-digestible carbohydrates into SCFAs [234]. The presence of SCFAs, as identified in the faecal pellet and bowel contents, causes activation of the G-protein coupled receptor 43 which has been proposed to constitute a molecular link between diet, microbiota and immune modulation [235], and also plays a major role in the regulation of energy balance [236]. In particular, the SCFA, butyrate, is important in the large bowel as a source of energy for colonocytes and is produced by beneficial colonic bacteria [237]. There were 4 butyrates yielded in the murine faecal pellet, methyl butyrate, ethyl butyrate, 1-methylethyl butyrate and fluorophenyl butyrate. The latter is rare as it was found only at week 3 in 33% of female mice, therefore is more likely to be an environmental contaminant rather than a biologically relevant compound. Upon

inspection of the chromatograms at this time point of other animals, a siloxane contaminant is present, thereby confirming our suspicions of fluorophenyl butyrate possibly being an environmental contaminant.

Ketones were the most common class of VOCs identified in the gas surrounding healthy murine faecal pellets. It is likely that acetone and 2-butanone arise from fatty acid carbohydrate metabolism [238]. The universal presence of 2, 3-butanedione is important as it has been reported to have potential health implications by impacting on the growth of yeast and some bacteria, either increasing or decreasing the growth [239], but does occur naturally as a by-product of fermentation [240]. The aldehydes, propanal, 2-methylpropanal, 3-methylpropanal, 2-methylbutanal, pentanal and hexanal were predominantly observed. Their presence suggests that their respective acids have undergone reduction or that their origin may be dietary as there have been reports of such compounds found in potatoes and carrots [241, 242]. Hexanal and 3-methylbutanal were amongst the most abundant compounds identified in the mouse feed; 3-methylbutanal has reportedly been included in feed for mice and rats as a feeding stimulant [243].

The faecal pellet VOC composition of C57BL/6 mice was assessed for eight time points from the age of 5 to 12 weeks old in male and female mice. It was demonstrated that healthy male and female mice form distinct clusters and further investigation also revealed a change in VOC metabolomic profiles as mice aged. C57BL/6 mice reach sexual maturity at 6-8 weeks old (experimental weeks 2-4), and, because of the hormonal changes occurring in both male and female mice (such as oestrogens and progesterone in female and androgen in males), the metabolites may vary. Won *et al.* investigated the metabolomics urinary profile of obese mice using NMR and reported significant gender-related differences [244]. This highlights the importance of the gender-specific differences and metabolic pathways for future studies.

Dissection of these known pathways and investigation into the mechanisms by which these differences arise will potentially lead to new diagnostic tests and understanding of the pathogenesis of health and disease. For example, it has been reported that certain metabolites related to mitochondrial energy metabolism were found to be different between gender and age [245]. It is important to note that dietary components may vary according to the time of day the faecal pellets were collected. This is something that was considered in preparation for this experiment, and controlled for.

Efficient absorption and metabolism of nutrients is the primary role of the small intestine. Here, various nuclear receptors have an important regulatory role in keeping homeostatic control of the digestive system [246]. This is achieved by mixing food with the digestive enzymes to increase contact with the absorptive cells of the luminal mucosa [247]. The small intestine secretes signalling molecules, such as gut hormones and cytokines, resulting in the liver and muscle tissue responding by modulating their own metabolism. There was a significant decrease in the number of VOCs identified in this study of the luminal content from the small intestine, compared to the faecal pellet and the luminal content from the large intestine. There was also an absence of ester compounds in the SI contents, perhaps explaining the significant decrease in number of VOCs. The number of bacteria in the gut increases distally, from the stomach to the large bowel, with microbial densities relatively low in the small intestine. Esters are produced from the metabolism of carbohydrates by the interaction of the gut bacteria with these complex polysaccharides [196], providing a possible explanation for this observation.

This study has investigated the faecal VOC metabolome from GF and non-GF mice using a non-invasive method, HS-SPME-GC-MS, and consequently, established very significant and reproducible profiles. It found specific groups of compounds responsible for these distinct VOC profiles. A number of alkanes were unique to GF faecal pellets in combination with an increase in the levels of aldehydes and a decrease in the levels of ketones, with a notable absence of acids and esters. The

synthesis of esters may be mediated by enzymes derived from the intestinal mucosa [248], which GF mice lack as demonstrated in this study. In addition, it is well-known that the gut microbiota is responsible for the degradation of most amino acids to synthesise SCFAs [249] [250]. The gut microbiota is responsible for the synthesis of essential vitamins (e.g. vitamin K and B) therefore GF mice have to be given these vitamins supplemented in their food [196]; a possible explanation for these differences noted between GF and non-GF animals. A reduction in the level of ketones is observed in fasted GF mice in this study, which may be explained by the lack of nutrients available to these mice. The colon is the most prominent site of microbial colonisation therefore it is no surprise that the faecal metabolome of GF mice is different from that of conventionally housed mice [233]. The microbiota of mice housed in SPF conditions is composed of well-established resident bacteria resulting from the long-term associations with the host from birth [251].

By comparing the colonic luminal metabolome of GF mice and non-GF mice using capillary electrophoresis-time of flight mass spectrometry (CE-TOFMS), Matsumoto *et al.* were able to obtain a novel profile of numerous metabolites present in the intestinal lumen unique to GF mice, which supports our findings [252]. Furthermore, Schwende *et al.* was able to show that by analysing urinary VOCs from mice of one strain may differ both quantitatively and qualitatively from those of another [253]. Here, it has been shown that the VOCs present in the HS gas of faecal pellets from mice of different strains, and geographical locations, differ.

Dysbiosis of the intestinal microbiota has been associated with a variety of diseases such as IBD and CRC [254]. This highlights the importance of improving our understanding of the molecular basis and metabolic pathways involved in host-microbe interactions and will increase the awareness of possible disease-associated shifts. These studies will aid future studies of chemically-induced IBD and CRC murine models, where one gender of mice will be used, taking into account these age-related VOC changes during the development of disease.

Chapter 4

Comparison of the Healthy Murine and Human Faecal Metabolome

4.1 INTRODUCTION

The GI tracts of mouse and human are similar in physiology and anatomical structure. Both species have a GI tract composed of a mouth, oesophagus, stomach, small intestine, large intestine and anus, and are also composed of the same cells in the small intestine e.g. enterocytes, goblet cells, Paneth cells, and the colon e.g. colonocytes, goblet cells, enteroendocrine cells [255]. However, due to the different diets, feeding patterns, body sizes and metabolic requirements, there are also prominent anatomical differences. Although the average ratio of intestinal surface area: body surface area is similar [256], the ratio differs along the length of the GI tract such that the small intestine: colon surface area ratio is 18 in mice versus 400 in humans and also the average small intestine: colon length ratio is 2.5 in mice compared to 7 in humans [255, 256]. Mice have a large caecum, relative to the rest of their GI tract **(Figure 4.1),** whereas the human caecum is relatively small with no clear function. The mouse caecum illustrates the adaption of the murine gut to digest larger amounts of 'indigestible' foods from the diet, such as the fermentation of plant materials and the production of vitamins K and B; mice reabsorb these nutrients through coprophagy [257]. Another significant difference is that humans have an appendix, but mice do not. In addition, the human large intestine contains sub-compartments made by haustral folds that support the fermentation of dietary carbohydrates in the human colon, which are absent in the mouse colon and are not observed in the caecum or appendix [255].

In addition, an example of the differences at cellular level between human and mouse includes the distribution of Paneth cells along the GI tract; they secrete antimicrobial compounds and are present along the small intestine, the colon and caecum of humans, but are uniquely found in the small intestine of mice [255]. The principal defence molecules secreted by Paneth cells are α-defensins, cells located in the mouse small intestine secrete >20, compared with two in human [258]. A consequence of cellular differences may suggest differences in local immune responses, also having a role to play in shaping the composition of the gut

microbiota. Such differences in the anatomical structure and cellular distribution of the GI tract may have an impact on the diversity and composition of the gut microbial communities of the colon, in turn affecting the breakdown of food components and the production of essential complements to the host, including SCFAs.

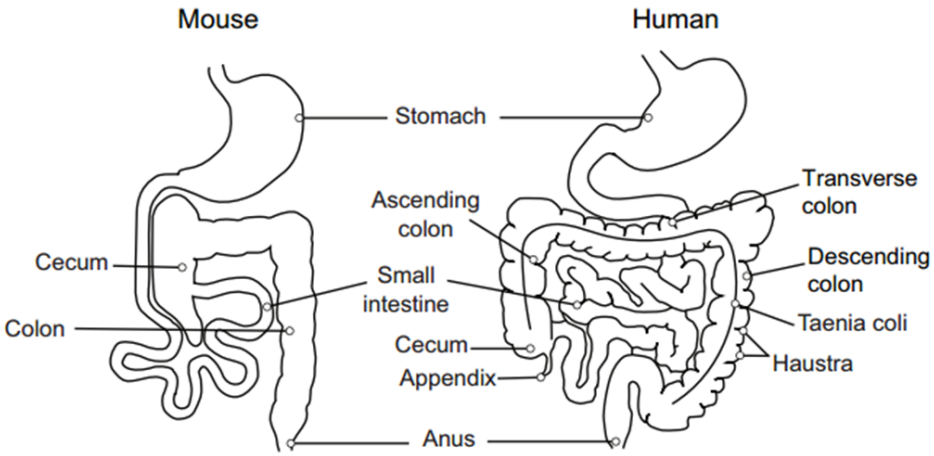

Figure 4.1 Gross anatomy of the human and mouse GI tract. The human colon is divided into ascending, transverse and descending colon sections, whereas the mouse colon is not [255]. Copyright has been granted and figure is used with permission.

The gut microbiota of both human and mouse are dominated by the two major phyla, Bacteroidetes and Firmicutes [259, 260]. However, although there is considerable similarity at divisional level, 85% of genera and microbial species found in mice are not seen in humans [261]. A recent analysis using *16S* rDNA found 79 genera occurring in both human and mouse gut microbiota. Dominant genera with high abundance in humans included *Prevotella, Faecalibacterium* and *Ruminococcus*, whereas *Lactobacillus*, *Alistipes* and *Turicibacter* were more abundant in mouse [255]. In contrast, *Clostridium, Bacteroides* and *Blautia* were present at a similar relative abundance in both organisms. A possible explanation for these differences may be that most human studies include the use of stool samples, whereas caecal contents are usually used in murine studies, with the exception of longitudinal studies when pellets are used. Other influencing factors include the age of the mice/human subjects, mouse strains/human populations, the

different microbiota pools in different laboratories and technological differences. Also, the presence of an SPF environment in murine studies may reduce the diversity of the mouse gut microbiota compared to wild mice, as evidenced by Linnenbrink *et al.* [262]. In conclusion, the observed differences may either be caused by intrinsic biological differences, or, by various confounding factors including diet, pathogen exposure and environment.

4.2 HYPOTHESIS

The hypotheses were:

- There will be notable similarities in the number and occurrence of VOCs in humans and mice.
- The differences between the human and murine faecal metabolome will reflect a varied diet and more complex intestinal microbiota in the human samples.

4.3 AIMS

1. Perform a qualitative comparison of the VOCs present in the headspace of faecal samples from healthy humans and mice.
2. Determine those VOCs that are unique to both humans and mice, and those that are shared between the two species.

4.4 METHODS

4.4.1 Experimental design

For the qualitative comparison of the faecal VOC profile from humans and mice, human samples were donated from a single healthy volunteer with informed consent collected as part of a method development study by Dr David Sawbridge in the in the Department of Gastroenterology, University of Liverpool. Samples (*n*=6)

used for this comparison were from a male aged between 30-40 years, who ate *ad lib* with no dietary restrictions. For the murine group, faecal pellet samples from male C57BL/6 mice at week 3 of the baseline study (**Chapter 3**) were used.

4.4.2 HS-SPME-GC-MS sample preparation and analysis

In brief, 10 pellets of murine stool sample was collected and stored in 2ml glass vials at -20°C. For human samples, 2g of faeces were collected and stored in a 10ml glass vial at -20°C. Prior to VOC extraction, samples were pre-incubated for 30 mins at 60°C before compound extraction using the solvent free SPME technique with a CAR/PDMS/DVB fibre for 20 mins prior to desorption into the GC oven [219]. For GC-MS conditions, please refer to **section 2.6.1.**

4.4.3 Data processing and statistical analysis

All raw data were processed and analysed as described in **Chapter 2**. Briefly, a batch report was produced in AMDIS and new compounds were added to the murine VOC library prior to batch report generation. A list of all compounds present and the corresponding corrected peak abundances were generated using Metab. As the volume of faeces differed between human and mouse in this comparison, there was no statistical analysis performed on the abundances of peaks. The presence or absence of each compound was determined for all samples, those VOCs unique to human or mouse, and those shared were also studied.

4.5 RESULTS

Generation of a report from the chromatograms of healthy human (*n*=6) and mouse (*n*=6) faecal samples containing VOCs present in the headspace yielded a total of 151 individual VOCs. Of these 151, 112 were present in humans and 89 in mice. There were 62 VOCs unique to the human samples, 39 unique to the mouse samples and 50 shared between the two giving a 33% overlap correlation **(Figure 4.2) (Table 4.1).**

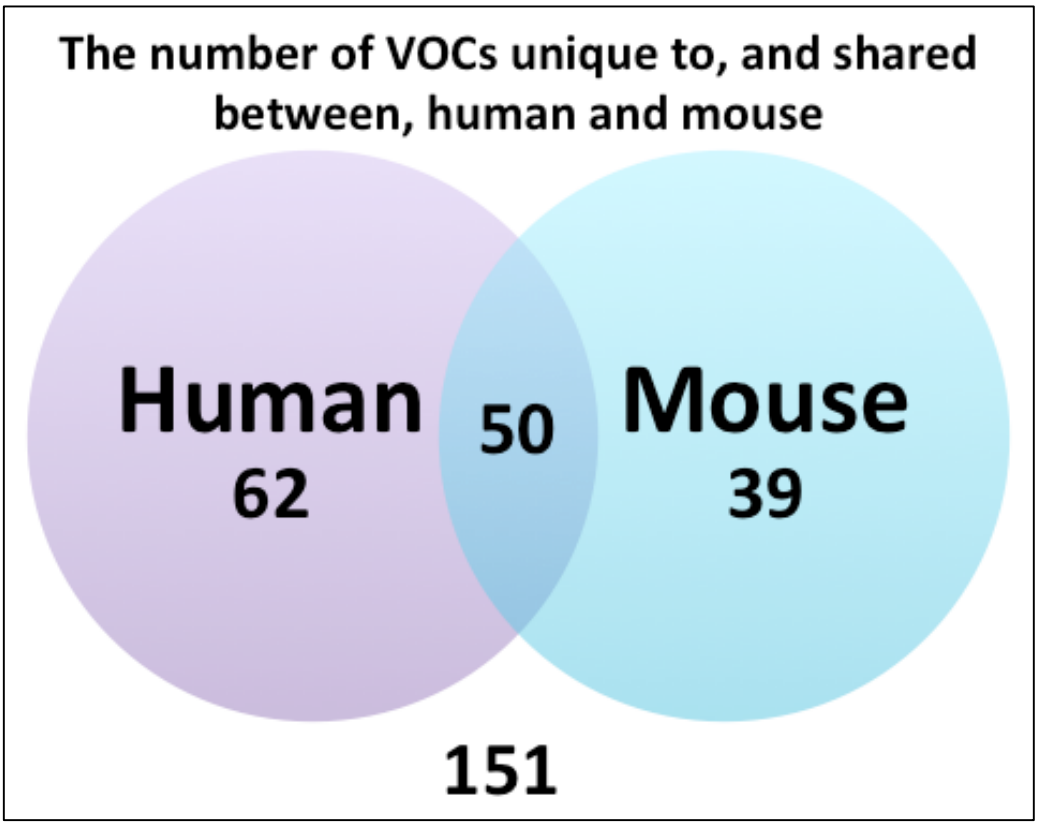

Figure 4.2 Venn diagram presenting the number of VOCs identified in the HS of human and mouse faecal samples.

4.5.1 Similarities in the faecal VOC metabolome between human and mice

The 50 VOCs shared between the human and murine samples include aldehydes, alcohols, ketones, acids, esters, alkanes, heterocyclic furan, benzene ring, sulphur and nitrogen containing compounds **(Table 4.1).** Aldehydes, acids and ketones were

the most commonly occurring compounds amongst humans and mice with 11, 10 and 8 present in each group, respectively. Acetone, 2-methyl propanal, 2-butanone, butanoic acid, xylene and benzaldehyde were present in 100% of samples in both the human and mouse group (*n*=6/group). Although the VOCs discussed here were all shared amongst humans and mice, the compounds present at high concentrations in each group differed. The 5 most abundant VOCs in the human group, present in more than 65% of samples, were indole (1,050,315,435 ±241,701,172), hexanoic acid (429,148,928 ±227,212,721), pentanoic acid (418,416,435 ±205,678,082), heptanoic acid (296,822,016 ±131,542,496), and 3-methyl butanoic acid (203,146,496 ±98,772,864) (mean abundance ±SEM). In comparison, the 5 most abundant VOCs in the murine group, present in 100% of samples, were acetic acid (1,260,126,208 ±48,441,145), butanoic acid (538,432,853 ±108,426,586), acetone (414,821,035 ±115,810,948), propanoic acid (241,188,864 ±28,876,877), and 2,3-butanedione (156,672,683 ±25,434,050) (mean abundance ±SEM). The shared compounds probably reflect a combination of the metabolic effluvia of common intestinal microbiota and mammalian physiology.

4.5.2 Differences in the faecal VOC metabolome between human and mice

There were 39 VOCs identified to be unique to the murine group, and 62 unique to the human group. Most notable in the murine group were ethanol, isopropanol, 1-propanol, 1-hydroxy-2-propanone, 3-hydroxy-2-butanone, 2,2,4,6,6-penta-methyl heptane, present in 100% of samples and absent from the human group. Furthermore, four of these commonly occurring VOCs were also amongst the most abundant VOCs specific to the murine group; 3-hydroxy-2-butanone (743,945,557 ±156,656,618), isopropanol (627,630,080 ±101,172,143), ethanol (89,643,008 ±7,839,467), and 1-hydroxy-2-propanone (11,339,051 ±988,069) (mean abundance ±SEM). Trimethylamine, acetic acid ethenyl ester and acetonitrile were also present at very high concentrations compared to the other VOCs unique to mouse, but only present in 17%, 33% and 83% of samples, respectively. Whereas alcohols, acids and ketones were the most commonly occurring compounds shared by humans and

mice, nitrogen-containing compounds were the most common group unique to the murine group with 8 identified in total, including trimethylamine, acetonitrile, and hydrogen azide. Several compounds found in the murine samples, that were not identified in the human samples probably reflect urine contamination from incontinent mice.

Chief compounds identified in the human group included 4-methyl phenol (2,140,809,899 ±141,657,253), D-limonene (1,918,599,168 ±201,023,554), 2,2-dimethyl-3-methylene-bicyclo[2.2.1]heptane (330,735,616 ±68,785,368), 1-(1,5-dimethyl-4-hexenyl)-4-methyl-benzene (291,588,779 ±49,118,453), dimethyl disulfide (265,988,779 ±60,329,640), 3-methylene-6-(1-methylethyl)-cyclohexene (256,698,778 ±62,613,587), benzeneacetaldehyde (233,732,779 ±80,361,107), α-pinene (223,176,021±70,508,920), 4-ethenyl-1,2-dimethyl-benzene (198,322,688 ±101,294,027), and β-pinene (153,371,989 ±27,116,088); all present in >80% of samples at high concentrations. Complex cycloalkenes such as terpenes were the most commonly occurring compounds with ketones and benzene-based compounds present in abundance. There was an absence of nitrogen-containing compounds identified specific to the human samples, only shared compounds e.g. indole. **Figure 4.3** shows representative chromatograms from healthy human and mouse faecal samples. The human chromatogram appears to be busier than the murine chromatogram, which appears to be lacking peaks towards the tail end of the run, after 30 minutes. These findings are in agreement with the VOC report produced from the analysis of samples.

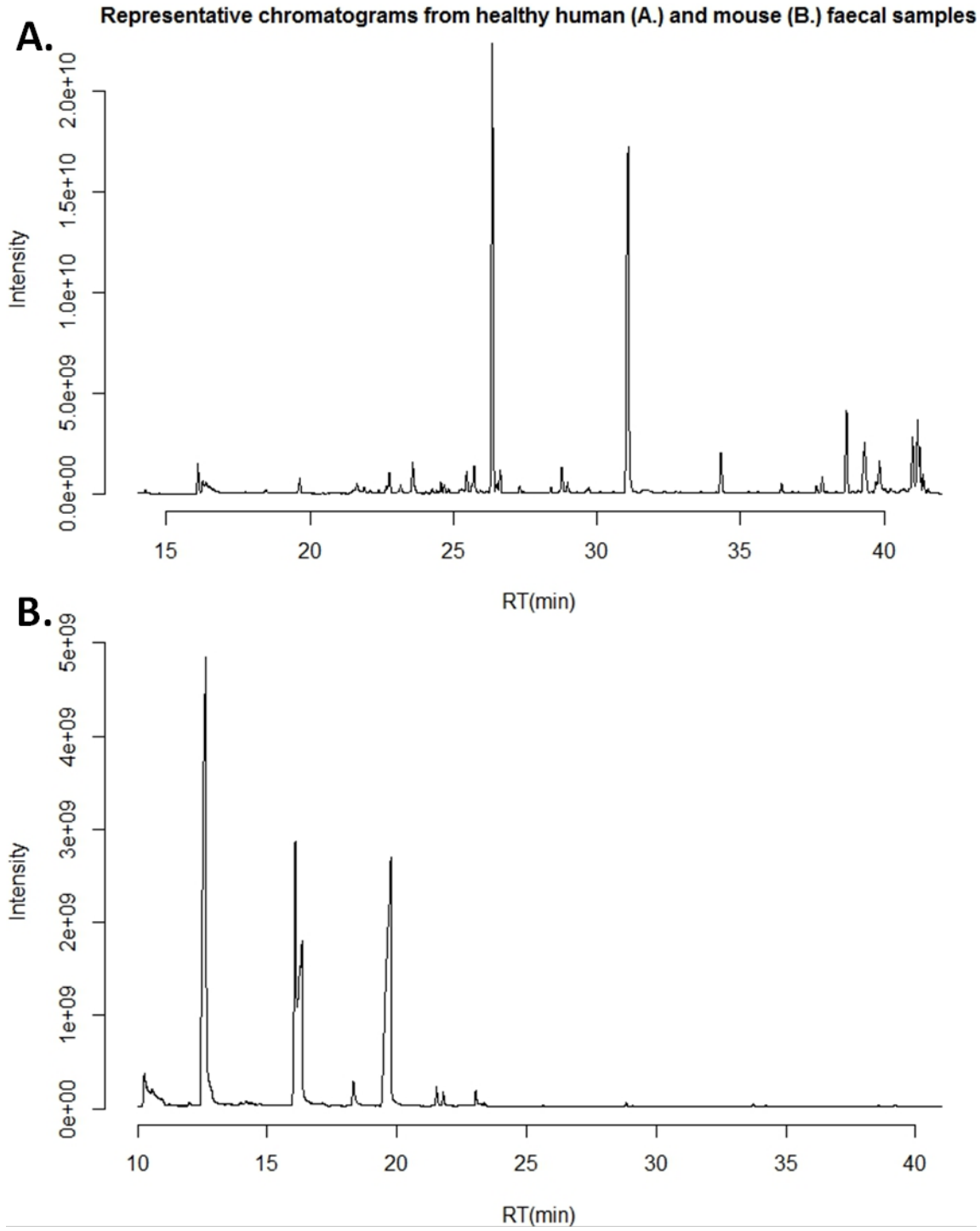

Figure 4.3 Representative chromatograms of healthy human (A) and mouse (B) faecal samples. Samples were run using the optimised HS-SPME-GC-MS method for the detection of VOCs.

Table 4.1 List of 151 VOCs identified in the HS of faecal samples from human (*n*=6) and mouse (*n*=6), by SPME-GC-MS.

RT_compound	Presence (+) or absence (-)		Occurrence (%)	
	Human	Mouse		
VOCs unique to human				
7.49_dimethyl sulfide	+	-	100	0
13.44_1-butanol	+	-	17	0
13.51_2-ethyl-furan	+	-	17	0
15.94_dimethyl disulfide	+	-	100	0
16.06_1-butanol, 3-methyl-	+	-	67	0
16.19_1-butanol, 2-methyl-	+	-	33	0
18.03_2-hexanone	+	-	17	0
18.10_methyl isobutyl ketone	+	-	83	0
18.51_2-butenal, 3-methyl-	+	-	17	0
18.60_methyl valerate	+	-	33	0
20.64_methyl vinyl ketone	+	-	17	0
20.96_2-hexanal	+	-	17	0
21.07_2-n-butyl furan	+	-	33	0
21.83_styrene	+	-	50	0
22.66_1,6-octadiene, 3,7-dimethyl-	+	-	100	0
22.77_ β-pinene	+	-	100	0
23.59_2,2-dimethyl-3-methylene-bicyclo[2.2.1]heptane	+	-	100	0
23.62_3-(methylthio)-propanal	+	-	67	0
24.04_2-octene, 2-methyl-6-methylene-	+	-	100	0
24.26_2,6-dimethyl-2-trans-6-octadiene	+	-	100	0
24.42_α-phellandrene	+	-	67	0
24.68_α-pinene	+	-	100	0
24.83_1,3-hexadiene, 3-ethyl-2,5-dimethyl-	+	-	100	0
24.94_butanoic acid, butyl ester	+	-	33	0
25.25_2,3-octanedione	+	-	33	0
25.34_dimethyltrisulphide	+	-	67	0
25.49_1,3-cyclohexadiene, 2-methyl-5-(1-methylethyl)-	+	-	83	0
25.52_3-octanone	+	-	17	0
25.57_2-octanone	+	-	83	0
26.34_D-limonene	+	-	100	0

Table 4.1 continued.				
26.45_benzene, 1-methyl-2-(1-methylethyl)-	+	-	100	0
26.63_cyclohexene, 3-methylene-6-(1-methylethyl)-	+	-	83	0
27.19_butanoic acid, 2-methylbutyl ester	+	-	17	0
27.25_butanoic acid, 3-methylbutyl ester	+	-	17	0
27.31_γ-terpinene	+	-	100	0
27.97_3-octen-2-one	+	-	33	0
28.32_pentanoic acid, pentyl ester	+	-	17	0
28.40_cyclohexene, 1-methyl-4-(1-methylethylidene)-	+	-	100	0
28.66_benzeneacetaldehyde	+	-	100	0
28.98_benzene, 4-ethenyl-1,2-dimethyl-	+	-	100	0
29.06_2-nonanone	+	-	100	0
29.34_acetophenone	+	-	100	0
29.57_nonanal	+	-	67	0
31.04_4-methyl-phenol	+	-	100	0
31.25_phenylethyl alcohol	+	-	17	0
31.73_hexyl ester, acid	+	-	17	0
31.81_2-nonenal	+	-	50	0
32.87_decanal	+	-	83	0
33.14_p-menth-1-en-8-ol	+	-	100	0
33.89_butane, 2,2-dimethyl-	+	-	33	0
33.91_4-ethyl-phenol	+	-	17	0
35.29_butanimidamide	+	-	50	0
36.42_benzeneacetaldehyde, a-ethylidene-	+	-	17	0
37.06_undecane, 4,7-dimethyl-	+	-	100	0
37.84_ α-copaene	+	-	100	0
38.01_zingiberene	+	-	33	0
39.56_benzene, (1,1-dimethylnonyl)-	+	-	100	0
39.63_hexadecane	+	-	50	0
39.71_cyclopentadecane	+	-	100	0
39.84_caryophyllene	+	-	100	0
40.23_1-pentadecene	+	-	50	0
40.99_benzene, 1-(1,5-dimethyl-4-hexenyl)-4-methy	+	-	100	0

Table 4.1 continued.

VOCs unique to mouse				
5.59_trimethylamine	-	+	0	17
6.42_pentane	-	+	0	50
6.61_ethanol	-	+	0	100
7.11_2-propenal	-	+	0	67
7.61_isopropanol	-	+	0	100
7.90_acetonitrile	-	+	0	83
9.57_1-propanol	-	+	0	100
10.40_nitromethane	-	+	0	33
10.74_acetic acid ethenyl ester	-	+	0	33
10.77_2-butanol	-	+	0	17
11.21_methyl propionate	-	+	0	50
12.22_isopropyl acetate	-	+	0	17
14.00_1-penten-3-ol	-	+	0	67
14.33_hydrogen azide	-	+	0	17
14.65_2-propanone, 1-hydroxy-	-	+	0	100
16.13_3-hydroxy-2-butanone	-	+	0	100
16.98_1-propanone, 1-cyclopropyl-	-	+	0	17
19.08_butanoic acid, 1-methylethyl ester	-	+	0	33
19.84_2,2-dimethyl-propanoic acid	-	+	0	67
20.82_2-pentanone, 4-hydroxy-	-	+	0	17
21.97_2-methyl-pentanal	-	+	0	17
22.56_pyrazine, 2,5-dimethyl-	-	+	0	17
23.37_2-acetyl-1-pyrroline	-	+	0	17
23.99_3-hepten-2-one	-	+	0	17
24.10_3-heptanone, 6-methyl-	-	+	0	17
24.22_heptane, 2,2,4,6,6-pentamethyl-	-	+	0	100
24.36_pentane, 2, 2, 3-trimethyl	-	+	0	17
24.80_1,3,5-triazine	-	+	0	33
24.96_1-hexene, 3,5-dimethyl-	-	+	0	17
25.12_1-octen-3-ol	-	+	0	50
25.63_(1H)pyrrole-3-carbonitrile, 2-methyl-	-	+	0	83
25.79_2(5H)-furanone	-	+	0	33

Table 4.1 continued.

25.82_unknown	-	+	0	17
26.66_dimethyl sulfone	-	+	0	83
26.79_2(3H)-furanone, dihydro-5-methyl-	-	+	0	33
27.53_7-exo-ethyl-5-methyl-6,8-dioxabicyclo[3.2.1]oct-3-ene	-	+	0	67
28.90_butyric acid, p-fluorophenyl ester	-	+	0	17
29.09_5-azacytosine	-	+	90	33
30.96_dodecane	-	+	0	33
VOCs shared between human and mouse				
5.12_acetylaldehyde	+	+	17	17
6.92_furan	+	+	33	17
7.21_propanal	+	+	17	100
7.41_acetone	+	+	100	100
7.82_thiourea	+	+	100	50
7.94_methyl acetate	+	+	33	67
8.32_cyclopentane	+	+	17	100
9.01_2-methyl-propanal	+	+	100	100
10.16_butanal	+	+	33	17
10.28_2,3-butanedione	+	+	83	100
10.32_furan, 3-methyl-	+	+	100	17
10.56_2-butanone	+	+	100	100
11.90_1-propanol, 2-methyl-	+	+	17	100
12.49_3-methyl-butanal	+	+	100	17
12.51_acetic acid	+	+	67	100
12.81_2-methyl-butanal	+	+	100	50
13.98_2-pentanone	+	+	100	83
14.16_2,3-pentanedione	+	+	100	67
14.20_pentanal	+	+	100	83
14.69_methyl butyrate	+	+	50	50
16.29_propanoic acid	+	+	33	100
16.47_2-pentanone, 3-methyl	+	+	17	17
16.58_toluene	+	+	100	17
17.45_1-pentanol	+	+	50	67
17.72_ethyl butyrate	+	+	33	50
18.26_2-methyl-propanoic acid	+	+	50	83
18.43_hexanal	+	+	100	83
19.62_butanoic acid	+	+	100	100
20.22_ethylbenzene	+	+	33	17
20.53_1,3-xylene	+	+	100	100

Table 4.1 continued.				
21.19_1-hexanol	+	+	67	100
21.51_3-methyl-butanoic acid	+	+	67	100
21.73_2-methyl-butanoic acid	+	+	83	100
22.11_2-heptanone	+	+	100	33
22.33_heptanal	+	+	50	17
23.14_pentanoic acid	+	+	83	100
23.27_unknown	+	+	17	100
24.89_1-heptanol	+	+	50	17
24.93_2-pentyl-furan	+	+	17	33
25.73_benzaldehyde	+	+	100	100
26.08_octanal	+	+	67	17
26.38_hexanoic acid	+	+	83	50
27.67_5-ethylcyclopent-1-enecarboxaldehyde	+	+	17	33
28.14_phenol	+	+	83	67
28.93_diiodomethane	+	+	17	67
29.72_heptanoic acid	+	+	67	17
30.27_2(3H)-furanone, 5-ethyldihydro-	+	+	17	17
33.74_benzene, 1, 3-bis(1,1-dimethylethyl)-	+	+	17	100
34.02_propanoic acid, 2,2-dimethyl-, sodium salt	+	+	17	33
38.66_indole	+	+	100	83

There are 62 VOCs unique to human samples, 39 unique to mouse and 50 VOCs are shared between the two species. The % occurrence is the number of times the VOC was present in the sample group.

4.6 SUMMARY OF RESULTS

1. A total of 151 VOCs were identified in this comparison of the human and mouse faecal metabolome, by HS-SPME-GC-MS. There were 50 VOCs shared between the two species giving a 33% overlap of total VOCs amongst the two species. Of these shared VOCs, aldehydes, acids and ketones were the most commonly occurring compounds. Indole and hexanoic acid were amongst the VOCs present at high concentration in the human group and acetic acid and butanoic acid in the murine group.

2. There were 89 of the total 151 VOCs found in the mouse faecal metabolome and 39 were unique to this species. Alcohol and ketone compounds were the most abundant VOCs in the murine metabolome being present in 100% of samples.

3. 112 VOCs were identified in the human faecal metabolome compared to mouse and 62 were unique to this species. Terpene and complex aromatic and cyclic benzenoid compounds were the most commonly occurring compounds in the human metabolome. Chromatograms highlighted the increased number of VOCs after 30 minutes in the human group, compared to the murine group.

4.7 DISCUSSION

This study has compared the faecal VOC profile emitted from healthy human and murine samples. There is a notable correlation between the two species and the differences in number and complexity of the VOCs found in the human, compared to the mouse, may reflect a varied diet and a more complex intestinal microbiome.

Terpenes are a large and diverse class of organic compounds and a number were found exclusively in human samples, including caryophyllene, γ-terpinene and D-limonene. They are often strong, yet pleasant smelling compounds, and are reportedly produced by a variety of plants, particularly conifers. Terpenes are constituents of the essential oils of many types of plants and flowers, which are also used as fragrances in perfumery, and in alternative medicines such as aromatherapy. Odorous plants, or parts of plants, including conifer wood (e.g. β-pinene), citrus fruits (e.g. D-limonene), eucalyptus, lavender, lemon grass, peppermint species, rosemary (e.g. α-pinene), coriander, sage and thyme all contain terpenes which are extracted and used to create fine perfumes (e.g. β-phellandrene and γ-terpinene), refine flavours and aromas of food and drink and to produce medicines [263].

Another example of the varied and diverse diet consumed by the human group is the identification of zingiberene, a monocyclic sesquiterpene that is the predominant constituent of the oil of ginger [264]. Zingiberene is also an ingredient in an herbal dietary supplement for weight loss in humans, along with rhubarb, red saga root, astragalus, and turmeric [265]. Derivatives of phenol were also detected exclusively in the human group, including 4-methyl phenol and 4-ethyl phenol. P-Cresol is another name for 4-methyl phenol, which has been reported as a component in human sweat [266], but has also been measured in the urine and faeces of humans [267].

Compounds shared between mouse and human include acetone, 2-methyl propanal, 2-butanone, butanoic acid, xylene and benzaldehyde. Acetone, 2-methyl propanal and 2-butanone probably arise from fatty acid and carbohydrate metabolism [268]. Traces of 2-methyl propanal has also been found in alcoholic beverages, tea, fresh fruits, breads, cooked pork and spearmint [268]. Benzaldehyde is occasionally found as a volatile component of urine [269], but is also used as an aromatic aldehyde in cosmetics as a denaturant, a flavouring agent, and a fragrance [270]. Butanoic acid is a SCFA and is a product of anaerobic bacterial fermentation of dietary carbohydrates in the colon, providing an explanation for the presence of butanoic acid in both humans and mice. Incubation of labelled butanoic acid with faeces by Garner *et al.* [242] found that esters are generated from acids, which may be mediated by a bacterial esterase such as is present in *E. coli* [271], or by the intestinal mucosa enzyme, ethanol-O-acyltransferase (AEAT) [272]. This may explain the increase in number of esters identified specific to the human group, compared to acids.

Fermentation of the aromatic amino acids, tyrosine and tryptophan, in human stool has been shown to produce the VOCs phenol and indole, respectively [242, 273]. Indole and phenol were shared between humans and mice suggesting a similar metabolism of amino acids by human and mouse colonic bacteria. It is likely that the presence of trimethylamine (TMA) in the murine group is from the urinary contamination of the stool samples. It is generally thought that the origin of urinary TMA is via the action of intestinal microbiota on precursors within the food such as choline. This has been confirmed by the absence of urinary TMA in germ-free mice and the significant reduction in antibiotic-treated mice. Subsequently, cohabitation of germ-free mice with conventional mice restored their ability to excrete TMA, suggesting an important role of the gut microbiota in the production of TMA [274].

Despite the notable differences between the faecal metabolome of human and mice outlined in this study, there are considerable similarities. Therefore, although the results from this thesis are primarily from murine models of human GI disease,

the translation of results to human disease and any conclusions will be made with caution.

Chapter 5

VOC Profiling of Chemically-Induced Acute Intestinal Inflammation

5.1 INTRODUCTION

IBD has two major phenotypes, CD and UC, and is characterised by chronic inflammation of the GI tract. Symptoms include severe abdominal pain, diarrhoea, rectal bleeding and weight loss and predominantly affects the younger population [5]. Currently, the pathogenesis of IBD is unknown but is hypothesised to result from an interaction of environmental factors (e.g. smoking, oral contraceptives, high-fat diet) affecting the intestinal microbiota, combined with an inappropriate immune response often, but not only, in a genetically predisposed person. The chronic inflammation in IBD is caused by activation of effector immune cells, producing pro-inflammatory cytokines, resulting in colonic tissue damage. The *NFκB* has been identified as one of the key regulators of the immunological setting in IBD [275]. Therefore, until we understand the cause of IBD, the diagnosis and treatment will remain difficult for clinicians.

The diagnosis and care of IBD patients remains difficult for clinicians due to the non-specific diagnostic methods currently used. They lack sensitivity and are often invasive, expensive and are found unpleasant by patients. Non-invasive methods of assessing the disease process, such as measuring faecal calprotectin concentration, are becoming increasing preferred. However, there is still room for improvement with regards to finding a non-invasive test with higher specificity and sensitivity for IBD. Faecal calprotectin is raised in other conditions, not just IBD [276, 277]. Recent studies strongly suggest that the accurate reproducible detection of VOCs from biological samples has great potential to develop into a non-invasive diagnostic test for IBD [131, 242, 278-280]. The untargeted analysis of VOCs in the faeces of IBD patients has potential as a non-invasive diagnostic method because of what the human stool represents; the end-product of diet, digestive and excretory processes, and colonic bacterial metabolism [185].

Oral administration of DSS is the most commonly used rodent model to induce colitis in experimental animals since 1990 [281] and to date there have been around 1000 papers published using this model [130]. DSS is administered orally in

sterile drinking water at a dose between 1-5% for 5 days, followed by 7 days normal drinking water to induce colitis. This experimental model shares clinical (diarrhoea, bloody stools and weight loss) and histological (crypt erosion, goblet cell depletion, ulceration) features with human ulcerative colitis [108]. The typical features appear by day 5, are maximally expressed by day 8 and present with signs of recovery by day 11. Depending on the concentration, the duration and the frequency of DSS administration, the animals may develop acute or chronic colitis. However, the exact mechanism of action of DSS-induced intestinal inflammation remains unknown. Mice lacking the *NFκB2* gene are resistant to DSS-induced colitis, compared to wild-type mice [54]

Quantitative profiling of the VOCs emitted from the faeces of mice administered DSS is a promising method to investigate the pathogenic mechanisms involved during the development of colitis by characterising the changes occurring in the levels of metabolites. In spite of this, there are currently a limited number of studies using a metabolomics approach to explore these metabolic changes [282-285]. Also, these studies primarily focus on the metabolite profile of plasma, urine and tissue using ^{1}H-NMR-based metabolomics, rather than the volatile component of the metabolomic profile emitted from the headspace of the faeces of these DSS-treated mice.

5.2 HYPOTHESIS

The hypotheses were:

- The presence and levels of VOCs detected in the HS of faeces by GC-MS will change during the development of murine colitis.
- The examination of these changes will achieve a detailed understanding of the pathogenesis of murine colitis on a metabolite level, and consequently human IBD.
- The faecal VOC profile from colitic mice will be significantly different to the profile from osmotic diarrhoea mice.

- *NFκB2* null mice will be resistant to colitis by DSS administration and will have a faecal VOC profile similar to untreated control animals, rather than DSS treated animals.

5.3 AIMS

1. To induce acute intestinal colitis in C57BL/6 WT female mice by oral administration of DSS.
2. To compare metabolic differences in the development of acute DSS-induced experimental colitis model to untreated controls.
3. To investigate the impact of an absence of the *NFκB2* gene on acute DSS-induced colitis, and the subsequent metabolic changes in the faecal VOC profile, compared to untreated controls and treated WT mice.
4. To induce secretory diarrhoea in WT mice by oral gavage of $MgSO_4$, and establish change in faecal VOC profile compared to healthy control and acute DSS-colitis.

5.4 METHODS

5.4.1 Experimental design

5.4.1.1 Induction of acute colitis by DSS administration

C57BL/6 female mice were administered 4.25% DSS (wt/vol) in their drinking water for 5 days followed by 6 days of normal water. Clinical parameters of body weight loss, stool consistency and the presence of rectal bleeding were assessed daily. This procedure aims to induce a mild to moderate form of colitis. Therefore, to ensure procedure and ethical guidelines were adhered to this experiment was split over 3 separate experiments, each time increasing the number of mice used. Experiments were reproducible and data was combined to produce results. Mice were sacrificed at experimental days 0 (*n*=11), 5 (*n*=11), 8 (*n*=11) and 11 (*n*=8); colonic, caecal, small intestine contents and mid-large bowel and distal small bowel tissue sections were

taken from each mouse and stored at -20°C prior to analysis by HS-SPME-GC-MS. The entire small and large intestine tissues were taken for histological analysis. Samples collected from mice euthanized at day 0 were treated as untreated control to be compared to days 5, 8 and 11.

This experiment was conducted to investigate the susceptibility of colitis in *NFκB2*$^{-/-}$ mice (*n*=6), mice were administered 2% DSS in their drinking water for 5 days and were euthanized at day 8. Three control groups were used: C57BL/6 untreated (WT) (*n*=4), C57BL/6 2% DSS treated (WT) (*n*=6) and *NFκB2*$^{-/-}$ untreated (*n*=4). Colon content collected upon necropsy was stored at -20°C prior to analysis by HS-SPME-GC-MS. Dr Jonathan Williams performed this experiment with the assistance of the author.

5.4.1.2 Induction of osmotic diarrhoea by $MgSO_4$

C57BL/6 mice were fasted overnight and were administered magnesium sulphate (2mg/kg) by oral gavage (*n*=5) with a control group receiving distilled water (*n*=3). Following the administration of the $MgSO_4$, the animals were placed on filter paper which was changed every hour. The amount and consistency of the faeces was assessed each hour for 6 hours. Faecal samples were collected every hour and at termination of the experiment. All samples were stored at -20°C prior to analysis by GC-MS. The VOC profile identified by HS-SPME-GC-MS of the resulting diarrhoea samples was compared to the colon content samples collected at day 8 of DSS-induced acute colitis.

5.4.2 HS-SPME-GC-MS sample preparation and analysis

In brief, where possible, 130mg (maximum volume) of stool sample was collected and stored in 2ml glass vials at -20°C. Prior to VOC extraction, samples were pre-incubated for 30 mins at 60°C before compound extraction using the solvent free

SPME technique with a CAR/PDMS/DVB fibre for 20 mins prior to desorption into the GC oven [221]. For GC-MS conditions, please refer to **section 2.6.1.**

5.4.3 Data processing and statistical analysis

All raw data were processed and analysed as described in **Chapter 2**. Briefly, batch reports are produced for each dataset in AMDIS and a list of all compounds present and their corresponding corrected peak abundances was then generated using Metab. Compounds present in less than 30% of at least one condition are removed. Chi-square test is used to determine compounds significantly more prevalent in one condition. NA was replaced with 1 and peak abundance was log transformed, and appropriate statistical analysis (Student's *t*-test or two-way ANOVA) was applied: all *p*-values are corrected for multiple comparison (Bonferroni). Hierarchical clustering and PCA was applied to illustrate the variation present between groups.

5.5 RESULTS

5.5.1 Clinical and histological symptoms confirm acute DSS-induced colitis

Acute colitis was induced by oral administration of 4.25% DSS in the drinking water of C57BL/6 female mice for 5 days followed by 6 days of normal water. A moderate to severe colitis was observed, characterized by a significant weight loss and bloody diarrhoea appearing at day 5, being most severe by day 8 and with signs of recovery by day 11. There was a significant decrease in relative body weight at day 5 with a loss of 3.8±1.3% (n=11, ANOVA with Tukey, p<0.001), and 27.3±1.6% at day 8 (n=10, ANOVA with Tukey, p<0.001), compared to a start weight of 19.1±0.7g at day 0 (mean±SEM, n=11). At day 11 (n=8), the relative body weight significantly increased compared to day 8 (ANOVA with Tukey, p<0.001) with a final weight of 20.2±0.6g (mean±SEM) **(Figure 5.1).**

A daily disease activity index (DAI) score was given to each animal based on the change in body weight, presence of diarrhoea and rectal bleeding to evaluate the general condition of the mice. The DAI markedly increased from day 5 to day 8 (Kruskal-Wallis, $p<0.001$) followed by a significant decrease from day 8 to day 11 (Kruskal-Wallis, $p<0.001$) at which point the experiment was finished **(Figure 5.2).** The DAI scores for the animals culled at days 5, 8 and 11 were all significantly different compared to the day 0 group (Kruskal-Wallis, $p<0.01$).

Histological examination of the distal colon with H&E staining found the degree of microscopic injury to be different according to the stage of colitis at the different time points. Day 0 showed an intact epithelial layer and crypts, signifying a healthy murine intestine. In contrast, day 5 and 8 samples showed inflammatory changes characterised by damaged crypts and a sub-mucosal layer with oedema and an infiltration of inflammatory cells such as neutrophils. Day 11 pathology showed the re-formation of the crypt infrastructure and a reduction in tissue inflammation in comparison to that observed at days 5 and 8. Significantly different histological scores between days 5 and 8, and 8 and 11 provide quantification of the pathological damage ($p<0.001$) **(Figure 5.3 & 5.4).**

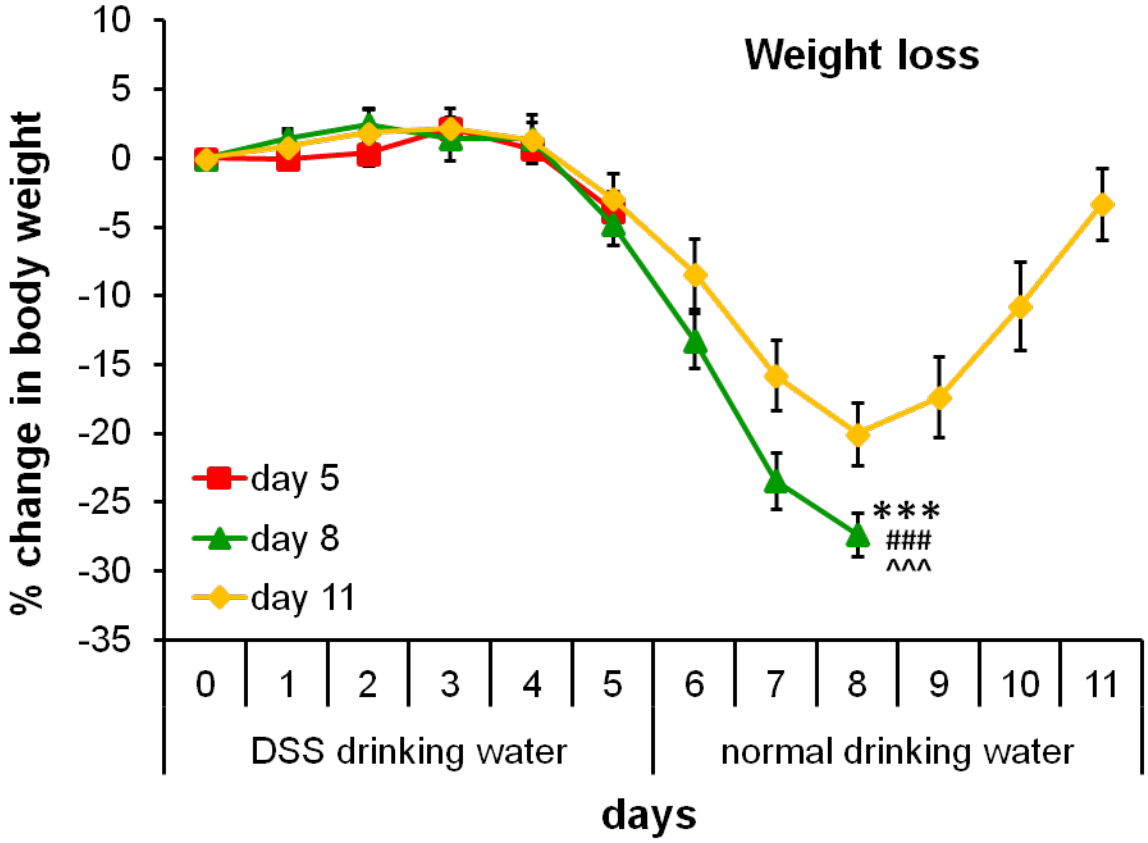

Figure 5.1 Weight loss. The change in the body weight (%) of C57BL/6 mice was measured daily to assess the degree of colitis. Data from 3 separate experiments combined and represented as mean±SEM, *n*=11, 11, 10, 8 for days 0, 5, 8 and 11, respectively. Statistical differences were assessed by one-way ANOVA followed by Tukey's HSD test, $p<0.001$*** compared to day 0, ### compared to day 5, ^^^ compared to day 11.

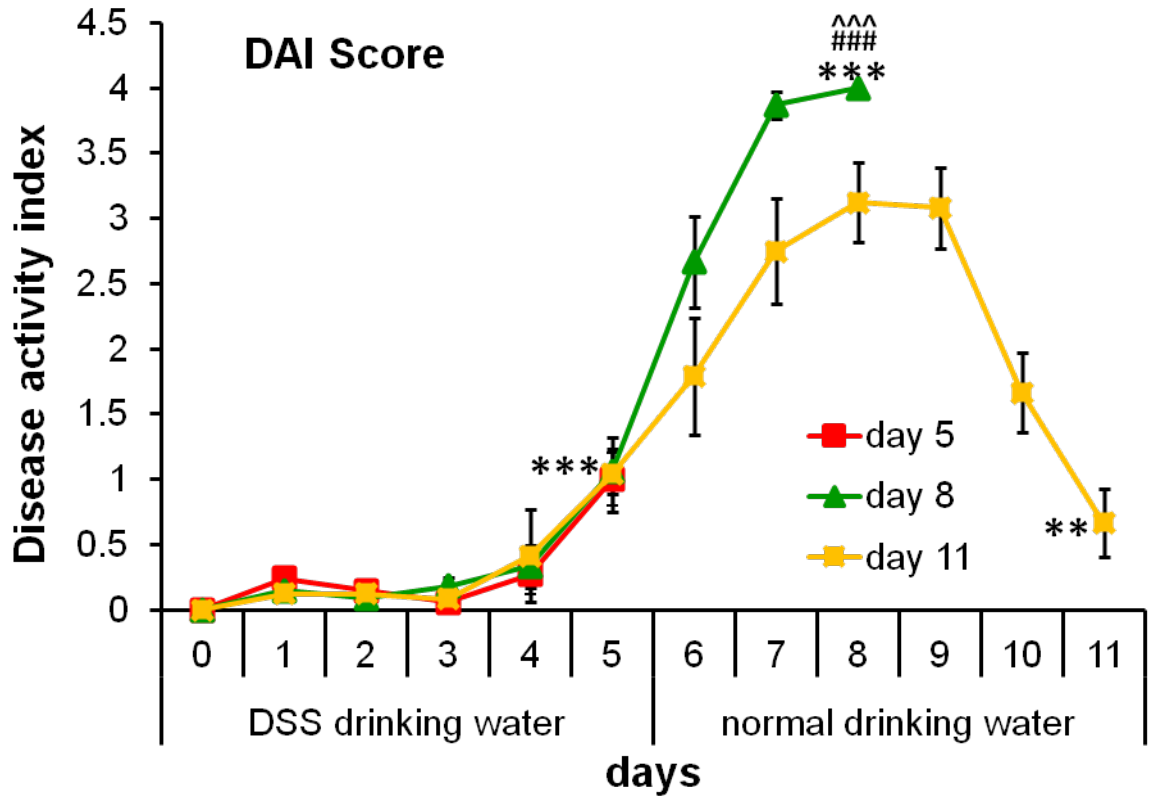

Figure 5.2 DAI. Assessment of disease activity index (DAI) daily for each animal (DAI = (combined score of weight loss, stool consistency and bleeding)/3). Data represented as mean±SEM, *n*=11, 11, 10, 8 for days 0, 5, 8 and 11, respectively. Statistical differences were assessed by Kruskal-Wallis Test followed by Mann-Whitney U tests between pairs of groups, $p<0.01$**, $p<0.001$*** compared to day 0, ### compared to day 5, ^^^ compared to day 11.

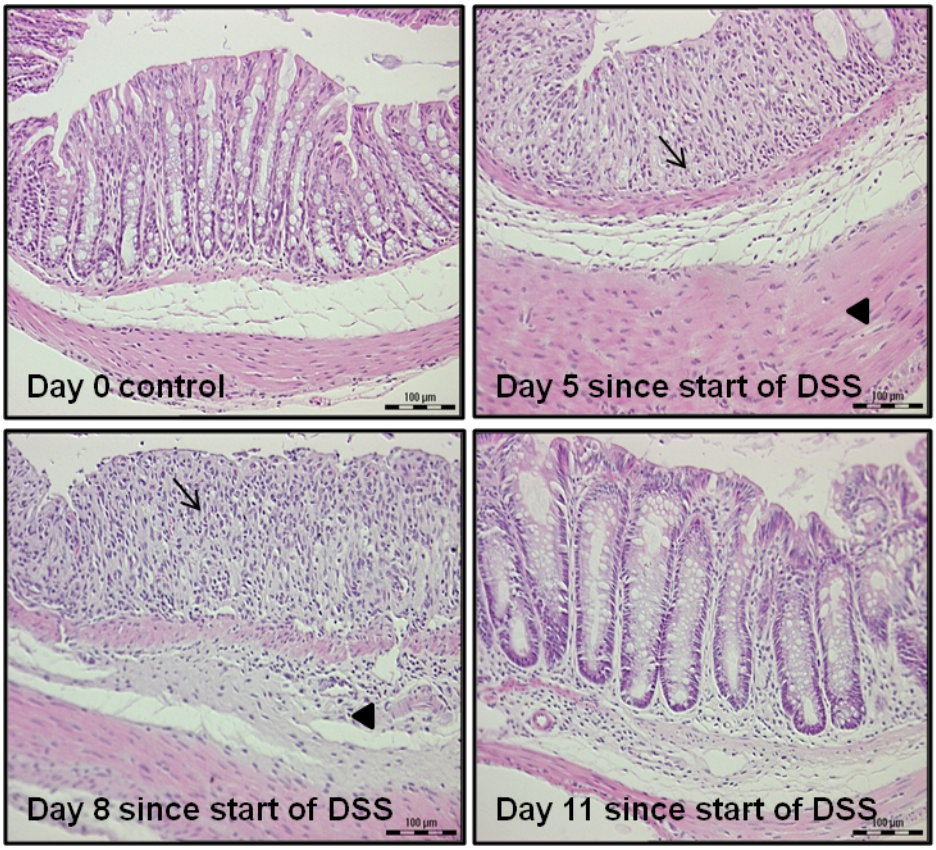

Figure 5.3 Representative images of H&E stained distal colonic sections at each time point. Mice were euthanized at days 0, 5, 8 and 11 since the start of DSS treatment at day 0. Arrows indicate damaged crypts; triangles indicate the submucosal layer with oedema and an infiltrate of inflammatory cells.

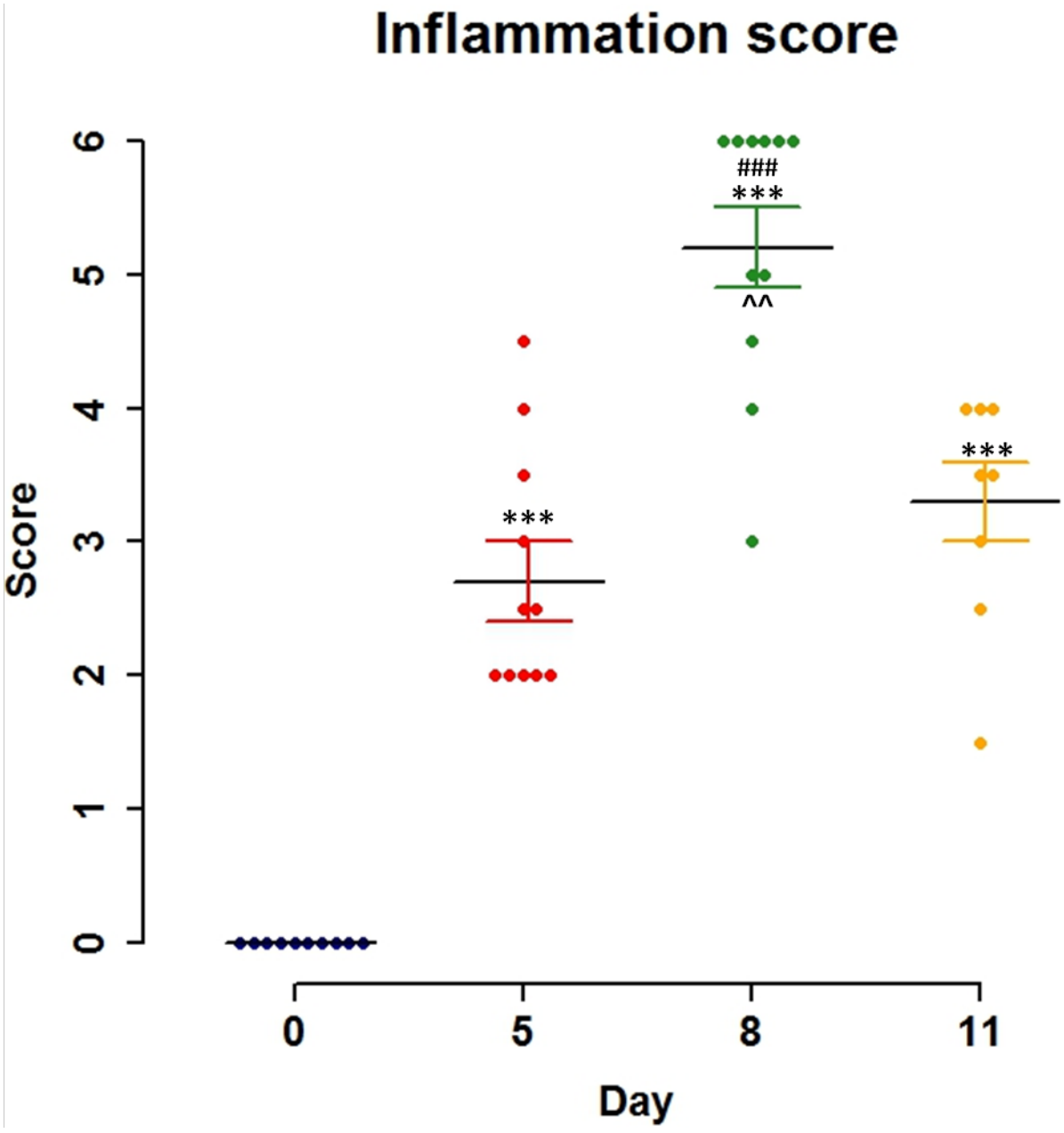

Figure 5.4 Histological (inflammation) scores of DSS-induced colitis in mice. Inflammation score of distal colon taken from C57BL/6 mice at day 0 (blue), day 5 (red), day 8 (green) and day 11 (orange) of a 5 day 4.25% DSS treatment. Each dot represents a score from one mouse and data are presented as mean±SEM, ***p<0.001 compared to day 0, ###p<0.001 compared to day 5, ^^p<0.01 compared to day 11 by Kruskal-Wallis test followed by follow-up Mann-Whitney U tests.

5.5.2 Variation in the faecal VOC metabolome of acute DSS-induced colitis

Mice were sacrificed at days 0, 5, 8 and 11 of experiment, tissues excised and colon contents collected for extraction of VOCs by HS-SPME-GC-MS. This has enabled the direct comparison of VOCs present in the headspace of the colonic luminal content during the development of acute DSS-induced colitis at days 0, 5, 8 and 11.

A total of 95 low molecular weight VOCs were identified across the four time points analysed present in at least 30% of samples in at least one group. 40% of these 95 VOCs were present in at least 50% of all samples at every time point, day 0, 5, 8 and 11, with acid, alcohol and aldehyde compounds as the most common compound classes. Ethanol, acetone, 2-methyl-propanal, 1-propanol, 2-methyl-butanal, butanoic acid, xylene, 3-methyl-butanoic acid and indole were ubiquitous compounds **(Table 5.1).** Of these 95 compounds, there were 59.1±2.5, 54.9±2.3, 47.9±2.6 and 49.6±4.2 VOCs identified at days 0, 5, 8 and 11, respectively (mean±SEM). The average number of VOCs identified decreased with the development of colitis, with a significant decrease at day 8 compared to day 0 (p<0.05). During the recovery phase of colitis, there was a minor increase between day 8 and 11 **(Figure 5.5).**

The chemical composition of the colon contents collected at the different time points of acute DSS-colitis was investigated. This was achieved by calculating the total number of alcohol, acid, ester, aldehyde, alkane, alicyclic, benzenoid, ether, heterocyclic, ketone, nitrogen containing, sulphur containing and unidentified compounds found in all samples and determining the presence of each group by percentage at each time point. Although the chemical composition does not appear to vary dramatically, there is a slight decrease in the number of ester compounds at day 8 (11%) compared to day 5 (14%). There is also a noticeable decrease in the number of alkane compounds (e.g. 3-methylpentane, hexane), and an increase in aldehydes and ketones in the presence of colitis at days 5 and 8, compared to days 0 and 11 **(Figure 5.6).**

Table 5.1 List of 95 compounds detected in the HS of colonic luminal content of DSS-treated mice at different time points, by SPME-GC-MS (*n*=11, 11, 10, 8 for days 0, 5, 8 and 11, respectively).

	Presence (%)			
RT_compound	**Day 0**	**Day 5**	**Day 8**	**Day 11**
5.12_acetylaldehyde	0	0	40	0
6.42_pentane	55	45	0	63
6.61_ethanol	100	100	100	100
6.92_furan	45	18	30	50
7.21_propanal	0	100	100	0
7.41_acetone	100	100	100	100
7.49_dimethyl sulfide	91	82	40	75
7.61_isopropanol	100	64	90	75
7.82_thiourea	91	91	60	75
7.94_methyl acetate	91	100	50	88
8.61_3-methyl-pentane	36	0	0	38
9.01_2-methyl-propanal	100	100	100	100
9.07_hexane	36	0	0	25
9.57_1-propanol	100	100	100	100
10.16_butanal	18	100	70	25
10.28_2,3-butanedione	82	100	100	100
10.32_furan, 3-methyl-	100	45	30	100
10.53_ethyl acetate	82	100	70	100
10.56_2-butanone	82	73	90	75
10.77_2-butanol	100	0	20	75
11.21_methyl propionate	55	100	50	88
11.90_1-propanol, 2-methyl-	82	82	60	88
12.49_3-methyl-butanal	91	100	90	88
12.51_acetic acid	91	100	100	100
12.81_2-methyl-butanal	100	100	100	100
13.44_1-butanol	73	73	50	88
13.51_2-ethyl-furan	36	9	10	0
13.98_2-pentanone	91	100	80	88
14.00_1-penten-3-ol	64	36	30	38
14.08_propanoic acid, ethyl ester	73	91	40	75
14.16_2,3-pentanedione	18	27	60	25
14.20_pentanal	9	36	10	13
14.26_propyl acetate	100	100	50	88
14.41_2-pentanol	64	9	0	75
14.69_methyl butyrate	91	100	50	88
16.08_1-butanol, 3-methyl-	73	45	30	38
16.13_3-hydroxy-2-butanone	9	55	90	63
16.19_1-butanol, 2-methyl-	45	9	40	25
16.29_propanoic acid	100	100	90	100
16.47_2-pentanone, 3-methyl	91	45	10	50

Table 5.1 continued.

RT_compound	Presence (%)			
	Day 0	Day 5	Day 8	Day 11
16.98_1-propanone, 1-cyclopropyl-	45	18	30	25
17.45_1-pentanol	55	55	60	38
17.72_ethyl butyrate	100	100	60	88
17.93_propanoic acid, propyl ester	45	18	40	63
17.94_oxirane, 2-methyl-2-(1-methylethyl)-	73	55	20	25
18.10_methyl isobutyl ketone	0	36	10	38
18.26_2-methyl-propanoic acid	100	100	100	88
18.43_hexanal	64	82	50	63
18.51_2-butenal, 3-methyl-	18	36	50	0
18.60_methyl valerate	45	9	0	0
19.62_butanoic acid	100	100	100	100
19.73_2-hydroxy-3-pentanone	0	9	60	13
20.22_ethylbenzene	64	73	80	50
20.53_xylene	100	100	100	100
20.56_N-benzyloxy-2-carbomethoxyaziridine	27	18	40	0
21.35_butanoic acid, propyl ester	64	45	10	13
21.49_1-hexanol	64	55	60	50
21.51_3-methyl-butanoic acid	100	100	100	100
21.73_2-methyl-butanoic acid	100	100	100	88
22.11_2-heptanone	100	82	90	100
22.16_2-heptanol	55	0	0	25
22.33_heptanal	9	82	80	13
23.14_pentanoic acid	100	100	100	88
23.27_unknown	27	9	40	0
23.62_3-(methylthio)-propanal	36	64	70	25
24.05_oxime-, methoxy-phenyl-	55	36	20	13
24.73_2-heptanone, 5-methyl-	91	73	30	63
24.80_1,3,5-triazine	9	36	30	13
24.89_1-heptanol	45	45	40	38
24.93_2-pentyl-furan	82	36	0	50
24.94_butanoic acid, butyl ester	55	45	0	0
25.12_1-octen-3-ol	55	55	60	88
25.52_3-octanone	91	73	30	63
25.73_benzaldehyde	91	100	100	88
26.38_hexanoic acid	55	73	30	25
26.50_1-propanol, 3-(methylthio)-	9	18	50	0
26.66_dimethyl sulfone	45	18	10	0
26.99_1-hexanol, 2-ethyl-	55	55	60	38
27.25_butanoic acid, 3-methylbutyl ester	36	18	0	0

Table 5.1 continued.

RT_compound	Presence (%)			
	Day 0	Day 5	Day 8	Day 11
27.67_5-ethylcyclopent-1-enecarboxaldehyde	82	73	20	63
28.14_phenol	100	91	90	50
28.62_2-octenal	82	73	50	50
28.64_benzyl alcohol	9	9	40	0
28.66_benzeneacetaldehyde	91	100	100	75
28.93_diiodomethane	36	0	20	25
29.06_2-nonanone	55	45	30	50
29.24_5-hydroxy-4-octanone	36	0	0	13
29.57_nonanal	36	36	50	13
29.77_benzenamine, 2-methyl-	73	45	20	0
31.25_phenylethyl alcohol	55	55	60	50
31.41_2-decanone	0	55	50	50
31.62_1-nonanol	55	0	0	25
31.81_2-nonenal	9	27	20	50
33.74_benzene, 1, 3-bis(1,1-dimethylethyl)-	64	9	0	13
38.66_indole	100	100	100	100

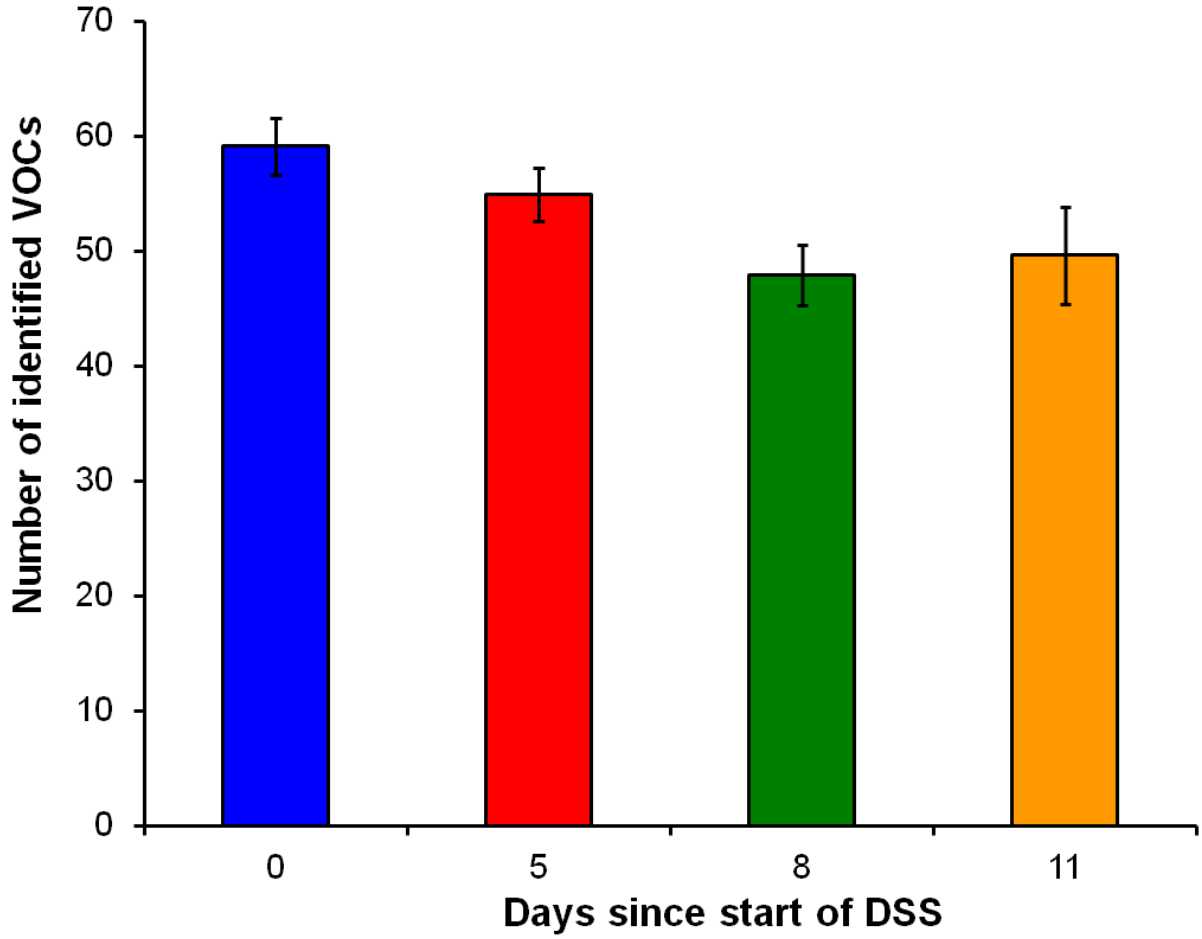

Figure 5.5 Variation in the presence of faecal VOCs during the development of acute colitis. The number of VOCs identified in the headspace of the colon contents collected at days 0, 5, 8 and 11 of the induction of acute colitis by administration of 4.25% DSS (data represented as mean±SEM, *n* =11, 11, 10, 8 for days 0, 5, 8 and 11, respectively; ANOVA followed by Tukey's test, *p<0.05).

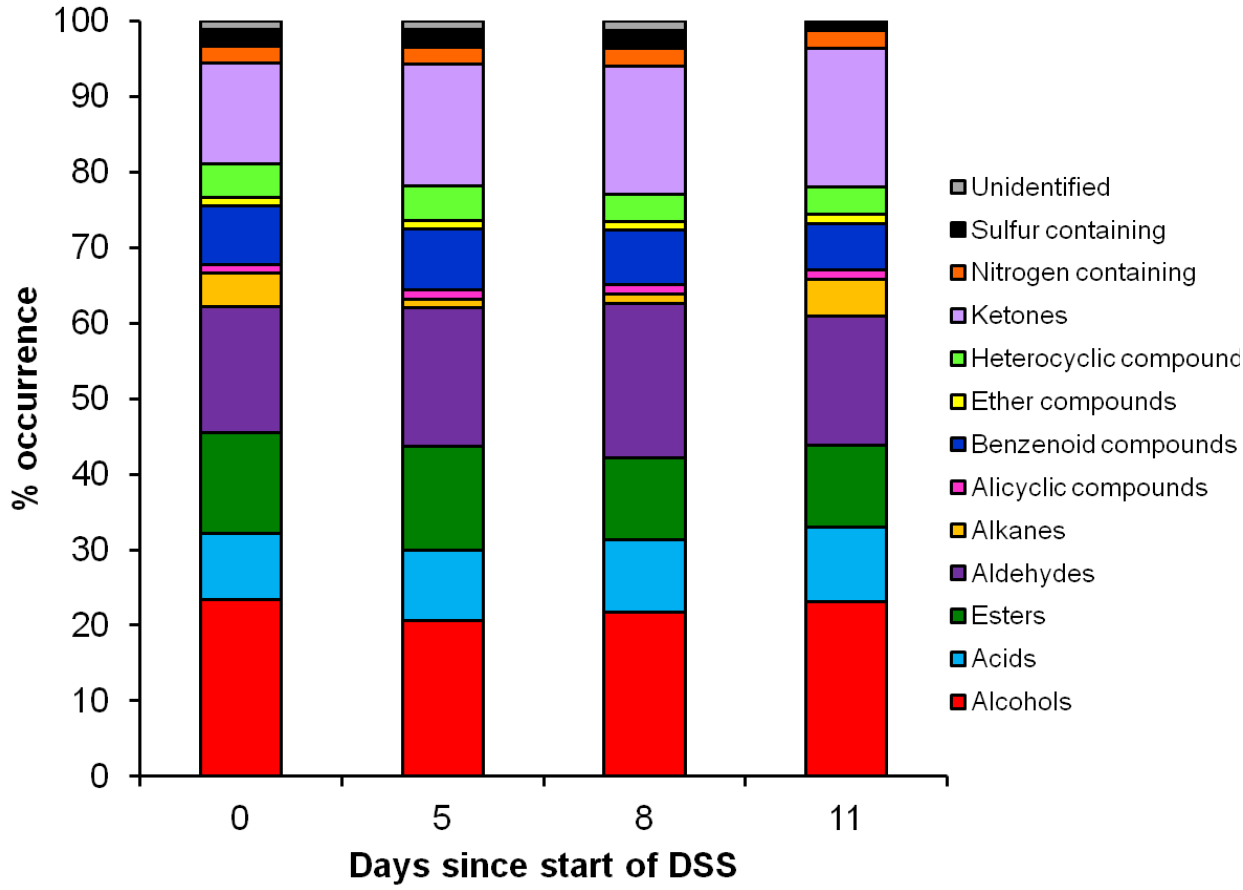

Figure 5.6 Variation in the chemical composition by percentage of faecal VOCs according to development of colitis. Bar plots demonstrating the compound chemical composition by percentage across all time points.

5.5.3 Quantitative VOC profile variation during the development of acute colitis

In order to further investigate the differences in faecal VOC profiles of colon content samples collected at days 0, 5, 8 and 11 of this experimental colitis murine model, the concentrations of the 95 identified VOCs in the colonic content were examined.

The peak abundances for all compounds in all samples were collated and a one-way ANOVA was performed on log-transformed data to identify those compounds significantly varying with the development of colitis. In the colonic luminal contents of DSS-treated mice, there were 46 compounds whose levels were significantly different between days 0, 5, 8 and 11 of treatment **(Table 5.2).** Of these 46 compounds, 32 significantly decreased at days 5 and 8, compared to day 0 and 11; in most cases the levels were seen to increase at day 11, to levels similar to those observed at day 0. In contrast, there were 14 compounds that significantly increased at days 5 and 8 when compared to the levels at days 0 and 11. The levels of nitrogen containing (e.g. indole), sulphur containing (e.g. dimethyl sulphide), fatty acids (e.g. 2-methyl-butanoic acid), esters (e.g. butanoic acid, propyl ester) and alcohols (e.g. 2-butanol) were all decreased during the acute phase of colitis (days 5 and 8). **Figure 5.7** shows each of the 46 significantly different compounds presented as a boxplot; a standardised way of displaying the distribution of data based on the minimum, first quartile, median, third quartile, and maximum. Presenting each significantly different compound in the form of a boxplot was a good way to visually identify outliers and to compare the distribution of presence/absence, abundance and spread of data across each time point.

Some of the 46 significantly different compounds may be significant with *p*-values less than 0.05 purely by chance. Therefore, these *p*-values were then corrected for multiple comparisons using the Bonferroni correction, resulting in 9 compounds being significantly different between days 0, 5, 8 and 11. A Tukey HSD test identified where these differences lie **(Table 5.3).** Propanal was identified in 100% of samples at days 5 and 8 at concentrations of 5,850,711±790,709 and 3,213,638

±495,214, respectively, but absent at days 0 and 11. A significant difference was therefore found when comparing days 5 and 8 to days 0 and 11 (p<0.001). 2-butanol was present in 100% and 75% of samples in days 0 and 11, respectively; it was absent at day 5 and showed a 22-fold significant decrease between day 0 and day 8 (only 20% of samples) (p<0.001), with a subsequent 6-fold increase between day 8 and day 11 (p<0.01). Butanal was detected in 18% of samples at day 0 and showed a significant 29-fold increase compared to day 5 (100% of samples) (p<0.001). The concentration of butanal then significantly decreased from 5,655,360 ±1,048,855 at day 5 to 1,485,786 ±630,022 at day 8 with a 14-fold decrease between day 8 and 11, resulting in a level similar to that seen at day 0. Heptanal behaved similar to propanal, significantly increasing at days 5 and 8 when compared to days 0 and 11, but was present at lower concentrations at days 0 and 11 unlike propanal. Ethanol was identified in 100% of samples at every time point with its concentration significantly decreasing at day 5 and 8 compared to day 0. Ethanol also significantly increased 2-fold between day 8 and 11 to a final concentration of 202,669,568 ±22,678,375, reverting back to levels more similar to that at day 0 (307,124,410 ±50,827,323), suggestive of signs of recovery. There was also a significant decrease in the levels of 2-pentanol when comparing days 5 (24-fold decrease) and 8 (absent) with days 0 and 11. The level of 3-methyl-butanoic acid started at 144,108,079 ±19,162,470 on day 0, increased slightly at day 5 then gradually decreased from day 5 to day 8 with a final concentration of 31,745,896±8,629,142 at day 11 and was also identified in 100% of samples at every time point (mean±SEM). 3-hydroxy-2-butanone was identified in the majority (90%) of samples at day 8 at a noticeably higher concentration than identified at days 5 (10-fold increase) and 11 (8-fold increase), but, interestingly, it was only present in one sample at day 0 at very low concentrations 2,846,628. Finally, furan, 3-methyl- showed a significant decrease in both the concentration and occurrence at days 5 and 8 compared to days 0 and 11.

It is also important to note that there are no significant differences between days 0 and day 11 with only one compound showing a significant difference between days 5 and 8 **(Table 5.3).**

To summarise, propanal, butanal, heptanal and 3-hydroxy-2-butanone were present in samples at day 8 at higher levels than at days 0 and 11. On the other hand, ethanol, 2-butanol, 2-pentanol, 3-methyl-furan and 3-methyl-butanoic acid were either absent or detected at significantly lower levels at day 8 than day 0 **(Figure 5.8).** At this point, it was noted that propanal, butanal, heptanal, ethanol, 2-butanol, 3-methyl-furan and 3-methyl-butanoic acid were also identified in the mouse chow **(Table 3.4).**

Table 5.2 List of the 46 significantly different compounds across time detected in the HS of colonic luminal content of DSS-treated mice, by SPME-GC-MS (*n*=11, 11, 10, 8 for days 0, 5, 8 and 11, respectively). Highlighted in bold are those VOCs still significant after Bonferroni correction.

	Abundance (mean±SEM)				*P*-value
RT_compound	**Day 0**	**Day 5**	**Day 8**	**Day 11**	
10.16_butanal	**194,951±130,834**	**5,655,360±1,048,855**	**1,485,786±630,022**	**380,257±305,951**	***P*<0.00**
10.32_furan, 3-methyl-	**1,119,436±75,840**	**725,662±274,024**	**207,343±108,584**	**1,192,496±248**	***P*<0.00**
10.77_2-butanol	**10,206,231±2,279,081**	**NA**	**462,670±314,178**	**2,944,264±937,262**	***P*<0.00**
14.26_n-propyl acetate	5,949,300±894,811	13,097,356±2,713,452	6,344,653±2,846,939	7,083,712±1,690,712	*P*<0.00
14.41_2-pentanol	**7,799,971±2,785,378**	**319,070±319,069**	**NA**	**4,141,792±1,772,331**	***P*<0.00**
16.13_3-hydroxy-2-butanone	**2,846,628±2,846,627**	**42,097,758±20,626,200**	**423,418,778±150,622,215**	**52,067,712±21,943,052**	***P*<0.00**
16.47_2-pentanone, 3-methyl	4,971,730±954,199	1,023,145±406,099	392,423±392,422	2,099,873±992,904	*P*<0.00
17.72_ethyl butyrate	33,141,132±9,759,791	4,486,156±1,050,183	1,892,808±662,034	6,974,176±2,829,829	*P*<0.00
19.73_2-hydroxy-3-pentanone	NA	290,235±290,234	6,097,357±2,168,733	194,177±194,176	*P*<0.00
20.53_1,3-xylene	2,030,627±155,608	1,722,624±172,033	2,026,496±238,410	1,080,292±240,972	*P*<0.00
21.51_3-methyl-butanoic acid	**144,108,079±19,162,470**	**192,230,493±56,667,181**	**74,954,650±15,587,067**	**31,745,896±8,629,143**	***P*<0.00**
22.16_2-heptanol	1,763,142±540,439	NA	NA	565,513±387,504	*P*<0.00
22.33_heptanal	**42,824±42,823**	**531,098±129,452**	**664,903±275,435**	**88,065±88,064**	***P*<0.00**

Table 5.2 continued.

RT_compound	Abundance (mean±SEM)				*P*-value
	Day 0	Day 5	Day 8	Day 11	
24.93_2-pentyl-furan	1,566,790±271,019	691,137±348,215	NA	1,259,609±536,636	*P*<0.00
24.94_butanoic acid, butyl ester	2,520,384±1,204,729	746,834±334,510	NA	NA	*P*<0.00
31.62_1-nonanol	269,426±82,907	NA	NA	124,717±81,845	*P*<0.00
33.74_benzene, 1, 3-bis(1,1-dimethylethyl)-	543,654±155,274	78,762±78,761	NA	160,177±160,176	*P*<0.00
5.12_acetylaldehyde	NA	NA	20,740,097±11,322,651	NA	*P*<0.00
6.61_ethanol	**307,124,410±50,827,323**	**122,771,642±14,804,044**	**75,989,709±13,431,387**	**202,669,568±22,678,375**	***P*<0.00**
7.21_propanal	**NA**	**5,850,711±790,709**	**3,213,638±495,214**	**NA**	***P*<0.00**
7.41_acetone	218,915,654±57,501,895	181,642,705±51,242,452	72,877,875±22,236,808	53,674,496±12,930,049	*P*<0.00
9.57_1-propanol	113,671,075±19,233,946	70,583,761±11,031,622	46,356,378±14,653,938	43,409,408±6,024,092	*P*<0.00
11.21_methyl propionate	866,374±316,465	6,592,291±1,647,556	1,637,863±635,804	6,046,552±1,868=3,814	0.01
14.69_methyl butyrate	4,475,805±957,096	1,992,919±354,263	513,972±195,107	1,764,420±544,620	0.01
18.60_methyl valerate	452,987±168,084	111,826±111,825	NA	NA	0.01
21.35_butanoic acid,	7,277,429±2,414,777	1,594,555±639,061	132,987±132,986	119,065±119,064	0.01

propyl ester					

Table 5.2 continued.

RT_compound	Abundances (mean±SEM)				P-value
	Day 0	Day 5	Day 8	Day 11	
21.73_2-methyl-butanoic acid	105,170,665±13,459,797	103,931,439±27,846,126	32,463,053±6,459,924	12,501,568±2,638,618	0.01
24.73_2-heptanone, 5-methyl-	2,504,035±376,554	1,205,661±296,457	236,871±126,365	957,864±401,046	0.01
25.52_3-octanone	1,425,460±333,004	2,072,371±1,112,261	236,193±121,533	906,280±314,466	0.01
28.14_phenol	11,601,437±4,188,859	17,074,810±7,664,201	67,305,715±26,344,602	1,339,153±723,287	0.01
29.77_benzenamine, 2-methyl-	679,919±203,564	687,490±349,396	241,095±168,891	NA	0.01
7.94_methyl acetate	13,298,548±2,856,056	15,561,356±2,664,082	3,878,068±1,578,805	9,981,696±2,172,581	0.01
10.28_2,3-butanedione	7,194,496±2,182,163	20,330,566±3,575,995	62,987,162±20,049,708	13,116,448±3,853,211	0.02
19.62_butanoic acid	999,817,216±160,950,090	797,625,251±128,372,772	443,548,058±109,004,878	501,849,216±123,912,530	0.02
27.67_5-ethylcyclopent-1-enecarboxaldehyde	499,292±79,691	503,912±135,476	100,442±69,121	572,130±230,400	0.02
31.41_2-decanone	NA	1,949,126±876,603	1,169,735±538,749	710,657±301,527	0.02
6.42_pentane	1,397,196±441,984	774,051±342,704	NA	1,634,438±649,195	0.02
8.61_3-methyl-pentane	471,942±250,342	NA	NA	218,723±109,612	0.02

Table 5.2 continued.

RT_compound	Abundances (mean±SEM)				P-value
	Day 0	Day 5	Day 8	Day 11	
26.50_1-propanol, 3-(methylthio)-	27,271±27,270	81,498±60,370	526,474±263,553	NA	0.03
29.24_5-hydroxy-4-octanone	312,001±138,112	NA	NA	63,289±63,288	0.03
7.49_dimethyl sulfide	2,052,841±359,095	1,395,596±374,376	410,797±231,724	1,604,312±531,780	0.03
17.94_oxirane, 2-methyl-2-(1-methylethyl)-	2,345,036±608,508	1,164,224±358,382	364,334±255,319	426,633±293,537	0.04
18.26_2-methyl-propanoic acid	66,311,633±11,822,925	68,957,370±17,949,426	30,914,842±7,055,699	14,576,256±3,446,318	0.04
28.66_benzeneacetaldehyde	2,224,093±551,654	8,800,047±1,413,856	7,669,888±1,755,801	2,723,560±1,352,426	0.04
9.07_hexane	1,178,815±974,180	NA	NA	443,097±294,567	0.04
38.66_indole	96,823,575±17,540,940	53,867,520±8,293,595	77,596,774±22,680,947	37,622,368±7,390,657	0.05

P-values were calculated according to a one-way ANOVA with the significant level of $p<0.05$. Compounds are ordered according to *p*-values (lowest to highest) with those compounds showing a larger significant difference across time at the top of the list. These *p*-values have not been corrected for multiple comparisons.

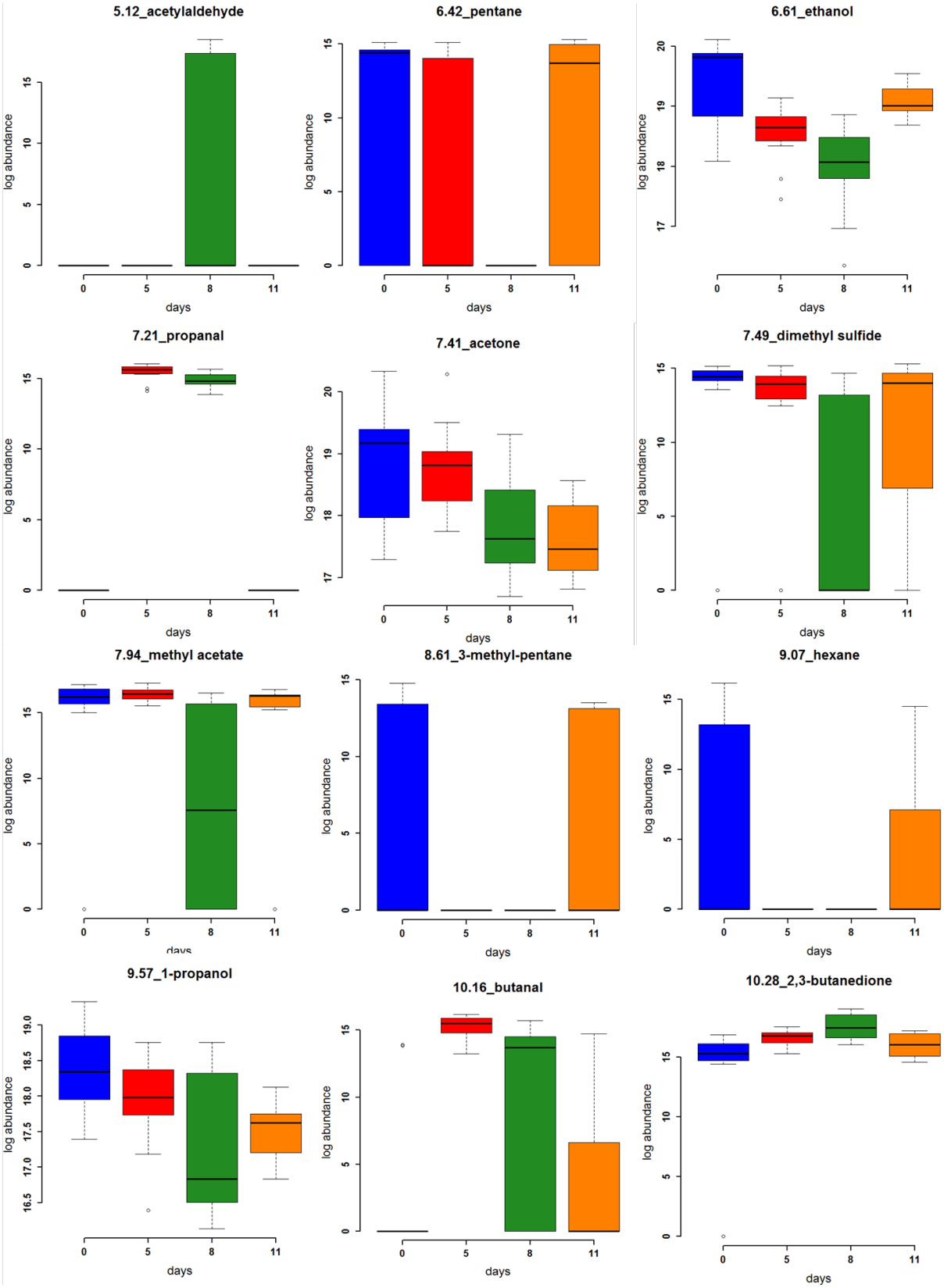

Figure 5.7 Box plots of the peak abundance (log scale) of the significantly different compounds. A one-way ANOVA was performed across the four time points and found 46 compounds to significantly vary across time (p<0.05). These p-values are shown in Table 5.2 and have not been corrected for multiple comparisons.

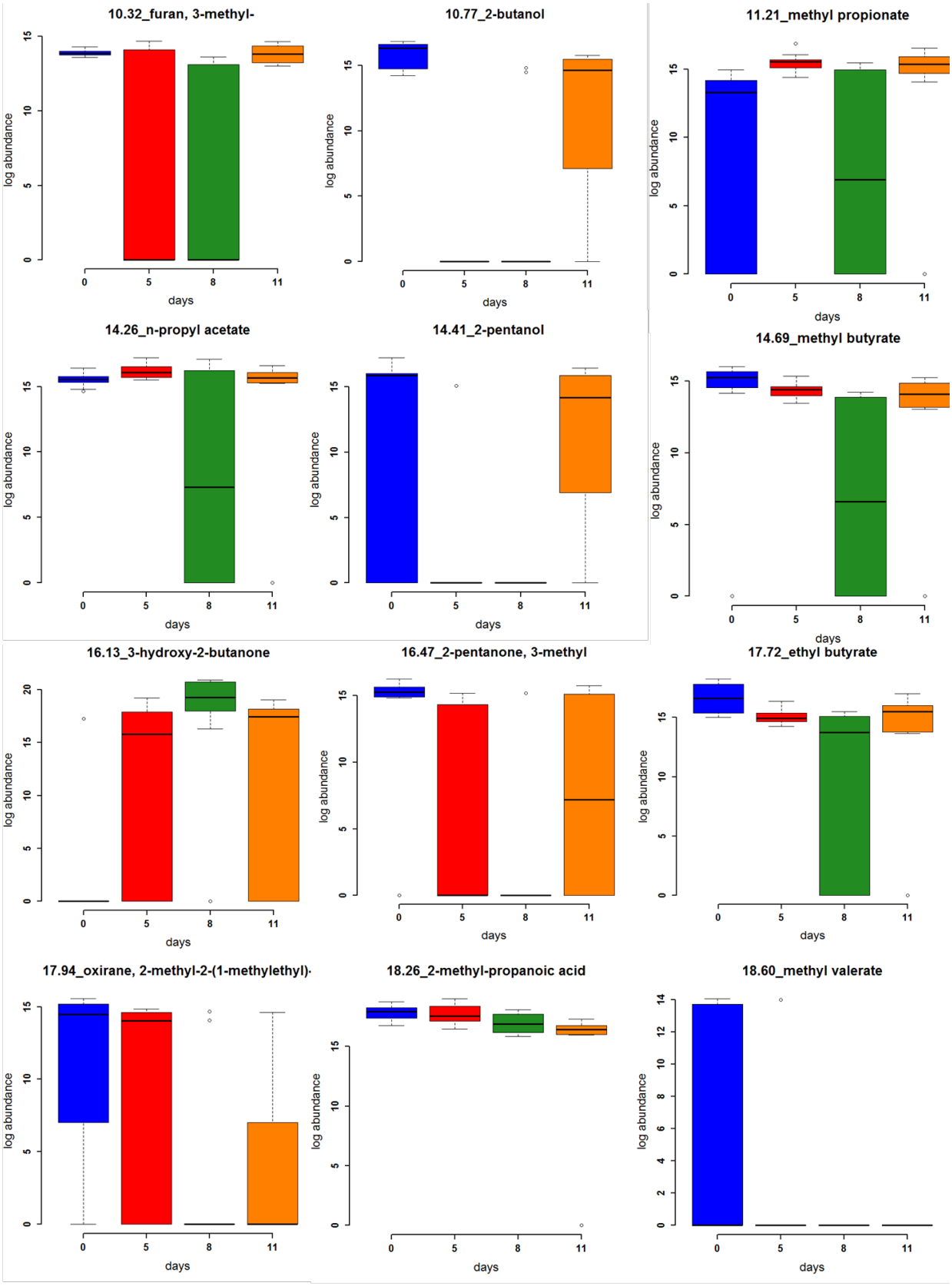

Figure 5.7 (continued). Box plots of the peak abundance (log scale) of the significantly different compounds. A one-way ANOVA was performed across the four time points and found 46 compounds to significantly vary across time (p<0.05). These p-values are shown in Table 5.2 and have not been corrected for multiple comparisons.

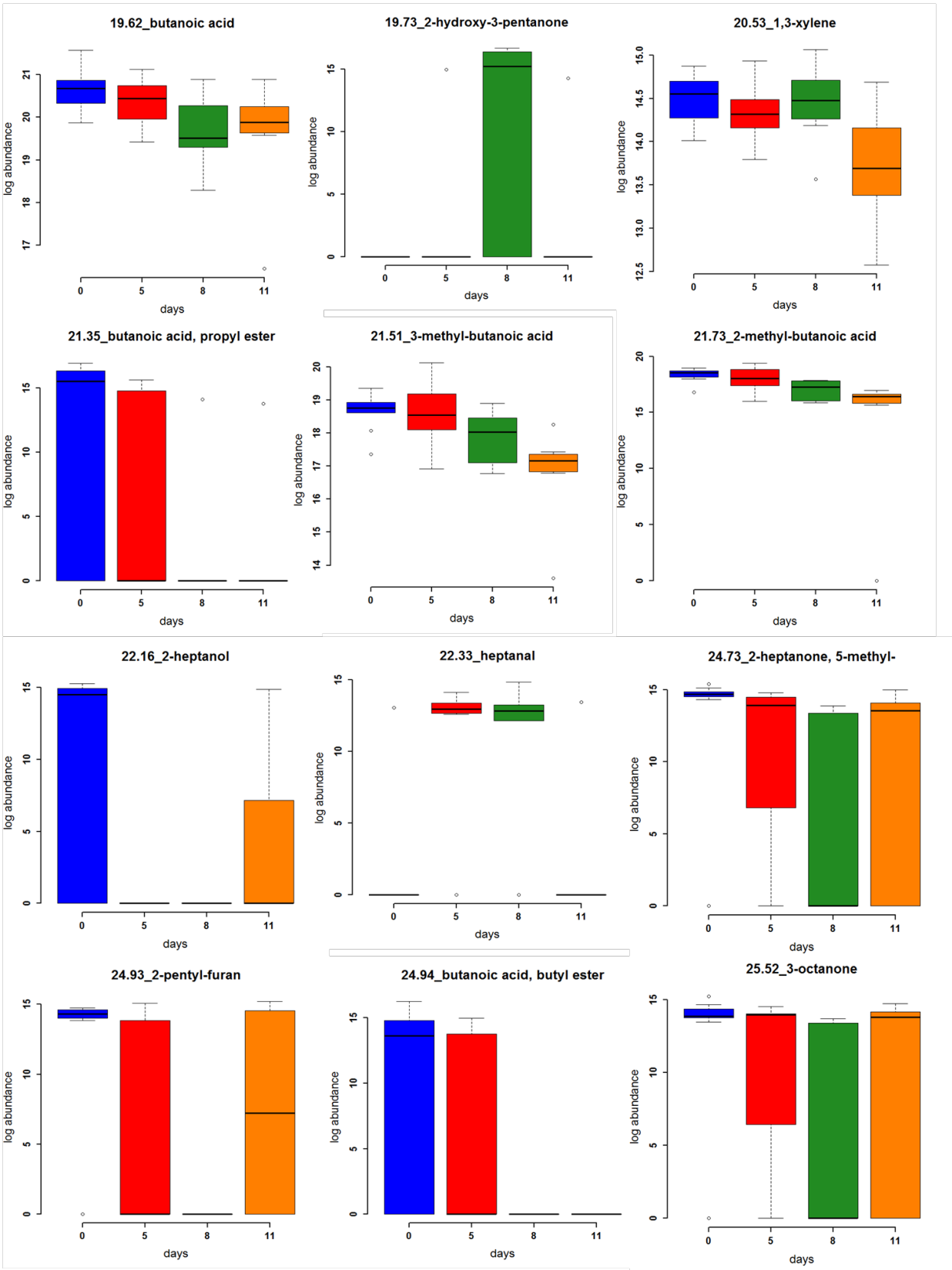

Figure 5.7 (continued). Box plots of the peak abundance (log scale) of the significantly different compounds. A one-way ANOVA was performed across the four time points and found 46 compounds to significantly vary across time (p<0.05). These p-values are shown in Table 5.2 and have not been corrected for multiple comparisons.

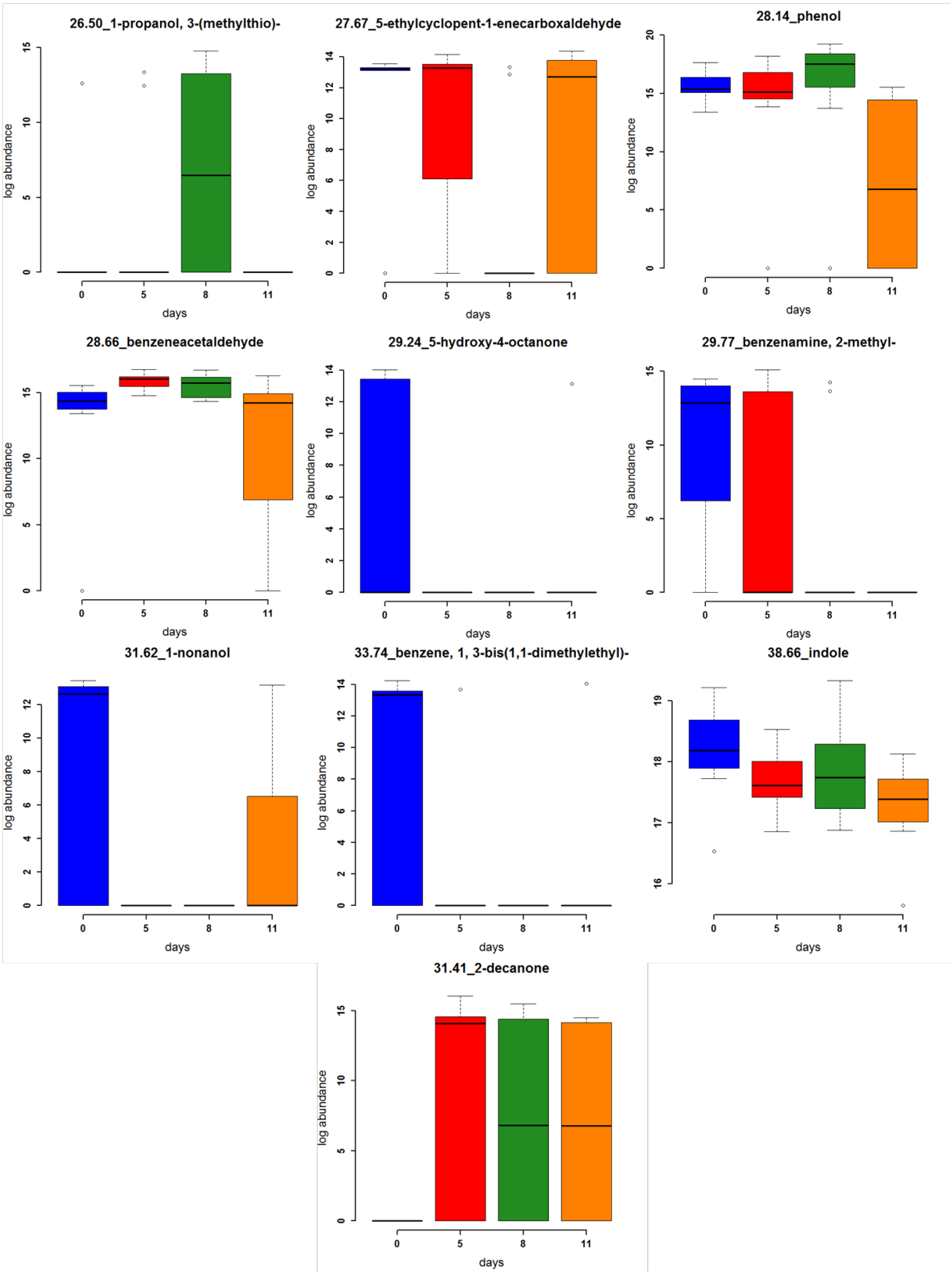

Figure 5.7 (continued). Box plots of the peak abundance (log scale) of the significantly different compounds. A one-way ANOVA was performed across the four time points and found 46 compounds to significantly vary across time (p<0.05). These p-values are shown in Table 5.2 and have not been corrected for multiple comparisons.

Table 5.3 List of the 9 significantly different compounds as a result of adjusting the *p*-values shown in **Table 5.2** for multiple comparisons by Bonferroni correction.

RT_compound	*P*-values						
	Bonferroni	Day 0 vs. 5	Day 0 vs. 8	Day 0 vs 11	Day 5 vs. 8	Day 5 vs. 11	Day 8 vs. 11
7.21_propanal	**0.0000**	**0.0000**	**0.0000**	1.0000	**0.0230**	**0.0000**	**0.0000**
10.16_butanal	**0.0008**	**0.0000**	**0.0159**	0.9798	0.1327	**0.0002**	0.0711
16.13_3-hydroxy-2-butanone	**0.0446**	0.0799	**0.0002**	**0.0451**	0.1172	0.9673	0.3552
22.33_heptanal	**0.0016**	**0.0003**	**0.0006**	0.9964	0.9995	**0.0018**	**0.0031**
6.61_ethanol	**0.0030**	**0.0144**	**0.0000**	0.7767	0.1402	0.2120	**0.0017**
10.32_furan, 3-methyl-	**0.0070**	**0.0081**	**0.0005**	1.0000	0.6937	**0.0185**	**0.0014**
10.77_2-butanol	**0.0000**	**0.0000**	**0.0000**	0.1448	0.4332	**0.0000**	**0.0016**
14.41_2-pentanol	**0.0063**	**0.0052**	**0.0015**	0.9813	0.9489	**0.0041**	**0.0013**
21.51_3-methyl-butanoic acid	**0.0353**	1.0000	0.2475	**0.0007**	0.2649	**0.0008**	0.0874

P-values were calculated according to a one-way ANOVA **(Table 5.2),** adjusted for multiple comparisons using Bonferroni correction, followed by Tukey's HSD test. **Red** indicates $p<0.05$, **blue** $p<0.01$ and **green** $p<0.001$.

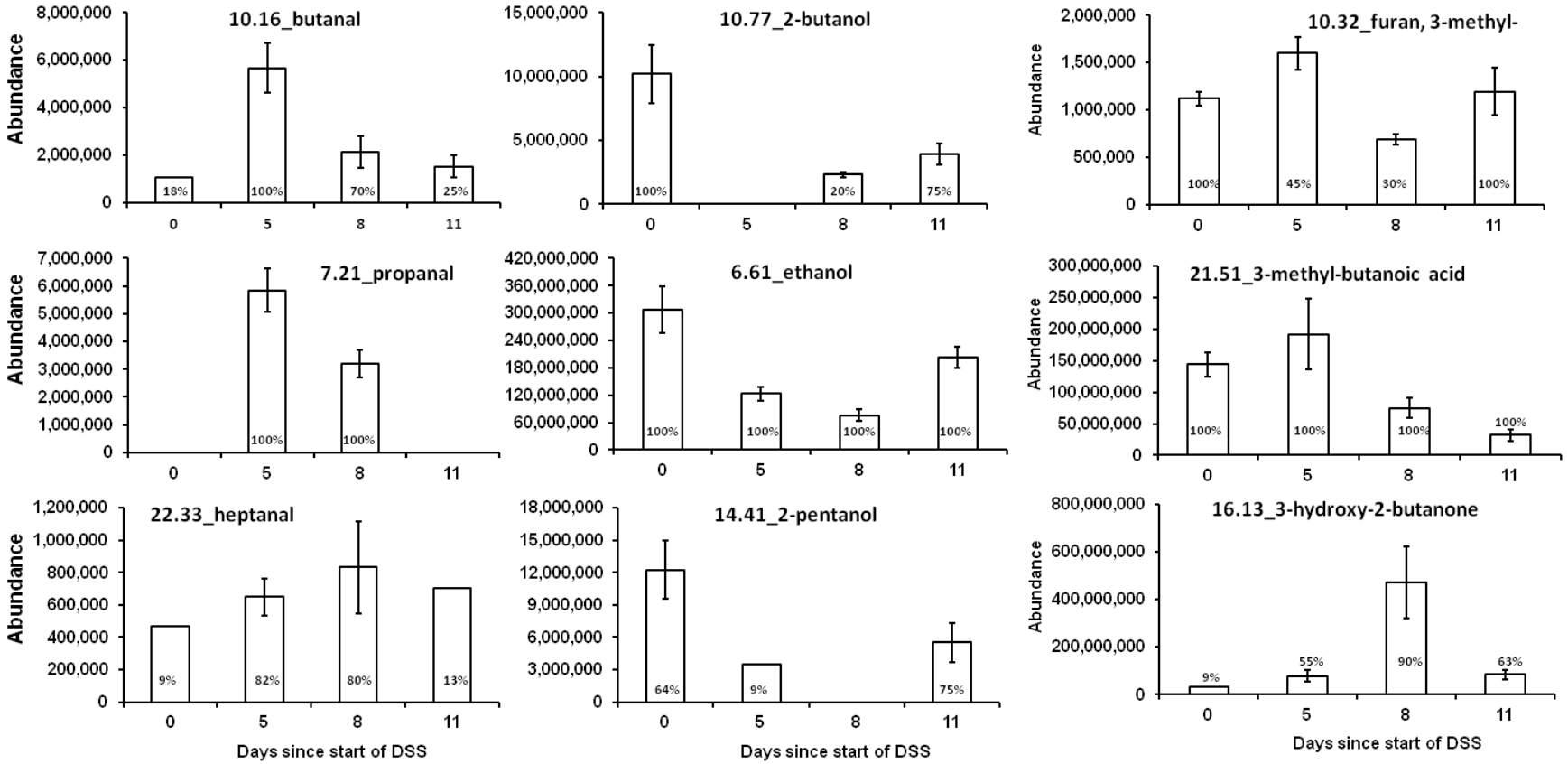

Figure 5.8 Bar plots of the peak abundance of 9 significantly different compounds. Table 5.3 shows the significant differences identified by a one-way ANOVA performed across the four time points and adjusted for multiple comparisons using Bonferroni correction (p<0.05). Data are expressed as mean±SEM peak abundance for each significant compound with the percentage occurrence of each compound at each time point presented.

5.5.4 Pattern recognition using multivariate statistics visually confirms variation during development of colitis

The patterns of variation in the levels of the 46 significantly different compounds detected in the HS of the colon contents of DSS-treated mice were analysed to examine the clustering of each time point according to multivariate statistics using PCA. This was performed using the abundance of the 46 significant compounds and showed distinct clustering and clear separation of the four time points **(Figure 5.9).** It is apparent from closer inspection of this analysis that the VOC profile from the colon contents of DSS-treated mice changes according to the different time points tested during the development of acute DSS-colitis. Specifically, samples from day 0 are grouped in the upper right hand quadrant of the plot, day 5 centre, day 8 to the left and day 11 grouped in the lower right hand quadrant with very little variation between day 0 and 11. These results visually suggest that the pathogenesis of DSS-induced colitis leads to variation in the faecal metabolome. Inspection of the variable factor map produced alongside the biplot of the PCA shows that the significant VOCs (p<0.05, Bonferroni) are responsible for the separation between the different time points. For example, butanal and 3-methylbutanoic acid are chief compounds at day 5, heptanal and 3-hydroxy-2-butanone at day 8, and 2-butanol and ethanol at day 0 and 11.

In order to further explore the differences between these significant VOC emissions from the different time points of DSS-colitis, a heat map was produced using cluster analysis according to the abundance of the 9 compounds selected (p<0.05, ANOVA followed by Bonferroni) **(Figure 5.10).** The resulting plots showed similar patterns with days 0 (control) and 11 (black) grouped together, and days 5 and 8 (red). It also visually shows how each of the 9 significantly different compounds change between the time points. For example, **Figure 5.8** shows that the concentration of ethanol decreases at days 5 and 8 compared to day 0 and 11. This decrease is represented by the heatmap with shades of red and shades of yellow representing higher concentrations of each compound.

To summarise, a one-way ANOVA followed by Tukey's HSD test, corrected for multiple comparison using the Bonferroni method, identified 9 significantly different compounds. Of these 9, there were 3 aldehydes, 3 alcohols, 1 ketone, 1 acid and 1 furan compound. All aldehydes and 3-hydroxy-2-butanone significantly increased in the presence of colitis and all alcohols, 3-methyl-butanoic acid and the furan compound significantly decreased. The visual cluster analyses confirm that these compounds are responsible for the differences observed according to the degree of colitis.

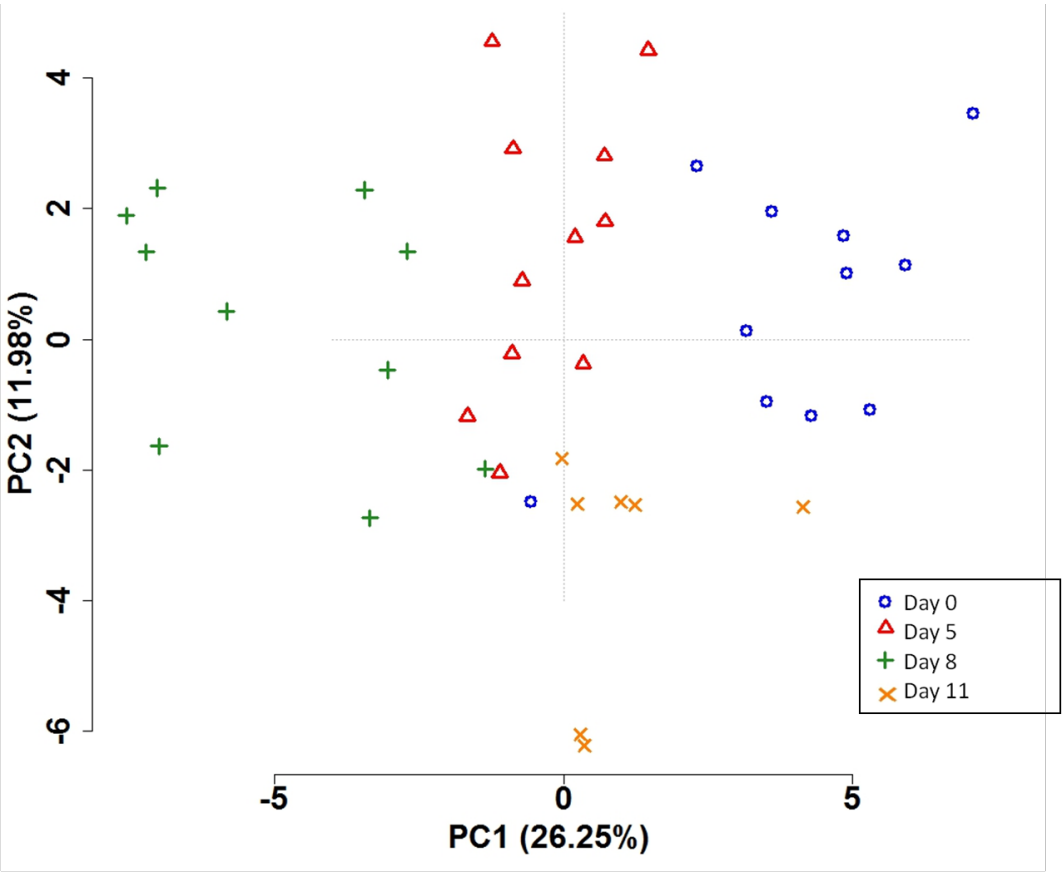

Figure 5.9 A PCA biplot for the colonic luminal content samples of DSS-treated mice. The first principal component has been plotted against the second principal component. The PCA was performed using the abundance of the 46 significant compounds from **Table 5.2**.

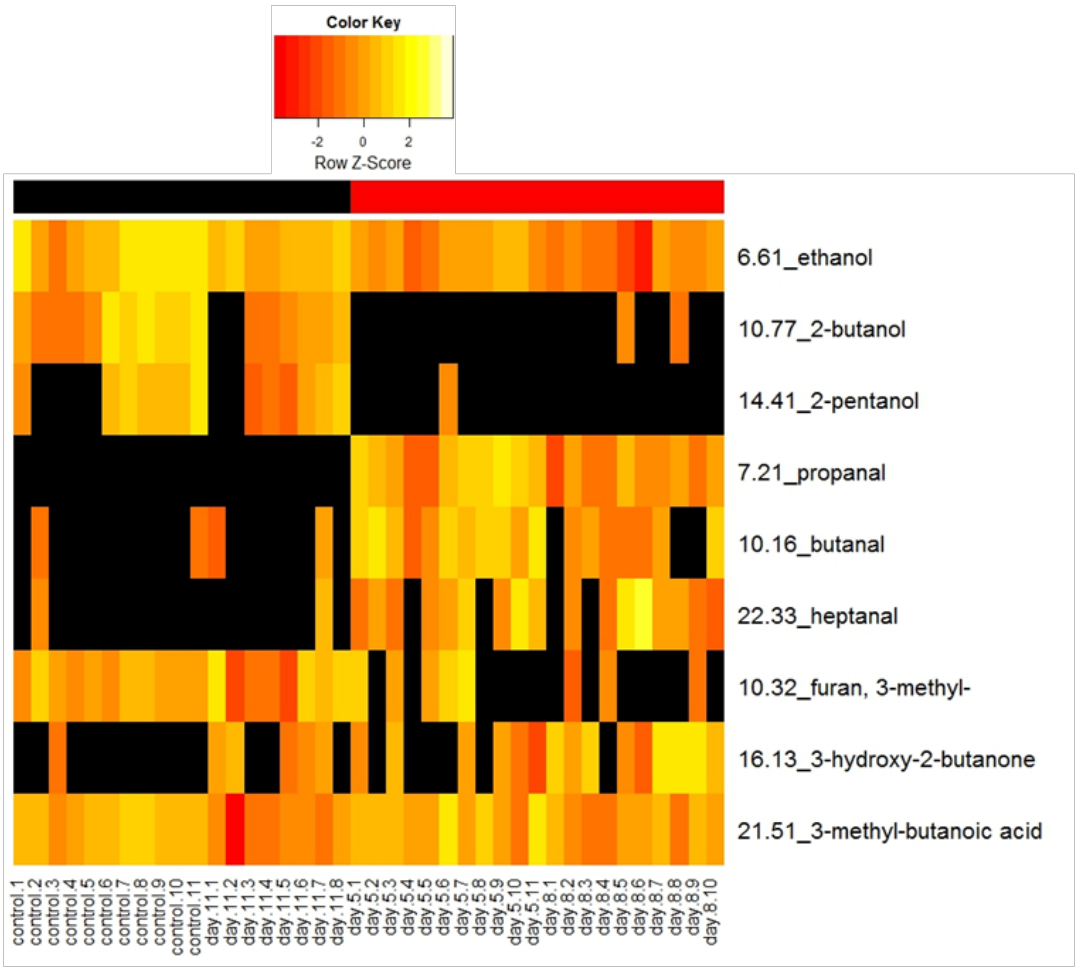

Figure 5.10 Hierarchical clustering. A heat map representing hierarchical clustering of the significantly different 9 compounds (ANOVA followed by Bonferroni correction) across the four different time points of DSS-induced colitis. Sample classes are indicated by the coloured bars (day 0 & day 11 = black, day 5 & day 8 = red). Columns represent individual murine faecal samples and rows refer to distinct compounds. Shades of yellow represent an increase in concentration of a compound and shades of red represent a decrease in concentration of a compound, grouping similar rows/columns using the complete-linkage clustering method.

5.5.5 Metabolomic effect of deleting *NFκB2* in acute DSS-induced colitis

This study specifically investigates the VOCs that may be associated with the role of the alternative *NFκB* pathway in the development of acute DSS-induced colitis. Clinical (weight loss and DAI) and histological features **(Figure 5.11C&D)** were assessed and confirmed the resistance of *NFκB2*$^{-/-}$ compared to WT treated mice following treatment with DSS. WT DSS treated mice lost 19.5±1.15% of their body weight at day 8, which was significantly more than *NFκB2*$^{-/-}$ treated mice (1.8±0.9% weight loss) and also the WT and *NFκB2*$^{-/-}$ untreated groups (p<0.001, ANOVA followed by Tukey's HSD test) **(Figure 5.11A).** The WT DSS treated mice were also significantly more physically unwell compared to WT untreated, *NFκB2*$^{-/-}$ untreated, and *NFκB2*$^{-/-}$ DSS treated animals (p<0.01, Kruskal Wallis Test followed by Mann-Whitney U) **(Figure 5.11B).**

A total of 100 VOCs were identified in the headspace of the colonic luminal content of the mice in all four groups. Univariate statistical analysis found 26 of these VOCs to be present at significantly different concentrations between the different groups (p<0.05, ANOVA and Bonferroni) **(Table 5.4).** Of these, 15 VOCs were absent in the WT and *NFκB2*$^{-/-}$ DSS treated group and were commonly alcohols. Inspection of the PCA **(Figure 5.12)** shows that based on the abundance of the 26 significant compounds, WT and *NFκB2*$^{-/-}$ untreated mice appear to have a similar faecal metabolome. The WT DSS-treated group appears to be very different to both the control groups with the *NFκB2*$^{-/-}$ DSS treated group lying in between the two clusters on the PCA. Although, clinically the *NFκB2*$^{-/-}$ DSS treated group behaved like the untreated control groups, the faecal VOC metabolome is significantly different, suggesting a role of *NFκB2* in the pathogenesis of DSS-induced colitis.

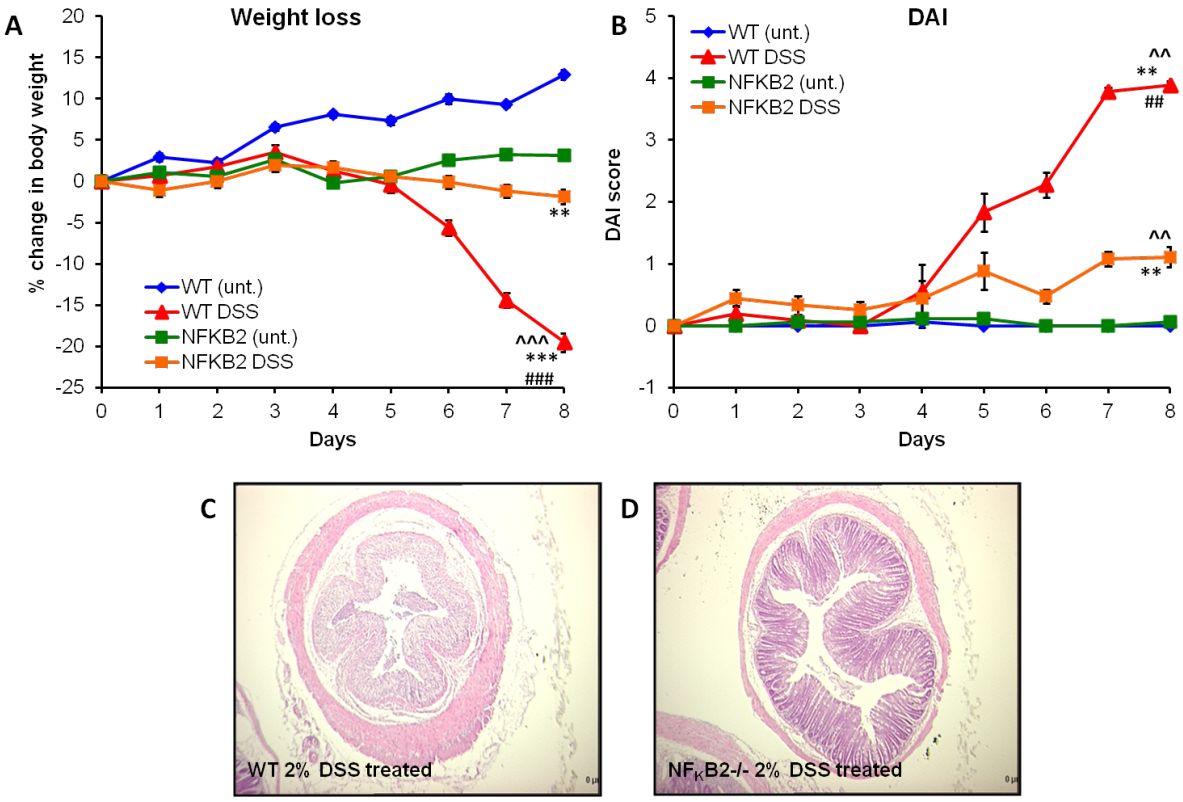

Figure 5.11 Clinical and histological features of acute DSS-induced colitis in WT and *NFκB2*$^{-/-}$ mice. A. Weight loss. B. Disease activity index (DAI); Data represented as mean±SEM, *n*=4, 6, 4, 6 for WT (unt.), WT DSS, *NFκB2*-/- (unt.) and *NFκB2*-/- DSS, respectively. Statistical differences were assessed by one-way ANOVA followed by Tukey's test for weight loss and Kruskal-Wallis Test followed by Mann-Whitney U for DAI, $p<0.01$ **, $p<0.001$ ***, ^^^, ### compared to WT (unt.), *NFκB2*-/- (unt.), *NFκB2*-/- DSS, respectively. C. & D. Representative images of H&E stained distal colonic sections for WT and *NFκB2*$^{-/-}$ DSS treated mice.

Table 5.4 List of the 26 significantly different compounds between WT and *NFκB2*$^{-/-}$ mice treated with and without 2% DSS.

RT_Compound	Abundance (mean±SEM)				*P*-value
	WT DSS-treated	WT untreated	*NFκB2*$^{-/-}$ DSS-treated	*NFκB2*$^{-/-}$ untreated	
26.99_1-hexanol, 2-ethyl-	NA	4,293,824±461,077	NA	2,823,744±111,612	0.0000
40.10_5,9-undecadien-2-ol, 6,10-dimethyl-	NA	6,320,576±773,170	NA	24,114,944±4,747,307	0.0000
16.19_1-butanol, 2-methyl-	NA	25,662,464±6,962,638	NA	14,029,568±2,975,937	0.0000
11.90_1-propanol, 2-methyl-	NA	5,085,568±1,051,529	NA	3,859,904±990,037	0.0000
17.45_1-pentanol	NA	4,209,088±1,034,285	NA	4,133,056±337,640	0.0000
31.25_phenylethyl alcohol	NA	13,751,552±3,973,018	NA	7,011,520±310,868	0.0000
21.19_1-hexanol	NA	26,988,224±6,589,116	NA	20,873,984±2,822,093	0.0000
25.12_1-octen-3-ol	NA	12,283,328±2,769,442	NA	15,430,144±4,198,912	0.0000
10.77_2-butanol	NA	6,767,104±1,555,738	NA	4,950,256±1,495,925	0.0000
14.41_2-pentanol	NA	6,107,472±2,132,947	NA	4,357,104±1,735,014	0.0000
24.89_1-heptanol	NA	1,612,816±363,086	NA	1,554,645±249,402	0.0002
26.50_1-propanol, 3-(methylthio)-	NA	1,772,395±535,956	NA	1,498,592±120,772	0.0002
31.62_1-nonanol	NA	658,683±90,728	NA	452,368±48,434	0.0002
13.44_1-butanol	NA	4,323,952±1,888,453	NA	8,490,837±1,647,241	0.0003
28.64_benzyl alcohol	NA	6,632,976±3,331,760	NA	1,428,736	0.0003
20.53_1,3-xylene	7,996,032±484,938	2,173,168±159,663	7,894,613±484,386	4,869,248±702,532	0.0000
35.82_1,2-benzisothiazole	1,783,808	5,888,640±1,658,803	7,309,653±1,606,850	6,075,136±1,299,329	0.0006
21.73_2-methyl-butanoic acid	9,474,133±2,895,488	93,830,656±24,504,667	37,910,699±9,004,976	69,857,024±16,370,365	0.0249
19.62_butanoic acid	125,237,931±40,154,797	611,123,200±164,712,772	647,350,955±94,764,949	663,744,512±167,684,275	0.0272

Table 5.4 continued.

33.74_benzene, 1, 3-bis(1,1-dimethylethyl)-	NA	422,480	2,241,909±235,028	1,790,784±576,388	0.0000
14.20_pentanal	NA	1,147,776	NA	1,663,568±287,732	0.0006
14.69_methyl butyrate	NA	2,612,780±1,035,401	1,570,672±363,524	1,590,560±478,802	0.0105
9.57_1-propanol	5,640,448	24,012,032±6,126,457	6,414,848	27,009,792±7,682,815	0.0153
18.60_methyl valerate	NA	1,057,493±155,322	NA	NA	0.0162
7.21_propanal	3,415,765±473,668	NA	2,326,784	1,082,752	0.0228
24.10_3-heptanone, 6-methyl-	NA	807,787±153,411	1,401,088±98,362	1,261,152±299,611	0.0369

P-values were calculated according to a one-way ANOVA adjusted for multiple comparisons using Bonferroni correction, followed by Tukey's HSD test.

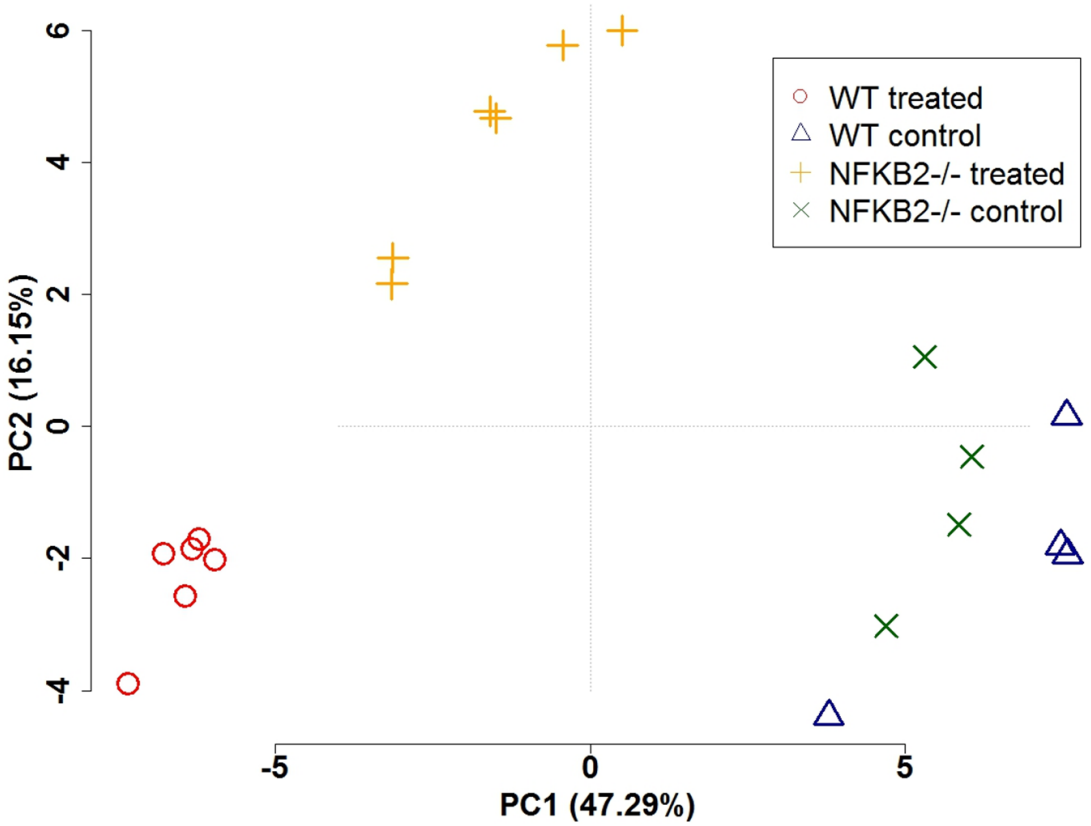

Figure 5.12 A PCA biplot for the colonic luminal content samples of WT and *NFκB2*$^{-/-}$ control and DSS-treated mice. The first principal component has been plotted against the second principal component. The PCA was performed using the abundance of the 26 significant compounds (p<0.05, ANOVA followed by Bonferroni).

5.5.6 Administration of $MgSO_4$ induces a quick onset of diarrhoea

Diarrhoea was induced by oral administration of magnesium sulphate at the dose of 2g/kg. Faecal samples were collected every hour and the amount and consistency of the faeces were assessed. Each animal was assigned a FOI (FOI = sum of consistency scores of all motions passed within 3 hours [286]). A mouse passing a stool of score 2 at least once was counted as suffering from diarrhoea. Diarrhoea was observed between 1 and 2 hours after administration of $MgSO_4$, peaking at 3 hours with a significantly different FOI between control and treated groups of mice (**Figure 5.13**). All faecal samples collected were analysed using the HS-SPME-GC-MS method of VOC detection and were later used as controls against the DSS colitis samples to isolate compounds changing or produced as a result of an inflammatory response.

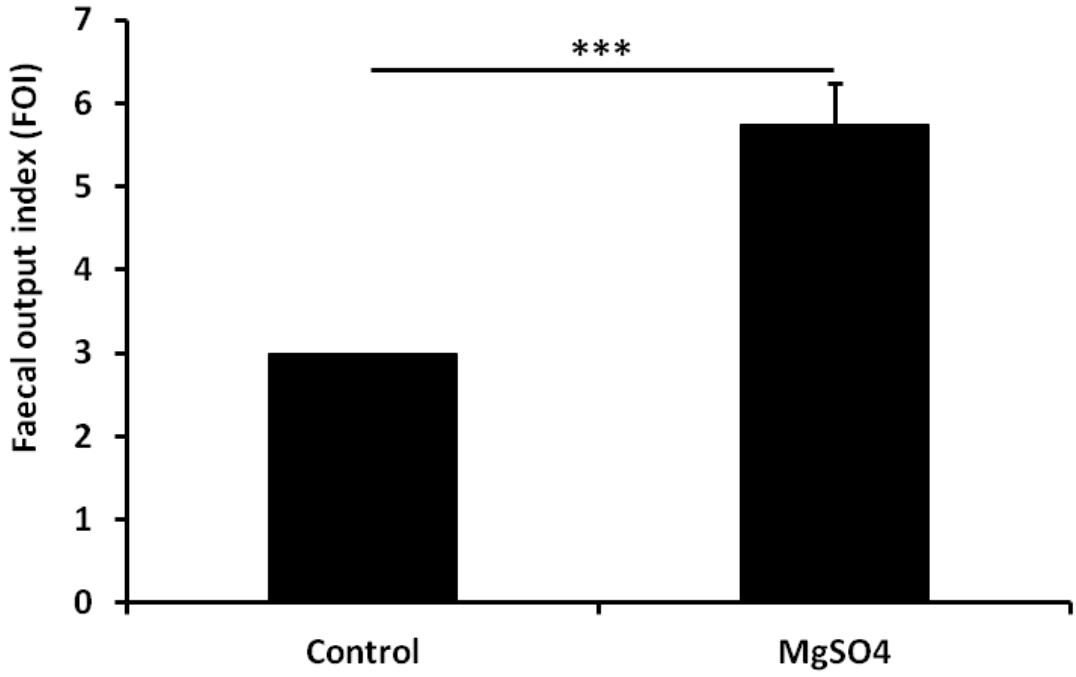

Figure 5.13 FOI for $MgSO_4$-induced diarrhoea at 3 hours. The FOI was defined as the sum of the consistency scores of all the motions passes within the observation period of 3 hours. A mouse passing a stool of score 2 at least once was counted as suffering from diarrhoea. Data expressed as mean±SD of FOI of each mouse for both control (n=3) and $MgSO_4$ group (n=5); t-test ***p<0.001.

5.5.7 Significantly different VOCs present with the onset of $MgSO_4$-induced diarrhoea

The detection of the VOCs emitted from the diarrhoea samples of mice 3 hours after being treated with $MgSO_4$ and their untreated controls yielded a total of 69 compounds with an average of 33.0±4.0 and 37.2±4.0 found in untreated controls and $MgSO_4$-treated mice, respectively (mean±SEM, $p>0.05$) **(Figure 5.14).** Of these, ketones, aldehydes, acids and alkanes were among the commonest groups of compounds across both groups with the number of ketones and aldehydes identified increasing in the diarrhoea group, compared to control. Phenol was the only compound found to be significantly more prevalent in the $MgSO_4$ group (5/5), compared to control (0/3) (Fisher's Exact, $p<0.05$).

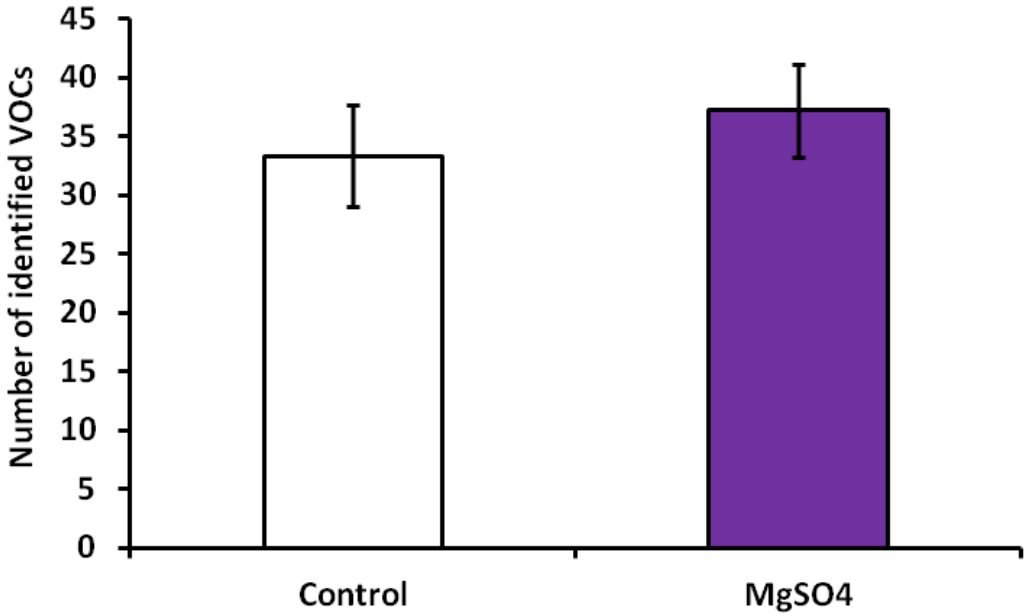

Figure 5.14 Administration of $MgSO_4$ causes in increase the number of identified VOCs. The number of VOCs identified in the HS of stool samples from mice administered with 2mg/kg MgSO4 (n=5) increased slightly compared to those identified from untreated controls (n=3). Data expressed as mean±SEM; t-test $p>0.05$ N.S.

Univariate statistical analysis resulted in 6 significantly different compounds (Student's *t*-test, $p<0.05$) **(Table 5.5).** Isopropanol was identified in 100% of samples from both the $MgSO_4$ and control groups but at a significantly lower concentration in $MgSO_4$ samples ($p=0.01$) with a 4.3-fold decrease. 3-hydroxy-2-butanone behaved in a similar way, but only had a prevalence of 20% in $MgSO_4$ compared to control (100%) with a 1.3-fold significant decrease ($p=0.02$). 2-methyl-propanal and 2-methyl-butanal were also found in 100% of $MgSO_4$ samples and both significantly increasing in $MgSO_4$ samples ($p<0.01$) by a 12.3 and 36.4-fold increase, respectively. Phenol and 3-(methylthio)-propanal were absent in the control group with 100 and 80% prevalence in the $MgSO_4$ group, respectively. These changes in abundance can be observed by inspection of the box and whisker plots in **Figure 5.15.** Phenol was the only compound to remain significantly different after undergoing the Bonferroni correction.

Furthermore, PCA illustrated the separation of $MgSO_4$-treated mice compared to the control group based on these significantly different VOCs **(Figure 5.16).** This suggests that the detection and analysis of VOCs is capable of distinguishing between healthy and diarrhoea faecal samples.

Table 5.5 List of the 6 significantly different compounds detected in the HS of diarrhoea samples from $MgSO_4$-treated mice compared to untreated controls, by SPME-GC-MS.

RT_compound	Presence (%)		Abundance (mean±SEM)			
	control (*n*=3)	$MgSO_4$(*n*=5)	control (*n*=3)	$MgSO_4$(*n*=5)	Fold change	*P*-value
7.61_isopropanol	100	100	92,575,061±19,183,304	21,470,617±7,927,192	4.3 ↓	0.0125
9.01_2-methylpropanal	100	100	2,761,514±652,764	33,999,974±12,072,443	12.3 ↑	0.0118
12.81_2-methylbutanal	100	100	2,027,776±570,594	73,876,428±30,147,287	36.4 ↑	0.0035
16.13_3-hydroxy-2-butanone	100	20	69,043,712±57,917,128	51,949,568	1.3 ↓	0.0167
23.62_3-(methylthio)-propanal	0	80	NA	1,730,448±849,691	Absent in control	0.0168
28.14_phenol	**0**	**100**	**NA**	**10,213,824±4,825,243**	**Absent in control**	**0.0000***

P-values were calculated according to a Student's *t*-test and performed on log-transformed data ($p<0.05$). Fold change shows an increase (↑) or decrease (↓) of the average peak abundance of each compound in the $MgSO_4$ group, compared to untreated control. *Bonferroni correction.

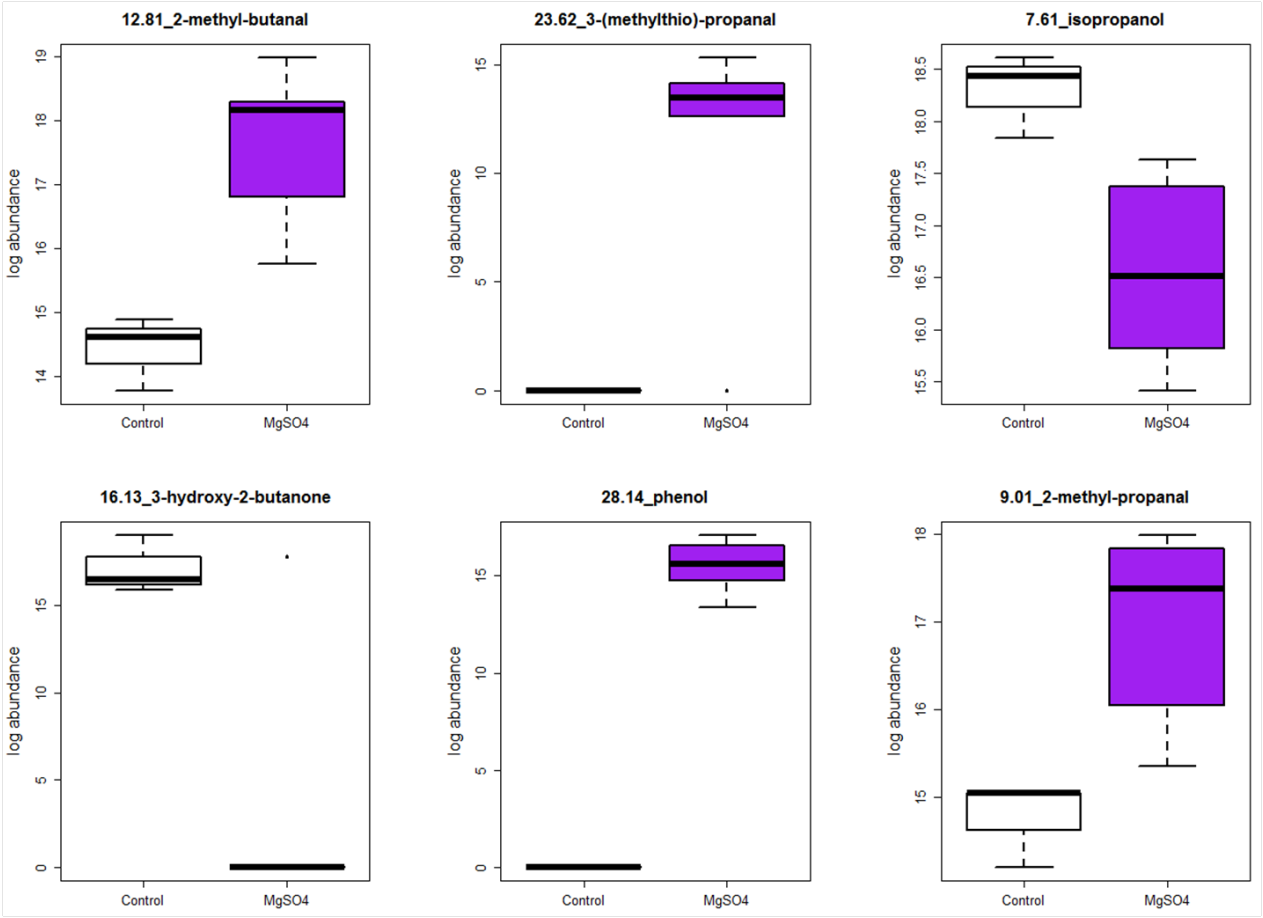

Figure 5.15 Box plots of the peak abundance (log scale) of the significantly different compounds. A Student's t-test was performed between the abundance of the 92 VOCs identified in the HS of stool samples from both groups. There were 6 compounds found to significantly vary and the p-values are shown in **Table 5.5.**

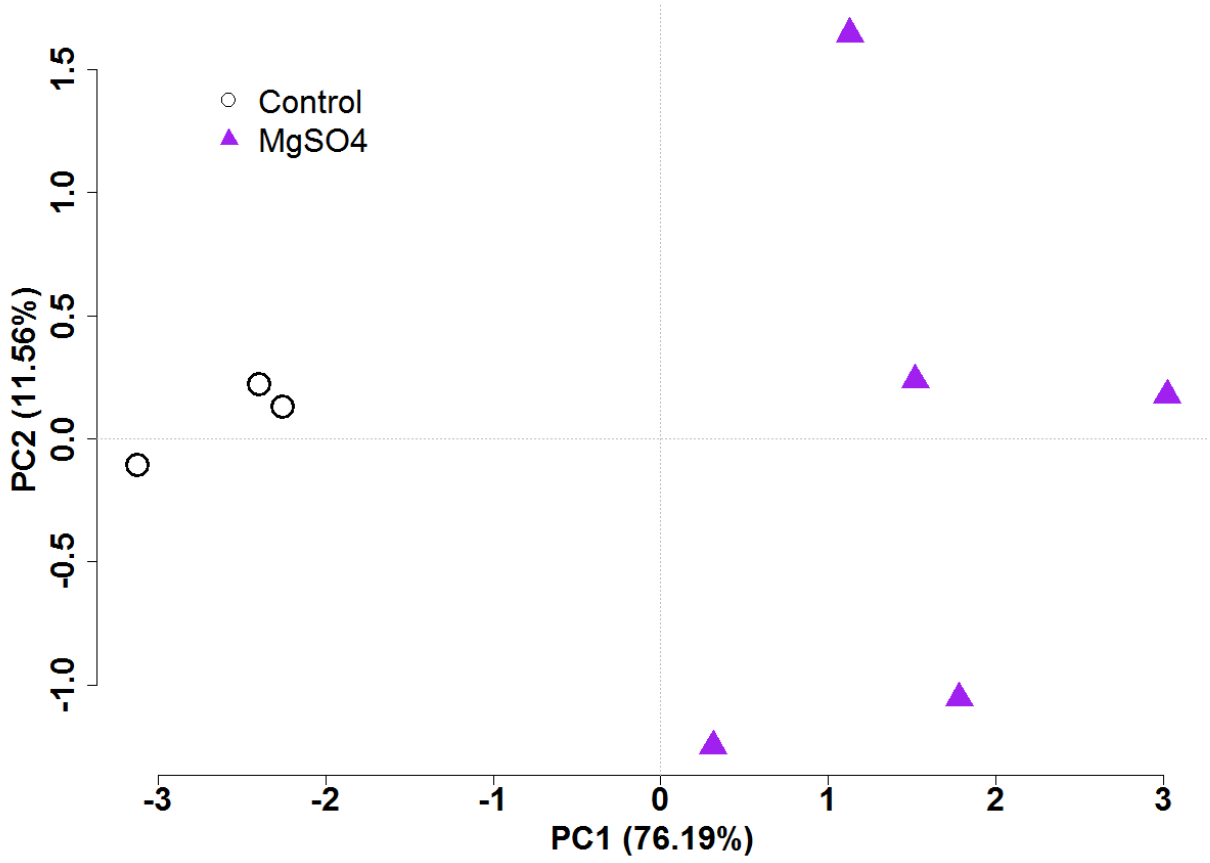

Figure 5.16 A PCA biplot for the diarrhoea faecal samples collected at 3 hours post $MgSO_4$ administration. The first principal component (76.19% of the total variation) has been plotted against the second principal component (11.56% of the total variation). The PCA was performed using the 6 significant compounds from **Table 5.5**.

5.5.8 VOC comparison of DSS-induced colitis and $MgSO_4$-induced diarrhoea

In order to identify compounds specific to the acute DSS-induced colitis faecal VOC profile, the colon contents collected at day 8 of acute DSS-colitis were compared to those produced from mice administered $MgSO_4$. The consistency of diarrhoea was scored hourly after administration of $MgSO_4$ with 3 hours receiving the highest score. Therefore, the samples collected at 3 hours (*n*=5) were directly compared with the samples from day 8 of the third and final acute DSS-colitis model (*n*=6).

Administration of $MgSO_4$ causes diarrhoea by accelerating the small intestinal transit time and reducing the intestinal absorption of fat, protein and carbohydrates, therefore acting as an osmotic laxative [287]. The onset of this watery diarrhoea is fast with a quick transit time through the intestine, resulting in a significantly lower number of VOCs identified (38.2±4.4) when compared to DSS-colitis (50.5±2.9) (mean±SEM, $p<0.05$) **(Figure 5.17).**

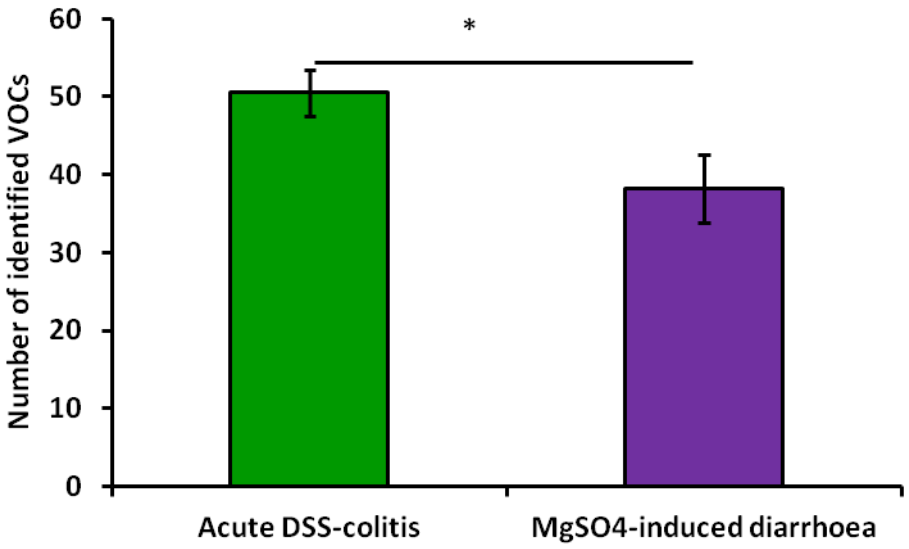

Figure 5.17 The number of VOCs identified from diarrhoea samples decreases for $MgSO_4$-treated mice compared to DSS-treated mice. The number of VOCs identified in the HS of colon contents of mice culled at day 8 of DSS-colitis (*n*=6) development significantly increased compared to $MgSO_4$-treated mice (*n*=5). Data expressed as mean±SEM; *$p<0.05$.

Of 92 compounds found in at least 30% of faecal samples in either group, 21 were noted to be significantly more prevalent in either the DSS-colitis or the $MgSO_4$-diarrhoea group **(Table 5.6**). The most significantly different compounds were 1-pentanol, 2-ethyl-1-hexanol and phenylethyl alcohol which were all present in 100% of DSS-colitis samples but absent from $MgSO_4$-diarrhoea samples (p<0.001). The majority of these significant compounds were more prevalent in the DSS-colitis group with alcohols appearing most frequently. These compounds were present in 60% of samples at day 8 of the acute colitis experiment, compared to 38% at day 11. This implies that the presence of these compounds may indicate the presence of inflammation-driven diarrhoea, or the absence may indicate osmotic laxative-induced diarrhoea.

In addition, there were 20 compounds found to significantly vary in concentration between the two groups (t-test; p<0.05). There were 12 compounds found exclusively in the DSS-colitis group (abundant in alcohols and ketones), 1 in the $MgSO_4$ (pentanal) and 7 compounds common to both groups **(Table 5.7).** The concentration of ethanol and 2-butanol significantly decreased at day 8 of DSS-colitis when compared to day 0, 5 and 11, whereas heptanal, butanal and propanal significantly increased at day 8. All mentioned compounds were present in the $MgSO_4$-diarrhoea group (>30% of samples) but with no significant difference in concentration to day 8 DSS-colitis. 2-pentanol was present at day 0, 5 and 11 of the DSS-colitis but absent at day 8 and also the $MgSO_4$-diarrhoea groups. These similarities indicate that these compounds are potential biomarkers for the presence of diarrhoea, not specific to IBD. Whereas, 3-hydroxy-2-butanone, which was present at day 8 DSS-colitis at a significantly higher concentration than day 0 (T-test, p<0.001), was present in only 1/5 samples in the $MgSO_4$ group **(Table 5.6 & 5.7).** A PCA plot using the abundances of these 20 significantly different compounds clearly demonstrates this separation (PC1 = 67.32% variation) of samples from mice administered either 4.25% DSS or 2mg/kg $MgSO_4$ based on their VOC profile **(Figure 5.18).** This shows that the faecal VOC profiles are significantly different between the different causes of murine diarrhoea.

Table 5.6 List of 21 compounds with a significantly different prevalence between DSS-induced colitis and $MgSO_4$-induced diarrhoea.

RT_compound	Present in DSS-colitis (%)	Present in $MgSO_4$-diarrhoea (%)	Chi^2 test *p*-value
17.45_1-pentanol	100	0	0.0009
26.99_1-hexanol, 2-ethyl-	100	0	0.0009
31.25_phenylethyl alcohol	100	0	0.0009
13.44_1-butanol	83	0	0.0057
19.73_2-hydroxy-3-pentanone	83	0	0.0057
25.33_1-octen-3-ol	83	0	0.0057
26.50_1-propanol, 3-(methylthio)-	83	0	0.0057
14.20_pentanal	0	80	0.0060
16.13_3-hydroxy-2-butanone	100	20	0.0060
21.49_1-hexanol	100	20	0.0060
25.12_1-nonen-3-ol	100	20	0.0060
16.19_1-butanol, 2-methyl-	67	0	0.0221
20.56_N-benzyloxy-2-carbomethoxyaziridine	67	0	0.0221
24.89_1-heptanol	67	0	0.0221
28.64_benzyl alcohol	67	0	0.0221
31.41_2-decanone	67	0	0.0221
11.90_1-propanol, 2-methyl-	100	40	0.0261
24.93_2-pentyl-furan	0	60	0.0261
26.34_D-limonene	0	60	0.0261
29.34_acetophenone	0	60	0.0261
26.66_dimethyl sulfone	17	80	0.0357

P-values were calculated according to the Chi-Square test to determine compounds significantly more or less prevalent in $MgSO_4$-treated (n=5) or DSS-treated mice (n=6) (p<0.05).

Table 5.7 List of 20 significantly different compounds between diarrhoea samples at 3 hours post $MgSO_4$ administration and day 8 acute DSS-colitis. Peak abundance of each compound expressed as mean±SEM and percentage occurrence of each compound in each group.

RT_compound	DSS (*n*=10)		MgSO4 (*n*=4)		
	mean±SEM	Prevalence (%)	mean±SEM	Prevalence (%)	*P*-value
17.45_1-pentanol	1,773,515±267,525	6/6 (100)	NA	0	0.0000
26.99_1-hexanol, 2-ethyl-	1,032,523±86,273	6/6 (100)	NA	0	0.0000
31.25_phenylethyl alcohol	9,522,837±3,708,046	6/6 (100)	NA	0	0.0000
19.73_2-hydroxy-3-pentanone	11,492,915±2,229,163	5/6 (83)	NA	0	0.0042
25.33_1-octen-3-ol	18,029,005±5,578,158	5/6 (83)	NA	0	0.0042
26.50_1-propanol, 3-(methylthio)-	1,052,947±380,771	5/6 (83)	NA	0	0.0042
13.44_1-butanol	15,762,330±8,775,427	5/6 (83)	NA	0	0.0045
25.12_1-nonen-3-ol	19,264,213±5,304,469	6/6 (100)	1,086,784	1/5 (20)	0.0074
21.49_1-hexanol	9,815,680±1,630,312	6/6 (100)	1,390,976	1/5 (20)	0.0094
16.13_3-hydroxy-2-butanone	586,330,283±228,375,228	6/6 (100)	51,949,568	1/5 (20)	0.0102
14.20_pentanal	NA	0	3,171,936±948,957	4/5 (80)	0.0164
28.14_phenol	94,737,920±38,409,969	6/6 (100)	10,213,824±4,825,243	5/5 (100)	0.0213
20.56_N-benzyloxy-2-carbomethoxyaziridine	1,950,768±208,789	4/6 (67)	NA	0	0.0251
16.19_1-butanol, 2-methyl-	15,589,760±3,725,321	4/6 (67)	NA	0	0.0252
28.64_benzyl alcohol	900,372±244,350	4/6 (67)	NA	0	0.0252
24.89_1-heptanol	1,750,160±470,750	4/6 (67)	NA	0	0.0253
31.41_2-decanone	2,483,344±817,373	4/6 (67)	NA	0	0.0253
26.66_dimethyl sulfone	477,776	1/6 (17)	1,608,052±508,239	4/5 (80)	0.0371
19.62_butanoic acid	493,524,992±176,378,555	6/6 (100)	120,535,603±91,190,829	5/5 (100)	0.0440
11.90_1-propanol, 2-methyl-	4,374,101±1,094,815	6/6 (100)	1,078,432±323,635	2/5 (40)	0.0465

P-values were calculated according to Student's *t*-test with the significant level of $p<0.05$. These *p*-values have not been corrected for multiple comparisons.

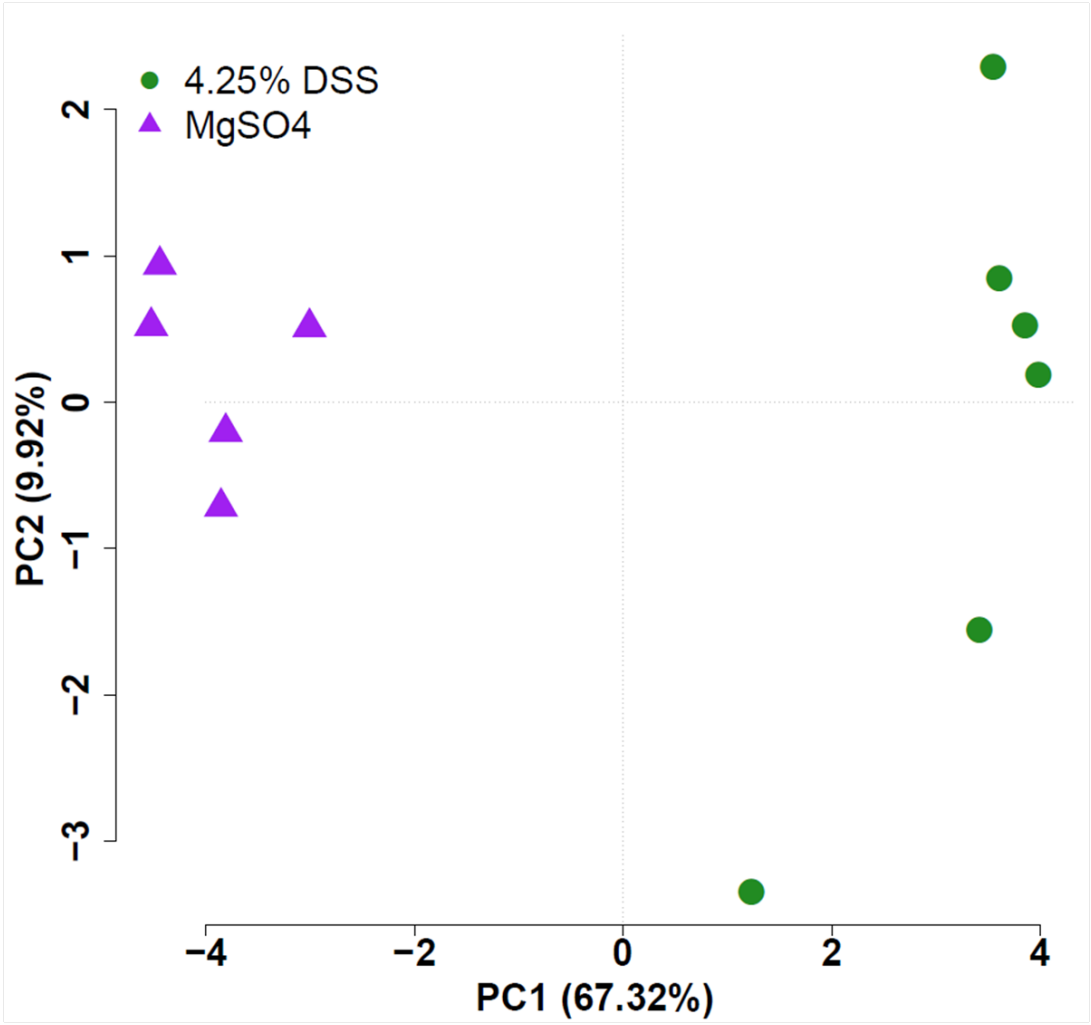

Figure 5.18 A PCA biplot for the diarrhoea samples from $MgSO_4$-treated mice compared to the colon contents from day 8 of DSS-colitis. The first principal component (67.32% of the total variation) has been plotted against the second principal component (9.92% of the total variation). The PCA was performed using the 20 significant compounds from **Table 5.6.**

5.6 SUMMARY OF RESULTS

1. Significant weight loss combined with a significant increase in both DAI and histological inflammation score at day 8 confirmed the onset of acute DSS-induced colitis. This was followed by a recovery at day 11 characterised by an increase in body weight and a significant decrease in DAI and histological inflammation score.

2. There were a total of 95 VOCs identified in the HS of the colonic content collected upon necropsy at days 0 (*n*=11), 5 (*n*=11), 8 (*n*=10) and 11 (*n*=8) of acute DSS-colitis. Acid, alcohol and aldehydes compounds were the most common compound classes identified across all time points with the chemical composition not appearing to vary dramatically between the different time points. A significant decrease in the average number of VOCs at day 8 compared to day 0 was also found.

3. Using these 46 VOCs, a PCA was plotted to examine the clustering of each time point according to the abundance of these significant compounds. This PCA provided results that suggest that the VOC profile changes according to the different time points tested during the development of acute DSS colitis.

4. A one-way ANOVA found 46 compounds that significantly varied in abundance during the development of acute colitis. Of these, 32 significantly decreased in the presence of colitis (days 5 & 8), compared to days 0 and 11, and 14 significantly increased. Multiple comparison *p*-value correction found 9 compounds which remained significantly different: propanal, 2-butanol, butanal, heptanal, ethanol, 2-pentanol, 3-methyl-butanoic acid, 3-hydroxy-2-butanone and 3-methyl-furan. A heatmap presented these differences in abundance of VOCs visually.

5. NFκB2 null mice were resistant to acute DSS-induced colitis. Unexpectedly, the faecal VOC profile of these mice was dissimilar to both the DSS treated C57BL/6 mice, and the untreated control groups.

6. $MgSO_4$-induced diarrhoea was observed 1-2 hours after administration with a high FOI at 3 hours which was significantly higher than untreated controls. However, there was no significant difference found between the average number of VOCs identified in untreated controls and $MgSO_4$-treated mice. Based on the significantly different VOCs by abundance, a PCA was able to clearly separate untreated and $MgSO_4$-treated faecal samples.

7. Day 8 acute DSS-colitis compared to 3-hour post- $MgSO_4$ administration found a significant decrease in average number of VOCs in $MgSO_4$ treated mice. There were a number of VOCs absent in $MgSO_4$-diarrhoea but were ubiquitous to the DSS-diarrhoea samples, implying potential markers of inflammation-driven diarrhoea. When considering the abundance of specific VOCs, comparison between these two groups also indicate VOCs as potential markers for the presence of diarrhoea, not specific to IBD. A PCA demonstrated this separation based on the VOC profiles.

5.7 DISCUSSION

There have been several studies that have applied a metabolomics approach to discriminate IBD patients from healthy controls, CD from UC and patients with active disease from patients in remission [131, 242, 280]. As a result, the involvement of the gut microbiota in the chronic mucosal immune activation underlying the pathogenesis of IBD has become more acceptable and has led to an increased interest and use of faecal samples to apply to metabolomics profiling studies. However, to date there have been few studies investigating the VOCs present in the faeces of IBD patients and murine models [65].

HS-SPME-GC-MS was performed using the colonic luminal contents from mice with DSS-induced colitis. The clinical and histological features observed in this study are consistent earlier studies of this model of IBD [132, 133]. The pathological appearance of the colon tissue at days 5 and 8 represented the damage induced by oral administration of the DSS molecules. An increase in body weight, an absence of diarrhoea and pathological improvements between day 8 and 11 suggest that this model of colitis also has a recovery phase. This study has detected compounds whose levels significantly vary along the development of colitis, indicating that the pathogenesis of colitis causes variations in the murine faecal metabolome. It has been shown that the faecal volatile metabolomic profiles significantly vary according to the stage of colitis with specific compounds responsible for these differences being grouped into the organic compound classes, aldehydes, alcohols and furans. In addition, the levels of nitrogen and sulphur containing, fatty acids and esters are all at significantly lower levels with the presence of colitis, compared to the untreated and recovery phases of colitis. These VOC profile changes correspond with the clinical and pathological differences.

A PCA plot based on the 46 significant compounds illustrated differences among the normal (day 0), acute (days 5-8) and recovery (day 11) phases of DSS-induced colitis **(Figure 5.9).** Upon dissection of the PCA plot, it was revealed from the loadings plot that several compounds strongly influenced the separation of each time point,

including 2-butanol, methyl-ketones and esters. Furthermore, based on the 9 compounds identified as highly significant between healthy and colitis **(Table 5.3),** a heatmap using a hierarchical clustering method provided visual evidence for these differences between the time points tested of acute DSS-colitis.

It has been reported that the characteristic changes in the levels of compounds occurring during acute DSS-induced colitis are a result of the disturbance of lipid and energy metabolism. Shiomi *et al.* found a significant decrease in the levels of tricarboxylic acid (TCA) cycle intermediates in the serum and colon tissue of DSS-treated mice as a result of a higher energy demand due to a decline in nutrient absorption through the damaged intestine [282]. The TCA cycle, lying at the heart of cellular metabolism, occurs within the mitochondria and is a sequence of chemical reactions used by all aerobic organisms to generate energy through the oxidation of acetate derived from carbohydrates, fats and proteins into CO_2 and chemical energy in the form of ATP. This study has resulted in a significant decrease in the levels of alcohols in combination with a significant increase in the levels of aldehydes in the presence of colitis. The higher energy demand during the development of DSS-colitis will see an increase in glucose breakdown to pyruvate, releasing free energy to form the required high energy compounds ATP and NADH. Consequently, there is an increased breakdown of pyruvate into acetate with aldehydes occurring as biproducts of this reaction, offering an explanation for the observed increase in levels of aldehydes in the presence of colitis.

Glutamine is considered one of the primary sources of amino acids in the intestinal mucosa, having a central role in colonocyte nutrition and integrity [288]. It has recently been reported that the oral administration of glutamine after the pathogenesis of DSS-colitis significantly decreases the severity of disease, therefore exerting a therapeutic effect on colitis [282]. Under normal conditions, it is a precursor for the synthesis of amino acids, proteins and nucleotides, conversely, it has been demonstrated that the tissue glutamine metabolism increases markedly in many stressful disease states. A decrease in the nitrogen- and sulphur-containing, fatty acids, esters and alcohol compounds could be explained by the decrease in the

essential amino acids, including glutamine. This decrease in amino acids is demonstrated by a recent study investigated the metabolic effects of DSS on intestinal epithelial cells using ^{1}H-NMR. They were able to show that Caco-2 cells incubated with DSS inhibits alanine synthesis with a 3 fold decrease, compared to untreated cells [289]. Glutamine is converted to alanine in the intestine, therefore the decrease in glutamine identified in the colon tissue explains the observed decrease of alanine [290].

Additionally, the levels of ROS are increased in the presence of DSS-induced colitis, therefore playing a vital role in the pathogenesis of this disease [291]. Damiani *et al.* made the interesting finding that a marker of lipoperoxidation is increased in DSS-treated rats [292]. Lipid peroxidation is a chain reaction, initiated by the removal of hydrogen atoms via the production of ROS, resulting in end-products including hydrocarbons such as ethane and pentane, but also aldehydes [293]. The number and levels of aldehydes compounds identified in the headspace of colon contents from DSS-treated mice in this study increased at day 5/8. However, there was a noticeable decrease in the number of alkanes detected at day 5/8, ethane was not identified and pentane was significantly decreased at day 5/8, compared to day 0.

The distal colon is characterised by an anaerobic microbiota with an abundance of metabolically active bacteria, constantly interacting with the host's epithelial cells and mucosal immune system. An altered microbial composition and function in the presence of IBD will result in an increased immune stimulation, an epithelial layer dysfunction leading to enhanced mucosal permeability [294]. It has been postulated that changes in the composition of the microbiota contributes to the pathogenesis of DSS-induced colitis [108]. Hence, the differences noted in this study according to stage of colitis may be a direct result of the changes in the gut luminal environment.

NFκB2 null mice have previously shown a significant reduction in the pro-inflammatory cytokine, TNF-α, and a significant increase in the levels of the anti-inflammatory cytokine, IL-4, following DSS treatment, compared to treated WT mice ([295] [54]). Therefore, the resistance of DSS-induced colitis observed in

NFκB2 null mice might be mediated by the significant down-regulation of TNF-α and the up-regulation of IL-4, exerting a protective effect against inflammation. The similarity of the faecal VOC metabolome in the WT and *NFκB2* null untreated groups suggest that the absence of the *NFκB2* gene does not significantly affect the faecal metabolome during health, whereas the administration of DSS to mice lacking the *NFκB2* induces a significant change to the faecal VOC metabolome. The DSS-treated *NFκB2* null group behaved similarly when considering that there was no significant weight loss and an absence of bloody diarrhoea. However, the significantly different faecal VOC metabolome suggest that at a metabolite level the *NFκB2* gene has a role to play in the pathogenesis of DSS-induced colitis, and appears to be in agreement with previous findings [54] that this role may be protective. This study provides evidence to support the hypothesis that *NFκB* does have a role to play in the pathogenesis of DSS-induced colitis, and human IBD. Using experimental murine models of colitis macrophages and epithelial cells isolated from inflamed gut were positive for the expression and activation of *NFκB* [296]. The amount of *NFκB* activation has also been found to be significantly correlated with the severity of intestinal inflammation [297].

Diarrhoea results from an imbalance between the absorptive and secretory mechanisms in the intestinal tract, which is accompanied by an excess loss of fluid in the faeces. $MgSO_4$ is an osmotic-acting laxative and has been reported to induce diarrhoea by increasing the volume of intestinal content through prevention of reabsorption of water [298]. The significant decrease identified between the average number of VOCs in the day 8 DSS diarrhoea and $MgSO_4$ diarrhoea samples may be explained by the higher content of water and an increase in colonic transit time of the $MgSO_4$ samples. Through the identification of VOCs and a direct comparison between metabolomic profiles of faeces from DSS-induced colitis and $MgSO_4$, these results highlight the differences between the mechanism of which diarrhoea occurs, and the metabolic pathways involved. To our knowledge, this is the first time this comparison has been reported.

The extraction of VOCs from the HS of colonic luminal content of mice collected at varying times during the development of DSS-induced acute colitis has revealed significant metabolomic profiles. This has provided evidence that this method is capable of producing reproducible and reliable results. Together with the clinical and histological confirmation, these VOC faecal profiles aid investigation into the pathogenesis of the acute DSS-colitis murine model.

Chapter 6

VOC Profiling of a Mouse Model of Inflammation-Associated Colorectal Cancer

6.1 INTRODUCTION

IBD is a chronic condition, characterised by acute inflammation of the intestine followed by periods of remission. It is likely to result from an interaction of environmental risk factors (e.g. smoking, diet) affecting the intestinal microbiota, with an inappropriate immune response often but not only, in a genetically predisposed person. Despite many years of extensive research, its pathogenesis is poorly understood. There have been numerous animal models developed to characterise the complexity of IBD. Oral exposure to DSS is the most widely used, inducing a colitis resembling UC. A single cycle of DSS induces acute inflammation, whereas multiple cycles of DSS induce chronic inflammation [299]. It has previously been reported that bacteria play a major role in initiation of inflammation in acute DSS colitis but not in chronic DSS colitis [300].

Individuals with chronic IBD are at increased risk for colorectal cancer (CRC). Although IBD-related CRC is only responsible for less than 2% of all CRC cases, the risk of developing CRC in IBD patients increases by 0.5-1% each year depending on the duration and extent of the disease [301]. Furthermore, individuals with either UC or CD and who have a family history of CRC have a relative risk of 2.5 and 3.7 of developing CRC, respectively, when compared to IBD patients with no family history [302]. The mean age of developing CRC in the setting of IBD (40 to 50 years) is lower than it is for sporadic CRC (60 years) [303]. The risk of developing CRC in the setting of IBD is increased; a possible explanation for this may be due to chronic inflammation leading to significant tissue damage. This enhances the epithelial cell turnover of the colonic mucosa, increasing the chance of errors in DNA repair [304]. The mechanisms that mediate the transition from intestinal inflammation to cancer have not been well identified. Clinical symptoms of IBD-associated CRC are not specific so prognosis is poor because of delayed diagnosis. CRC usually arises from dysplasia-associated lesions following a progressive scenario from non-dysplastic lesions to low-grade, then to high-grade dysplasia and ultimately to invasive CRC.

Patients with IBD are currently screened for dysplasia after 10 years of IBD diagnosis and due to the relatively young age of such patients, attempts have been made to stratify patients at the greatest risk. A number of cohort studies have demonstrated improved survival in patients with IBD undergoing colonoscopy [305, 306]. A recent review of the literature states that surveillance is now recommended by the American Gastroenterological Association (AGA), the American College of Gastroenterology (ACG), the American Society for Gastrointestinal Endoscopy (ASGE), and the British Society of Gastroenterology (BSG) [303]. The main goal of surveillance is to detect the presence of dysplasia, which is associated with a high risk of CRC. Therefore, an ideal surveillance strategy would include a cost-effective and sensitive detection system. It is evident that surveillance significantly improves patient survival. For instance, 149 patients with IBD-associated CRC included 23 who had undergone colonoscopic surveillance prior to the discovery of CRC, while 126 patients had not. When considering the five-year survival, 100% of patients in the prior surveillance group survived compared to 74% in the non-surveillance group [307]. However, the colonoscopy approach generally suffers from poor patient compliance, thus a non-invasive diagnostic tool is desirable.

Increasing availability of high-throughput methodologies has opened up new possibilities and has led to the development of a metabolomics-based approach for the early detection of CRC. The use of metabolomics applied in the field of oncology has the potential to identify marker metabolites specific for the diagnosis of certain cancers. In addition, metabolomics may be able to differentiate between harmless changes and abnormalities that precede the disease, allowing the detection of the disease at an early stage. Nishiumi *et al.* recently performed a serum metabolome analysis using GC-MS: the resulting model for the prediction of CRC was composed of 2-hydroxybutyrate, aspartic acid, kynurenine, and cystamine and had 85% sensitivity, specificity and accuracy [308].

6.2 HYPOTHESIS

The onset of IBD causes dysbiosis and a change to the normal metabolic state. Dysplasia will lead to a further change in the metabolome. This change may be used to detect dysplasia and offer a novel, cheaper, non-invasive method of diagnosing IBD and also an effective screening tool for early CRC detection.

6.3 AIMS

1. To induce chronic intestinal inflammation in C57BL/6 WT female mice by cyclic oral administration of DSS.
2. To induce inflammation-associated colorectal cancer in WT mice by i.p. administration of AOM and cycles of DSS.
3. To investigate metabolic differences by detecting VOCs in the headspace of faecal samples from murine models of colitis, colitis-associated cancer and untreated controls.

6.4 METHODS

6.4.1 Experimental design

6.4.1.1 Induction of chronic colitis by DSS administration

Mice were administered 0.75% DSS (wt/vol) in their drinking water for 5 days, followed by 7 days of normal water. This cycle was repeated three further times to induce chronic colitis; the DSS concentration increased slightly, to 1%, for cycles two and three and to 1.25% for cycle four. The control group of mice remained on normal drinking water throughout the course of the experiment (*n*=6 control; *n*=6 treated). Clinical parameters of body weight loss, stool consistency and the presence of rectal bleeding were assessed daily. Faecal samples were collected on experimental days 5, 8 and 11 of each cycle. Animals were sacrificed on day 45 with colonic, caecal, small intestine contents collected and stored at -20°C prior to

analysis by GC-MS and intestinal tissues taken for histological analysis. MT stain was used to evaluate the degree of fibrosis, as a method to distinguish between acute and chronic colitis.

6.4.1.2 Induction of inflammation-associated colorectal cancer using AOM/DSS

As described in detail in **Chapter 2**, mice were administered one dose of 12.5mg/kg AOM i.p. Mice were then orally exposed to 1.5% DSS for 5 days followed by 16 days of ordinary water. This DSS cycle was repeated twice more (or just twice) with animals sacrificed 12 days after final cycle. Faecal samples were collected weekly and stored at -20°C prior to analysis by GC-MS. Tissues were taken for histological analysis following necropsy. HID-AB staining was used to visualise pre-malignant lesions in the form of MDF, in sections of distal colonic tissues.

6.4.2 HS-SPME-GC-MS sample preparation and analysis

In brief, where possible, 130mg or 10 pellets (maximum volume) of stool sample was collected and stored in 2ml glass vials at -20°C. Prior to VOC extraction, samples were pre-incubated for 30 mins at 60°C before compound extraction using the solvent free SPME technique with a CAR/PDMS/DVB fibre for 20 mins prior to desorption into the GC oven [221]. For GC-MS conditions, please refer to **section 2.6.1.**

6.4.3 Data processing and statistical analysis

All raw data were processed and analysed as described in **Chapter 2**. Briefly, batch reports are produced for each dataset in AMDIS and a list of all compounds present and their corresponding corrected peak abundances are then generated using Metab. Compounds present in less than 30% of at least one condition were removed. NA was replaced with 1 and peak abundance was log transformed, and appropriate statistical analysis (Student's *t*-test or two-way ANOVA) was applied: all

p-values are corrected for multiple comparison (Bonferroni). Hierarchical clustering and PCA was applied to illustrate variation present between groups.

6.5 RESULTS

6.5.1 Clinical and histological confirmation of chronic DSS-induced colitis

Mice were administered 0.75% DSS (wt/vol) in their drinking water for 5 days, followed by 6 days of normal water. This cycle was repeated three further times to induce chronic colitis [309]. The DSS concentration was increased slightly to 1% for cycles two and three and to 1.25% for cycle four.

Mice were weighed daily to assess the degree of colitis. Weight loss was first observed in the fourth and final cycle of DSS and was accompanied by diarrhoea and rectal bleeding **(Figure 6.1).** At necropsy, the colons of DSS treated mice were white with extreme mucosal thickening and decreased length compared to untreated controls. H&E stained distal colon tissue sections showed an inflammatory cell infiltrate into the submucosal layer and a breakdown of the epithelial layer and crypt structure in the DSS treated mice **(Figure 6.2). Figure 6.3** shows that the untreated controls were free from inflammation, compared to an average inflammation score of 3 for the DSS-treated group ($p<0.001$, Mann-Whitney U test).

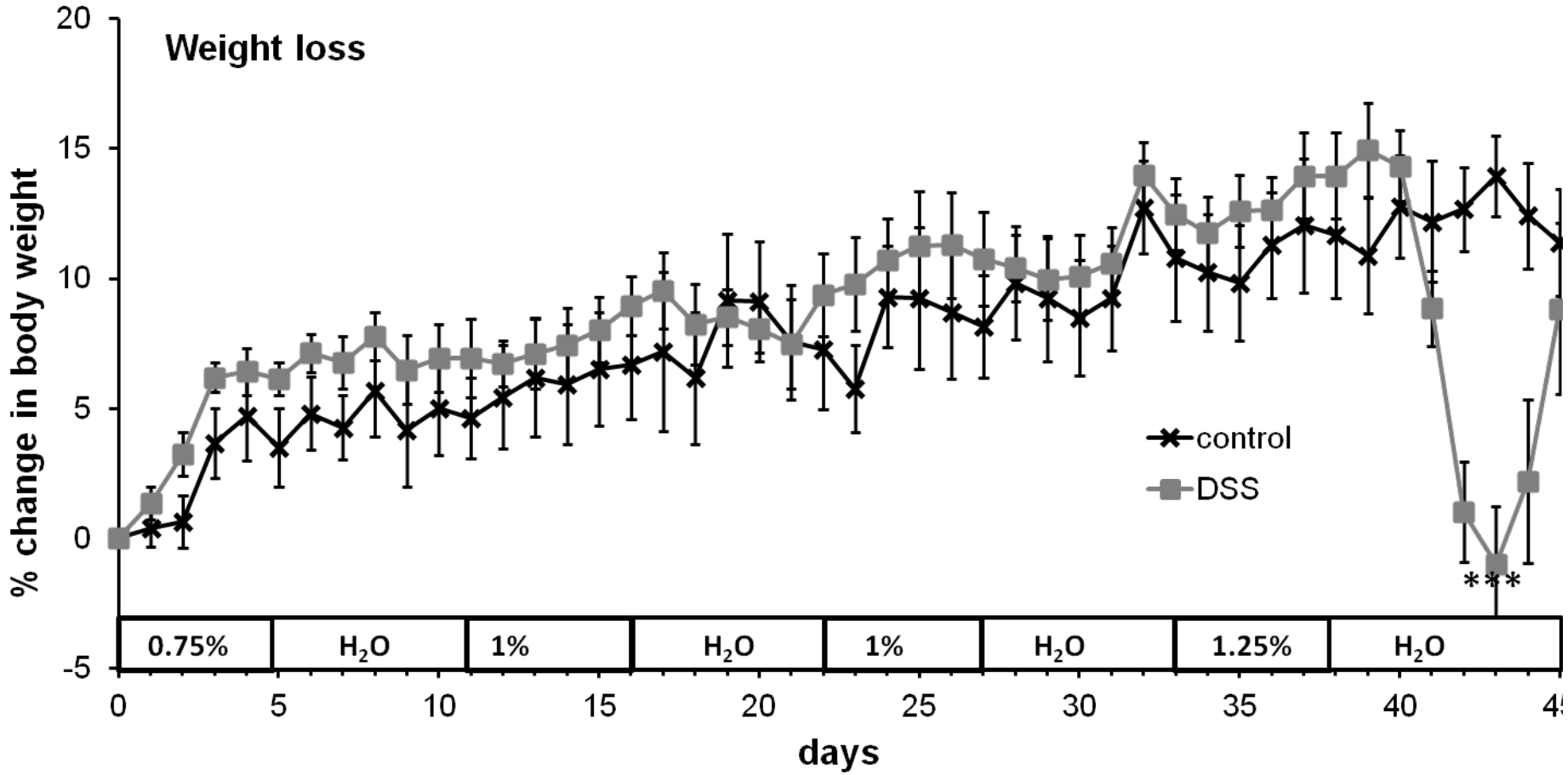

Figure 6.1 Weight change in mice undergoing chronic DSS treatment and controls. The percentage change in the body weight was used to assess the degree of colitis. Data represented as mean±SEM, *n*=6/group. Statistical differences at day 43 were assessed by Student's t-test, $p<0.001$*** for weight loss in the DSS treated group at day 43 compared to untreated control.

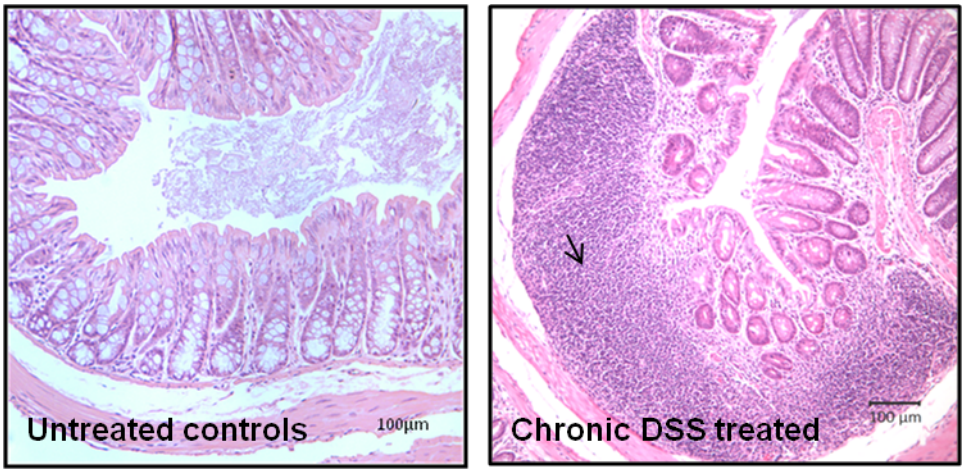

Figure 6.2 Representative images of H&E stained distal colonic sections of untreated controls and DSS treated mice. Mice were euthanized at experimental day 45 since the start of DSS treatment at day 0. Arrows indicate damaged crypts in the DSS treated group accompanied by a damaged epithelium, compared to untreated controls.

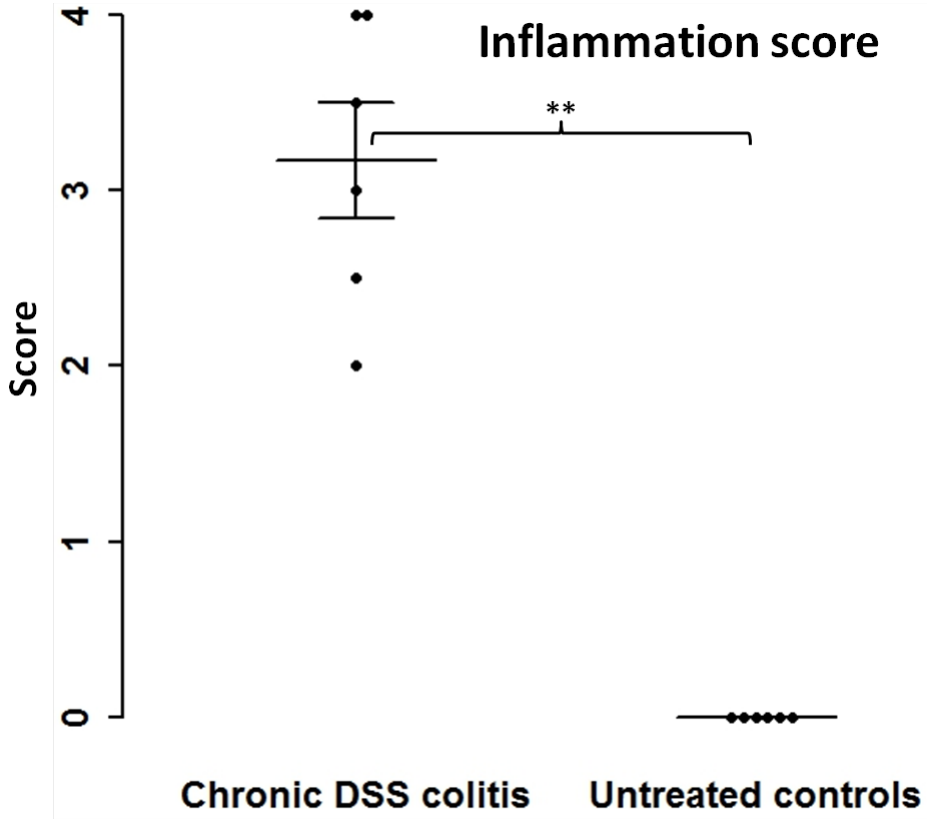

Figure 6.3 Histological (inflammation) scores of DSS-induced chronic colitis in mice. Inflammation score of distal colon taken from C57BL/6 mice at day 45 from chronic DSS treated and untreated control groups. Each dot represents the score from one mouse and data are presented as mean±SEM, $^{**}p<0.01$ by Mann-Whitney U test.

6.5.2 Longitudinal VOC analysis of the development of chronic colitis

Mice were sacrificed on day 45 of the experiment, tissues excised and colon contents were collected for extraction of VOCs by HS-SPME-GC-MS. This enabled the direct comparison of VOCs present in the headspace of the colon luminal content of chronic DSS-treated mice. Faecal samples were also collected during the experiment on days 5, 8 and 11 of each cycle. The faecal VOC profiles from experimental days 0, 8, 20, 31, 42 and 45 from both untreated control and the DSS treated groups were compared.

One hundred and seventy VOCs were identified in two treatment groups during the experiment. There was no difference in the average number of VOCs identified on experimental days 0, 8, 20, 31, 42 and 45 between the untreated control and DSS-treated C57BL/6 mice assessed by a two-way ANOVA. No significant interaction effect was found, indicating that when considering both group and time, there were no significant differences with the effect of time on the number of VOCs for control or DSS-treated mice, $F(5,58) = 1.44$, $p>0.05$). There was no significant main effect of group, $F(1, 58) = 2.09$, $p>0.05$. This means if other dependent variables (time) are ignored, the average number of VOCs identified did not vary significantly according to disease group. There was, however, a significant main effect of time, $F(5, 58) = 2.92$, $p<0.05$. This effect means if group is ignored, the number of VOCs were different between days 0, 8, 20, 31, 42 and 45. In order to further investigate where this time related significant difference occured, a Tukey HSD test was performed irrespective of group. The number of VOCs identified were significantly lower at day 42 compared to day 8 **(Figure 6.4).**

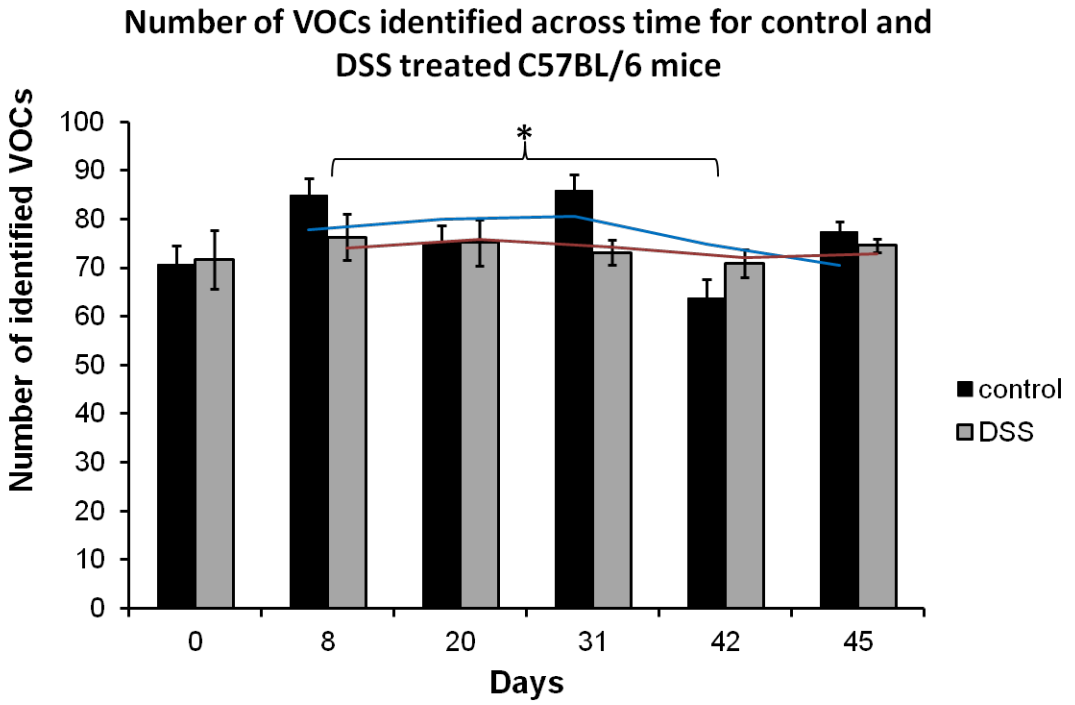

Figure 6.4 Variation in the presence of faecal VOCs during the development of chronic colitis. The number of VOCs identified in the headspace of the faecal pellets collected at days 0, 8, 20, 31, 42 and 45 from untreated control and DSS-treated mice. Data represented as mean±SEM, *n*=6/group. Statistical differences were assessed by two-way ANOVA, $p<0.05$* for combined number of VOCs at day 8 compared to day 42. The blue line is the rolling average for control mice and the red line is the rolling average for DSS-treated mice, both showing the trend of number of VOCs over time for both groups.

Next, the concentrations each compound were compared. Of the 170 compounds identified across the 6 time points tested, 165 were found in the DSS treated group, 167 in the untreated control group with 3 and 5 being unique to the DSS and untreated group, respectively. In the DSS treated group, 19 VOCs varied significantly in abundance across days 0, 8, 20, 31, 42 and 45 (ANOVA followed by Bonferroni, $p<0.05$). A PCA plot using these 19 compounds showed clear separation of each time point, in particular on day 45 **(Figure 6.5).** Eight of the 19 compounds also significantly varied over time in the untreated control group (1-pentanol, 1-penten-3-ol, 2-methyl-propanal, 1-butanol, 1-hexanol, α-pinene, nonanal, dodecane); therefore, it was concluded that these compounds were not specific to chronic colitis and were dismissed for further analysis into VOC markers of chronic inflammation. In addition, a number of these significant compounds were also found to significantly vary as healthy mice aged **(section 3.5.6).** Consequently, the

11 remaining compounds found to vary significantly exclusively in the DSS group were considered as potential markers of inflammation **(Figure 6.6).** The concentration of each compound was plotted to illustrate how the profile varied during the development of chronic colitis in both untreated control mice and DSS-treated mice. Clinically, the DSS treated mice showed signs of colitis between days 40 and 45 (time points 10-12); acetone, propanoic acid propyl ester, 5-methyl-2-heptanone, 2-octanone, tetra-methyl-pyrazine, 1,3-xylene, 2-acetoxy-3-butanone and 2-decanone were all present at higher concentrations, whereas 2-methyl-propanal, hexanal and benzene, 1,3-bis (1-1-dimethylethyl)- were present at lower concentrations in the DSS treated faeces compared to the untreated control group.

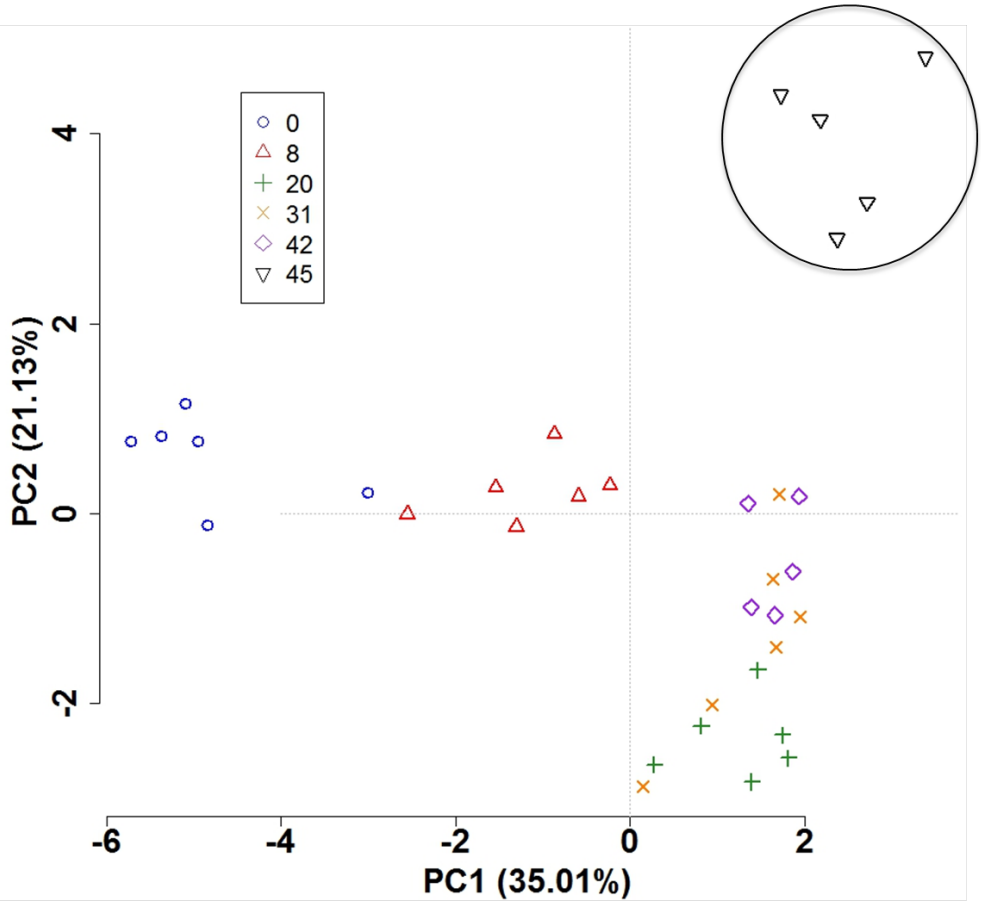

Figure 6.5 A PCA biplot for the faecal pellets of DSS treated mice from experimental days 0, 8, 20, 31, 42 and 45. The PCA shows the variation within the DSS group and was performed using the abundance of the 19 significant different compounds over time (ANOVA followed by Bonferroni, $p<0.05$). The last time point tested, day 45, is circled.

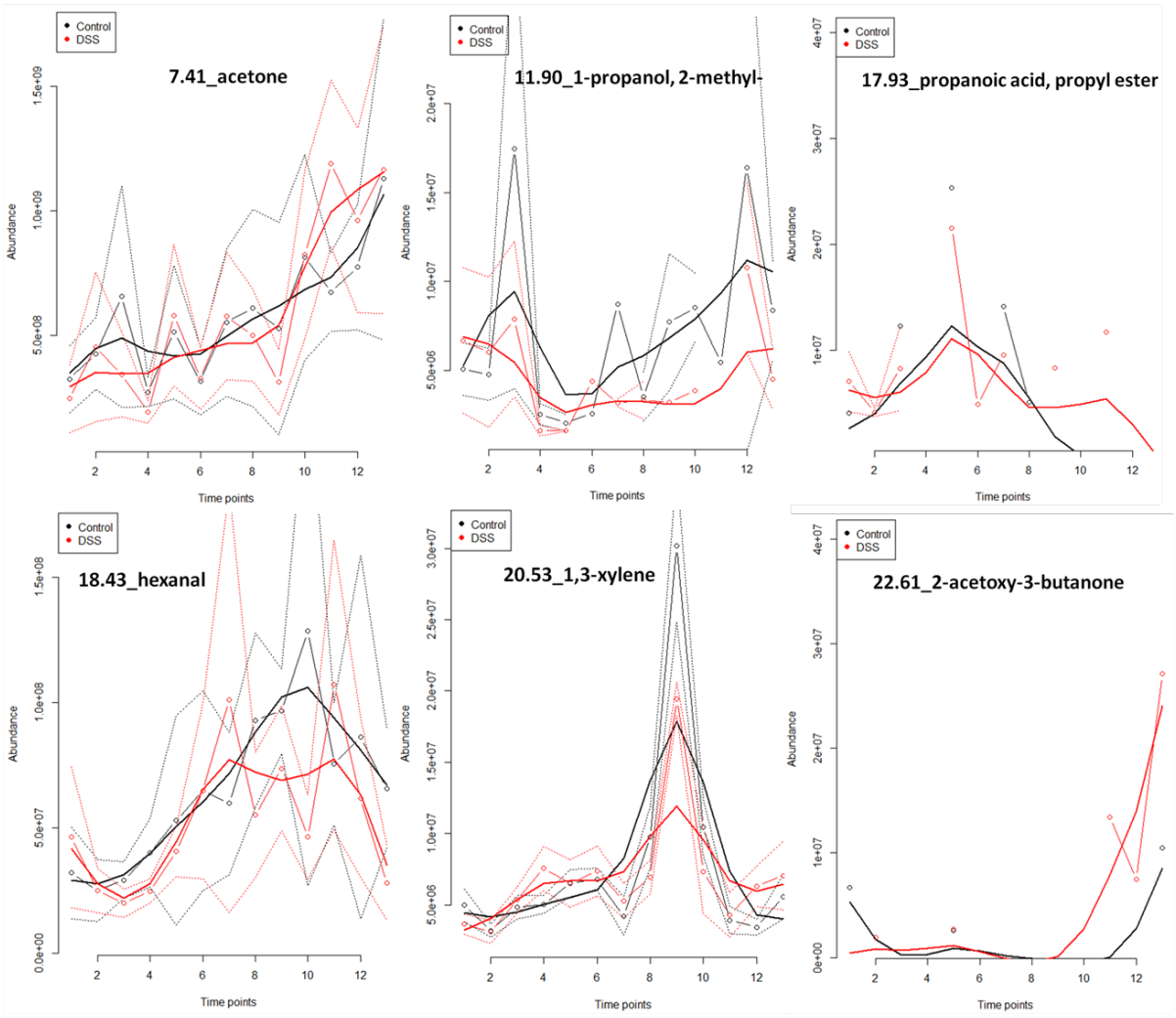

Figure 6.6 Time series abundance plots of prominent VOCs from chronic DSS-induced colitis and untreated controls. The mean peak abundance of the 11 compounds found to vary significantly over time is plotted at 12 time points over the space of 45 days of which mice were administered four cycles of DSS (red lines) (p<0.05; ANOVA followed by Bonferroni). The concentration of each compound in the untreated control group is also included to compare VOC profiles (black lines). Dashed lines represent the standard deviation (n=6/treatment group).

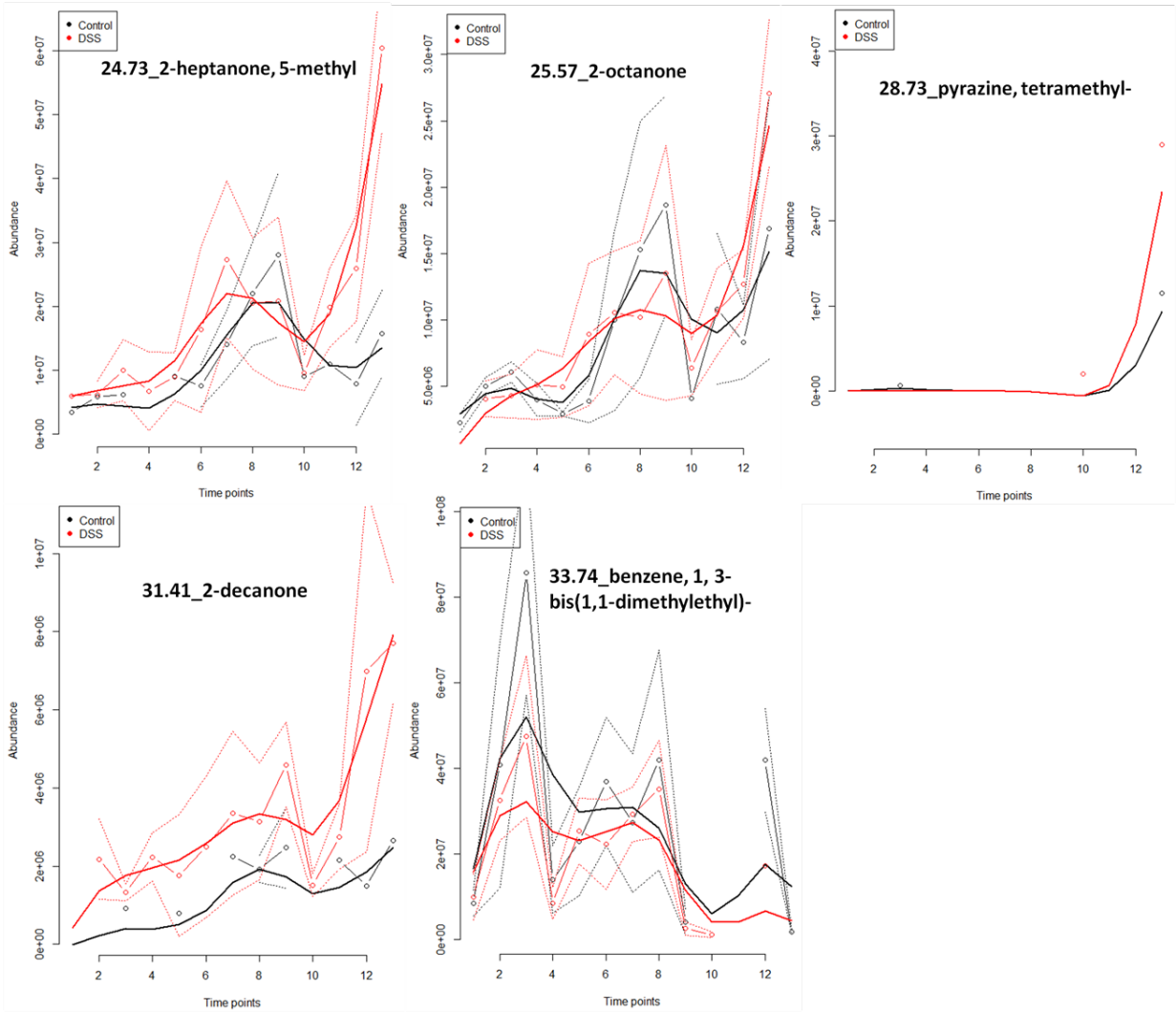

Figure 6.6 continued. Time series abundance plots of prominent VOCs from chronic DSS-induced colitis and untreated controls. The mean peak abundance of the 11 compounds found to vary significantly over time is plotted at 12 time points over the space of 45 days of which mice were administered four cycles of DSS (red lines) (p<0.05; ANOVA followed by Bonferroni). The concentration of each compound in the untreated control group is also included to compare VOC profiles (black lines). Dashed lines represent the standard deviation (n=6/treatment group).

The distinct cluster of the DSS treated faecal samples at day 45 in the top right hand quarter of the PCA plot **(Figure 6.5)** suggests that the VOC profile is capable of representing a change in disease state. We have identified potential markers of both acute and chronic inflammation during the development of colitis by administration of 1-4 cycles of DSS, therefore, the VOC profile observed at day 45 was then directly compared to the untreated control group **(Figure 6.7 and 6.8)**. Although there appears to be more variation within each sample group, there were 14 significantly different compounds between the two groups and when plotted using a PCA, the separation was clear (Student's *t*-test followed by Bonferroni, $p<0.05$). Eight of these 14 were present at significantly higher levels in the DSS treated group compared to untreated controls, 4 were absent in the DSS group, and 2 were absent in the untreated control group **(Figure 6.8).** Benzene, 1, 3-bis(1,1-dimethylethyl)- significantly varied over time in the DSS-treated group and was also found to be significantly different at day 45 between the DSS-treated group and the control group.

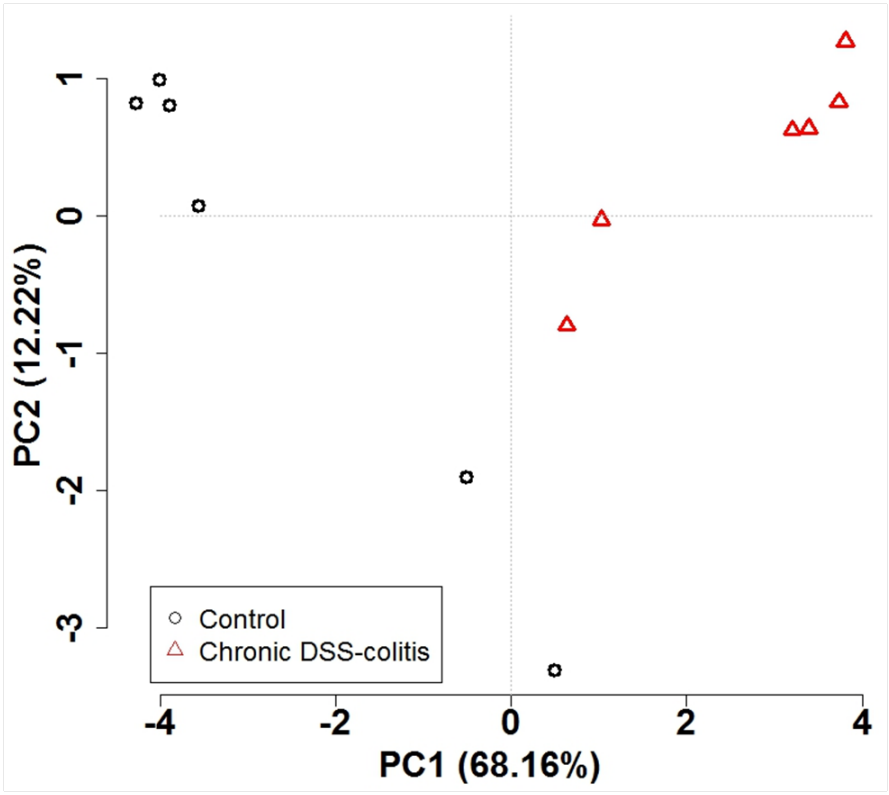

Figure 6.7 A PCA biplot for the faecal pellets of DSS treated mice compared to untreated control mice at experimental day 45. The first principal component has been plotted against the second principal component. The PCA was performed using the abundance of the 14 significant different compounds between the two groups (Student's *t*-test followed by Bonferroni, $p<0.05$) **(Figure 6.8)**.

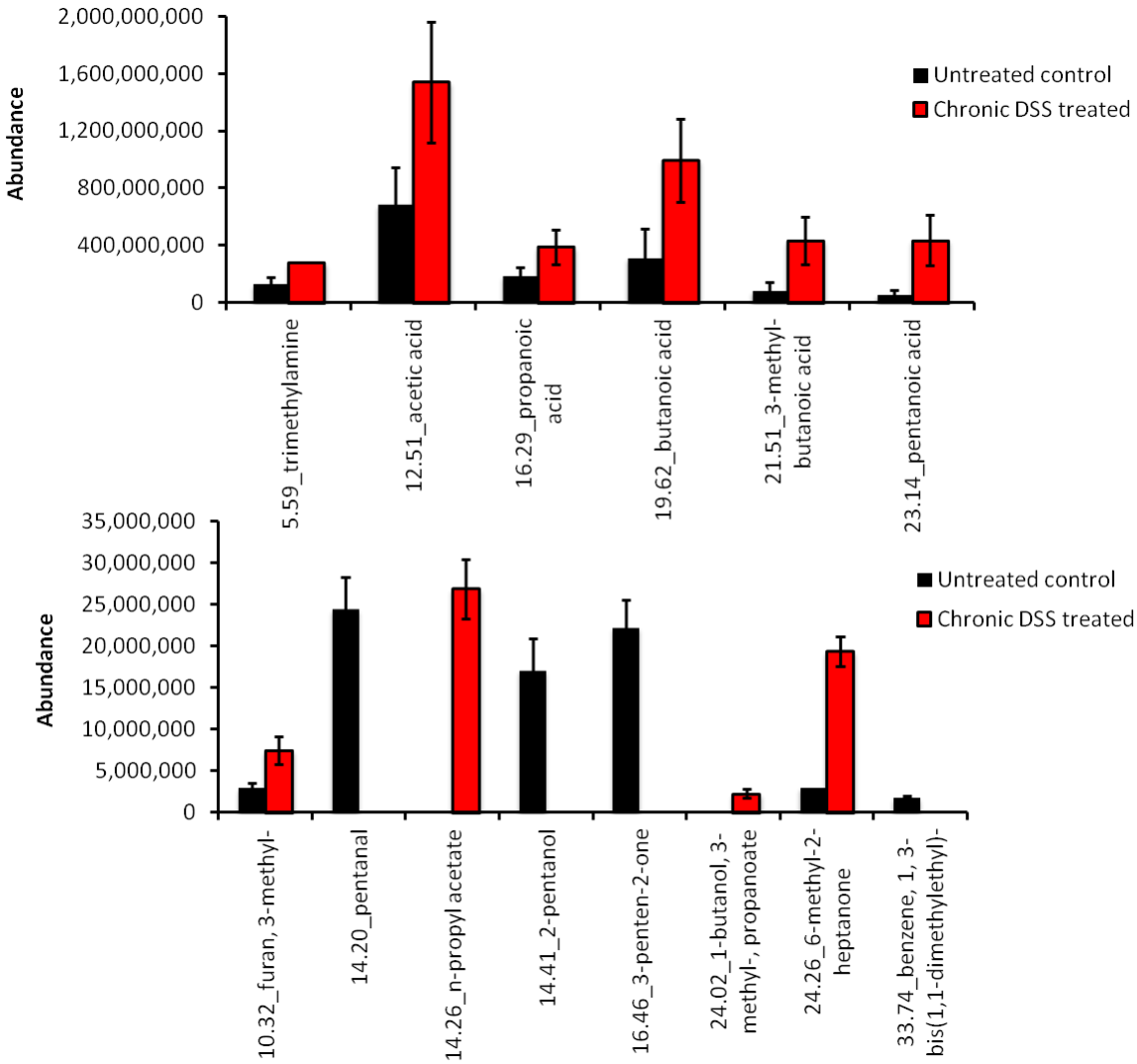

Figure 6.8 Bar plots of the peak abundance. Comparison of compound concentrations at day 45 between untreated control and DSS treated mice resulted in 14 significantly different compounds (Student's *t*-test followed by Bonferroni, (p<0.05)). Data are expressed as mean±SEM peak abundance for each significant compound.

6.5.3 Histological differences between acute and chronic DSS-induced colitis

Clinical and histological analyses have previously confirmed the presence of both acute **(section 5.5.1)** and chronic (**section 6.5.1**) DSS-induced colitis. Distal colonic sections taken from mice induced with both acute and chronic mice were evaluated for the degree of fibrosis using the MT method. A tissue section was also stained with H&E at the same time to directly compare the degree of inflammation **(Figure 6.10).** In order to quantify the amount of fibrosis in acute colitis, chronic colitis and untreated control mice, an accredited murine pathologist assessed each slide for the degree of fibrosis and the percent of tissue in which it was present; a fibrosis score was then given to each animal based on the sum of these two parameters. The fibrosis score was higher in the chronic colitis mice compared to the acute colitis mice and significantly higher than the untreated control group (p<0.01, Mann Whitney U).

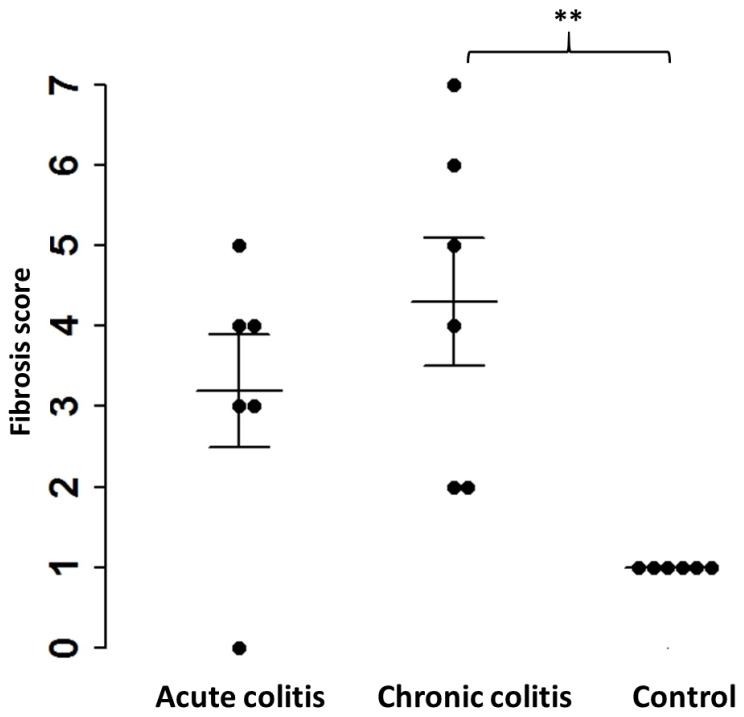

Figure 6.9 Histological fibrosis score. Fibrosis score of distal colonic tissue sections stained with MT stain from mice induced with acute and chronic colitis, also compared to untreated controls. The fibrosis score for each animal is the sum of the degree of fibrosis score and the percent involvement. Each dot represents a score from one mouse and data are presented as mean±SEM **p<0.01 by Mann-Whitney U test.

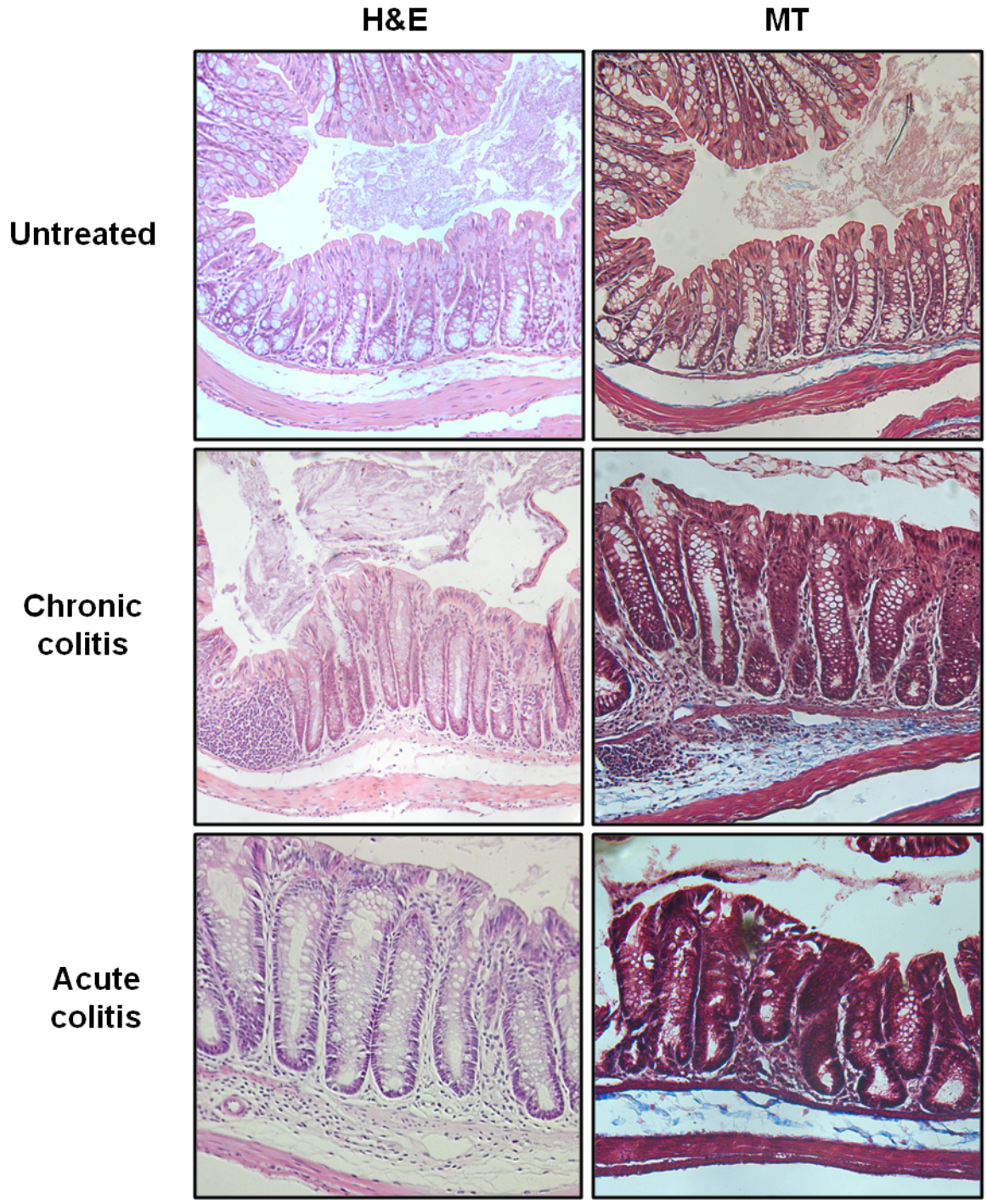

Figure 6.10 Evaluation of fibrosis. Representative images of distal colon sections from untreated controls and DSS treated mice with either chronic or acute inflammation. Slides were stained using the MT method to evaluate the amount of fibrosis, and H&E to assess the degree of inflammation.

6.5.4 Significantly different faecal VOC profiles between acute and chronic DSS-induced colitis

Clinical and histological analysis confirmed induction of acute and chronic colitis in the respective groups. Significantly different VOC profiles were found in each condition. The specific VOCs responsible for the differences observed during the development of acute colitis and between control and chronic colitis were not the same. With acute colitis, there was a significant increase in the levels of aldehydes and a decrease in alcohols. Chronic colitis was associated with a significant increase in the bacterial products, methyl-ketones, and also carboxylic acids. A direct comparison between day 11 acute and day 45 chronic colitis showed a significant increase in the number of compounds identified in chronic (75±1.5) compared to acute colitis (49±4.0) (mean±SEM, *t*-test, $p<0.001$) **(Figure 6.11A)**. The levels of 2,3-butandione (FC=49.2), 2-heptanone (FC=37.8) and acetone (FC=20.7) were all significantly increased in chronic compared to acute colitis with a notable absence of 1-butanol in chronic colitis and an absence of 2-acetoxy-3-butanone, 2,4,6-trimethyl-octane and 7-ethyl-5-methyl-6,8-dioxabicyclo[3.2.1]oct-3-ene in acute colitis. Nonanal and 2-octanone were identified in only one sample of the acute colitis group compared to 100% of the chronic colitis group with 109.7 and 93.4 fold increase, respectively, in chronic compared to acute colitis **(Table 6.1).** A PCA showed the separation of acute and chronic colitis based on the significant VOCs present in the headspace of the colonic content **(Figure 6.11B).**

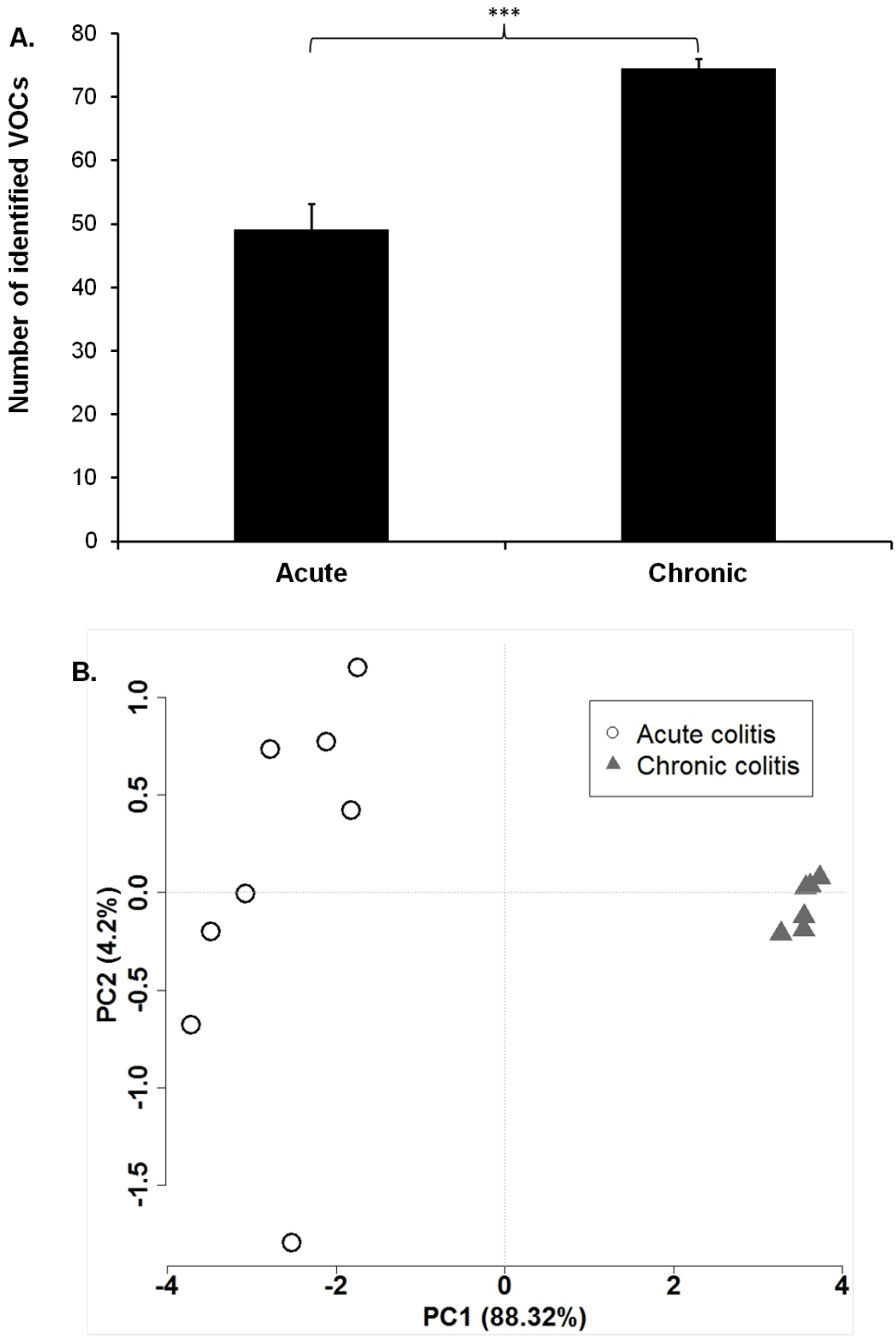

Figure 6.11 Comparison of VOC profiles from mice with acute and chronic colitis. (A) The number of VOCs identified in the headspace of the colon contents collected at the final day of the acute (*n*=8) and chronic (*n*=6) colitis experiments (mean±SEM, Student's *t*-test, ***$p<0.001$). (B) A PCA biplot with the first principal component plotted against the second principal component representing 88.32% and 4.2% of the variation, respectively. The PCA was performed using the 11 significant compounds from **Table 6.1.**

Table 6.1 List of the 11 significantly different compounds detected in the HS of colon content samples from mice with acute (day 11) and chronic (day 45) colitis, by SPME-GC-MS.

RT_compound	Presence (%)		Abundance (mean±SEM)			
	Acute (*n*=8)	Chronic (*n*=6)	Acute	Chronic	Fold change	*P*-valu
7.41_acetone	100	100	53,674,496±2,930,049	1,111,553,365±453,789,761	20.7 ↑	0.000
10.28_2,3-butanedione	100	100	13,116,448±3,853,211	645,977,429±263,719,181	49.2 ↑	0.000
10.32_furan, 3-methyl-	100	100	1,192,496±248,478	7,458,304±3,044,840	6.3 ↑	0.006
13.44_1-butanol	87.5	NA	22,807,776±13,397,620	NA	Absent in chronic	0.028
20.53_1,3-xylene	100	100	1,080,292±240,972	6,910,976±2,821,394	6.4 ↑	0.001
22.11_2-heptanone	100	100	5,919,840±1,607,085	223,645,696±91,302,973	37.8 ↑	0.001
22.61_2-acetoxy-3-butanone	NA	100	NA	41,806,037±17,067,243	Absent in acute	0.000
25.57_2-octanone	12.5	100	266,689	24,915,968±10,171,901	93.4 ↑	0.007
27.53_7-ethyl-5-methyl-6,8-dioxabicyclo[3.2.1]oct-3-ene	NA	100	NA	17,735,040±7,240,300	Absent in acute	0.000
29.57_nonanal	12.5	100	62,867	6,893,781±2,814,374	109.7 ↑	0.005
39.63_octane, 2,4,6-trimethyl-	NA	100	NA	3,434,837±1,402,266	Absent in acute	0.000

P-values were calculated according to a Student's *t*-test, corrected for multiple comparison by Bonferroni and performed on log-transformed data ($p<0.05$). Fold change shows an increase (↑) or decrease (↓) of the average peak abundance of each compound in the acute colitis group, compared to chronic colitis.

6.5.5 Pre-malignant changes in an inflammation-associated CRC model

C57BL/6 female mice (*n*=6) were housed individually and were administered one dose of 12.5mg/kg AOM. This was followed by oral exposure to 1.5% DSS for 5 days followed by 16 days of ordinary water. This DSS cycle was repeated twice with animals being sacrificed 12 days after final cycle. There were 2 control groups included in the analysis: an untreated control group (*n*=6) and mice treated with cycles of DSS alone (chronic colitis) (*n*=6). Faecal samples were collected weekly and tissues were taken for histological analysis upon necropsy. After treatment, DSS-treated mice weighed significantly less than the untreated mice with a difference of 17.7±4.3%, 9.1±2.7% and 11.2±1.6% on days 13, 34 and 57, respectively (Student's *t*-test; mean±SEM) **(Figure 6.12).** This weight loss was accompanied by mild diarrhoea. The AOM/DSS inflammation-associated CRC model is expected to produce large colonic tumours, however inspection of the colon at necropsy showed no tumours. Tissues were prepared for histological examination for signs of pre-malignancy.

All animals treated with AOM/DSS showed signs of pre-malignancy, visualised by HID/AB staining of colonic sections. Signs included hyperplasic and occasionally dysplastic crypts and were assessed for the number of MDF by both the author and an accredited murine pathologist **(Figure 6.13).** The criterion used to define an MDF is described in **section 2.4.6.** There were significantly more MDF in the AOM/DSS treated group compared to the DSS-alone treated group with 3.7±0.7 and 1.2±0.2 MDF identified respectively (mean±SEM, Student's *t*-test, $p<0.05$); no MDF were identified in untreated control mice **(Figure 6.14).**

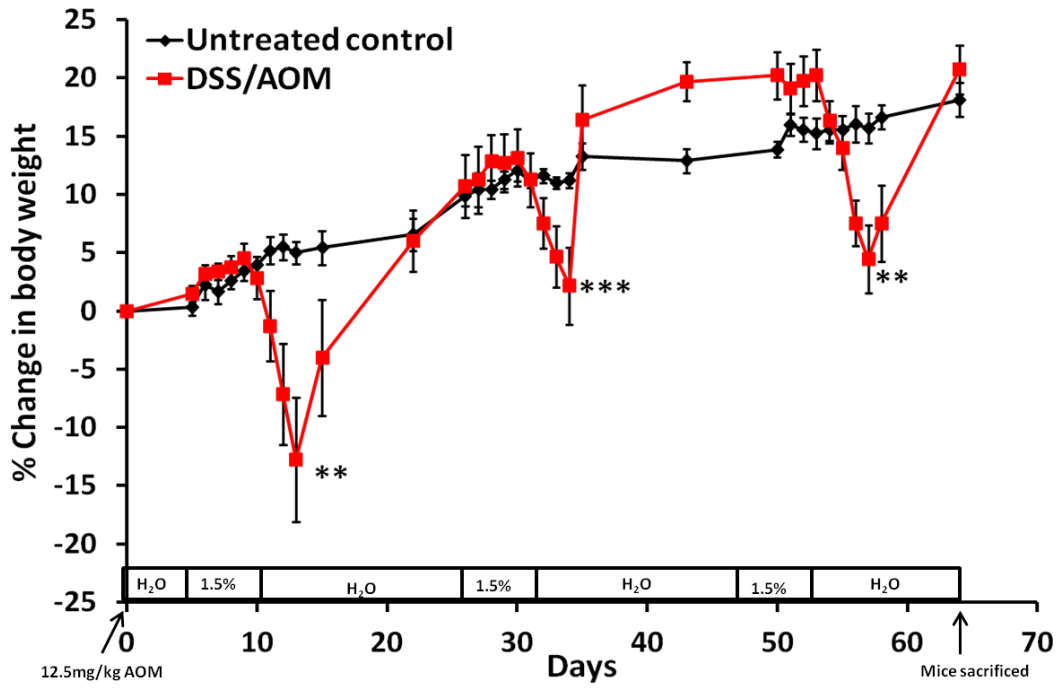

Figure 6.12 Weight loss of DSS/AOM treated mice compared to untreated control. The change in the body weight (%) of mice was measured daily during each DSS cycle. Data are represented as mean±SEM, *n*=6/group. Statistical differences were assessed by Student's t-test, $p<0.01$** for weight loss in the AOM/DSS treated group at days 13 and 57, $p<0.001$*** at day 34 compared to untreated control.

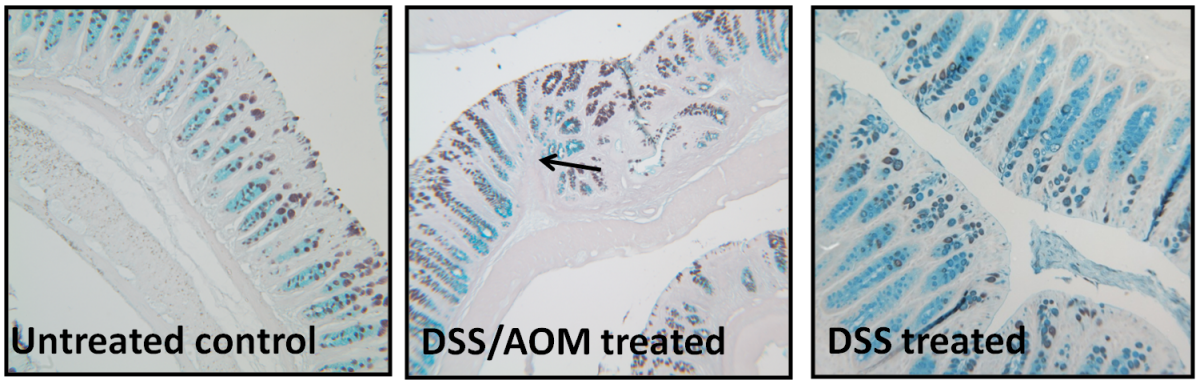

Figure 6.13 Representative images of HID/AB stained distal colonic section for untreated controls, AOM/DSS and DSS-alone treated mice (x20 magnification). The untreated control group and the AOM/DSS treated group were euthanized at experimental day 64 and the DSS-alone treated mice were euthanized at day 45 since the start of DSS/AOM treatment at day 0. The arrow indicates damaged crypts in the AOM/DSS treated group accompanied by a damaged epithelium, compared to untreated controls.

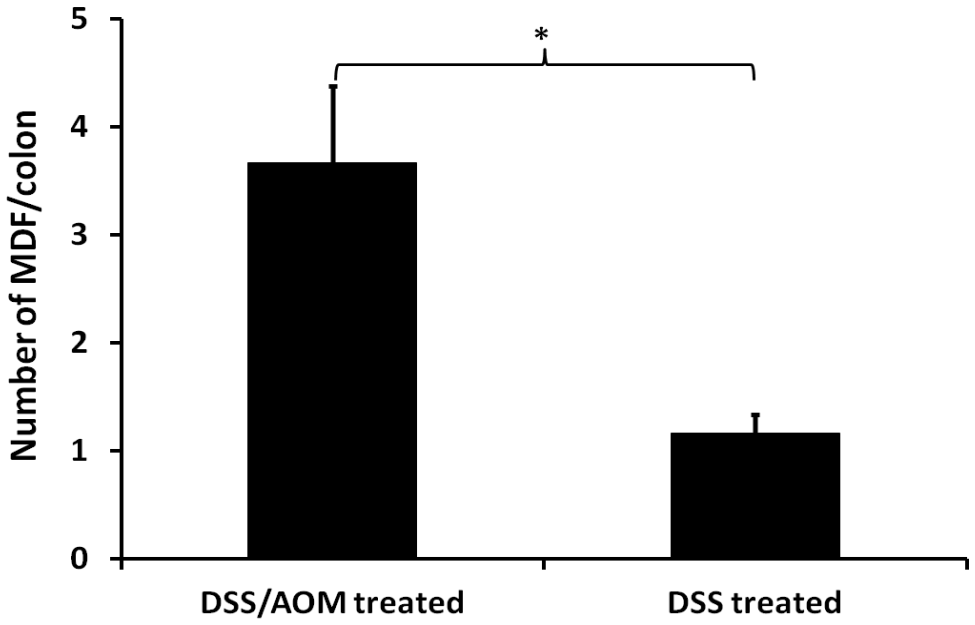

Figure 6.14 Number of MDF/colon. Identification of morphologically distinctive pre-invasive mucosal lesions, MDF, characterised by dysplastic crypts devoid of mucins. The number of MDF/colon was significantly higher in the AOM/DSS treated mice compared to the DSS-alone treated mice (*n*=6/group; Student's *t*-test, $p<0.05$*).

6.5.6 VOC profiles as indicators of early lesions in murine colitis associated CRC

In the first instance, the faecal VOC profiles were compared between the AOM/DSS group and untreated controls. Faecal pellet samples collected from each animal and samples from experimental weeks 1, 4, 7 and 10 were compared. A total of 138 VOCs were identified across the four time points from both groups; the largest number of VOCs identified was at week 4, in both groups, and the lowest at week 10. A two-way ANOVA found a significant effect of time, $F(3, 40) = 29.20$, $p<0.001$, but no significant interaction effect or main effect of group was found. This suggests that if group is ignored, the number of VOCs was different between weeks 1, 4, 7 and 10. In order to further investigate where this time related significant difference occurs, a Tukey HSD test was performed irrespective of group. The number of VOCs identified were significantly lower at week 1 and week 7 compared to week 4, and week 10 compared to weeks 1, 4 and 7 **(Figure 6.15).**

The abundance of 47 VOCs varied significantly with time, in the AOM/DSS group (ANOVA followed by Bonferroni, $p<0.05$). A PCA using these 47 VOCs shows the difference between week 1 and week 10 **(Figure 6.16)**.

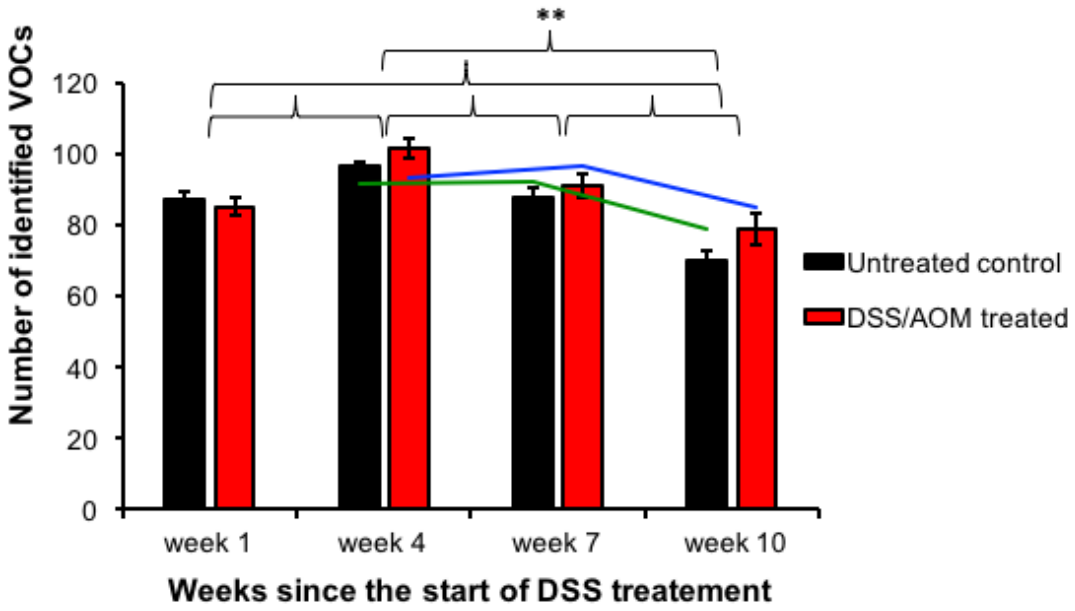

Figure 6.15 Variation in the number of faecal VOCs identified during the development of inflammation-driven CRC. The number of VOCs identified in the headspace of the faecal pellets collected at weeks 1, 4, 7 and 10 from untreated control and AOM/DSS treated mice. Data represented as mean±SEM, n=6/group. Statistical differences were assessed by two-way ANOVA, $p<0.01$** for combined number of VOCs from the untreated control and AOM/DSS treated groups between weeks 1, 4, 7 and 10. The green line is the rolling average for the untreated control group and the blue line is the rolling average for AOM/DSS treated mice, both showing the trend of number of VOCs over time for both groups.

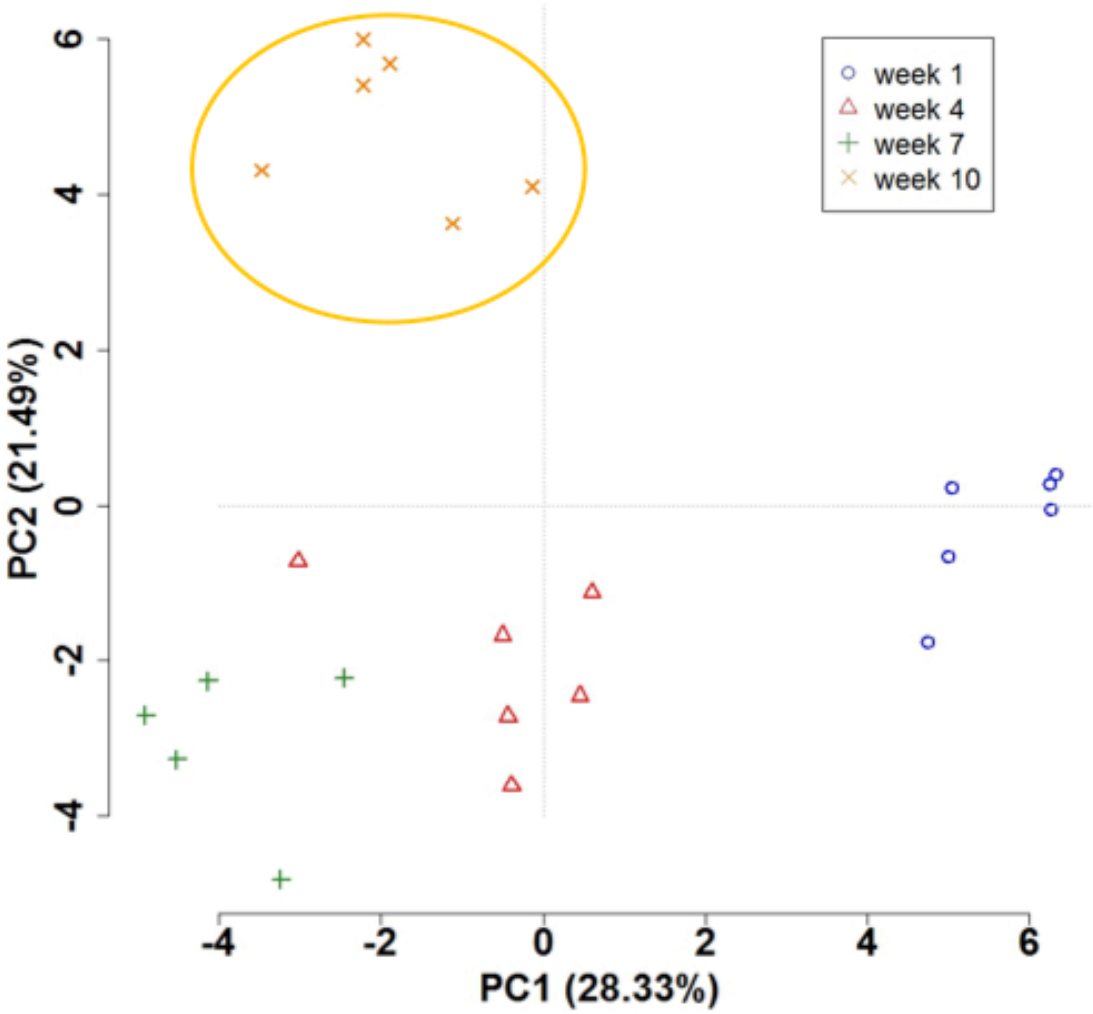

Figure 6.16 A PCA biplot for the faecal pellets of AOM/DSS treated mice from weeks 1, 4, 7 and 10. The PCA shows the variation within the AOM/DSS group and was performed using the abundance of the 47 significantly different compounds (p<0.05; ANOVA followed by Bonferroni). The last time point tested, week 10, is circled.

Faecal VOC analysis at week 10 yielded 93 compounds, 11 of which were significantly different between the two groups (Student's t-test, p<0.01). A PCA plot was able to clearly distinguish between untreated and treated mice based on VOCs present in the HS of faecal samples, using all VOCs and when just using those VOCs that significantly varied between the two groups, as shown in **Figure 6.17.** Of these significantly different compounds found to vary between treated and untreated mice at the end time point, 10 were increased and one (propanoic acid, 2-methyl-, anhydride) decreased **(Figure 6.18)**. The 10 compounds found to be higher in the AOM/DSS treated group were either aldehydes, or ketones.

Representative chromatograms from week 10 clearly show these differences in the presence or levels of peaks, which correlate to the 11 significantly different compounds and their absence or decrease in untreated controls. For example, 2-heptanone, 5-methyl-2-heptanone, 6-methyl-2-heptanone, 2H-pyran-2-one, tetrahydro- and benzeneacetaldehyde **(Figure 6.19).**

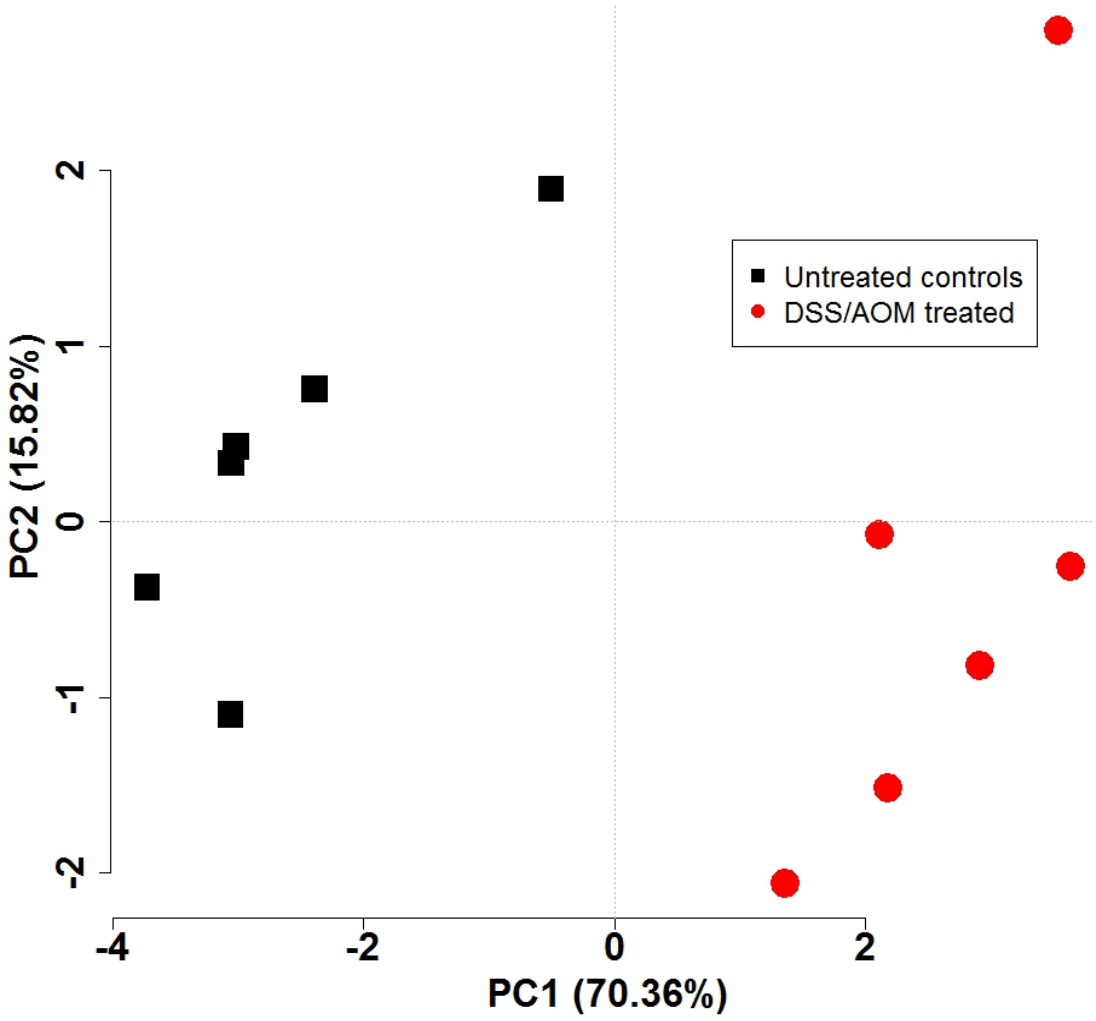

Figure 6.17 A PCA biplot for the faecal pellets of AOM/DSS treated mice compared to untreated control mice at experimental week 10. The PCA was performed using the abundance of the 11 significantly different compounds between the two groups (Student's *t*-test followed by Bonferroni, $p<0.05$).

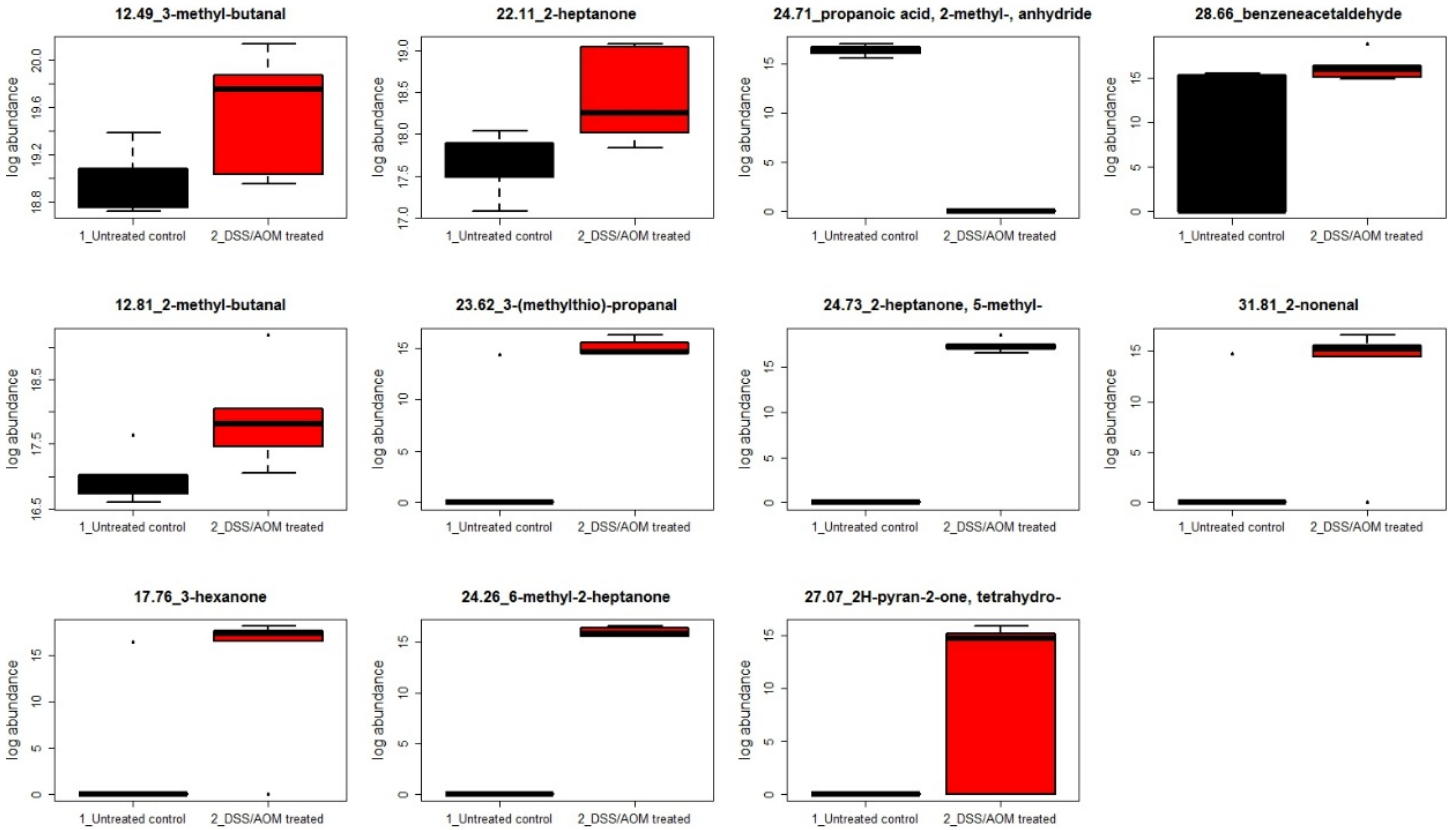

Figure 6.18 Box plots of the peak abundance (log scale) of the significantly different compounds. A Student's *t*-test, followed by Bonferroni multiple comparison correction, was performed between AOM/DSS treated and untreated control groups and found 11 compounds to significantly vary across time (p<0.05).

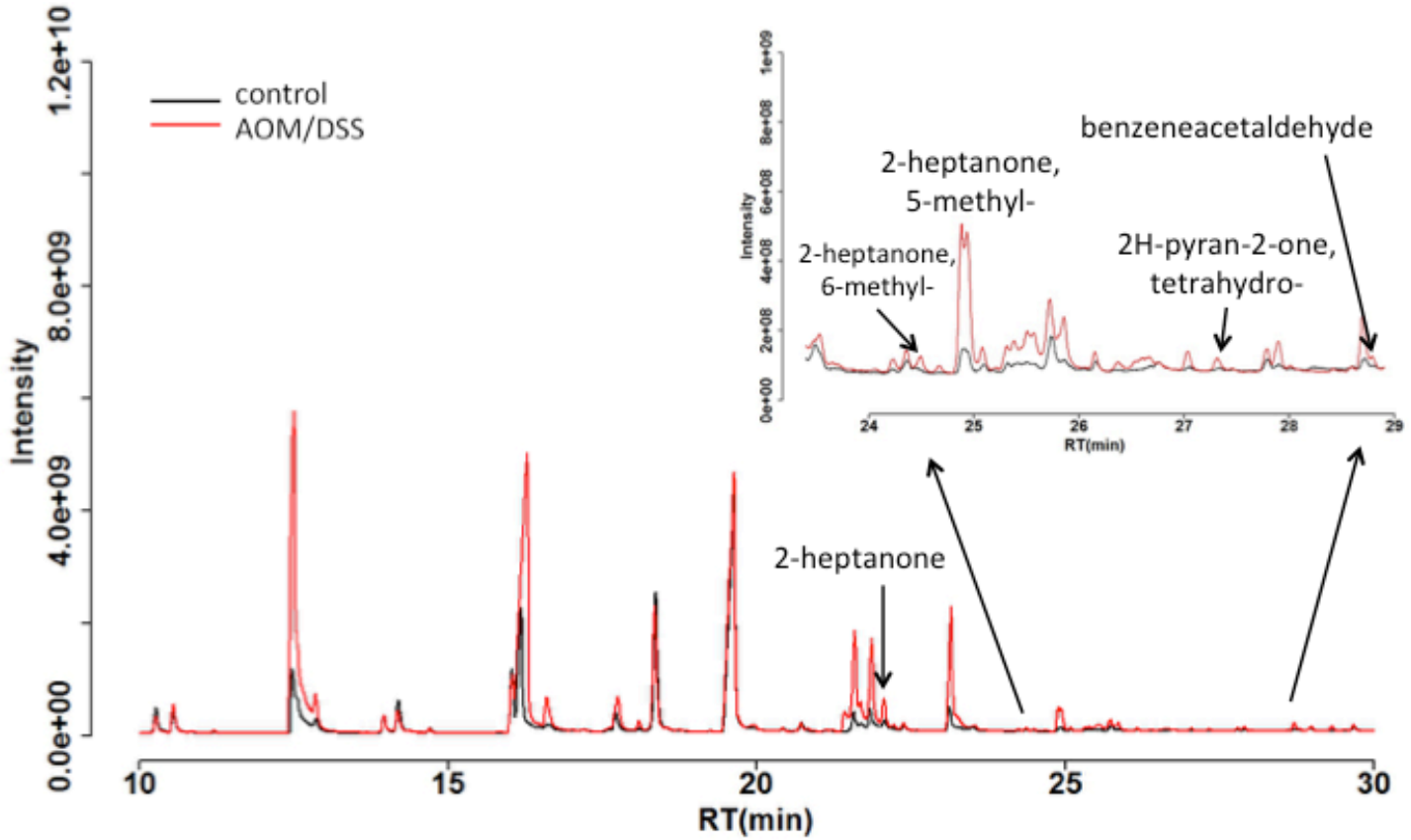

Figure 6.19 Representative chromatograms from experimental week 10. This demonstrates the differences in peaks between an untreated control faecal sample compared to a AOM/DSS mouse sample. A number of the significant VOCs are highlighted (Student's *t*-test, $p<0.05$).

In order to further explore the differences between the VOC profiles from weeks 1, 4, 7 and 10 of untreated and AOM/DSS treated mice, a heat map was produced using cluster analysis using the 75 significantly different VOCs (found by two-way ANOVA, using the time-series metabolomics online tool, MetAtt [225] **(Figure 6.20).**

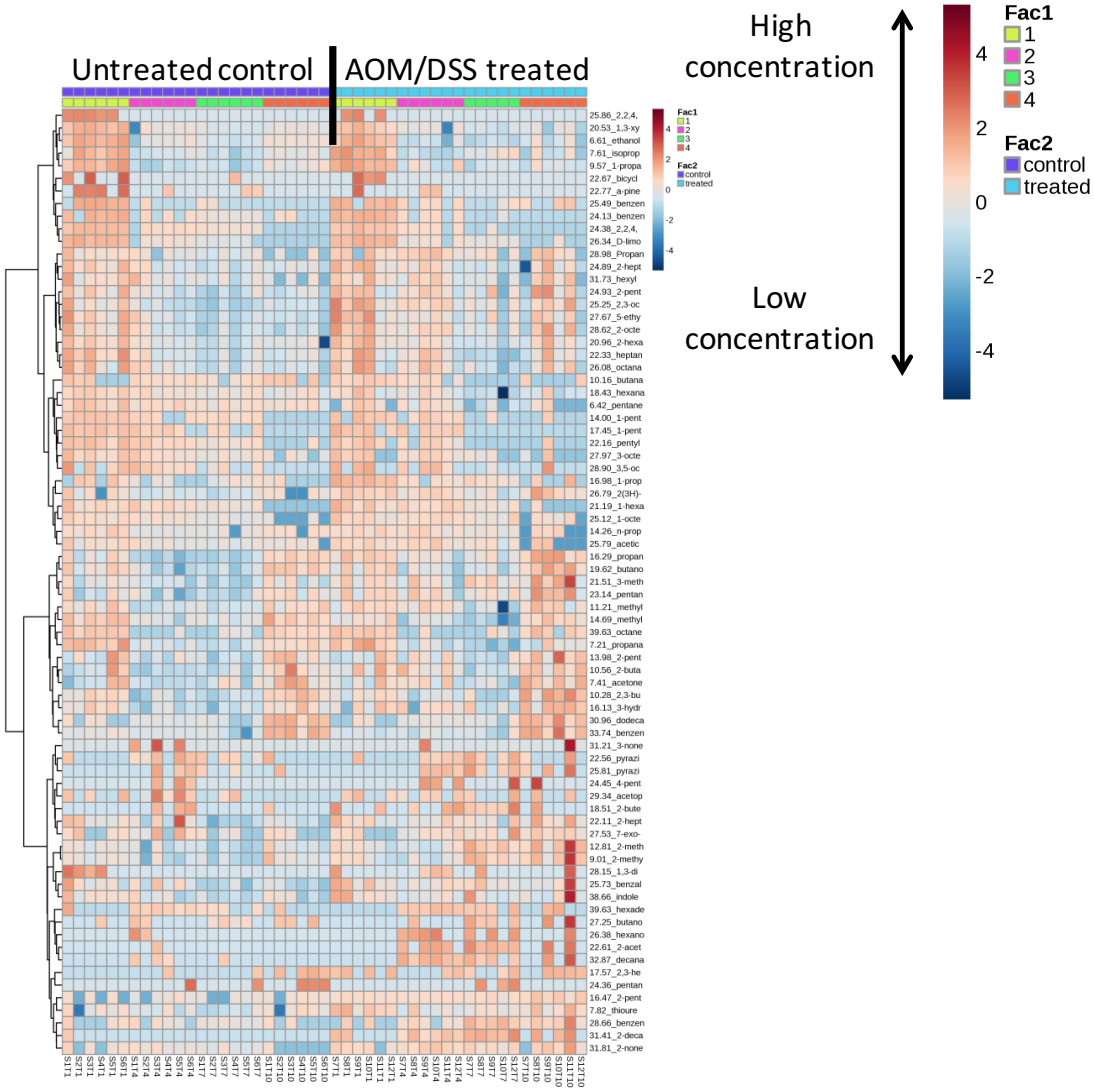

Figure 6.20 Heat map representing hierarchical clustering of 75 compounds identified in the faeces of untreated, and AOM/DSS treated mice at 4 different time points (weeks 1, 4, 7, and 10). The untreated control group is indicated by the purple left-hand panel and the AOM/DSS treated group is indicated by the blue right-hand side panel. Columns represent individual murine faecal samples and rows refer to distinct compounds. Shades of red represent an increase in concentration of a compound and shades of blue represent a decrease in concentration of a compound.

In order to demonstrate that the markers of pre-malignancy are specific to the presence of malignant changes, and are not markers of chronic inflammation, the VOC profiles from week 10 of AOM/DSS treated mice was directly compared to day 45 chronic DSS only treated mice. 26 compounds were significantly different; 10 were increased in the chronic colitis group and 16 in the inflammation-carcinogen group **(Table 6.2).** A PCA plotted using these significant compounds is able to clearly distinguish between the two groups **(Figure 6.21).**

Table 6.2 List of the 26 significantly different compounds detected in the HS of faecal pellet samples from mice treated with AOM/DSS by SPME-GC-MS.

RT_compound	Presence (%)		Abundance (mean±SEM)		
	DSS	AOM/DSS	DSS	AOM/DSS	*P*-value
6.61_ethanol	100	100	480,156,331±159,522,185	61,950,123±15,761,211	0.0085
7.21_propanal	33.3	100	12,402,048±4,704,010	9,047,637±2,182,796	0.0264
7.49_dimethyl sulfide	66.7	0	8,266,224±3,912,603	NA	0.0256
7.61_isopropanol	100	100	66,871,467±14,796,772	24,212,651±4,510,725	0.0098
9.57_1-propanol	100	100	49,677,483±21,472,805	12,274,517±2,101,616	0.0373
10.56_2-butanone	100	100	843,795,797±206,663,769	214,717,099±26,504,314	0.0231
11.90_1-propanol, 2-methyl-	100	33.3	4,458,453±618,098	6,742,400±2,252,276	0.0275
14.20_pentanal	0	100	NA	53,717,504±23,817,831	0.0000
16.46_3-penten-2-one	0	66.7	NA	9,268,224±4,831,905	0.0255
16.58_toluene	16.7	83.3	1,805,056	7,846,246±1,360,117	0.0132
17.57_2,3-hexanedione	0	66.7	NA	140,064,768±17,121,344	0.0251
18.51_2-butenal, 3-methyl-	83.3	16.7	3,547,341±331,371	6,165,248±2,097,536	0.0206
20.53_1,3-xylene	100	100	6,910,976±893,127	37,793,621±6,930,503	0.0003
20.96_2-hexanal	33.3	100	4,039,168±275,946	4,722,987±1,232,157	0.0248
21.07_2-n-butyl furan	0	66.7	NA	6,226,656±2,097,536	0.0253
21.49_4-heptanone, 3-methyl-	16.7	83.3	9,399,296	39,231,693±12,556,693	0.0142
22.61_2-acetoxy-3-butanone	100	33.3	41,806,037±16,909,092	23,981,056±2,528,000	0.0237
24.10_3-heptanone, 6-methyl-	66. 7	0	27,705,344±14,418,736	NA	0.0259
25.25_2,3-octanedione	16.7	100	4,801,536	23,892,480±5,321,259	0.0025
25.52_3-octanone	83.3	16.7	23,896,883±5,517,636	20,142,080	0.0179
27.01_6,8-dioxabicyclo[3.2.1]octane, 7-ethyl-5-methyl-, (1R-exo)-	66.7	0	6,995,456±319,122	NA	0.0250

Table 6.2 continued.

28.14_phenol	100	16.7	45,255,168±29,198,521	2,038,038,52	0.0130
30.96_dodecane	0	100	NA	20,571,605±8,629,327	0.0000
31.41_2-hexanone, 5-methyl-	0	83.3	NA	2,467,853±707,320	0.0251
33.74_benzene, 1, 3-bis(1,1-dimethylethyl)-	0	100	NA	75,492,864±35,440,076	0.0000
37.06_Undecane, 4,7-dimethyl-	50	100	1,919,808±276,549	7,936,299±2,148,834	0.0456

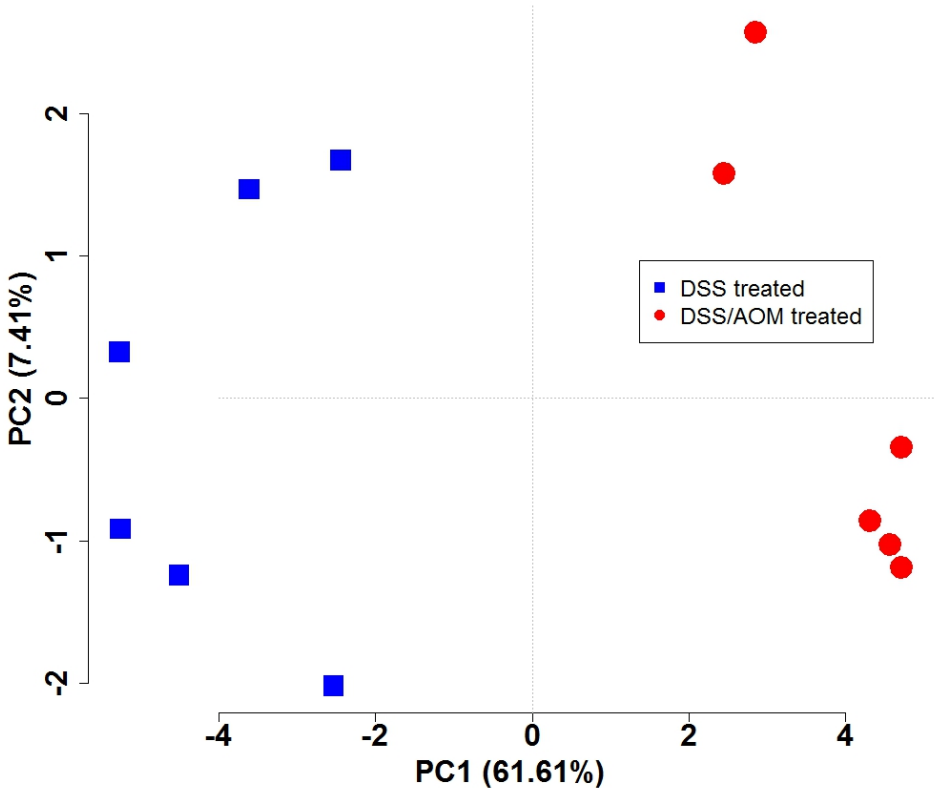

Figure 6.21 A PCA biplot for the faecal pellets of AOM/DSS treated mice compared to DSS alone treated mice. The PCA was performed using the abundance of the 26 significantly different compounds between the two groups (Student's *t*-test followed by Bonferroni, $p<0.05$).

6.6 SUMMARY OF RESULTS

1. After 4 cycles of DSS, chronic colitis was induced as characterised by significant weight loss and histological changes. Analysis of the longitudinal faecal VOC profile found significant differences compared to untreated healthy control mice. There were specific VOCs associated with chronic colitis; these were 5-methyl-2-heptanone, 2-octanone and 2-decanone.

2. There was significantly more fibrosis in mice treated with chronic DSS compared to those given acute DSS treatment only. The clinical difference was associated with significantly different VOC profiles.

3. Administration of a single dose of AOM followed by 3 cycles of 1.5% DSS did not result in the induction of distal colonic tumours, but was associated with pre-malignant MDF lesions, as visualised by HID/AB.

4. There was a significant increase in the abundance and prevalence of methyl ketones and aldehydes in AOM/DSS treated mice compared to untreated controls. Furthermore, the specific compounds were associated with either the AOM/DSS or the DSS groups and may be markers of pre-malignancy.

6.7 DISCUSSION

This study has demonstrated that HS-SPME-GC-MS analysis can be used to differentiate VOC profiles of healthy untreated, chronic colitis and CRC AOM/DSS treated murine faecal samples. Potential markers for chronic intestinal inflammation and the presence of very early stage CRC as well as possible markers of disease progression were identified. Even early lesions of colitis-associated CRC were associated with significant metabolic alterations in the faeces of mice treated with AOM/DSS.

Among the chemically-induced CRC models, the combination of a single dose of AOM with 1-week exposure to DSS in rodents has proven to dramatically shorten the latency time for induction of CRC and to rapidly recapitulate the aberrant crypt foci–adenoma–carcinoma sequence that occurs in human CRC. This study used this CRC model and identified morphologically distinctive pre-invasive mucosal lesions to help elucidate the early steps of CRC, which included the characterisation of so-called MDF, formed by dysplastic crypts devoid of mucins [310].

There were specific VOCs identified in AOM/DSS treated mice, which had premalignant changes in the colon, including 3-(methylthio)-propanal, 2-nonenal, 3-hexanone and 6-methyl-2-heptanone. In addition, markers of chronic inflammation were found, including ethanol, 3-methyl-2-butenal, 3-octanone, 2-butanone and 2-acetoxy-3-butanone. Overproduction of ROS combined with the occurrence of lipid peroxidation has been widely proposed as a possible mechanism for intestinal inflammation of the mucosa and intestinal lumen. An increase in the number of ROS causes an increase in toxic VOCs, including aldehydes and alkanes, which in turn have a toxic effect on the surrounding tissue [311]. Further work to investigate whether or not these markers that we have identified are markers of oxidative stress or markers of alternative metabolic pathways associated with CRC (e.g. those involved in the transformation from normal epithelium to benign neoplasia [312]), would include taking an *in vitro* approach. A recent review has identified current

challenges in the investigations of VOCs as potential cancer biomarkers and this approach shows the rationale for further study [313].

A recent study was able to demonstrate the use of travelling wave ion mobility mass spectrometry (TWIMMS) technology as a fast and efficient method for metabolomics profiling of human CRC [314]. The authors discovered alterations in fatty acid biosynthesis and oxidative, glycolytic, and polyamine pathways that distinguish tumours from non-malignant colonic epithelium as well as various stages of CRC. In addition, it has been shown recently that a study using selected-ion flow-tube mass spectrometry (SIFT-MS) was able to correctly classify samples into either high risk or low risk of developing CRC with a specificity of 78% and a sensitivity of 72% [315].

Overall, data produced from this study combined with previous studies suggest that a difference can be predicted between faecal samples from individuals or animal models with CRC compared to healthy control samples, based on their VOC profile. A multivariate predictive method of modelling this data may enable the development of a predictive tool to be used in a clinical setting to determine whether or not individuals are may already have preneoplasia, and are at risk of developing CRC.

Chapter 7

VOC Profiling of a Sporadic Colon Cancer Murine Model

7.1 INTRODUCTION

CRC is the fourth most common cancer [67] and, with more than 600,000 deaths annually, it is the second leading cause of cancer related death in both men and women in the UK [316]. CRC often evolves over a number a years, therefore providing a window of opportunity for early detection. However, the prognosis of CRC for many patients is poor due to late detection and, despite the growing evidence to support an increased understanding of the pathogenesis of CRC, reliable disease-specific biomarkers for screening and surveillance are lacking. There are currently no reliable markers for early diagnosis of CRC or its precursor lesions, and therefore this remains an overwhelming challenge [317].

As previously described, there is an increased risk of developing CRC associated with the duration and extent of IBD [56]. However, most CRC occurs independent of IBD and is directly influenced by diet, genetic and environmental factors [318]. Individuals who do not have a family history of CRC or adenomas, or a history of non-polyposis syndromes or IBD are classified as having sporadic CRC. Approximately 75% of patients have sporadic CRC with no known risk factors for their disease [319].

In England, all men and women aged 60-74 are invited to carry out an FOB test at home to check for the presence of blood in a stool sample as a way of screening for early signs of CRC [320]. While non-invasive stool-based screening tests are used for the early detection of CRC concerns have been raised about their sensitivity and specificity. Thus, as previously mentioned, there is an opportunity for the development of a metabolomics-based approach to the non-invasive diagnosis of CRC. Metabolomics involves the comprehensive profiling of low MW compounds emitted from biological samples or fluids, and has been used to classify CRC on the basis of tumour classification [321], to identify new diagnostic or prognostic markers [322] and to discover new targets for future therapeutic interventions [323].

Understanding the metabolome of human CRC will also provide insights into the critical metabolic pathways involved in CRC. Montrose *et al.* determined whether metabolic changes can be detected in the faeces and plasma during AOM-induced CRC using ultra-performance liquid chromatography tandem mass spectrometry (UPLC/MS/MS) and GC/MS. They were able to provide evidence that CRC was associated with significant metabolic alterations in both the faeces and plasma, including elevated levels of sarcosine in the faeces, and increased levels of 2-hydroxyglutarate in the plasma [324]. Here, we use HS-SPME-GC-MS to investigate the metabolic odorous 'smell' emitted from faeces of a AOM-induced CRC model.

7.2 HYPOTHESIS

The hypotheses were:

- The induction of sporadic CRC will cause a significant change to the faecal VOC profile of mice compared to untreated controls.
- The VOCs responsible for these changes will be different to those identified as markers of inflammation-associated CRC.

7.3 AIMS

1. To determine the appropriate dose of AOM to induce sporadic CRC.
2. To determine whether metabolic changes can be detected in the faeces during AOM-induced CRC.
3. To investigate whether the tumour was a potential source for altered levels of metabolites in faeces.

7.4 METHODS

7.4.1 Experimental design

7.4.1.1 Induction of sporadic colorectal cancer using AOM

Briefly, female C57BL/6 mice were given 6 injections (I.P.) of 12.5mg/kg AOM solution once a week over the first 6 weeks of the experiment. Faecal samples were collected once a week until week 30 when mice were sacrificed and colons were assessed for tumours. A pilot study was performed using a control and AOM-treated group (*n*=4/group) in order to investigate the outcome of using 12.5mg/kg of AOM (ended at week 20 due to profuse rectal bleeding). This was followed by a subsequent study using *n*=6 mice in each group as a repeat study which continued until week 30.

7.4.2 HS-SPME-GC-MS

In brief, where possible, 10 pellets of stool sample was collected and stored in 2ml glass vials at -20°C. Prior to VOC extraction, samples were pre-incubated for 30 mins at 60°C before compound extraction using the solvent free SPME technique with a CAR/PDMS/DVB fibre for 20 mins prior to desorption into the GC oven [221]. For GC-MS conditions, please refer to **section 2.6.1.**

7.4.3 Data processing and statistical analysis

All raw data were processed and analysed as described in **Chapter 2.** Briefly, batch reports were produced for each dataset in AMDIS and a list of all compounds present and their corresponding corrected peak abundances was generated using Metab. Compounds present in less than 30% of at least one condition were removed. NA was replaced with 1 and peak abundance was log transformed, and appropriate statistical analysis (Student's *t*-test or two-way ANOVA) was applied: all

p-values are corrected for multiple comparison (Bonferroni). Hierarchical clustering and PCA was applied to illustrate variation present between groups.

7.5 RESULTS

7.5.1 Pilot Study: measurement of distal colonic tumours

In order to monitor the health of the animals, mice were weighed daily and percentage body weight loss was determined. Unlike the observations of mice treated with DSS alone and in combination with AOM, in which mice lost weight, the weight of AOM-alone treated mice remained stable or increased throughout the experiment **(Figure 7.1).** Between weeks 14 and 20, the weight of the untreated control group continued to increase whereas the weight plateaued in the AOM treated group with a significant difference at week 16 ($p<0.05$, *t*-test). At week 16, rectal bleeding was also observed in the AOM treated animals, which may explain the difference in weight, so the decision was made to end the experiment prematurely at week 20, before the planned end at week 30.

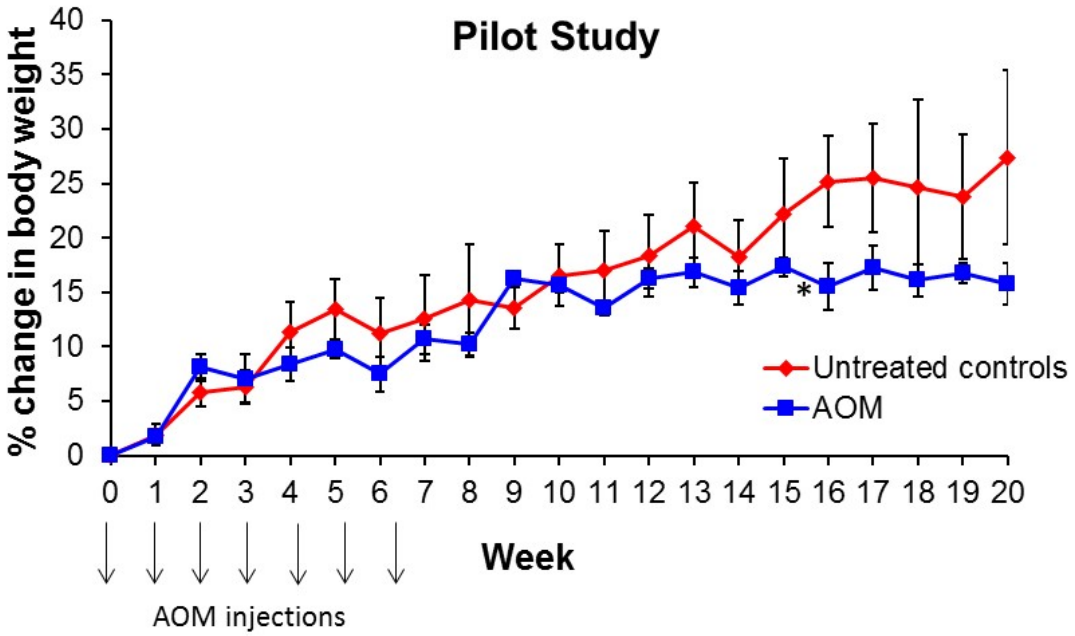

Figure 7.1 Weight change in mice undergoing sporadic AOM treatment and controls (Pilot Study). Data represented as mean±SEM, *n*=4/group. Statistical differences were assessed by Student's t-test at each week, $p<0.05$* for weight loss in the AOM treated group at week 16 only compared to untreated control.

In this pilot study, all mice in the AOM treated group (*n*=4) received 6 doses of 12.5mg/kg AOM; 3 mice developed colonic tumours but in 1 no tumour was found **(Table 7.1).** Tumours were mainly located within the distal and middle thirds of the colon, as shown in **Figure 7.2.** These locations correlate with previous findings [325] and imply that the protocol was effective [144]. Microscopic examination of H&E stained colonic sections found that the tumours were mainly broad-based adenomas and they did not penetrate the muscularis mucosa **(Figure 7.3).**

Table 7.1 Tumour load analysis.

Animal I.D.	Treatment	Number of tumours	Average tumour size (mm)
5	6 x i.p. 12.5 mg/kg	1	3
6	6 x i.p. 12.5 mg/kg	0	0
7	6 x i.p. 12.5 mg/kg	5	2.6
8	6 x i.p. 12.5 mg/kg	2	5

Number of visible colonic tumours per mouse following sporadic tumour induction using AOM and the average tumour size.

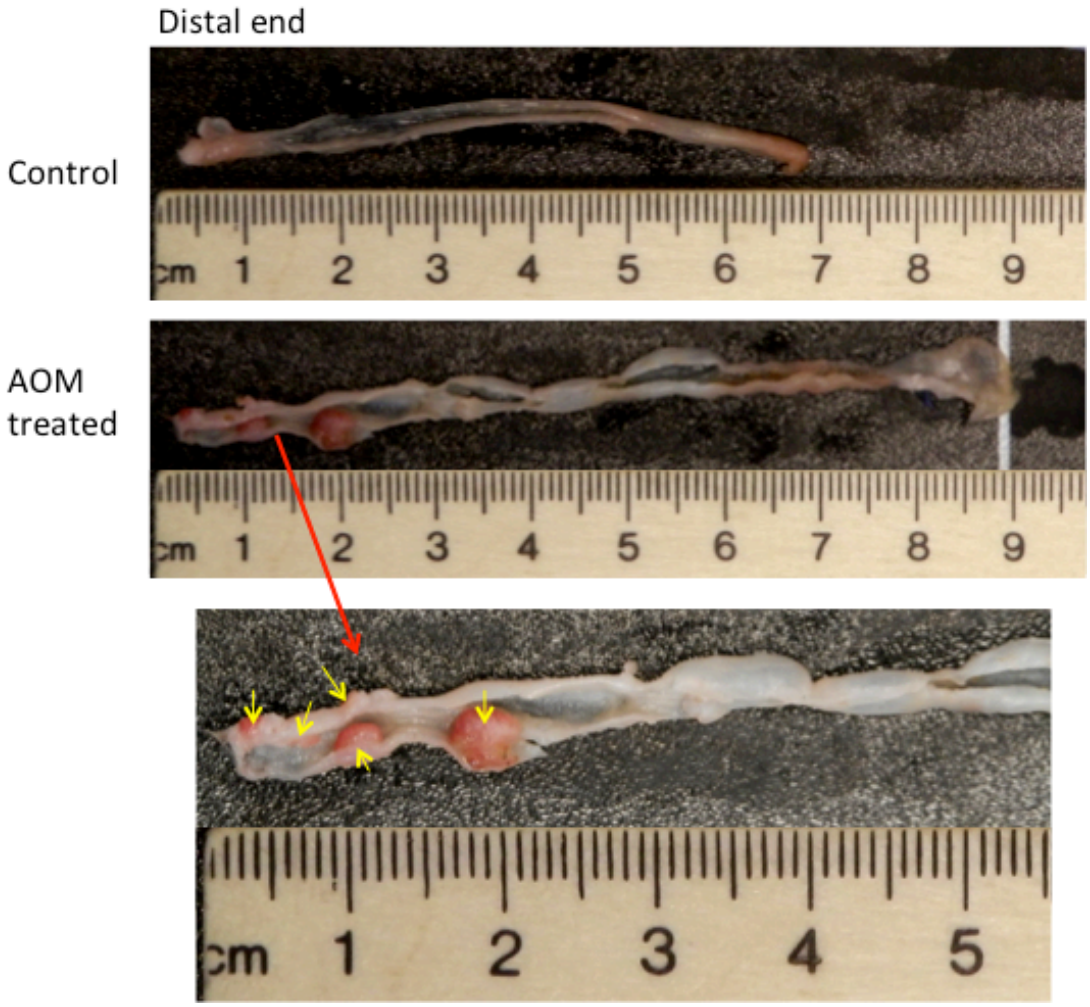

Figure 7.2 Representative gross images. Macroscopic view of longitudinally open colon mice following tumour induction by AOM treatment. A scaled ruler was used to measure the size of the formed tumours (yellow arrows indicate visible tumours).

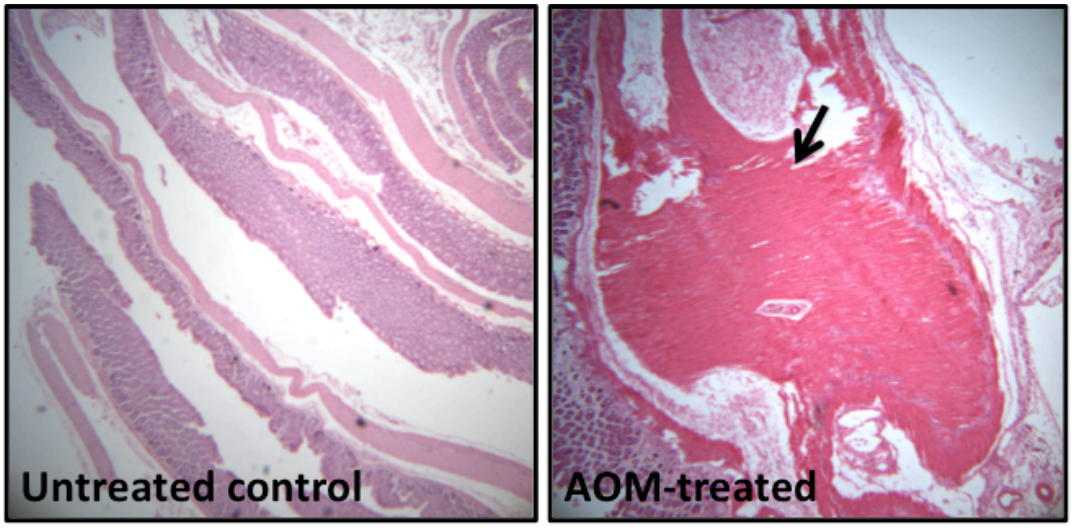

Figure 7.3 Representative H&E stained colonic sections from mice following tumour induction using AOM. Histology of colonic tumours in sections (Swiss roll) at 20x objective magnification (arrows indicate the formed polyps).

7.5.2 Pilot Study: metabolomics VOC profile of AOM-induced colonic tumours

A total of 208 VOCs were identified in the faecal pellets from both groups across weeks 1, 5, 10, 15 and 20. Comparison of the average number of VOCs identified across time, and between treatment group, found no significant interaction effect, indicating that there is no significant differences in the effect of time on the number of VOCs for control or AOM-treated mice, $F(4,20) = 0.30$, $p>0.05$). There was also no significant main effect of group, $F(1, 20) = 3.24$, $p>0.05$. However, there was a significant main effect of time, $F(4, 20) = 8.45$, $p<0.001$; the number of VOCs identified were significantly lower at weeks 15 and 20 compared to weeks 1, 5 and 10 in both groups (ANOVA followed by Tukey HSD test, $p<0.01$) **(Figure 7.4).**

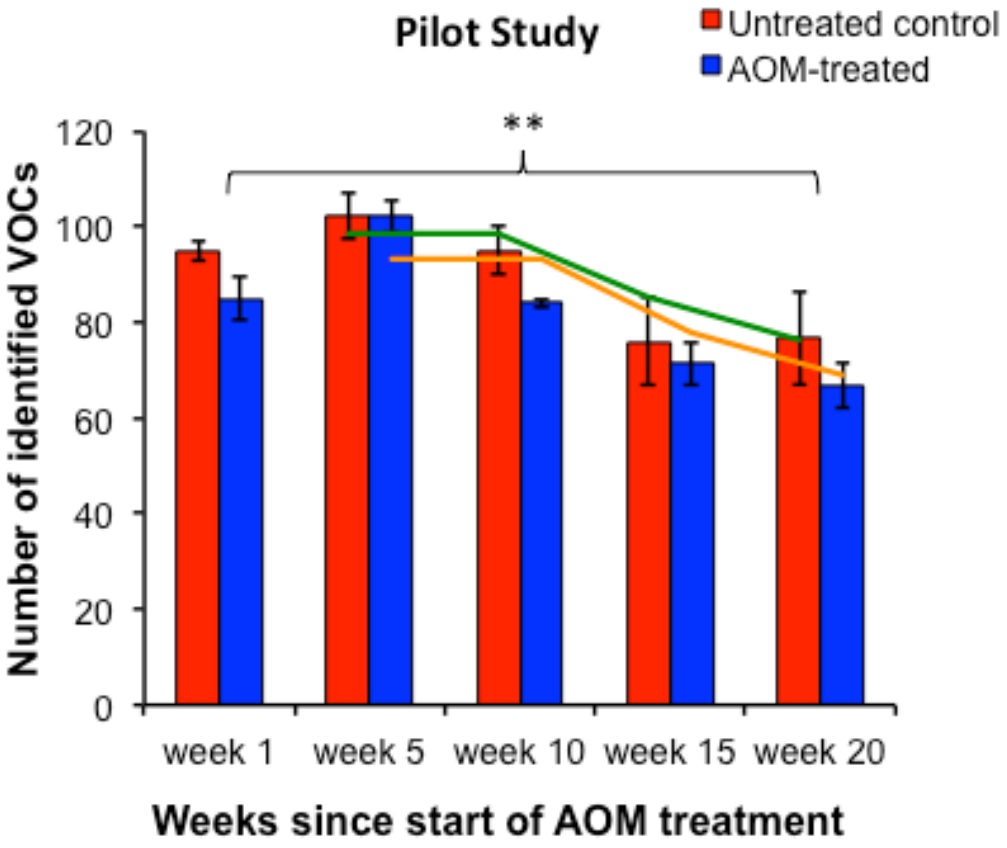

Figure 7.4 Number of faecal VOCs identified during the treatment of AOM in the Pilot Study. The number of VOCs identified in the headspace of the faecal pellets collected at weeks 1, 5, 10, 15 and 20 from untreated control and AOM treated mice. Data represented as mean±SEM, *n*=6/group. Statistical differences were assessed by two-way ANOVA, $p<0.01$** for combined number of VOCs compared between weeks 1 and 15, 1 and 20, 5 and 15, 5 and 20, 10 and 15, and 10 and 20. The green line is the rolling average for the untreated control group and the orange line is the rolling average for AOM-treated mice, both showing the trend of number of VOCs over time for both groups.

A two-way ANOVA was then performed to identify variations between groups over time according to the concentration of each of the 208 VOCs. There were only 8 compounds found to vary significantly over time when comparing the concentrations between the untreated control and the AOM-treated groups. Of these significant VOCs, 2,2,4,-tetramethyloctane, 2,2,4,6,6-pentamethylheptane, D-limonene and cyclopentane were only present in the AOM-treated group at week 10 ($p<0.001$), isopropanol ($p<0.001$) and 5-hydroxy-4-octanone ($p<0.05$) were present at significantly higher concentrations, whereas 1,3-xylene ($p<0.01$) and 2-ethyl-1-hexanol ($p<0.05$) were present at significantly lower concentrations in the untreated control group at week 10 (MetAtt). A heat map illustrates the total

variation of the 208 VOC identified between both groups and how they vary over time from week 1 to week 20 **(Figure 7.5).** These results indicate that there is a change in VOC profile at week 10, which also corresponds with the plateau in the weight loss in the AOM-treated group.

Analysis of the VOCs present across both groups at the end time point was performed. At week 20 one compound was significantly different between the untreated control and AOM-treated groups; 1,3-difluoro-2-propanone was absent in the control group and in all four samples at 24,909,824±12,511,196 in the AOM-treated group (mean±SEM, Student's *t*-test). A PCA was produced using the total 208 VOCs but resulted in poor separation of the two groups, which may be explained by the small *n* number (*n*=3 untreated control, *n*=4 AOM-treated mice) **(Figure 7.6).**

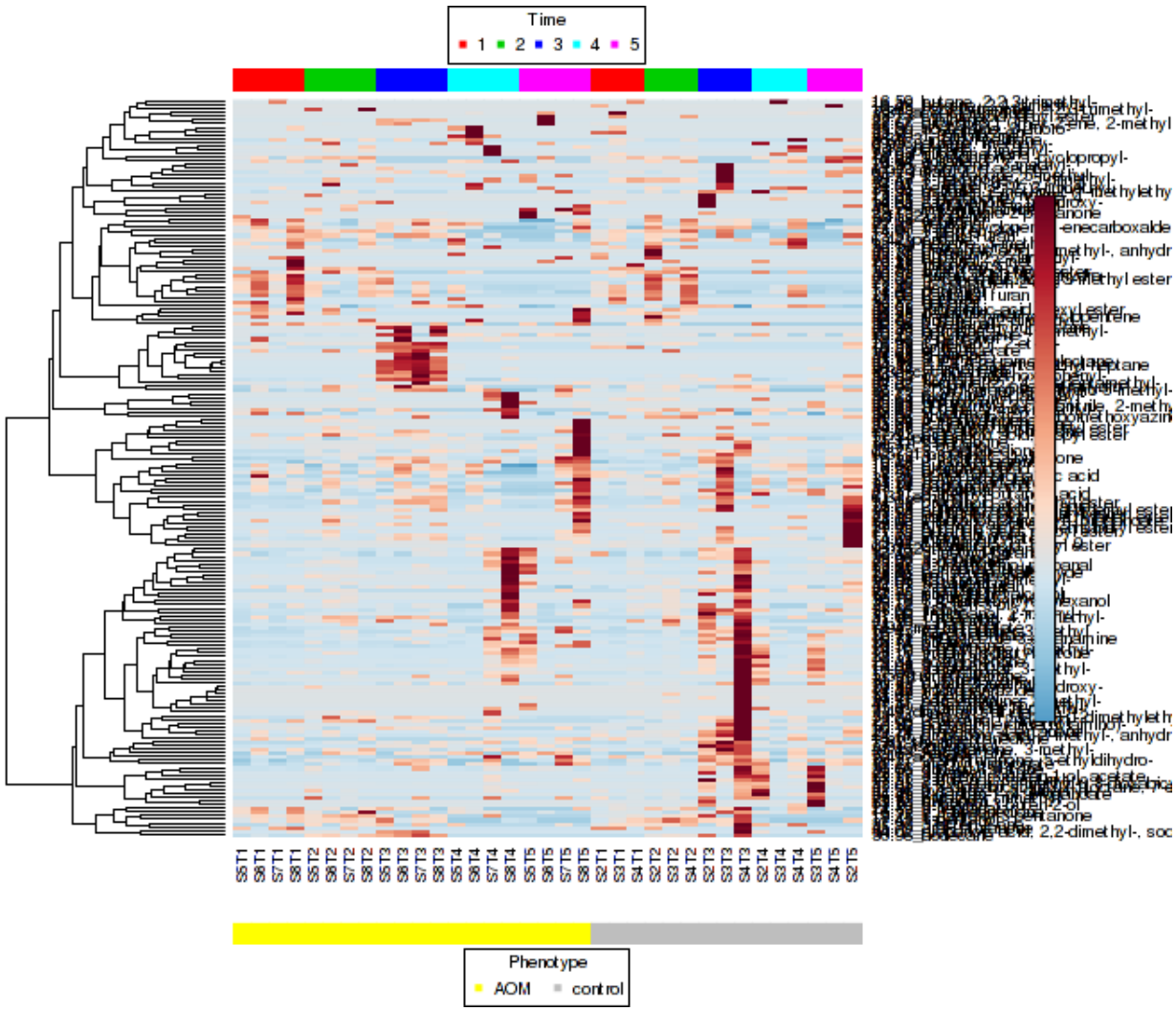

Figure 7.5 Hierarchical clustering. A heat map representing hierarchical clustering of the VOCs identified across the five different time points of AOM-induced CRC. Sample classes are indicated by the coloured bars (AOM-treated mice = yellow, untreated control = grey). Columns represent individual murine faecal samples and rows refer to distinct compounds. Shades of red represent an increase in concentration of a compound and shades of blue represent a decrease in concentration of a compound.

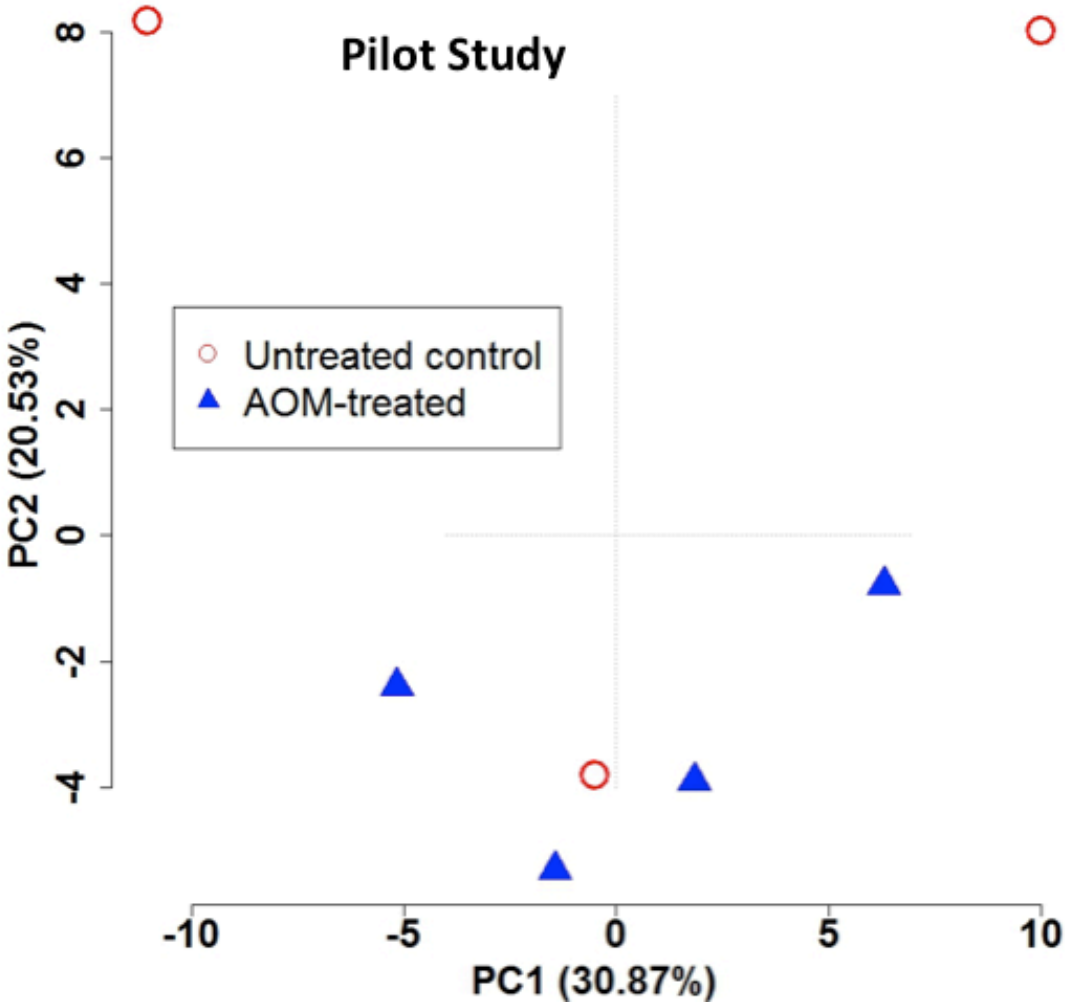

Figure 7.6 A PCA biplot for the faecal pellets of AOM-treated mice compared to untreated control mice at experimental week 20 in the Pilot Study. The first principal component has been plotted against the second principal component representing 30.87% and 20.53% of the total variation, respectively. The PCA was performed using the abundance of the 136 VOCs present at week 20.

7.5.3 Repeat Study: measurement of distal colonic tumours

As the Pilot Study resulted in the successful induction of distal colonic tumours, the method, including the AOM concentration, used for the repeat study was an exact replica of the Pilot Study but with *n*=6 mice in each group. The only difference between the two studies was that the repeat study continued until week 30, rather than week 20.

The weight of the AOM-treated group continued to increase alongside the untreated control group. There was a significant difference in body weight at weeks 18, 20 and 24; however this was not accompanied by rectal bleeding **(Figure 7.7).** Upon dissection of the intestines, there was an absence of distal colonic tumours, which was unexpected. Possible reasons to explain this may be that the AOM dose was too low or that there was variation between the different litters of the C57BL/6 mouse strain causing one to have a low susceptibility.

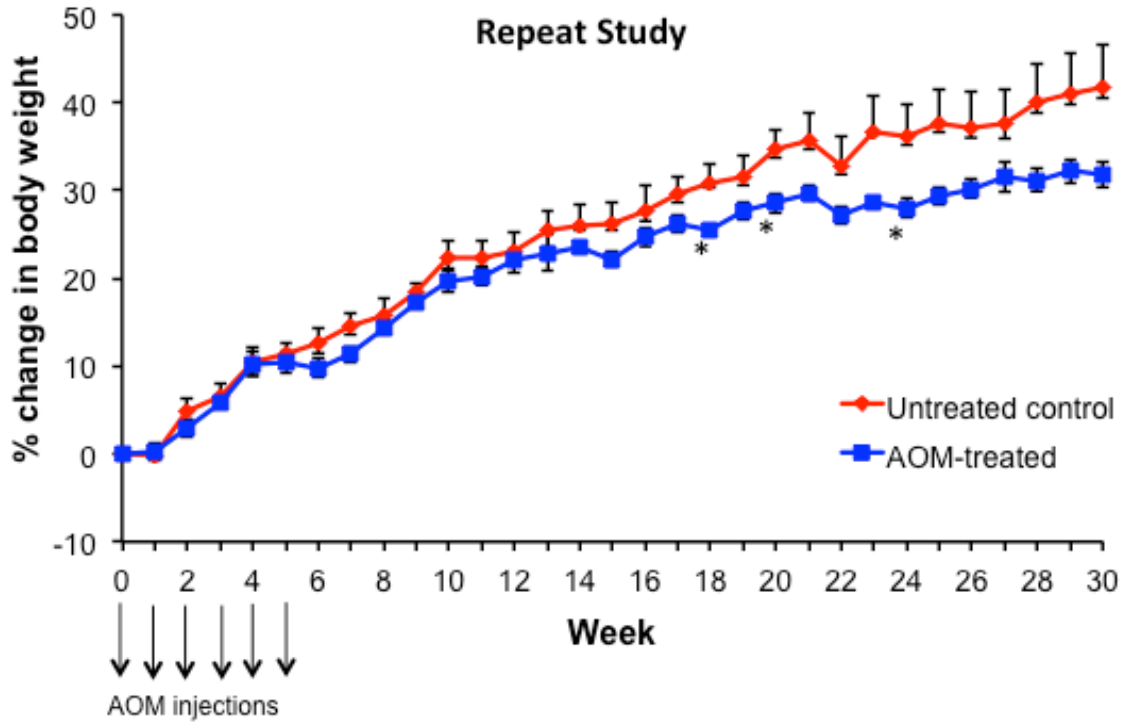

Figure 7.7 Weight change in mice undergoing sporadic AOM treatment and controls (Repeat Study). Data represented as mean±SEM, *n*=6/group. Statistical differences were assessed by Student's t-test at each week, $p<0.05$* for weight loss in the AOM treated group at weeks 18, 20 and 24 compared to untreated control.

7.5.4 Repeat Study: metabolomics VOC profile of AOM-induced colonic tumours

Although this study did not result in the induction of distal colonic tumours, as expected, the faecal samples still underwent analysis for the detection of VOCs. There were 207 VOCs were identified in the faecal pellets from both groups across weeks 1, 8, 15, 23 and 30, similar to the 208 in the Pilot Study. The number of VOCs at each group also followed a similar pattern with the lowest number of VOCs

identified towards the end of the experiment. Comparison of the average number of VOCs produced the same pattern as found in the Pilot Study; there was no significant interaction effect, F (4,30) = 0.39, p>0.05), no significant main effect of group, F (1, 30) = 0.99, p>0.05, and a significant main effect of time, F (4, 30) = 3.83, p<0.01. When grouping the untreated control and AOM treated groups together, the number of VOCs identified were significantly lower at week 1 compared to week 15, week 8 compared to week 15, week 30 compared to week 15, and week 30 compared to week 23 (ANOVA followed by Tukey HSD test, p<0.01) **(Figure 7.8).**

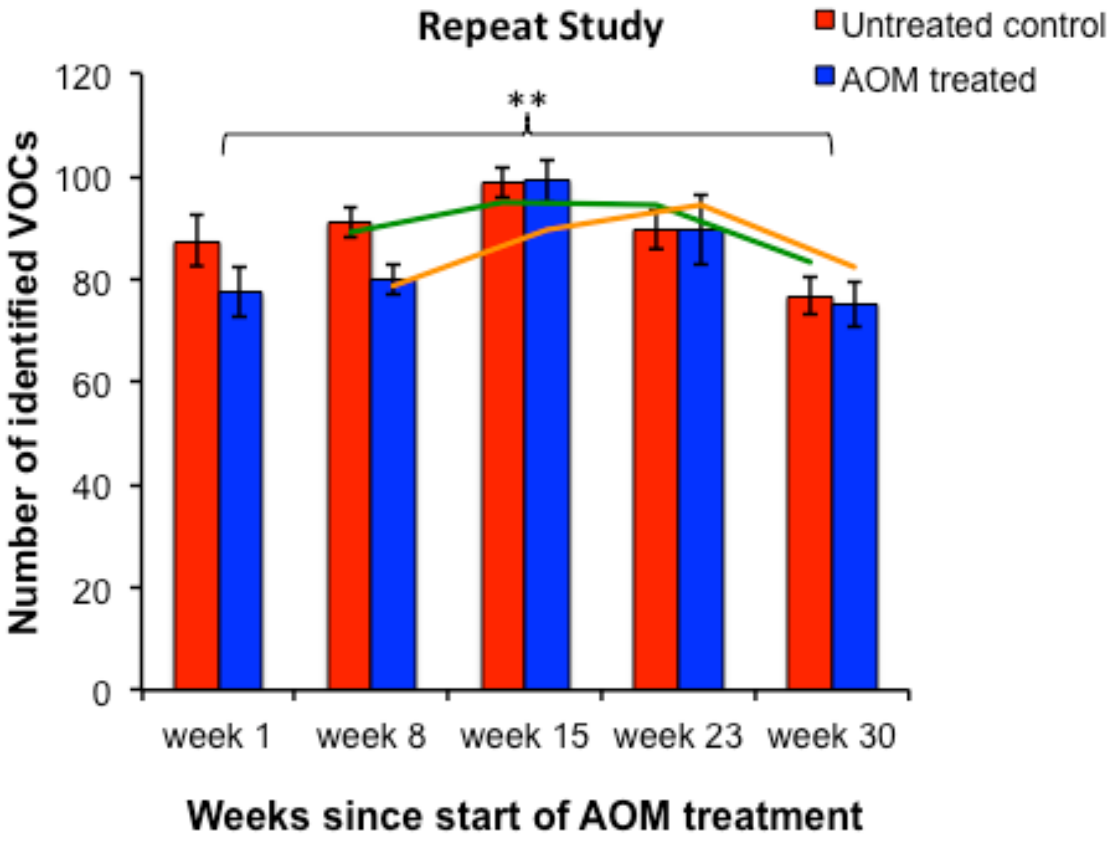

Figure 7.8 Number of faecal VOCs identified during the treatment of AOM in the Repeat Study. The number of VOCs identified in the headspace of the faecal pellets collected at weeks 1, 8, 15, 23 and 30 from untreated control and AOM treated mice. Data represented as mean±SEM, n=6/group. Statistical differences were assessed by two-way ANOVA, p<0.01** for combined number of VOCs compared between weeks 1 and 15, 8 and 15, 15 and 30, and 23 and 30. The green line is the rolling average for the untreated control group and the orange line is the rolling average for AOM-treated mice, both showing the trend of number of VOCs over time for both groups.

Unlike the Pilot Study, a multivariate quantitative analysis performed on this dataset showed no significant differences between the concentrations of the 207 VOCs between the untreated control and AOM-treated groups (MetAtt). The heat map demonstrates this by showing similar VOC profiles over time for both groups **(Figure 7.9).** Furthermore, the analysis of VOCs at week 30 resulted in only four significantly different compounds; 1-cyclopropyl-1-propanone and 3-methylbutyl ester-butanoic acid are absent in the AOM-treated group, and toluene and 2-butanol were increased in AOM compared to the untreated control group (Student's *t*-test, $p<0.05$). A PCA was produced using the total 207 VOCs, which were not able to differentiate samples according to AOM treatment **(Figure 7.10).**

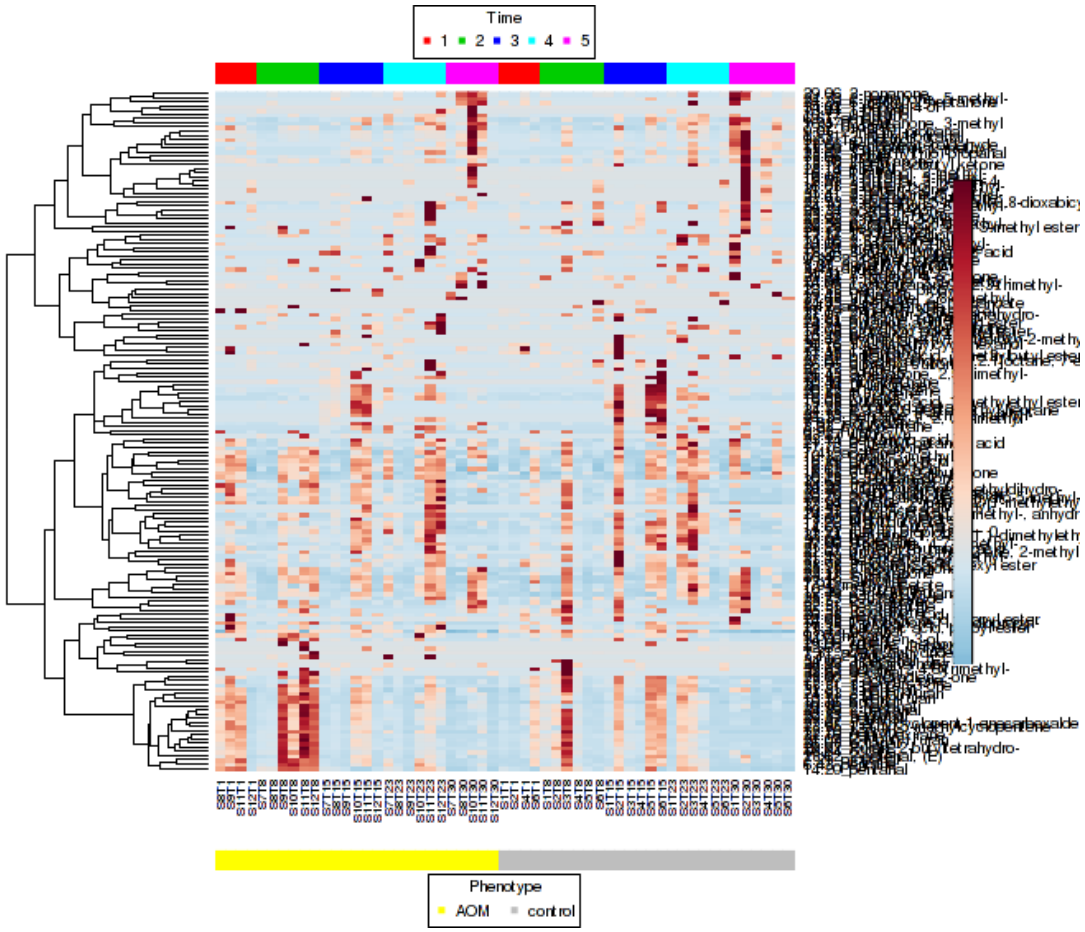

Figure 7.9 Hierarchical clustering. As with the Pilot Study, a heat map representing hierarchical clustering of the VOCs identified across the five different time points. Sample classes are indicated by the coloured bars (AOM-treated mice = yellow, untreated control = grey). Columns represent individual murine faecal samples and rows refer to distinct compounds. Shades of red represent an increase in concentration of a compound and shades of blue represent a decrease in concentration of a compound.

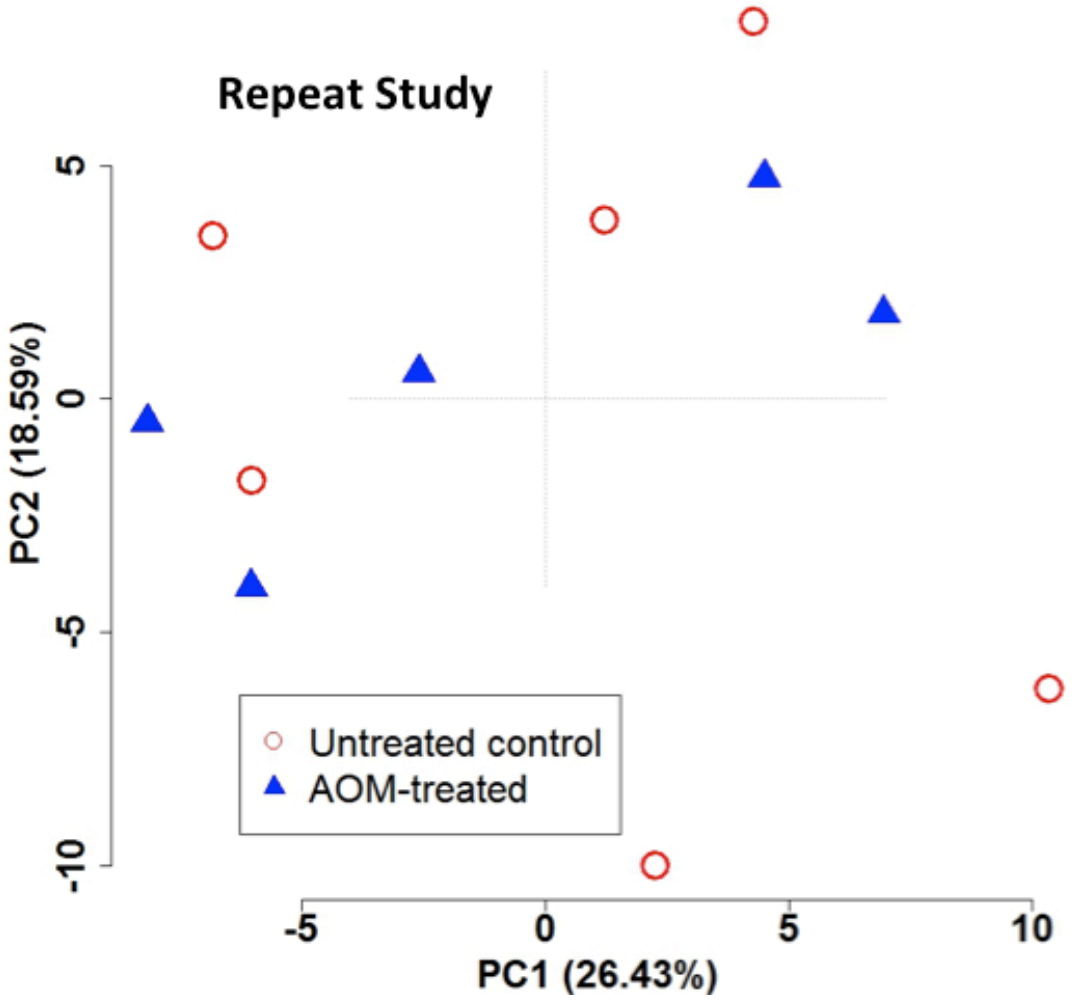

Figure 7.10 A PCA biplot for the faecal pellets of AOM-treated mice compared to untreated control mice at experimental week 30 in the Repeat Study. The first principal component has been plotted against the second principal component representing 26.43% and 18.59% of the total variation, respectively. The PCA was performed using the abundance of the 163 VOCs present at week 30.

7.6 SUMMARY OF RESULTS

1. Following AOM administration mice developed distal colonic tumours with slightly different faecal VOC profiles from week 15 to week 20.
2. Unfortunately the repeat study did not yield the anticipated results as there were no distal colonic tumours present. Therefore, a more susceptible mouse strain would ideally be used in future experiments to produce more reliable results when using AOM to induce CRC with high penetrance and low mortality.

7.7 DISCUSSION

The objective of this study was to provide strong rationale for carrying out human studies with the goal of both defining the metabolic changes that occur in tumour tissue during CRC and possibly identifying metabolites in faeces that reflect CRC. However, the study did not produce the expected results. AOM is known for being very reliable in inducing CRC with high penetrance in highly susceptible mouse strains with 3-10 tumours in 80-100% of animals with a mortality rate below 10% [144]. There are a number of factors reported to influence tumourigenesis such as genetic predisposition [325] and the colonic microflora [326], both of which play a role in the activation cascade of AOM. Consequently, the genetic heterogeneity within inbred strains and variation in the intestinal microbiota between animal facilities will influence the development of tumours after AOM administration. C57BL/6 mice have a lower susceptibility to AOM-induced CRC compared to those strains less resistant to AOM such as C3H/HeN and Balb/c [327]. It was for this reason that the dose of AOM was increased from 10 to 12.5 mg/kg. It has been recommended to perform dose-response experiments to optimise conditions for the specific mouse strain, animal facility and preparation of AOM that is used [144]. However, as each experiment lasted up to 6 months there was insufficient time to dose optimise the AOM.

Metabolomic profiling has previously been shown to identify biomarkers of AOM-induced colorectal neoplasia in mice using ultra-performance liquid chromatography tandem mass spectrometry and GC-MS [324]. Haem, changed with disease progression, increasing over time, which is consistent with enhanced GI bleeding. However, haem may also be increased in non-cancerous conditions. Wang *et al.* collected blood from 16 CRC patients and 20 healthy controls, and using SPME-GC-MS they found that phenyl methylcarbamate, ethylhexanol and 6-t-butyl-2,2,9,9-tetramethyl-3,5-decadien-7-yne were at significantly lower concentrations, and 1,1,4,4-tetramethyl-2,5-dimethylene-cyclohexane at a higher concentration in the CRC group compared to the normal group [328]. In addition, tumour growth also involves several metabolic changes leading to the production of specific VOCs that have been detected in exhaled breath. Altomare *et al.* used mathematical modelling to identify a pattern of VOCs emitted from exhaled breath to discriminate between CRC patients and healthy controls with an accuracy of 85% [329]. Furthermore, detection of CRC by urinary VOC analysis using ion mobility spectroscopy (FAIMS) has also shown potential as a novel screening tool [330].

There is increasing evidence to suggest that CRC exhibits a distinct faecal, blood, urine and breathe metabolic profile with respect to VOCs. Further investigation and optimisation of AOM to induce CRC in mice will aid the development of VOC profiling as a potential clinical application for human CRC screening, and diagnosis.

Chapter 8

Faecal Calprotectin as a Non-Specific Marker of Inflammatory Diseases

8.1 INTRODUCTION

Calprotectin is a calcium-binding protein found in neutrophils. Faecal calprotectin is a substance that is released into the intestinal lumen by an influx of neutrophils when there is any inflammation present and so can act as a marker for inflammatory conditions of the lower GI tract. Its presence may suggest a person has active IBD. As the symptoms of IBD and some non-inflammatory bowel conditions such as IBS are similar, people with IBS may undergo unnecessary invasive hospital investigations before their condition is diagnosed. Therefore, faecal calprotectin testing is recommended by NICE as an option to help clinicians distinguish between IBD and non-inflammatory bowel diseases, such as IBS.

Several technologies that measure the level of calprotectin in stool samples have been evaluated, including fully quantitative laboratory-based tests (e.g. an enzyme-linked immunosorbent assay (ELISA) platform), fully quantitative rapid tests and semi-quantitative point-of-care tests (POCTs). Due to the fact that faecal calprotectin concentration correlated with the level of bowel inflammation, results are interpreted in the context of a cut-off value, below which the test is deemed negative and above which is deemed positive, thereby supporting an IBD diagnosis. The most common cut-off recommended by test manufacturers is 50µg/g [331].

Advantages of using the faecal calprotectin test in the diagnosis and management of IBD include the fact that it is a simple, relatively cheap non-invasive test and has increased specificity by the more direct assessment of intestinal inflammation, compared to serum markers. However, there are a number of disadvantages, including the poor assessment of ileal inflammation, detection of neutrophil-related inflammation only and the inability to distinguish IBD from infections and pathologies that bleed [332].

Diagnostic tests are often carried out to exclude conditions rather than to diagnose them, leading to repeat visits and unpleasant investigations. Faecal calprotectin still has some disadvantages and can only be used as a complementary test. Here, we

used stool samples from murine models of GI disease to assess the sensitivity of faecal calprotectin concentration as a diagnostic marker for IBD.

8.2 HYPOTHESIS

The faecal calprotectin test will be positive in stool samples from murine models of IBD and CRC.

8.3 AIMS

1. Detection of calprotectin in the stool samples from murine models of DSS-induced colitis, and AOM/DSS-induced, and AOM-induced CRC.
2. Quantification of the calprotectin concentration, and test for differences between groups.

8.4 METHODS

8.4.1 Faecal samples

Faecal samples used in this study were collected during the experiments performed throughout this project: acute DSS-induced colitis (**Chapter 5**), chronic DSS-induced colitis (**Chapter 6**), AOM/DSS-induced CRC (**Chapter 6**), and AOM-induced CRC (Pilot Study) (**Chapter 7**). Each group was run in triplicate (*n*=3) and each sample was run in duplicate wells. For the acute and chronic DSS-induced colitis groups, the faecal samples were in the form of colon contents, whereas the faecal samples used for the AOM±DSS-induced CRC were faecal pellets.

8.4.2 Calprotectin mouse ELISA

Quantitative determination of calprotectin was performed using a sandwich S100A8/S100A9 (Calprotectin) ELISA technique in a 96-well plate format with a commercial kit supplied by Biohit Healthcare, UK who are the UK suppliers for the

manufacturers, Immundiagnostik, Germany. A detailed protocol for the calprotectin mouse ELISA is included in section 2.5 of **Chapter 2**. Samples were extracted 1:50 in extraction buffer and centrifuged for 5 minutes at 13000g prior to beginning the ELISA.

8.4.3 Statistical analysis

The average concentration of calprotectin in each sample (*n*=2) was calculated by finding the mean of each replicate (*n*=2) using the standard curve, subsequently the average concentration for each group (*n*=3) and differences between the average calprotectin concentrations of the different treatment groups were determined. Statistical analysis was performed in SPSS. For normally distributed data, a *t*-test was used to test for differences in the concentration of calprotectin between two groups. A one-way ANOVA was used when there were more than two groups. *P*-values less than 0.05 were considered statistically significant.

8.5 RESULTS

8.5.1 Measurement of calprotectin in acute DSS-induced colitis

Faecal calprotectin concentration during induction and resolution of acute DSS-colitis was measured to examine the level of inflammation in DSS-treated mice. DSS-induced colitis can be in the form of an acute, or chronic colitis. First, we assessed the concentrations of calprotectin in the colonic luminal content of mice treated with 4.25% DSS in an acute model of colitis (chapter 5). Mice were sacrificed via cervical dislocation at experimental days 0 (*n*=11), 5 (*n*=11), 8 (*n*=10) and 11 (*n*=8); samples from three mice in each group were used in duplicate for this experiment. As expected, the concentration of faecal calprotectin increased from 48.0±5.9 ng/ml at day 0 (prior to DSS treatment), to 62.6±25.9 ng/ml at day 5 and 84.9±34.2 ng/ml at day 8 when mice were clinically unwell (mean±SEM). The amount of inflammation appeared to decrease at day 11 due to the improvement in histological and clinical parameters, therefore the calprotectin concentration was

expected to decrease. However, the levels at day 11 (127.6±62.0 ng/ml) were higher than those at day 8, but no significant difference was found which can be explained by the variability between the individual mice ($p>0.05$, ANOVA) **(Figure 8.1).**

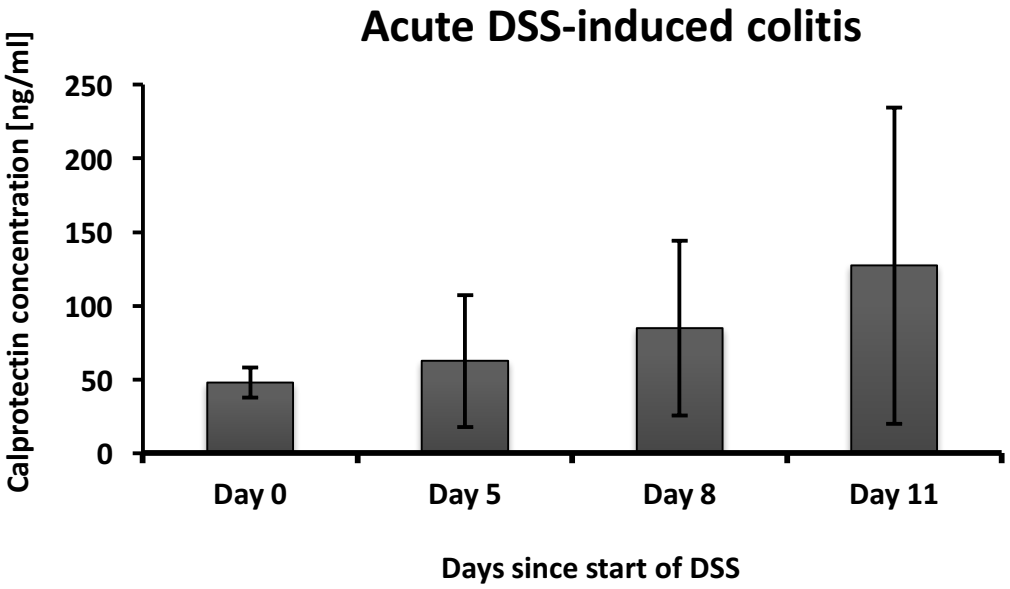

Figure 8.1 Faecal calprotectin concentration [ng/ml] in the colonic luminal contents from mice of an acute DSS-induced colitis model. Female C57BL/6 mice were administered 4.25% DSS in their drinking water for 5 days followed by 6 days of ordinary water. Mice were sacrificed on experimental days 0, 5, 8 and 11 and colonic luminal contents were collected and stored at -20°C until analysis by HS-SPME-GC-MS and then detection of calprotectin by ELISA (data expressed as mean±SD, *n*=3/group; *p*>0.05, ANOVA).

8.5.2 Measurement of faecal calprotectin concentration in chronic DSS-induced colitis

Following the assessment of acute DSS-induced colitis, the concentration of calprotectin was assessed in the colonic luminal content of mice (*n*=6) treated with four cycles of 0.75-1.25% DSS in a chronic model of colitis (**Chapter 6**). There was an untreated control group (*n*=6). All mice were sacrificed via cervical dislocation at day 45; samples from three mice in each group were used in duplicate for this experiment. The concentration of faecal calprotectin increased from 15.7±3.7 ng/ml

in the control group to 45.2±23.8 ng/ml in the DSS treated group (p=0.37, *t*-test) **(Figure 8.2).**

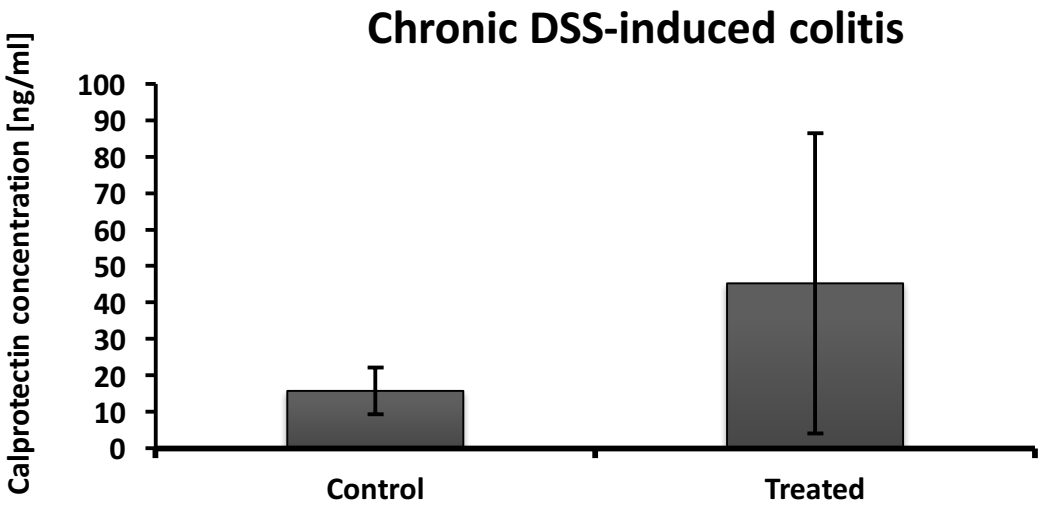

Figure 8.2 Faecal calprotectin concentration [ng/ml] in the colonic luminal contents from mice of a chronic DSS-induced colitis model. Female C57BL/6 mice were administered four cycles of DSS in their drinking water at doses from 0.75-1.25%. Each cycle included 5 days of DSS followed by 6 days of ordinary water. A control and treated group were included and all mice were sacrificed on day 45 at the end of the experiment and colonic luminal contents were collected and stored at -20°C until analysis by HS-SPME-GC-MS and then detection of calprotectin by ELISA (data expressed as mean±SD, *n*=3/group; *p*>0.05, *t*-test).

8.5.3 Measurement of faecal calprotectin concentration in inflammation-associated CRC

A murine model of inflammation-associated CRC included one injection of a carcinogen, 12.5mg/kg AOM followed by 3 cycles of 1.5% DSS (**Chapter 6**). Animals were sacrificed at day 64 and due to the presence of cancerous lesions within the mucosal surface of the distal colon, fresh faecal pellets were collected from the cages instead of colonic luminal contents; samples from three mice in each group were used in duplicate for this experiment. The concentration of faecal calprotectin increased from 18.1±1.8 ng/ml in the control group to 42.2±13.6 ng/ml in the AOM/DSS treated group (p=0.22, *t*-test) **(Figure 8.3).**

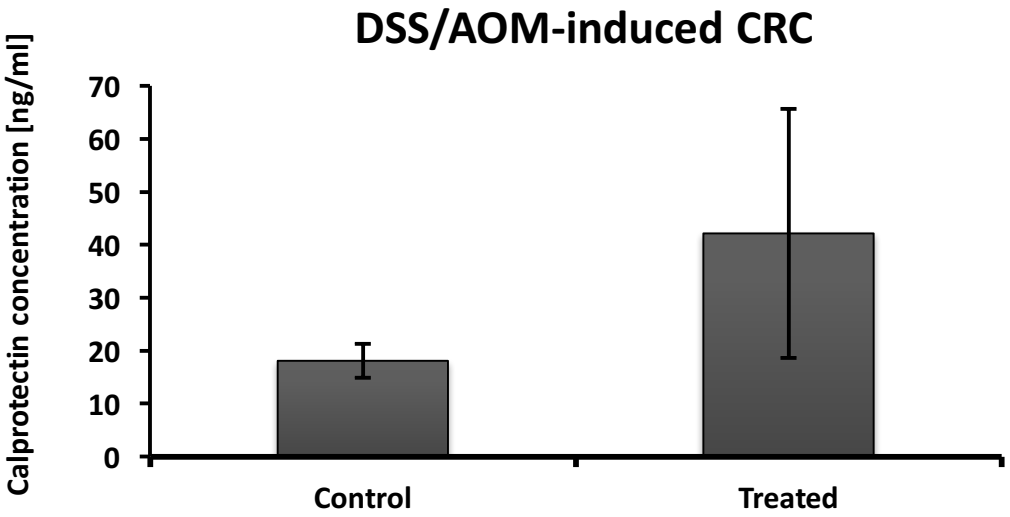

Figure 8.3 Faecal calprotectin concentration [ng/ml] in the faecal pellets from mice of an inflammation-associated CRC model. Female C57BL/6 mice received one injection (i.p.) of 12.5mg/kg AOM and were administered three cycles of 1.5% DSS in their drinking water. A control and treated group were included and all mice were sacrificed at week 10 at the end of the experiment and colonic luminal contents were collected and stored at -20°C until analysis by HS-SPME-GC-MS and then detection of calprotectin by ELISA (data expressed as mean±SD, *n*=3/group; $p>0.05$, *t*-test).

8.5.4 Measurement of faecal calprotectin concentration in sporadic CRC

A murine model of sporadic CRC included six weekly injections of a carcinogen, 12.5mg/kg AOM and lasted 6 months for the growth of colonic adenomas (**Chapter 7**). Animals were sacrificed at the end of week 20 (Pilot Study) and similar to samples from the AOM/DSS study, fresh faecal pellets were collected from the cages instead of colonic luminal contents; samples from three mice in each group were used in duplicate for this experiment. The concentration of faecal calprotectin increased from 22.6±5.1 ng/ml in the control group to 68.7±27.3 ng/ml in the AOM treated group (p=0.25, *t*-test) **(Figure 8.4).**

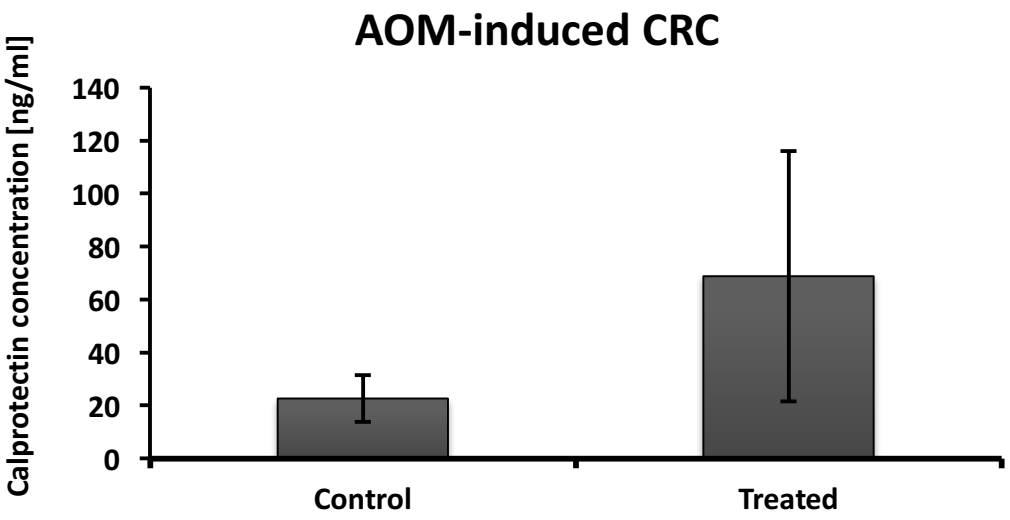

Figure 8.4 Faecal calprotectin concentration [ng/ml] in the faecal pellets from mice of a sporadic CRC model. Female C57BL/6 mice received six weekly injections (i.p.) of 12.5mg/kg AOM. A control and treated group were included and all mice were sacrificed at week 20 at the end of the experiment and colonic luminal contents were collected and stored at -20°C until analysis by HS-SPME-GC-MS and then detection of calprotectin by ELISA (data expressed as mean±SD, *n*=3/group; $p>0.05$, *t*-test).

8.6 DISCUSSION

Calprotectin constitutes 60% of neutrophil proteins and is abundant in all bodily fluids at levels dependent on the neutrophil migration toward the intestinal tract and thus, the degree of inflammation. Faecal calprotectin has a number of clinical advantages, which makes it a robust test. It is resistant to bacterial degradation in the gut and is also stable in stool samples at room temperature for up to a week, therefore tolerating any interruption or delay in the transportation of the sample to the laboratory [333].

The measurement of faecal calprotectin in both the acute, and chronic DSS-induced colitis model yielded expected results. The levels of calprotectin increased in the presence of inflammation, illustrated by the clinical and histological data and demonstrated by the step-wise increase in faecal calprotectin. However, the levels were not significantly different due to the wide error bars; future repeats should include a larger *n* number to achieve tighter error bars and a significant difference.

These results are in agreement with human studies. Measurement of calprotectin in stool samples from healthy, chronic IBD, and IBS patients showed that it was able to differentiate between chronic IBD and IBS [334]. Additionally, a second study found that faecal calprotectin was strongly associated with colorectal inflammation [335], providing strong evidence for the clinical use of the faecal calprotectin test when distinguishing between IBS and IBD. It is also useful for monitoring disease activity by reliably discriminating between inactive disease from mild, moderate and highly active diseases, demonstrated by the overall accuracy for the detection of endoscopically active disease being 89% for calprotectin [336]. Furthermore, evidence shows it might also be useful in predicting an impending clinical relapse [337].

In humans, the sensitivity and specificity of calprotectin in distinguishing between CD and IBD is 67.7% and 66.7%, respectively [338]. Although this is high, there may still be room for improvement with a novel diagnostic test. The lack of sensitivity

and specificity may be caused by the occurrence of false positive results. False positive calprotectin readings may be the result of any bleeding in the body over 100ml, e.g. menstrual bleeding. Also, the presence of non-steroidal anti-inflammatory drugs (NSAIDs) may cause an increase in calprotectin levels in patients without IBD [270]. Likewise, levels of faecal calprotectin increase in any condition that causes neutrophil migration to the gut, including neoplasms and infections, therefore the sensitivity and specificity of faecal calprotectin is limited and is not as high as desired.

Faecal calprotectin in stool samples from murine models of inflammation-associated, and sporadic CRC also produced positive results, compared to untreated control groups. Kristinsson *et al.* showed that the majority of patients with CRC have increased faecal concentrations of calprotectin [276]. They recruited 155 patients with newly diagnosed CRC and found that 87% of all patients had elevated faecal calprotectin concentrations; 79% had levels above 15mg/l and 74% had levels above 20mg/l. Furthermore, the calprotectin levels in faecal samples collected after bowel resection surgery fell significantly from a preoperative median value of 45 mg/l to 14 mg/l after the resection. Although this study suggests that the measurement of faecal calprotectin may be a marker for CRC, similar to FOBT, faecal calprotectin is non-specific for colorectal pathology.

These results provide evidence that the faecal calprotectin test may not be a specific IBD or CRC diagnostic marker in murine models and are in agreement with current studies testing the effectiveness of faecal calprotectin in human GI disease. However, the assay was only performed once and in order to validate these results further, it would need to be repeated on a larger scale. Furthermore, there appears to be a lack of evidence to support the use of this assay to specifically measure colonic inflammation in the faeces of colitis murine models. Investigation of the variability of the healthy mouse microbiota of five common lab mouse strains using *16S* rDNA pyrosequencing found the murine enterotype to show a striking resemblance to human, which was also associated with calprotectin levels [339]. Mice expressing an increase in Enterobacteriaceae, which has previously been

associated with induction of low grade inflammation, also had increased levels of caecal calprotectin; providing confirmation that low-grade inflammation can occur in healthy SPF mice. In addition, calprotectin is also reportedly increased in plaques from a diabetic murine model [340], brain hemispheres of an Alzheimer's disease model [341], and in the serum of LPS-induced septic shock mice [342]. Therefore, as with human studies, the specificity of faecal calprotectin as a marker of colonic inflammation in mice is questioned.

Chapter 9

Discussion

9.1 CONCLUDING DISCUSSION

The different 'omic' approaches, including genomics, transcriptomics and proteomics, are currently applied to identifying novel diagnostic, disease-specific biomarkers. These approaches also aim to characterise the link between the gut microbiota and host metabolism and to investigate the pathophysiology underlying diseases. Metabolomics can be defined as 'the non-biased identification and quantification of all metabolites in a biological system' [343], integrating the effects of gene regulation, post-transcriptional regulation and the resulting pathway interactions [344]. This approach, ultimately, provides us with a direct molecular readout of the cell status, reflecting the physiological phenotype. Furthermore, metabolomic profiling reflects the environmental and dietary factors of the host, which do not affect the genome.

Here, we have characterised the healthy murine faecal metabolome and assessed the effect of inducing disease of the GI tract for the first time using HS-SPME-GC-MS. As a result, our analysis of the murine faecal metabolome has enabled the isolation and detection of specific VOCs, and certain groups of VOCs, that are associated with both health and disease states. Only subtle differences were identified between individual mice therefore providing confidence in the use of this species for subsequent studies. This also demonstrated the robustness of our optimised HS-SPME-GC-MS method. Furthermore, comparison of the human faecal VOC profile with the murine profile highlighted the diversity of the human intestinal microbiota with 62 VOCs found to be unique to this group compared to 39 in the murine group. This is likely due to a more varied human diet and changes in their environment. The consequent focus on the murine VOC metabolome found significant effects of age and gender; which were expected, and led to the use of one gender (females) in future experiments to decrease variation, and to ensure that time related differences in VOC profiles of GI disease were already recognised. Differences between males and females were most notable when mice were 5, 8, 10 and 12 weeks old where the majority of VOCs were significantly higher in males compared to females, or completely absent in females. This may be explained by

hormonal differences. Female was the chosen gender for future experiments due to the slightly lower variation in abundance of VOCs over time; 27.8% of VOCs significantly varied over time for females, compared to 28.2% for males. A significant decrease in both the number of VOCs and the abundance of specific VOCs in the small intestine was found compared to the large bowel and the faecal pellet of healthy mice which could be explained by the increase in the numbers of bacteria from the stomach to the colon. This was also considered an important finding to take into account when planning future experiments; for instance, making sure to not directly compare the VOC profiles of samples obtained directly from the large bowel with faecal pellets.

IBD is often difficult for clinicians to diagnose. It can also be traumatic and unpleasant for a patient to have to undergo unnecessary invasive tests. This can also be said for the diagnosis of cancer, in particular, IBD-associated CRC. The earlier the cancer is detected, the better the chances of the patient recovering, as prognosis is better and appropriate treatment can be started sooner. Earlier diagnosis and screening would therefore result in a better prognosis for CRC patients of all types. This thesis thus far has discussed the underlying need for the development of new methods for the early detection of CRC as current non-invasive tests lack sensitivity and specificity, and a colonoscopy is required to confirm a positive result. Ideally, a novel screening tool would have 100% accuracy with fewer false positives than FOBT, thus reducing the number of unnecessary colonoscopies. The focus of this work has been a metabolomics approach, specifically, the analysis of VOCs emitted from the faeces of mice with or without GI diseases with the aim of producing results that may aid future studies of human disease.

A mouse model mimicking human UC was used and, after performing a number of DSS dose response studies, a reproducible protocol was established that resulted in weight loss, rectal bleeding and diarrhoea. A VOC profile was identified that changed significantly during the onset and recovery of acute colitis, characterised by an increase in aldehydes, specifically, propanal, butanal, and heptanal, and a

decrease in alcohols, namely 2-butanol, 2-pentanol and ethanol at days 5 and 8 compared to days 0 and 11. A similar pattern with an increase in aldehydes and a decrease in alcohols was also found in a mouse model of osmotic diarrhoea when compared to untreated controls, but different marker compounds, including 2-methyl-propanal, 2-methyl-butanal and phenol were found. Phenol was the only compound to remain significantly different between $MgSO_4$-treated mice and untreated controls after *p*-values were corrected for multiple comparisons; this is believed to originate from the microbial degradation of tyrosine in the intestinal tract [345]. This similarity indicates that a combination of increased aldehydes and decreased alcohols may be a marker of acute diarrhoea in mice. A comparison of DSS-treated mice with $MgSO_4$-treated mice showed a significantly lower average number of VOCs in the $MgSO_4$-treated group (38.2) compared to DSS-treated (50.5); possibly due to the decreased intestinal transit time and the increased amount of water present in the faeces in $MgSO_4$-treated mice. Previous results have shown alcohol compounds to be indicative of a healthy murine gut due to the significant decrease observed in diarrhoea samples obtained from both $MgSO_4$-treated and DSS-treated mice. A DSS vs $MgSO_4$ comparison found that a number of alcohols were either absent (12) from or significantly decreased (6) in the $MgSO_4$ group, and based on these significant compounds, a PCA was able to clearly distinguish between these two groups. This suggests that the metabolic pathways involved in the pathogenesis of colitis are independent from those involved in the onset of diarrhoea that was not associated with colitis, which is also supported by previous findings [346]. Decreased bacterial diversity characterises the altered gut microbiome present in IBD; the observed decrease in 'health'-associated alcohol compounds and the reported role that these compounds play in providing an ecological niche [242] therefore fits with this hypothesis. The differences in the levels of specific alcohols associated with health, colitis and osmotic diarrhoea suggests that identification of disease-associated VOC concentration ranges combined with specific marker compounds would potentially increase the likelihood of finding an IBD-specific faecal VOC marker profile.

Administration of DSS induces an acute or chronic form of colitis, depending on its dose and duration of administration, and it has been postulated that the initiation of these disease types may be caused by different mechanisms [138]. In addition to identification of individual VOC profiles for acute and chronic DSS colitis, we have shown that metabolomic faecal VOC profiling is capable of distinguishing between chemically-induced murine acute and chronic colitis. Ten VOCs were detected at significantly higher concentrations in chronic colitis compared to acute colitis, amongst them were 5 ketones (acetone, 2,3-butanedione, 2-heptanone, 2-octanone, 2-acetoxy-3-butanone). The immune system is essential to prevent infection but is also important in the process of repair and recovery from any type of injury, such as intestinal inflammation. It has a role to play in the control of the resident microbiota which is essential to metabolic health and is highly energy demanding on all immune cells [347]. It has been reported that the adaptive immune system is not required for acute colitis, but is likely to play an important role in the pathogenesis of chronic colitis, therefore indicating the involvement of different immune responses. In addition, ketones were the most common type of VOC found in healthy mice, and were found to significantly decrease in germ free samples suggesting that the origin of ketones in the gut is likely to be from the presence of bacteria. Samples from another pre-clinical chronic colitis murine model, the CD4+CD62L+ T cell transfer-mediated colitis, were kindly provided by Dr Jim Wilson, Epistem, Manchester. Similar to the DSS-induced chronic colitis, our method was able to also distinguish between VOC profiles of healthy and T cell transfer-mediated colitis (**Appendix 2**) with marker compounds including 3-methyl-2-pentanone and 2,5-dimethyl-3-hexanone being decreased in colitic mice 28 days after T-cell transfer. Methyl ketones may therefore be a marker of chronic colitis as this group of compounds were also responsible for the different VOC profile between untreated controls and the DSS-induced chronic colitis model used in this thesis, and have interestingly been reported to be produced by many species of bacteria and fungi [242].

Colorectal tumours shed cells and sometimes bleed, therefore faeces provide the ideal matrix for identifying markers of intestinal changes. However, the induction of

CRC using AOM±DSS is a time-consuming experiment and requires troubleshooting to ensure the correct doses of both AOM and DSS are used. Unfortunately, this was not achieved in the timeframe that the work in this thesis was performed. That said, the absence of distal colonic tumours from the AOM±DSS experiment was surprising due to the clinical GI symptoms noted throughout. Significant weight loss and the presence of mild diarrhoea suggested that the DSS was administered at the correct dose and that there may have been further dose studies required for the AOM in order to initiate the CRC cascade. The pilot study using 12.5mg/kg resulted in 3 out of 4 mice developing tumours, but repeating this with and without DSS, did not. Interpreting this result in terms of the method suggests that batch-to-batch variation may exist for AOM (obtained from Sigma Aldrich).

The premalignant lesions, MDF, are associated with the future development of CRC and can be visualised by staining with HID-AB, as reported by [327]. Although there were no invasive tumours, the administration of AOM/DSS did promote MDF development in this study. Therefore, we demonstrated that VOC profiling is capable of detecting metabolic differences at an earlier stage than we originally anticipated. MDF were first described in 2003, and like most colorectal tumours, also show constitutive activation of the Wnt-signalling pathway with cytoplasmic and nuclear accumulation of β-catenin [348]. They are also characterised by an *APC* mutation [349]. Specific VOCs were identified in AOM/DSS treated compared to untreated mice, which provides evidence that they may be markers for the presence of MDF, including 3-(methylthio)-propanal, 2-nonenal, 3-hexanone and 6-methyl-2-heptanone. In addition, by comparison of AOM/DSS vs DSS alone treated mice, markers of chronic inflammation were found, including ethanol, 3-methyl-2-butenal, 3-octanone, 2-butanone and 2-acetoxy-3-butanone, in agreement with previous findings when comparing chronic DSS-induced colitis to untreated controls. Investigation of the VOCs produced by cancerous cells *in vitro* would help with determining the true origin of these identified marker compounds.

Current non-invasive markers for IBD include the measurement of calprotectin in a patient's stool sample. However, the specificity for IBD has been questioned. The

levels of faecal calprotectin were therefore tested in samples from acute and chronic DSS-induced colitis, and AOM±DSS-induced CRC. As expected, faecal calprotectin concentration was increased compared to healthy control samples in all groups. Raised faecal calprotectin concentration is a direct consequence of neutrophil degranulation due to mucosal damage and can also be increased in some patients with IBS. The same can be said of the FOBT which is currently used for CRC screening. Taken together, the lack of specificity of current non-invasive IBD diagnostic tests and CRC screening tests combined with our method showing capabilities of distinguishing between health and disease based on a VOC profile, suggests that there may be a need to develop a novel non-invasive test that is cost-efficient with a high level of specificity. Furthermore, the lack of characteristic early clinical signs in most forms of cancer highlights the importance of investigating new methods for early tumour detection.

Although MS-based metabolomics is being increasingly used to characterise the complex metabolic interactions involved in disease pathogenesis, and as we have shown, also as a method of detecting odorous disease markers, there are still limitations which slow down the progress of this innovative area. For instance, the lack of well established and standardised methods and protocols between different laboratories and research groups. Therefore, I firstly set out to establish a reproducible, robust method for the untargeted detection of HS VOCs emitted from murine faecal samples. This method, along with the detection of HS VOCs from human faecal samples, has since been peer-reviewed and shared [221]. Care was taken throughout all studies performed in this thesis with regards to sample collection and storage, the quality performance of all instruments used (e.g. GC-MS), the extraction of raw data and the identification and interpretation of both individual VOCs, and disease specific VOC profiles. The analysis of data in this thesis was performed by the author but under the guidance of a bioinformatician. Similar to a lack of standardised protocol for the extraction of VOCs, there is currently no standardised method for both the univariate or multivariate analysis of these data. It is well known that altering even one step of a protocol may cause a significant

change in results, further highlighting the importance of establishing a standardised method.

Limitations such as these mean that results from different research groups are currently difficult to compare and thus, the interpretation of results between studies needs to be done with caution. That said, the increased levels of aldehydes in the presence of colitis seen in this work may be explained by the higher energy demand due to a decline in nutrient absorption through the damaged intestine; this was also demonstrated by the observed decrease in levels of TCA cycle intermediates in a study performed by Shiomi *et al* [282].

9.2 IMPLICATIONS FOR FUTURE STUDIES

VOCs are reportedly emitted from the HS of body specimens, such as blood [328], urine [186], faeces [242], and breath [329]. However, currently none of these matrices are ideal for looking for potential disease biomarkers because of the uncertainty with regards to the origin of the detected VOCs. This may be explained by the fact that the patterns of VOCs identified may depend not only on the disease state, but also on other contributing variables such as genetics, the environment, age and gender. A relatively newer matrix is the HS of cells *in vitro [350]*. Advantages of *in vitro* studies over other commonly used matrices, in particular breath or faeces, include easier control of experimental variables and perhaps, more easily interpreted results, due to less biological variation as a result of factors such as gender, age or diet. Investigations of the VOC profiles produced by tumours at the microcellular level by sample preparation of cells or tumours have been reported to be a valuable tool in advancing the aim of cancer diagnosis [313]. Future studies should therefore use complementary *in vivo* and *in vitro* studies to provide possible explanations for the presence of particular compounds found in a chromatogram. This may also enable the identification of markers of oxidative stress and metabolic pathways.

Preliminary investigations performed as part of this thesis consisted of the VOC analysis by HS-SPME-GC-MS analysis of isolated colonic epithelial cells incubated with and without DSS, and also the analysis of colonic tissue from mice treated with and without DSS. Results included chromatograms with no peaks, indicating the lack of VOCs emitted from these matrices. Optimisation of sample preparation is therefore required for further analysis into the VOC profiles by this method. These results did lead to the conclusion, however, that the VOCs identified from faecal samples are likely to originate from the presence of the intestinal microbiota. That said, this study has also investigated the faecal VOC metabolome from GF mice, resulting in the isolation of compounds specific to this profile when compared to a non-GF control group. These findings are in agreement with previous studies [252] and emphasise the importance of microbial colonisation in the metabolism of food and the production of waste matter. Due to the increasing awareness of the role of the microbiota in the pathogenesis of IBD [197], metabolomics studies using murine models of colitis in GF mice may provide further evidence for this.

As previously stated, murine models are a crucial component of gut microbiome research. Having established the healthy murine faecal metabolome of WT C57BL/6 mice and *NFκB2*$^{-/-}$ mice, studies leading on from this work should therefore include murine models using strains of a multitude of genetic backgrounds and experimental setups. Specifically, genetic variation contributes to 19% to the variance in the murine gut microbiota composition [339]. Future identification of the faecal metabolome of genetically engineered murine colitis models including the *IL-10*$^{-/-}$ spontaneous colitis model with or without the addition of *Helicobacter hepaticus* (previously shown to develop severe colitis when *IL-10-/-* mice are reconstituted with *H. hepaticus* [351]), would deepen our understanding of the complex pathogenesis of colitis. Calprotectin is raised in the blood and faeces as a marker of inflammation [352], therefore a comparison between the serum and faecal metabolome of all future animals and humans is recommended to determine which correlates highly with intestinal inflammation.

Immediate future work should first of all include repeat AOM±DSS studies in order to induce invasive tumours arising from both the sporadic AOM-induced adenoma-carcinoma cascade, and the AOM/DSS-induced inflammation-dysplasia-carcinoma sequence. In addition, we would ideally compare the anticipated early VOC changes detected from these CRC murine models to a spontaneous intestinal adenoma mouse model (e.g. *Apc(Min/+)*) to look for common VOC changes in both models.

The quality of an animal model should be determined by how well it reproduces a human disease on a molecular basis rather than simply phenotype; genomics and metabolomics are just two of the emerging fields capable of achieving this. A recent review by Takao *et al.* evaluated gene expression datasets from both humans and mice and found significant correlations between mouse models and humans with conditions including burn, trauma, and sepsis [353]. Analysis also revealed a number of commonly regulated pathways by these conditions in both humans and mice. The linkage of human and animal models of IBD remains unclear. Studying disease in patients is much more complex than studying model systems, therefore prior to the performance of any future studies involving murine models, it would be ideal to increase our understanding of how well such murine models mimic human inflammatory diseases in patients. For instance, the investigation of the faecal metabolome of a number of different murine models in combination, rather than the use of a single mechanistic model may be provide a better reflection of human disease.

References

1. HELLIER, M.D. &WILLIAMS, J.G. 2007. The burden of gastrointestinal disease: implications for the provision of care in the UK. *Gut,* 56**,** 165-6.
2. WILLIAMS, J.G., ROBERTS, S.E., ALI, M.F., CHEUNG, W.Y., COHEN, D.R., DEMERY, G., EDWARDS, A., GREER, M., HELLIER, M.D., HUTCHINGS, H.A., IP, B., LONGO, M.F., RUSSELL, I.T., SNOOKS, H.A. &WILLIAMS, J.C. 2007. Gastroenterology services in the UK. The burden of disease, and the organisation and delivery of services for gastrointestinal and liver disorders: a review of the evidence. *Gut,* 56**,** 1-113.
3. LIEVIN-LE MOAL, V. &SERVIN, A.L. 2006. The front line of enteric host defense against unwelcome intrusion of harmful microorganisms: mucins, antimicrobial peptides, and microbiota. *Clinical Microbiology Reviews,* 19**,** 315-37.
4. HANAUER, S.B. 2006. Inflammatory bowel disease: Epidemiology, pathogenesis, and therapeutic opportunities. *Inflammatory Bowel Diseases,* 12**,** S3-S9.
5. KNIGHTS, D., LASSEN, K.G. &XAVIER, R.J. 2013. Advances in inflammatory bowel disease pathogenesis: linking host genetics and the microbiome. *Gut,* 62**,** 1505-10.
6. ISKANDAR, H.N. &CIORBA, M.A. 2012. Biomarkers in inflammatory bowel disease: current practices and recent advances. *Transl Res,* 159**,** 313-25.
7. BERNSTEIN, C.N., BLANCHARD, J.F., RAWSTHORNE, P. &WAJDA, A. 1999. Epidemiology of Crohn's disease and ulcerative colitis in a central Canadian province: a population-based study. *American Journal of Epidemiology,* 149**,** 916-24.
8. ANANTHAKRISHNAN, A.N. 2015. Epidemiology and risk factors for IBD. *Nat Rev Gastroenterol Hepatol,* 12**,** 205-217.
9. MOLODECKY, N.A., SOON, I.S., RABI, D.M., GHALI, W.A., FERRIS, M., CHERNOFF, G., BENCHIMOL, E.I., PANACCIONE, R., GHOSH, S., BARKEMA, H.W. &KAPLAN, G.G. 2012. Increasing incidence and prevalence of the inflammatory bowel diseases with time, based on systematic review. *Gastroenterology,* 142**,** 46-54 e42; quiz e30.
10. EWALD, P.W. &SWAIN EWALD, H.A. 2013. An evolutionary perspective on the causes and treatment of inflammatory bowel disease. *Curr Opin Gastroenterol,* 29**,** 350-6.
11. GROUP, T.I.S. 2009. *Quality Care: Service Standards for the healthcare of people who have Inflammatory Bowel Disease (IBD)* [Online]. Available: http://www.bsg.org.uk/attachments/160_IBDstandards.pdf.

12. NICE. 2015. *Inflammtory bowel disease* [Online]. Available: https://www.nice.org.uk/guidance/qs81/resources/guidance-inflammatory-bowel-disease-pdf.

13. M'KOMA, A.E. 2013. Inflammatory bowel disease: an expanding global health problem. *Clin Med Insights Gastroenterol,* 6**,** 33-47.

14. BURISCH, J., JESS, T., MARTINATO, M., LAKATOS, P.L. &EPICOM, E. 2013. The burden of inflammatory bowel disease in Europe. *J Crohns Colitis,* 7**,** 322-37.

15. BERNSTEIN, C.N. &SHANAHAN, F. 2008. Disorders of a modern lifestyle: reconciling the epidemiology of inflammatory bowel diseases. *Gut,* 57**,** 1185-91.

16. SALIM, S.A.Y. &SÖDERHOLM, J.D. 2011. Importance of disrupted intestinal barrier in inflammatory bowel diseases. *Inflammatory Bowel Diseases,* 17**,** 362-381.

17. JOSTINS, L., RIPKE, S., WEERSMA, R.K., DUERR, R.H., MCGOVERN, D.P., HUI, K.Y., LEE, J.C., PHILIP SCHUMM, L., SHARMA, Y., ANDERSON, C.A., ESSERS, J., MITROVIC, M., NING, K., CLEYNEN, I., THEATRE, E., SPAIN, S.L., RAYCHAUDHURI, S., GOYETTE, P., WEI, Z., ABRAHAM, C., ACHKAR, J.-P., AHMAD, T., AMININEJAD, L., ANANTHAKRISHNAN, A.N., ANDERSEN, V., ANDREWS, J.M., BAIDOO, L., BALSCHUN, T., BAMPTON, P.A., BITTON, A., BOUCHER, G., BRAND, S., BUNING, C., COHAIN, A., CICHON, S., D/'AMATO, M., DE JONG, D., DEVANEY, K.L., DUBINSKY, M., EDWARDS, C., ELLINGHAUS, D., FERGUSON, L.R., FRANCHIMONT, D., FRANSEN, K., GEARRY, R., GEORGES, M., GIEGER, C., GLAS, J., HARITUNIANS, T., HART, A., HAWKEY, C., HEDL, M., HU, X., KARLSEN, T.H., KUPCINSKAS, L., KUGATHASAN, S., LATIANO, A., LAUKENS, D., LAWRANCE, I.C., LEES, C.W., LOUIS, E., MAHY, G., MANSFIELD, J., MORGAN, A.R., MOWAT, C., NEWMAN, W., PALMIERI, O., PONSIOEN, C.Y., POTOCNIK, U., PRESCOTT, N.J., REGUEIRO, M., ROTTER, J.I., RUSSELL, R.K., SANDERSON, J.D., SANS, M., SATSANGI, J., SCHREIBER, S., SIMMS, L.A., SVENTORAITYTE, J., TARGAN, S.R., TAYLOR, K.D., TREMELLING, M., VERSPAGET, H.W., DE VOS, M., WIJMENGA, C., WILSON, D.C., WINKELMANN, J., XAVIER, R.J., ZEISSIG, S., ZHANG, B., ZHANG, C.K., ZHAO, H., SILVERBERG, M.S., ANNESE, V., HAKONARSON, H., BRANT, S.R., RADFORD-SMITH, G., MATHEW, C.G., RIOUX, J.D., SCHADT, E.E., et al. 2012. Host-microbe interactions have shaped the genetic architecture of inflammatory bowel disease. *Nature,* 491**,** 119-124.

18. MCGOVERN, D.P.B., GARDET, A., TORKVIST, L., GOYETTE, P., ESSERS, J., TAYLOR, K.D., NEALE, B.M., ONG, R.T.H., LAGACE, C., LI, C., GREEN, T., STEVENS, C.R., BEAUCHAMP, C., FLESHNER, P.R., CARLSON, M., D'AMATO, M., HALFVARSON, J.,

HIBBERD, M.L., LORDAL, M., PADYUKOV, L., ANDRIULLI, A., COLOMBO, E., LATIANO, A., PALMIERI, O., BERNARD, E.J., DESLANDRES, C., HOMMES, D.W., DE JONG, D.J., STOKKERS, P.C., WEERSMA, R.K., SHARMA, Y., SILVERBERG, M.S., CHO, J.H., WU, J., ROEDER, K., BRANT, S.R., SCHUMM, L.P., DUERR, R.H., DUBINSKY, M.C., GLAZER, N.L., HARITUNIANS, T., IPPOLITI, A., MELMED, G.Y., SISCOVICK, D.S., VASILIAUSKAS, E.A., TARGAN, S.R., ANNESE, V., WIJMENGA, C., PETTERSSON, S., ROTTER, J.I., XAVIER, R.J., DALY, M.J., RIOUX, J.D., SEIELSTAD, M. &CONSORTIUM, N.I.G. 2011. Genome-wide association identifies multiple ulcerative colitis susceptibility loci (vol 42, pg 332, 2010). *Nature Genetics,* 43**,** 388-388.

19. ATREYA, I., ATREYA, R. &NEURATH, M.F. 2008. NF-kappaB in inflammatory bowel disease. *Journal of Internal Medicine,* 263**,** 591-6.
20. ANDERSSON, R.E., OLAISON, G., TYSK, C. &EKBOM, A. 2001. Appendectomy and protection against ulcerative colitis. *N Engl J Med,* 344**,** 808-14.
21. MAHMUD, N. &WEIR, D.G. 2001. The urban diet and Crohn's disease: is there a relationship? *European Journal of Gastroenterology & Hepatology,* 13**,** 93-95.
22. HAQ, O., ALI, T., MORTON, J., MADHOUN, M.F. &KANE, S.V. 2012. Awareness Among Practitioners Regarding Efficacy of Oral Contraceptives With Concomitant use of Antibiotics in Inflammatory Bowel Disease (IBD) Patients. *Gastroenterology,* 142**,** S250-S250.
23. HIGUCHI, L.M., KHALILI, H., CHAN, A.T., RICHTER, J.M., BOUSVAROS, A. &FUCHS, C.S. 2012. A prospective study of cigarette smoking and the risk of inflammatory bowel disease in women. *Am J Gastroenterol,* 107**,** 1399-406.
24. SARTOR, R.B. &MAZMANIAN, S.K. 2012. Intestinal Microbes in Inflammatory Bowel Diseases. *Am J Gastroenterol Suppl,* 1**,** 15-21.
25. ECKBURG, P.B., BIK, E.M., BERNSTEIN, C.N., PURDOM, E., DETHLEFSEN, L., SARGENT, M., GILL, S.R., NELSON, K.E. &RELMAN, D.A. 2005. Diversity of the human intestinal microbial flora. *Science,* 308**,** 1635-8.
26. ELSON, C.O., CONG, Y., MCCRACKEN, V.J., DIMMITT, R.A., LORENZ, R.G. &WEAVER, C.T. 2005. Experimental models of inflammatory bowel disease reveal innate, adaptive, and regulatory mechanisms of host dialogue with the microbiota. *Immunological Reviews,* 206**,** 260-76.
27. KOSTIC, A.D., XAVIER, R.J. &GEVERS, D. 2014. The microbiome in inflammatory bowel disease: current status and the future ahead. *Gastroenterology,* 146**,** 1489-99.

28. EBERL, G. 2010. A new vision of immunity: homeostasis of the superorganism. *Mucosal Immunology,* 3**,** 450-60.

29. NATIVIDAD, J.M., PINTO-SANCHEZ, M.I., GALIPEAU, H.J., JURY, J., JORDANA, M., REINISCH, W., COLLINS, S.M., BERCIK, P., SURETTE, M.G., ALLEN-VERCOE, E. &VERDU, E.F. 2015. Ecobiology rich in firmicutes decreases susceptibility to colitis in a humanized gnotobiotic mouse model. *Inflamm Bowel Dis,* 0**,** 1-11.

30. FRANK, D.N., ST AMAND, A.L., FELDMAN, R.A., BOEDEKER, E.C., HARPAZ, N. &PACE, N.R. 2007. Molecular-phylogenetic characterization of microbial community imbalances in human inflammatory bowel diseases. *Proc Natl Acad Sci U S A,* 104**,** 13780-5.

31. ANDOH, A., SAKATA, S., KOIZUMI, Y., MITSUYAMA, K., FUJIYOMA, Y. &BENNO, Y. 2007. Terminal restriction fragment length polymorphism analysis of the diversity of fecal microbiota in patients with ulcerative colitis. *Inflammatory Bowel Diseases,* 13**,** 955-962.

32. MARTINEZ-MEDINA, M., DENIZOT, J., DREUX, N., ROBIN, F., BILLARD, E., BONNET, R., DARFEUILLE-MICHAUD, A. &BARNICH, N. 2014. Western diet induces dysbiosis with increased E coli in CEABAC10 mice, alters host barrier function favouring AIEC colonisation. *Gut,* 63**,** 116-124.

33. DARFEUILLE-MICHAUD, A., NEUT, C., BARNICH, N., LEDERMAN, E., DI MARTINO, P., DESREUMAUX, P., GAMBIEZ, L., JOLY, B., CORTOT, A. &COLOMBEL, J.F. 1998. Presence of adherent Escherichia coli strains in ileal mucosa of patients with Crohn's disease. *Gastroenterology,* 115**,** 1405-13.

34. KNOSEL, T., SCHEWE, C., PETERSEN, N., DIETEL, M. &PETERSEN, I. 2009. Prevalence of infectious pathogens in Crohn's disease. *Pathology Research and Practice,* 205**,** 223-30.

35. KIM, H., RHEE, S.H., POTHOULAKIS, C. &LAMONT, J.T. 2007. Inflammation and apoptosis in Clostridium difficile enteritis is mediated by PGE(2) up-regulation of Fas ligand. *Gastroenterology,* 133**,** 875-886.

36. ROBIZADEH, S., RHEE, K.J., WU, S.G., HUSO, D., GAN, C.M., GOLUB, J.E., WU, X.Q., ZHANG, M. &SEARS, C.L. 2007. Enterotoxigenic bacteroides fragilis: A potential instigator of colitis. *Inflammatory Bowel Diseases,* 13**,** 1475-1483.

37. SHEEHAN, D., MORAN, C. &SHANAHAN, F. 2015. The microbiota in inflammatory bowel disease. *Journal of Gastroenterology,* 50**,** 495-507.

38. MOYES, D.L. &NAGLIK, J.R. 2012. The Mycobiome: Influencing IBD Severity. *Cell Host & Microbe,* 11**,** 551-552.

39. BRANDT, L.J. 2012. Fecal transplantation for the treatment of Clostridium difficile infection. *Gastroenterol Hepatol (N Y),* 8**,** 191-4.

40. COLMAN, R.J. &RUBIN, D.T. 2014. Fecal microbiota transplantation as therapy for inflammatory bowel disease: A systematic review and meta-analysis. *Journal of Crohns & Colitis,* 8**,** 1569-1581.

41. YANG, H., MCELREE, C., ROTH, M.P., SHANAHAN, F., TARGAN, S.R. &ROTTER, J.I. 1993. Familial Empirical Risks for Inflammatory Bowel-Disease - Differences between Jews and Non-Jews. *Gut,* 34**,** 517-524.

42. HALME, L., PAAVOLA-SAKKI, P., TURUNEN, U., LAPPALAINEN, M., FARKKILA, M. &KONTULA, K. 2006. Family and twin studies in inflammatory bowel disease. *World Journal of Gastroenterology,* 12**,** 3668-3672.

43. HUGOT, J.P., CHAMAILLARD, M., ZOUALI, H., LESAGE, S., CEZARD, J.P., BELAICHE, J., ALMER, S., TYSK, C., O'MORAIN, C.A., GASSULL, M., BINDER, V., FINKEL, Y., CORTOT, A., MODIGLIANI, R., LAURENT-PUIG, P., GOWER-ROUSSEAU, C., MACRY, J., COLOMBEL, J.F., SAHBATOU, M. &THOMAS, G. 2001. Association of NOD2 leucine-rich repeat variants with susceptibility to Crohn's disease. *Nature,* 411**,** 599-603.

44. OGURA, Y., BONEN, D.K., INOHARA, N., NICOLAE, D.L., CHEN, F.F., RAMOS, R., BRITTON, H., MORAN, T., KARALIUSKAS, R., DUERR, R.H., ACHKAR, J.P., BRANT, S.R., BAYLESS, T.M., KIRSCHNER, B.S., HANAUER, S.B., NUNEZ, G. &CHO, J.H. 2001. A frameshift mutation in NOD2 associated with susceptibility to Crohn's disease. *Nature,* 411**,** 603-6.

45. FRANKISH, H. 2001. Crohn's gene identified. *Lancet,* 357**,** 1678.

46. KHOR, B., GARDET, A. &XAVIER, R.J. 2011. Genetics and pathogenesis of inflammatory bowel disease. *Nature,* 474**,** 307-17.

47. DIXON, L.J., KABI, A., NICKERSON, K.P. &MCDONALD, C. 2015. Combinatorial effects of diet and genetics on inflammatory bowel disease pathogenesis. *Inflammatory Bowel Diseases,* 21**,** 912-22.

48. VAN LIMBERGEN, J., RADFORD-SMITH, G. &SATSANGI, J. 2014. Advances in IBD genetics. *Nat Rev Gastroenterol Hepatol,* 11**,** 372-85.

49. KOLOSKI, N.A., BRET, L. &RADFORD-SMITH, G. 2008. Hygiene hypothesis in inflammatory bowel disease: A critical review of the literature. *World Journal of Gastroenterology,* 14**,** 165-173.

50. SIEBENLIST, U., FRANZOSO, G. &BROWN, K. 1994. Structure, regulation and function of NF-kappa B. *Annu Rev Cell Biol,* 10**,** 405-55.

51. LAWRENCE, T. 2009. The nuclear factor NF-kappaB pathway in inflammation. *Cold Spring Harb Perspect Biol,* 1**,** a001651.

52. SCHREIBER, S., NIKOLAUS, S. &HAMPE, J. 1998. Activation of nuclear factor kappa B inflammatory bowel disease. *Gut,* 42**,** 477-84.

53. STEINBRECHER, K.A., HARMEL-LAWS, E., SITCHERAN, R. &BALDWIN, A.S. 2008. Loss of epithelial RelA results in deregulated intestinal proliferative/apoptotic homeostasis and susceptibility to inflammation. *J Immunol,* 180**,** 2588-99.

54. BURKITT, M.D., HANEDI, A.F., DUCKWORTH, C.A., WILLIAMS, J.M., TANG, J.M., O'REILLY, L.A., PUTOCZKI, T.L., GERONDAKIS, S., DIMALINE, R., CAAMANO, J.H. &PRITCHARD, D.M. 2015. NF-κB1, NF-κB2 and c-Rel differentially regulate susceptibility to colitis-associated adenoma development in C57BL/6 mice. *The Journal of Pathology***,** n/a-n/a.

55. KAMADA, N., SEO, S.U., CHEN, G.Y. &NUNEZ, G. 2013. Role of the gut microbiota in immunity and inflammatory disease. *Nature Reviews Immunology,* 13**,** 321-335.

56. KIM, E.R. &CHANG, D.K. 2014. Colorectal cancer in inflammatory bowel disease: the risk, pathogenesis, prevention and diagnosis. *World J Gastroenterol,* 20**,** 9872-81.

57. KULAYLAT, M.N. &DAYTON, M.T. 2010. Ulcerative colitis and cancer. *Journal of Surgical Oncology,* 101**,** 706-12.

58. EADEN, J.A., ABRAMS, K.R. &MAYBERRY, J.F. 2001. The risk of colorectal cancer in ulcerative colitis: a meta-analysis. *Gut,* 48**,** 526-35.

59. CHOI, C.H.R., RUTTER, M.D., ASKARI, A., LEE, G.H., WARUSAVITARNE, J., MOORGHEN, M., THOMAS-GIBSON, S., SAUNDERS, B.P., GRAHAM, T.A. &HART, A.L. 2015. Forty-Year Analysis of Colonoscopic Surveillance Program for Neoplasia in Ulcerative Colitis: An Updated Overview. *American Journal of Gastroenterology,* 110**,** 1022-1034.

60. TRIANTAFILLIDIS, J.K., NASIOULAS, G. &KOSMIDIS, P.A. 2009. Colorectal cancer and inflammatory bowel disease: epidemiology, risk factors, mechanisms of carcinogenesis and prevention strategies. *Anticancer Res,* 29**,** 2727-37.

61. UK, C.S.A.C. 2013. *Tests and Investigations for IBD* [Online]. Available: http://www.crohnsandcolitis.org.uk/Resources/CrohnsAndColitisUK/Documents/Publications/Info-Sheets/tests-and-investigations-for-ibd.pdf [Accessed 11/05 2015].

62. NAPPO, A., IACOVIELLO, L., FRATERMAN, A., GONZALEZ-GIL, E.M., HADJIGEORGIOU, C., MARILD, S., MOLNAR, D., MORENO, L.A., PEPLIES, J., SIOEN, I., VEIDEBAUM, T., SIANI, A. &RUSSO, P. 2013. High-sensitivity C-reactive Protein is a Predictive Factor of Adiposity in Children: Results of the Identification and prevention of Dietary- and lifestyle-induced health Effects in Children and InfantS (IDEFICS) Study. *Journal of the American Heart Association,* 2.

63. WAUGH, N., CUMMINS, E., ROYLE, P., KANDALA, N.B., SHYANGDAN, D., ARASARADNAM, R., CLAR, C. &JOHNSTON, R. 2013. Faecal calprotectin testing for differentiating amongst inflammatory and non-inflammatory bowel diseases: systematic review and economic evaluation. *Health Technology Assessment,* 17**,** 1-+.

64. PROBERT, C.S.J. 2011. Role of faecal gas analysis for the diagnosis of IBD. *Biochemical Society Transactions,* 39**,** 1079-1080.

65. PROBERT, C.S., READE, S. &AHMED, I. 2014. Fecal volatile organic compounds: a novel, cheaper method of diagnosing inflammatory bowel disease? *Expert Rev Clin Immunol,* 10**,** 1129-31.

66. HAGGAR, F.A. &BOUSHEY, R.P. 2009. Colorectal cancer epidemiology: incidence, mortality, survival, and risk factors. *Clin Colon Rectal Surg,* 22**,** 191-7.

67. UK, C.R. Available: http://www.cancerresearchuk.org/cancer-info/cancerstats/types/bowel/incidence/uk-bowel-cancer-incidence-statistics#source1 [Accessed May 2015].

68. ARVELO, F., SOJO, F. &COTTE, C. 2015. Biology of colorectal cancer. *Ecancermedicalscience,* 9**,** 520.

69. BAILEY, C.E., HU, C.Y., YOU, N., BEDNARSKI, B.K., RODRIGUEZ-BIGAS, M.A., SKIBBER, J.M., CANTOR, S.B. &CHANG, G.J. 2015. Increasing Disparities in the Age-Related Incidences of Colon and Rectal Cancers in the United States, 1975-2010. *JAMA Surg,* 150**,** 17-22.

70. DE JONG, A.E., MORREAU, H., NAGENGAST, F.M., MATHUS-VLIEGEN, E.M.H., KLEIBEUKER, J.H., GRIFFIOEN, G., CATS, A. &VASEN, H.F.A. 2005. Prevalence of adenomas among young individuals at average risk for colorectal cancer. *American Journal of Gastroenterology,* 100**,** 139-143.

71. MECKLIN, J.P. &DELEON, M.P. 1994. Epidemiology of Hnpcc. *Anticancer Res,* 14**,** 1625-1629.

72. JENKINS, M.A., DOWTY, J.G., OUAKRIM, D.A., MATHEWS, J.D., HOPPER, J.L., DROUET, Y., LASSET, C., BONADONA, V. &WIN, A.K. 2015. Short-Term Risk of Colorectal Cancer in Individuals With Lynch Syndrome: A Meta-Analysis. *Journal of Clinical Oncology,* 33**,** 326-U193.

73. VAN NIEUWENHUYSEN, T., NAERT, T., TRAN, H.T., VAN IMSCHOOT, G., GEURS, S., SANDERS, E., CREYTENS, D., VAN ROY, F. &VLEMINCKX, K. 2015. TALEN-mediated apc mutation in Xenopus tropicalis phenocopies familial adenomatous polyposis. *Oncoscience,* 2**,** 555-66.

74. BARROW, P., KHAN, M., LALLOO, F., EVANS, D.G. &HILL, J. 2013. Systematic review of the impact of registration and screening on colorectal cancer incidence and mortality in familial adenomatous polyposis and Lynch syndrome. *Br J Surg,* 100**,** 1719-31.

75. 2014. *Colorectal (Colon) Cancer* [Online]. Available: http://www.cdc.gov/cancer/colorectal/basic_info/risk_factors.htm [Accessed July 2015].

76. BOTTERI, E., IODICE, S., RAIMONDI, S., MAISONNEUVE, P. &LOWENFELS, A.B. 2008. Cigarette smoking and adenomatous polyps: A meta-analysis. *Gastroenterology,* 134**,** 388-395.

77. TANAKA, T. 2009. Colorectal carcinogenesis: Review of human and experimental animal studies. *J Carcinog,* 8**,** 5.

78. CROHN, B., AND ROSENBURG, H. 1925. The sigmoidoscopic picture of chronic ulcerative colitis (non-specifc). . *Am. J. Med. Sci,* 170**,** 220-228.

79. WARREN, S. &SOMMERS, S.C. 1948. Cicatrizing enteritis as a pathologic entity; analysis of 120 cases. *American Journal of Pathology,* 24**,** 475-501.

80. AMERSI, F., AGUSTIN, M. &KO, C.Y. 2005. Colorectal cancer: epidemiology, risk factors, and health services. *Clin Colon Rectal Surg,* 18**,** 133-40.

81. HANAHAN, D. &WEINBERG, R.A. 2011. Hallmarks of Cancer: The Next Generation. *Cell,* 144**,** 646-674.

82. RUTTER, M.D., SAUNDERS, B.P., WILKINSON, K.H., RUMBLES, S., SCHOFIELD, G., KAMM, M.A., WILLIAMS, C.B., PRICE, A.B., TALBOT, I.C. &FORBES, A. 2004. Cancer surveillance in longstanding ulcerative colitis: endoscopic appearances help predict cancer risk. *Gut,* 53**,** 1813-6.

83. AZER, S.A. 2013. Overview of molecular pathways in inflammatory bowel disease associated with colorectal cancer development. *Eur J Gastroenterol Hepatol,* 25**,** 271-81.

84. ITZKOWITZ, S.H. &YIO, X. 2004. Inflammation and cancer IV. Colorectal cancer in inflammatory bowel disease: the role of inflammation. *Am J Physiol Gastrointest Liver Physiol,* 287**,** G7-17.

85. CLEVERS, H. 2006. Colon cancer - Understanding how NSAIDs work. *New England Journal of Medicine,* 354**,** 761-763.

86. FUKATA, M., CHEN, A., VAMADEVAN, A.S., COHEN, J., BREGLIO, K., KRISHNAREDDY, S., HSU, D., XU, R., HARPAZ, N., DANNENBERG, A.J., SUBBARAMAIAH, K., COOPER, H.S., ITZKOWITZ, S.H. &ABREU, M.T. 2007. Toll-like receptor-4 promotes the development of colitis-associated colorectal tumors. *Gastroenterology,* 133**,** 1869-1881.

87. BIRD, R.P. 1987. Observation and quantification of aberrant crypts in the murine colon treated with a colon carcinogen: preliminary findings. *Cancer Letters,* 37**,** 147-51.

88. TAKAYAMA, T., KATSUKI, S., TAKAHASHI, Y., OHI, M., NOJIRI, S., SAKAMAKI, S., KATO, J., KOGAWA, K., MIYAKE, H. &NIITSU, Y. 1998. Aberrant crypt foci of the colon as precursors of adenoma and cancer. *N Engl J Med,* 339**,** 1277-84.

89. RONCUCCI, L., STAMP, D., MEDLINE, A., CULLEN, J.B. &BRUCE, W.R. 1991. Identification and quantification of aberrant crypt foci and microadenomas in the human colon. *Hum Pathol,* 22**,** 287-94.

90. MORI, H., HATA, K., YAMADA, Y., KUNO, T. &HARA, A. 2005. Significance and role of early-lesions in experimental colorectal carcinogenesis. *Chem Biol Interact,* 155**,** 1-9.

91. FURUKAWA, F., NISHIKAWA, A., KITAHORI, Y., TANAKAMARU, Z. &HIROSE, M. 2002. Spontaneous development of aberrant crypt foci in F344 rats. *J Exp Clin Cancer Res,* 21**,** 197-201.

92. MAGNUSON, B.A. &BIRD, R.P. 1993. Reduction of aberrant crypt foci induced in rat colon with azoxymethane or methylnitrosourea by feeding cholic acid. *Cancer Letters,* 68**,** 15-23.

93. FEMIA, A.P., DOLARA, P. &CADERNI, G. 2004. Mucin-depleted foci (MDF) in the colon of rats treated with azoxymethane (AOM) are useful biomarkers for colon carcinogenesis. *Carcinogenesis,* 25**,** 277-81.

94. FEMIA, A.P., GIANNINI, A., FAZI, M., TARQUINI, E., SALVADORI, M., RONCUCCI, L., TONELLI, F., DOLARA, P. &CADERNI, G. 2008. Identification of mucin depleted foci in the human colon. *Cancer Prev Res (Phila),* 1**,** 562-7.

95. DE ROBERTIS, M., MASSI, E., POETA, M.L., CAROTTI, S., MORINI, S., CECCHETELLI, L., SIGNORI, E. &FAZIO, V.M. 2011. The AOM/DSS murine model for the study of colon carcinogenesis: From pathways to diagnosis and therapy studies. *J Carcinog,* 10**,** 9.

96. GUINA, T., BIASI, F., CALFAPIETRA, S., NANO, M. &POLI, G. 2015. Inflammatory and redox reactions in colorectal carcinogenesis. *Cellular and Environmental Stressors in Biology and Medicine,* 1340**,** 95-103.

97. JUHASZ, A., GE, Y., MARKEL, S., CHIU, A., MATSUMOTO, L., VAN BALGOOY, J., ROY, K. &DOROSHOW, J.H. 2009. Expression of NADPH oxidase homologues and accessory genes in human cancer cell lines, tumours and adjacent normal tissues. *Free Radic Res,* 43**,** 523-32.

98. KEKU, T.O., DULAL, S., DEVEAUX, A., JOVOV, B. &HAN, X. 2015. The gastrointestinal microbiota and colorectal cancer. *Am J Physiol Gastrointest Liver Physiol,* 308**,** G351-63.

99. LOH, Y.H., JAKSZYN, P., LUBEN, R.N., MULLIGAN, A.A., MITROU, P.N. &KHAW, K.T. 2011. N-nitroso compounds and cancer incidence: the European Prospective Investigation into Cancer and Nutrition (EPIC)-Norfolk Study. *American Journal of Clinical Nutrition,* 93**,** 1053-1061.

100. ABNET, C.C. 2007. Carcinogenic food contaminants. *Cancer Investigation,* 25**,** 189-196.

101. BASTIDE, N.M., PIERRE, F.H.F. &CORPET, D.E. 2011. Heme Iron from Meat and Risk of Colorectal Cancer: A Meta-analysis and a Review of the Mechanisms Involved. *Cancer Prevention Research,* 4**,** 177-184.

102. BISHEHSARI, F., MAHDAVINIA, M., VACCA, M., MALEKZADEH, R. &MARIANI-COSTANTINI, R. 2014. Epidemiological transition of colorectal cancer in developing countries: Environmental factors, molecular pathways, and opportunities for prevention. *World Journal of Gastroenterology,* 20**,** 6055-6072.

103. WINAWER, S.J. 2015. The history of colorectal cancer screening: a personal perspective. *Dig Dis Sci,* 60**,** 596-608.

104. DUKES, C.E. 1932. The classification of cancer of the rectum. *The Journal of Pathology and Bacteriology,* 35**,** 323-332.

105. NHS. 2015. *Bowel cancer screening* [Online]. Available: http://www.nhs.uk/Conditions/bowel-cancer-screening/Pages/bowel-scope-screening.aspx [Accessed January 2016].

106. CARMONA, F.J., AZUARA, D., BERENGUER-LLERGO, A., FERNANDEZ, A.F., BIONDO, S., DE OCA, J., RODRIGUEZ-MORANTA, F., SALAZAR, R., VILLANUEVA, A., FRAGA, M.F., GUARDIOLA, J., CAPELLA, G., ESTELLER, M. &MORENO, V. 2013. DNA methylation biomarkers for noninvasive diagnosis of colorectal cancer. *Cancer Prev Res (Phila),* 6**,** 656-65.

107. HARDOUIN, S.N. &NAGY, A. 2000. Mouse models for human disease. *Clin Genet,* 57**,** 237-44.

108. PERSE, M. &CERAR, A. 2012. Dextran sodium sulphate colitis mouse model: traps and tricks. *J Biomed Biotechnol,* 2012**,** 718617.

109. GOYAL, N., RANA, A., AHLAWAT, A., BIJJEM, K.R. &KUMAR, P. 2014. Animal models of inflammatory bowel disease: a review. *Inflammopharmacology,* 22**,** 219-33.

110. PRATTIS, S. &JURJUS, A. 2015. Spontaneous and transgenic rodent models of inflammatory bowel disease. *Lab Anim Res,* 31**,** 47-68.

111. MURDOCH, T.B., FU, H., MACFARLANE, S., SYDORA, B.C., FEDORAK, R.N. &SLUPSKY, C.M. 2008. Urinary metabolic profiles of inflammatory bowel disease in interleukin-10 gene-deficient mice. *Anal Chem,* 80**,** 5524-31.

112. BAUR, P., MARTIN, F.P., GRUBER, L., BOSCO, N., BRAHMBHATT, V., COLLINO, S., GUY, P., MONTOLIU, I., ROZMAN, J., KLINGENSPOR, M., TAVAZZI, I., THORIMBERT, A., REZZI, S., KOCHHAR, S., BENYACOUB, J., KOLLIAS, G. &HALLER, D. 2011. Metabolic phenotyping of the Crohn's disease-like IBD etiopathology in the TNF(DeltaARE/WT) mouse model. *J Proteome Res,* 10**,** 5523-35.

113. HAHM, K.B., IM, Y.H., PARKS, T.W., PARK, S.H., MARKOWITZ, S., JUNG, H.Y., GREEN, J. &KIM, S.J. 2001. Loss of transforming growth factor beta signalling in the intestine contributes to tissue injury in inflammatory bowel disease. *Gut,* 49**,** 190-8.

114. VAN DER SLUIS, M., DE KONING, B.A.E., DE BRUIJN, A.C.J.M., VELCICH, A., MEIJERINK, J.P.P., VAN GOUDOEVER, J.B., BULLER, H.A., DEKKER, J., VAN SEUNINGEN, I., RENES, I.B. &EINERHAND, A.W.C. 2006. Muc2-deficient mice spontaneously develop colitis, indicating that Muc2 is critical for colonic protection. *Gastroenterology,* 131**,** 117-129.

115. PANWALA, C.M., JONES, J.C. &VINEY, J.L. 1998. A novel model of inflammatory bowel disease: Mice deficient for the multiple drug resistance gene, mdr1a, spontaneously develop colitis. *Journal of Immunology,* 161**,** 5733-5744.

116. KUHN, R., LOHLER, J., RENNICK, D., RAJEWSKY, K. &MULLER, W. 1993. Interleukin-10-Deficient Mice Develop Chronic Enterocolitis. *Cell,* 75**,** 263-274.

117. KIESLER, P., FUSS, I.J. &STROBER, W. 2015. Experimental Models of Inflammatory Bowel Diseases. *Cell Mol Gastroenterol Hepatol,* 1**,** 154-170.

118. FRANKE, A., BALSCHUN, T., KARLSEN, T.H., SVENTORAITYTE, J., NIKOLAUS, S., MAYR, G., DOMINGUES, F.S., ALBRECHT, M., NOTHNAGEL, M., ELLINGHAUS, D., SINA, C., ONNIE, C.M., WEERSMA, R.K., STOKKERS, P.C.F., WIJMENGA, C., GAZOULI, M., STRACHAN, D., MCARDLE, W.L., VERMEIRE, S., RUTGEERTS, P., ROSENSTIEL, P., KRAWCZAK, M., VATN, M.H., MATHEW, C.G., SCHREIBER, S. &GRP, I.S. 2008. Sequence variants in IL10, ARPC2 and multiple other loci contribute to ulcerative colitis susceptibility. *Nature Genetics,* 40**,** 1319-1323.

119. FRANKE, A., MCGOVERN, D.P.B., BARRETT, J.C., WANG, K., RADFORD-SMITH, G.L., AHMAD, T., LEES, C.W., BALSCHUN, T., LEE, J., ROBERTS, R., ANDERSON, C.A., BIS, J.C., BUMPSTEAD, S., ELLINGHAUS, D., FESTEN, E.M., GEORGES, M., GREEN, T., HARITUNIANS, T., JOSTINS, L., LATIANO, A., MATHEW, C.G., MONTGOMERY, G.W., PRESCOTT, N.J., RAYCHAUDHURI, S., ROTTER, J.I., SCHUMM, P., SHARMA, Y., SIMMS, L.A., TAYLOR, K.D., WHITEMAN, D., WIJMENGA, C., BALDASSANO, R.N., BARCLAY, M., BAYLESS, T.M., BRAND, S., BUNING, C., COHEN, A., COLOMBEL, J.F., COTTONE, M., STRONATI, L., DENSON, T., DE VOS, M., D'INCA, R., DUBINSKY, M., EDWARDS, C., FLORIN, T., FRANCHIMONT, D., GEARRY, R., GLAS, J., VAN GOSSUM, A., GUTHERY, S.L., HALFVARSON, J., VERSPAGET, H.W., HUGOT, J.P., KARBAN, A., LAUKENS, D., LAWRANCE, I., LEMANN, M., LEVINE, A., LIBIOULLE, C., LOUIS, E., MOWAT, C., NEWMAN, W., PANES, J., PHILLIPS, A., PROCTOR, D.D., REGUEIRO, M., RUSSELL, R., RUTGEERTS, P., SANDERSON, J., SANS, M., SEIBOLD, F., STEINHART, A.H., STOKKERS, P.C.F., TORKVIST, L., KULLAK-UBLICK, G., WILSON, D., WALTERS, T., TARGAN, S.R., BRANT, S.R., RIOUX, J.D., D'AMATO, M., WEERSMA, R.K., KUGATHASAN, S., GRIFFITHS, A.M., MANSFIELD, J.C., VERMEIRE, S., DUERR, R.H., SILVERBERG, M.S., SATSANGI, J., SCHREIBER, S., CHO, J.H., ANNESE, V., HAKONARSON, H., DALY, M.J. &PARKES, M. 2010. Genome-wide meta-analysis increases to 71 the number of confirmed Crohn's disease susceptibility loci. *Nature Genetics,* 42**,** 1118-+.

120. GLOCKER, E.O., KOTLARZ, D., BOZTUG, K., GERTZ, E.M., SCHAFFER, A.A., NOYAN, F., PERRO, M., DIESTELHORST, J., ALLROTH, A., MURUGAN, D., HATSCHER, N., PFEIFER, D., SYKORA, K.W., SAUER, M., KREIPE, H., LACHER, M., NUSTEDE, R., WOELLNER, C., BAUMANN, U., SALZER, U., KOLETZKO, S., SHAH, N., SEGAL, A.W., SAUERBREY, A., BUDERUS, S., SNAPPER, S.B., GRIMBACHER, B. &KLEIN, C. 2009. Inflammatory Bowel Disease and Mutations Affecting the Interleukin-10 Receptor. *New England Journal of Medicine,* 361**,** 2033-2045.

121. RANDHAWA, P.K., SINGH, K., SINGH, N. &JAGGI, A.S. 2014. A review on chemical-induced inflammatory bowel disease models in rodents. *Korean J Physiol Pharmacol,* 18**,** 279-88.

122. MCCAFFERTY, D.M. &ZEITLIN, I.J. 1989. Short chain fatty acid-induced colitis in mice. *Int J Tissue React,* 11**,** 165-8.

123. KRASNA, I.H. &KIM, H. 1992. Indomethacin administration after temporary ischemia causes bowel necrosis in mice. *Journal of Pediatric Surgery,* 27**,** 805-7.

124. PALMEN, M.J., DIELEMAN, L.A., VAN DER ENDE, M.B., UYTERLINDE, A., PENA, A.S., MEUWISSEN, S.G. &VAN REES, E.P. 1995. Non-lymphoid and lymphoid cells in acute, chronic and relapsing experimental colitis. *Clinical and Experimental Immunology,* 99**,** 226-32.

125. YAMADA, T., SARTOR, R.B., MARSHALL, S., SPECIAN, R.D. &GRISHAM, M.B. 1993. Mucosal injury and inflammation in a model of chronic granulomatous colitis in rats. *Gastroenterology,* 104**,** 759-71.

126. PRICOLO, V.E., MADHERE, S.M., FINKELSTEIN, S.D. &REICHNER, J.S. 1996. Effects of lambda-carrageenan induced experimental enterocolitis on splenocyte function and nitric oxide production. *J Surg Res,* 66**,** 6-11.

127. BOIRIVANT, M., FUSS, I.J., CHU, A. &STROBER, W. 1998. Oxazolone colitis: A murine model of T helper cell type 2 colitis treatable with antibodies to interleukin 4. *J Exp Med,* 188**,** 1929-39.

128. FOX, J.G., GE, Z., WHARY, M.T., ERDMAN, S.E. &HORWITZ, B.H. 2011. Helicobacter hepaticus infection in mice: models for understanding lower bowel inflammation and cancer. *Mucosal Immunology,* 4**,** 22-30.

129. OKAYASU, I., HATAKEYAMA, S., YAMADA, M., OHKUSA, T., INAGAKI, Y. &NAKAYA, R. 1990. A novel method in the induction of reliable experimental acute and chronic ulcerative colitis in mice. *Gastroenterology,* 98**,** 694-702.

130. MAXWELL, J.R., BROWN, W.A., SMITH, C.L., BYRNE, F.R. &VINEY, J.L. 2009. Methods of inducing inflammatory bowel disease in mice. *Curr Protoc Pharmacol,* Chapter 5**,** Unit5 58.

131. ARASARADNAM, R.P., OUARET, N., THOMAS, M.G., QURAISHI, N., HEATHERINGTON, E., NWOKOLO, C.U., BARDHAN, K.D. &COVINGTON, J.A. 2013. A novel tool for noninvasive diagnosis and tracking of patients with inflammatory bowel disease. *Inflammatory Bowel Diseases,* 19**,** 999-1003.

132. LAROUI, H., YAN, Y.T., INGERSOLL, S., XIAO, B., CHARANIA, M.A., AYYADURAI, S., SITARAMAN, S.V. &MERLIN, D. 2012. Dextran Sodium Sulfate (DSS) Induces Colitis in Mice by Forming Nano-Lipocomplexes With Medium-Chain-Length Fatty Acids in the Colon. *Gastroenterology,* 142**,** S720-S720.

133. CHASSAING, B., AITKEN, J.D., MALLESHAPPA, M. &VIJAY-KUMAR, M. 2014. Dextran sulfate sodium (DSS)-induced colitis in mice. *Curr Protoc Immunol,* 104**,** Unit 15 25.

134. KITAJIMA, S., TAKUMA, S. &MORIMOTO, M. 2000. Histological analysis of murine colitis induced by dextran sulfate sodium of different molecular weights. *Exp Anim,* 49**,** 9-15.

135. MAHLER, M., BRISTOL, I.J., LEITER, E.H., WORKMAN, A.E., BIRKENMEIER, E.H., ELSON, C.O. &SUNDBERG, J.P. 1998. Differential susceptibility of inbred mouse strains to dextran sulfate sodium-induced colitis. *American Journal of Physiology-Gastrointestinal and Liver Physiology,* 274**,** G544-G551.

136. MELGAR, S., KARLSSON, A. &MICHAELSSON, E. 2005. Acute colitis induced by dextran sulfate sodium progresses to chronicity in C57BL/6 but not in BALB/c mice: correlation between symptoms and inflammation. *Am J Physiol Gastrointest Liver Physiol,* 288**,** 6.

137. HUDCOVIC, T., STEPANKOVA, R., CEBRA, J. &TLASKALOVA-HOGENOVA, H. 2001. The role of microflora in the development of intestinal inflammation: Acute and chronic colitis induced by dextran sulfate in germ-free and conventionally reared immunocompetent and immunodeficient mice. *Folia Microbiologica,* 46**,** 565-572.

138. HANS, W., SCHOLMERICH, J., GROSS, V. &FALK, W. 2000. The role of the resident intestinal flora in acute and chronic dextran sulfate sodium-induced colitis in mice. *European Journal of Gastroenterology & Hepatology,* 12**,** 267-273.

139. KITAJIMA, S., MORIMOTO, M. &SAGARA, E. 2002. A model for dextran sodium sulfate (DSS)-induced mouse colitis: Bacterial degradation of DSS does not occur after incubation with mouse cecal contents. *Experimental Animals,* 51**,** 203-206.

140. HALE, L.P. &GREER, P.K. 2012. A novel murine model of inflammatory bowel disease and inflammation-associated colon cancer with ulcerative colitis-like features. *PLoS One,* 7**,** e41797.

141. RUBIN, D.C., SHAKER, A. &LEVIN, M.S. 2012. Chronic intestinal inflammation: inflammatory bowel disease and colitis-associated colon cancer. *Front Immunol,* 3**,** 107.

142. JOHNSON, R.L. &FLEET, J.C. 2013. Animal models of colorectal cancer. *Cancer Metastasis Rev,* 32**,** 39-61.

143. YAMADA, Y., YOSHIMI, N., HIROSE, Y., KAWABATA, K., MATSUNAGA, K., SHIMIZU, M., HARA, A. &MORI, H. 2000. Frequent beta-catenin gene mutations and accumulations of the protein in the putative preneoplastic lesions lacking macroscopic aberrant crypt foci appearance, in rat colon carcinogenesis. *Cancer Research,* 60**,** 3323-3327.

144. NEUFERT, C., BECKER, C. &NEURATH, M.F. 2007. An inducible mouse model of colon carcinogenesis for the analysis of sporadic and inflammation-driven tumor progression. *Nat Protoc,* 2**,** 1998-2004.

145. BIRD, R.P. &GOOD, C.K. 2000. The significance of aberrant crypt foci in understanding the pathogenesis of colon cancer. *Toxicol Lett,* 112-113**,** 395-402.

146. GU, S., CHEN, D., ZHANG, J.N., LV, X., WANG, K., DUAN, L.P., NIE, Y. &WU, X.L. 2013. Bacterial community mapping of the mouse gastrointestinal tract. *PLoS One,* 8**,** e74957.

147. HAKANSSON, A., TORMO-BADIA, N., BARIDI, A., XU, J., MOLIN, G., HAGSLATT, M.L., KARLSSON, C., JEPPSSON, B., CILIO, C.M. &AHRNE, S. 2015. Immunological alteration and changes of gut microbiota after dextran sulfate sodium (DSS) administration in mice. *Clinical and Experimental Medicine,* 15**,** 107-20.

148. GKOUSKOU, K.K., DELIGIANNI, C., TSATSANIS, C. &ELIOPOULOS, A.G. 2014. The gut microbiota in mouse models of inflammatory bowel disease. *Front Cell Infect Microbiol,* 4.

149. DENNIS, K.L., WANG, Y., BLATNER, N.R., WANG, S., SAADALLA, A., TRUDEAU, E., ROERS, A., WEAVER, C.T., LEE, J.J., GILBERT, J.A., CHANG, E.B. &KHAZAIE, K. 2013. Adenomatous polyps are driven by microbe-instigated focal inflammation and are controlled by IL-10-producing T cells. *Cancer Research,* 73**,** 5905-13.

150. DOVE, W.F., CLIPSON, L., GOULD, K.A., LUONGO, C., MARSHALL, D.J., MOSER, A.R., NEWTON, M.A. &JACOBY, R.F. 1997. Intestinal neoplasia in the ApcMin mouse:

independence from the microbial and natural killer (beige locus) status. *Cancer Research,* 57**,** 812-4.

151. SELLON, R.K., TONKONOGY, S., SCHULTZ, M., DIELEMAN, L.A., GRENTHER, W., BALISH, E., RENNICK, D.M. &SARTOR, R.B. 1998. Resident enteric bacteria are necessary for development of spontaneous colitis and immune system activation in interleukin-10-deficient mice. *Infection and Immunity,* 66**,** 5224-31.

152. RATH, H.C., SCHULTZ, M., FREITAG, R., DIELEMAN, L.A., LI, F., LINDE, H.J., SCHOLMERICH, J. &SARTOR, R.B. 2001. Different subsets of enteric bacteria induce and perpetuate experimental colitis in rats and mice. *Infection and Immunity,* 69**,** 2277-85.

153. ISAACS, K. &HERFARTH, H. 2008. Role of probiotic therapy in IBD. *Inflammatory Bowel Diseases,* 14**,** 1597-605.

154. ARTHUR, J.C., GHARAIBEH, R.Z., URONIS, J.M., PEREZ-CHANONA, E., SHA, W., TOMKOVICH, S., MUHLBAUER, M., FODOR, A.A. &JOBIN, C. 2013. VSL#3 probiotic modifies mucosal microbial composition but does not reduce colitis-associated colorectal cancer. *Sci Rep,* 3**,** 2868.

155. ARTHUR, J.C., PEREZ-CHANONA, E., MUHLBAUER, M., TOMKOVICH, S., URONIS, J.M., FAN, T.J., CAMPBELL, B.J., ABUJAMEL, T., DOGAN, B., ROGERS, A.B., RHODES, J.M., STINTZI, A., SIMPSON, K.W., HANSEN, J.J., KEKU, T.O., FODOR, A.A. &JOBIN, C. 2012. Intestinal inflammation targets cancer-inducing activity of the microbiota. *Science,* 338**,** 120-3.

156. YANG, I., EIBACH, D., KOPS, F., BRENNEKE, B., WOLTEMATE, S., SCHULZE, J., BLEICH, A., GRUBER, A.D., MUTHUPALANI, S., FOX, J.G., JOSENHANS, C. &SUERBAUM, S. 2013. Intestinal microbiota composition of interleukin-10 deficient C57BL/6J mice and susceptibility to Helicobacter hepaticus-induced colitis. *PLoS One,* 8**,** e70783.

157. ETTREIKI, C., GADONNA-WIDEHEM, P., MANGIN, I., COEFFIER, M., DELAYRE-ORTHEZ, C. &ANTON, P.M. 2012. Juvenile ferric iron prevents microbiota dysbiosis and colitis in adult rodents. *World J Gastroenterol,* 18**,** 2619-29.

158. WILSON, A.D. &BAIETTO, M. 2011. Advances in electronic-nose technologies developed for biomedical applications. *Sensors (Basel),* 11**,** 1105-76.

159. ADAMS, F. 1994. Hippocratic writings: Aphorisms IV, V. *The Internet Classic Archive; Stevenson, D.C., Ed.; Web Atomics: New York, NY, USA***,** 1-10.

160. SHAMSI, M., HAGHVERDI, F. &CHANGIZI ASHTIYANI, S. 2014. A brief review of Rhazes, Avicenna, and Jorjani's views on diagnosis of diseases through urine examination. *Iran J Kidney Dis,* 8**,** 278-85.

161. PORTER, R. 1977. The early years *The Greatest Benefit to Mankind: A Medical History of Humanity from Antiquity to the Present; Porter, R., Ed.: Harper Collins: London, UK.* **,** 147-162.

162. ZHAO, H.L., TONG, P.C. &CHAN, J.C. 2006. Traditional Chinese medicine in the treatment of diabetes. *Nestle Nutr Workshop Ser Clin Perform Programme,* 11**,** 15-25; discussion 25-9.

163. PETTERS, W. 1857. Untersuchungen uber die Honigharnruhr. *Prager Vierteljahrsschr. Praktischer Heilkunde,* 55**,** 81-94.

164. MUELLER, J. 1898. Uber die Ausscheidungsst ¨ atten des Acetons ¨ und die Bestimmung desselben in der Athemluft und den Hautausdunstungen des Menschen. *Arch. Exp. Pathol. Pharmacol,* 40**,** 315-62.

165. KOCH, R. 1876. Investigations into bacteria: V. The etiology of anthrax, based on the ontogenesis of Bacillus anthracis. . *Cohns Beitrage zur Biologie der Pflanzen,* 2**,** 277-310.

166. OMELIANSKI, V.L. 1923. Aroma-Producing Microorganisms. *J Bacteriol,* 8**,** 393-419.

167. DAVIES, T. &HAYWARD, N.J. 1984. Volatile products from acetylcholine as markers in the rapid urine test using head-space gas-liquid chromatography. *J Chromatogr,* 307**,** 11-21.

168. CONTI-NIBALI, S., BALDARI, S., VITULO, F., SFERLAZZAS, C., RUSSO, E., TEDESCHI, A., BONANNO, N. &MAGAZZU, G. 1990. The 14CO2 urea breath test for Helicobacter pylori infection. *J Pediatr Gastroenterol Nutr,* 11**,** 284-5.

169. LIKIC, V.A., MCCONVILLE, M.J., LITHGOW, T. &BACIC, A. 2010. Systems biology: the next frontier for bioinformatics. *Adv Bioinformatics***,** 268925.

170. MONTEIRO, M.S., CARVALHO, M., BASTOS, M.L. &GUEDES DE PINHO, P. 2013. Metabolomics analysis for biomarker discovery: advances and challenges. *Curr Med Chem,* 20**,** 257-71.

171. AMANN, A., COSTELLO BDE, L., MIEKISCH, W., SCHUBERT, J., BUSZEWSKI, B., PLEIL, J., RATCLIFFE, N. &RISBY, T. 2014. The human volatilome: volatile organic compounds (VOCs) in exhaled breath, skin emanations, urine, feces and saliva. *Journal of Breath Research,* 8**,** 034001.

172. COSTELLO, B.D., AMANN, A., AL-KATEB, H., FLYNN, C., FILIPIAK, W., KHALID, T., OSBORNE, D. &RATCLIFFE, N.M. 2014. A review of the volatiles from the healthy human body. *Journal of Breath Research,* 8.

173. FILIPIAK, W., RUZSANYI, V., MOCHALSKI, P., FILIPIAK, A., BAJTAREVIC, A., AGER, C., DENZ, H., HILBE, W., JAMNIG, H., HACKL, M., DZIEN, A. &AMANN, A. 2012. Dependence of exhaled breath composition on exogenous factors, smoking habits and exposure to air pollutants. *Journal of Breath Research,* 6**,** 036008.

174. MIEKISCH, W., SCHUBERT, J.K. &NOELDGE-SCHOMBURG, G.F.E. 2004. Diagnostic potential of breath analysis - focus on volatile organic compounds. *Clinica Chimica Acta,* 347**,** 25-39.

175. FOSTER, W.M., JIANG, L., STETKIEWICZ, P.T. &RISBY, T.H. 1996. Breath isoprene: Temporal changes in respiratory output after exposure to ozone. *Journal of Applied Physiology,* 80**,** 706-710.

176. LEBOVITZ, H.E. 1995. Diabetic-Ketoacidosis. *Lancet,* 345**,** 767-772.

177. POLI, D., CARBOGNANI, P., CORRADI, M., GOLDONI, M., ACAMPA, O., BALBI, B., BIANCHI, L., RUSCA, M. &MUTTI, A. 2005. Exhaled volatile organic compounds in patients with non-small cell lung cancer: cross sectional and nested short-term follow-up study. *Respir Res,* 6**,** 71.

178. SCOTT-THOMAS, A.J., SYHRE, M., PATTEMORE, P.K., EPTON, M., LAING, R., PEARSON, J. &CHAMBERS, S.T. 2010. 2-Aminoacetophenone as a potential breath biomarker for Pseudomonas aeruginosa in the cystic fibrosis lung. *Bmc Pulmonary Medicine,* 10**,** 56.

179. YATES, D.H., KRISHNAN, A., CHOW, S. &THOMAS, P.S. 2011. Non-invasive assessment of exhaled biomarkers in lung transplantation. *Journal of Breath Research,* 5**,** 024001.

180. KOHL, I., BEAUCHAMP, J., CAKAR-BECK, F., HERBIG, J., DUNKL, J., TIETJE, O., TIEFENTHALER, M., BOESMUELLER, C., WISTHALER, A., BREITENLECHNER, M., LANGEBNER, S., ZABERNIGG, A., REINSTALLER, F., WINKLER, K., GUTMANN, R. &HANSEL, A. 2013. First observation of a potential non-invasive breath gas biomarker for kidney function. *Journal of Breath Research,* 7**,** 017110.

181. SMITH, S., BURDEN, H., PERSAD, R., WHITTINGTON, K., COSTELLO, B.D., RATCLIFFE, N.M. &PROBERT, C.S. 2008. A comparative study of the analysis of human urine headspace using gas chromatography-mass spectrometry. *Journal of Breath Research,* 2.

182. MILLS, G.A. &WALKER, V. 2001. Headspace solid-phase microextraction profiling of volatile compounds in urine: application to metabolic investigations. *J Chromatogr B Biomed Sci Appl,* 753**,** 259-68.

183. GUERNION, N., RATCLIFFE, N.M., SPENCER-PHILLIPS, P.T. &HOWE, R.A. 2001. Identifying bacteria in human urine: current practice and the potential for rapid, near-patient diagnosis by sensing volatile organic compounds. *Clinical Chemistry and Laboratory Medicine,* 39**,** 893-906.

184. ARASARADNAM, R.P., MCFARLANE, M., DAULTON, E., WESTENBRINK, E., O'CONNELL, N., WURIE, S., NWOKOLO, C.U., BARDHAN, K.D., SAVAGE, R.S. &COVINGTON, J.A. 2015. Non-invasive distinction of non-alcoholic fatty liver disease using urinary volatile organic compound analysis: early results. *J Gastrointestin Liver Dis,* 24**,** 197-201.

185. PROBERT, C.S.J., AHMED, I., KHALID, T., JOHNSON, E., SMITH, S. &RATCLIFFE, N. 2009. Volatile Organic Compounds as Diagnostic Biomarkers in Gastrointestinal and Liver Diseases. *Journal of Gastrointestinal and Liver Diseases,* 18**,** 337-343.

186. ARASARADNAM, R.P., COVINGTON, J.A., HARMSTON, C. &NWOKOLO, C.U. 2014. Review article: next generation diagnostic modalities in gastroenterology--gas phase volatile compound biomarker detection. *Aliment Pharmacol Ther,* 39**,** 780-9.

187. TAIT, E., HILL, K.A., PERRY, J.D., STANFORTH, S.P. &DEAN, J.R. 2014. Development of a novel method for detection of Clostridium difficile using HS-SPME-GC-MS. *J Appl Microbiol,* 116**,** 1010-9.

188. GARNER, C.E., SMITH, S., DE LACY COSTELLO, B., WHITE, P., SPENCER, R., PROBERT, C.S. &RATCLIFFE, N.M. 2007. Volatile organic compounds from feces and their potential for diagnosis of gastrointestinal disease. *FASEB J,* 21**,** 1675-88.

189. WALTON, C., FOWLER, D.P., TURNER, C., JIA, W., WHITEHEAD, R.N., GRIFFITHS, L., DAWSON, C., WARING, R.H., RAMSDEN, D.B., COLE, J.A., CAUCHI, M., BESSANT, C. &HUNTER, J.O. 2013. Analysis of volatile organic compounds of bacterial origin in chronic gastrointestinal diseases. *Inflammatory Bowel Diseases,* 19**,** 2069-78.

190. DE MEIJ, T.G., DE BOER, N.K., BENNINGA, M.A., LENTFERINK, Y.E., DE GROOT, E.F., VAN DE VELDE, M.E., VAN BODEGRAVEN, A.A. &VAN DER SCHEE, M.P. 2014. Faecal gas analysis by electronic nose as novel, non-invasive method for assessment of active and quiescent paediatric inflammatory bowel disease: Proof of principle study. *J Crohns Colitis*.

191. HANG, B. 2010. Formation and repair of tobacco carcinogen-derived bulky DNA adducts. *J Nucleic Acids,* 2010**,** 709521.

192. SANTO-PIETRO, K.A. 2006. *The Environmental Reporter* [Online]. Available: https://www.emlab.com/s/sampling/env-report-04-2006.html [Accessed July 2015].

193. SAGAR, N.M., CREE, I.A., COVINGTON, J.A. &ARASARADNAM, R.P. 2015. The Interplay of the Gut Microbiome, Bile Acids, and Volatile Organic Compounds. *Gastroenterology Research and Practice*.

194. CARBONERO, F., BENEFIEL, A.C., ALIZADEH-GHAMSARI, A.H. &GASKINS, H.R. 2012. Microbial pathways in colonic sulfur metabolism and links with health and disease. *Frontiers in Physiology,* 3**,** 448.

195. RAJAIE, S. &ESMAILLZADEH, A. 2011. Dietary choline and betaine intakes and risk of cardiovascular diseases: review of epidemiological evidence. *ARYA Atheroscler,* 7**,** 78-86.

196. HOOPER, L.V., MIDTVEDT, T. &GORDON, J.I. 2002. How host-microbial interactions shape the nutrient environment of the mammalian intestine. *Annu Rev Nutr,* 22**,** 283-307.

197. GUINANE, C.M. &COTTER, P.D. 2013. Role of the gut microbiota in health and chronic gastrointestinal disease: understanding a hidden metabolic organ. *Therap Adv Gastroenterol,* 6**,** 295-308.

198. TURNER, A.P. &MAGAN, N. 2004. Electronic noses and disease diagnostics. *Nat Rev Microbiol,* 2**,** 161-6.

199. MCCULLOCH, M., JEZIERSKI, T., BROFFMAN, M., HUBBARD, A., TURNER, K. &JANECKI, T. 2006. Diagnostic accuracy of canine scent detection in early- and late-stage lung and breast cancers. *Integr Cancer Ther,* 5**,** 30-9.

200. SONODA, H., KOHNOE, S., YAMAZATO, T., SATOH, Y., MORIZONO, G., SHIKATA, K., MORITA, M., WATANABE, A., MORITA, M., KAKEJI, Y., INOUE, F. &MAEHARA, Y. 2011. Colorectal cancer screening with odour material by canine scent detection. *Gut,* 60**,** 814-9.

201. COOPER, H.S., MURTHY, S.N., SHAH, R.S. &SEDERGRAN, D.J. 1993. Clinicopathologic study of dextran sulfate sodium experimental murine colitis. *Lab Invest,* 69**,** 238-49.

202. TSO, V.K., SYDORA, B.C., FOSHAUG, R.R., CHURCHILL, T.A., DOYLE, J., SLUPSKY, C.M. &FEDORAK, R.N. 2013. Metabolomic profiles are gender, disease and time specific

in the interleukin-10 gene-deficient mouse model of inflammatory bowel disease. *PLoS One,* 8**,** e67654.

203. AEPPLI, C., BERG, M., HOFSTETTER, T.B., KIPFER, R. &SCHWARZENBACH, R.P. 2008. Simultaneous quantification of polar and non-polar volatile organic compounds in water samples by direct aqueous injection-gas chromatography/mass spectrometry. *Journal of Chromatography A,* 1181**,** 116-124.

204. ARTHUR, C.L. &PAWLISZYN, J. 1990. Solid-Phase Microextraction with Thermal-Desorption Using Fused-Silica Optical Fibers. *Analytical Chemistry,* 62**,** 2145-2148.

205. GROB, R.L., & BARRY, E, F., (ed.) 2004. *Modern Practice of Gas Chromatography* John Wiley & Sons, Inc. .

206. ZHANG, Z.Y. &PAWLISZYN, J. 1993. Headspace Solid-Phase Microextraction. *Analytical Chemistry,* 65**,** 1843-1852.

207. SMITH, S. 2007. The Analysis of Organic Compounds as a Tool for Diagnosis of Disease; PhD Thesis. *University of West of England, Bristol, UK*.

208. PARKINSON, N., HARDISTY-HUGHES, R.E., TATEOSSIAN, H., TSAI, H.T., BROOKER, D., MORSE, S., LALANE, Z., MACKENZIE, F., FRAY, M., GLENISTER, P., WOODWARD, A.M., POLLEY, S., BARBARIC, I., DEAR, N., HOUGH, T.A., HUNTER, A.J., CHEESEMAN, M.T. &BROWN, S.D.M. 2006. Mutation at the Evi1 locus in Junbo mice causes susceptibility to otitis media. *Plos Genetics,* 2**,** 1556-1564.

209. DEY, S.K., HIRA, A., HOWLADER, M.S.I., AHMED, A., HOSSAIN, H. &JAHAN, I.A. 2014. Antioxidant and antidiarrheal activities of ethanol extract of Ardisia elliptica fruits. *Pharmaceutical Biology,* 52**,** 213-220.

210. NAMBIAR, P.R., GIRNUN, G., LILLO, N.A., GUDA, K., WHITELEY, H.E. &ROSENBERG, D.W. 2003. Preliminary analysis of azoxymethane induced colon tumors in inbred mice commonly used as transgenic/knockout progenitors. *International Journal of Oncology,* 22**,** 145-150.

211. GRETEN, F.R., ECKMANN, L., GRETEN, T.F., PARK, J.M., LI, Z.W., EGAN, L.J., KAGNOFF, M.F. &KARIN, M. 2004. IKKbeta links inflammation and tumorigenesis in a mouse model of colitis-associated cancer. *Cell,* 118**,** 285-96.

212. MOOLENBEEK, C. &RUITENBERG, E.J. 1981. The Swiss Roll - a Simple Technique for Histological Studies of the Rodent Intestine. *Laboratory Animals,* 15**,** 57-59.

213. SPICER, S.S. 1965. Diamine Methods for Differentiating Mucosubstances Histochemically. *Journal of Histochemistry & Cytochemistry,* 13**,** 211-&.

214. MURTHY, S.N., COOPER, H.S., SHIM, H., SHAH, R.S., IBRAHIM, S.A. &SEDERGRAN, D.J. 1993. Treatment of dextran sulfate sodium-induced murine colitis by intracolonic cyclosporin. *Dig Dis Sci,* 38**,** 1722-34.

215. BAUER, C., DUEWELL, P., MAYER, C., LEHR, H.A., FITZGERALD, K.A., DAUER, M., TSCHOPP, J., ENDRES, S., LATZ, E. &SCHNURR, M. 2010. Colitis induced in mice with dextran sulfate sodium (DSS) is mediated by the NLRP3 inflammasome. *Gut,* 59**,** 1192-9.

216. DING, S., WALTON, K.L., BLUE, R.E., MCNAUGHTON, K., MAGNESS, S.T. &LUND, P.K. 2012. Mucosal healing and fibrosis after acute or chronic inflammation in wild type FVB-N mice and C57BL6 procollagen alpha1(I)-promoter-GFP reporter mice. *PLoS One,* 7**,** e42568.

217. ROBERT, F.S.M. &RAO, J.P. 1996. Evidence for possible involvement of guanylate cyclase in diarrhoea induced by castor oil in mice. *Journal of Diarrhoeal Diseases Research,* 14**,** 218-219.

218. CADERNI, G., FEMIA, A.P., GIANNINI, A., FAVUZZA, A., LUCERI, C., SALVADORI, M. &DOLARA, P. 2003. Identification of mucin-depleted foci in the unsectioned colon of azoxymethane-treated rats: Correlation with carcinogenesis. *Cancer Research,* 63**,** 2388-2392.

219. READE S, M.A., AGGIO R, KHALID T, PRITCHARD DM, EWER, AK, PROBERT CS. 2014. Optimisation of Sample Preparation for Direct SPME-GC-MS Analysis of Murine and Human Faecal Volatile Organic Compounds for Metabolomic Studies. *J Anal Bioanal Tech,* 5.

220. DIXON, E., CLUBB, C., PITTMAN, S., AMMANN, L., RASHEED, Z., KAZMI, N., KESHAVARZIAN, A., GILLEVET, P., RANGWALA, H. &COUCH, R.D. 2011. Solid-Phase Microextraction and the Human Fecal VOC Metabolome. *PLoS One,* 6.

221. READE, S., MAYOR, A., AGGIO, R., KHALID, T., PRITCHARD, D.M., EWER, A.K. &PROBERT, C.S. 2014. Optimisation of Sample Preparation for Direct SPME-GC-MS Analysis of Murine and Human Faecal Volatile Organic Compounds for Metabolomic Studies. *J Anal Bioanal Tech,* 5.

222. AGGIO, R., VILLAS-BOAS, S. G., & RUGGIERO, K. 2011. Metab: an R package for high-throughput analysis of metabolomics data generated by GC-MS. *Bioinformatics,* 27**,** 2316-2318.

223. HRYDZIUSZKO, O. &VIANT, M.R. 2012. Missing values in mass spectrometry based metabolomics: an undervalued step in the data processing pipeline. *Metabolomics,* 8**,** S161-S174.

224. VAN DEN BERG, R.A., HOEFSLOOT, H.C.J., WESTERHUIS, J.A., SMILDE, A.K. &VAN DER WERF, M.J. 2006. Centering, scaling, and transformations: improving the biological information content of metabolomics data. *Bmc Genomics,* 7.

225. XIA, J., SINELNIKOV, I.V. &WISHART, D.S. 2011. MetATT: a web-based metabolomics tool for analyzing time-series and two-factor datasets. *Bioinformatics,* 27**,** 2455-6.

226. TURNBAUGH, P.J. &GORDON, J.I. 2008. An invitation to the marriage of metagenomics and metabolomics. *Cell,* 134**,** 708-713.

227. ROGERS, G.B., KOZLOWSKA, J., KEEBLE, J., METCALFE, K., FAO, M., DOWD, S.E., MASON, A.J., MCGUCKIN, M.A. &BRUCE, K.D. 2014. Functional divergence in gastrointestinal microbiota in physically-separated genetically identical mice. *Sci Rep,* 4.

228. STANLEY, E.G., BAILEY, N.J.C., BOLLARD, M.E., HASELDEN, J.N., WATERFIELD, C.J., HOLMES, E. &NICHOLSON, J.K. 2005. Sexual dimorphism in urinary metabolite profiles of Han Wistar rats revealed by nuclear-magnetic-resonance-based metabonomics. *Anal Biochem,* 343**,** 195-202.

229. GOODRICH, B.S., GAMBALE, S., PENNCUIK, P.R. &REDHEAD, T.D. 1990. Volatile compounds from excreta of laboratory mice (Mus musculus) : Preliminary examination of composition and effects on behavior. *Journal of Chemical Ecology,* 16**,** 2107-20.

230. GOODRICH, B.S., GAMBALE, S., PENNYCUIK, P.R. &REDHEAD, T.D. 1990. Volatiles from feces of wild male house mice : Chemistry and effects on behavior and heart Rate. *Journal of Chemical Ecology,* 16**,** 2091-106.

231. DRABOVICH, A.P., PAVLOU, M.P., BATRUCH, I. &DIAMANDIS, E.P. 2013. Chapter 2 - Proteomic and Mass Spectrometry Technologies for Biomarker Discovery. *In:* VEENSTRA, H.J.I.D. (ed.) *Proteomic and Metabolomic Approaches to Biomarker Discovery.* Boston: Academic Press.

232. COMBES, R.D. &BALLS, M. 2014. The Three Rs - Opportunities for Improving Animal Welfare and the Quality of Scientific Research. *Atla-Alternatives to Laboratory Animals,* 42**,** 245-259.

233. EL AIDY, S., DERRIEN, M., MERRIFIELD, C.A., LEVENEZ, F., DORE, J., BOEKSCHOTEN, M.V., DEKKER, J., HOLMES, E., ZOETENDAL, E.G., VAN BAARLEN, P., CLAUS, S.P. &KLEEREBEZEM, M. 2013. Gut bacteria-host metabolic interplay during conventionalisation of the mouse germfree colon. *ISME J,* 7**,** 743-55.

234. BACKHED, F., DING, H., WANG, T., HOOPER, L.V., KOH, G.Y., NAGY, A., SEMENKOVICH, C.F. &GORDON, J.I. 2004. The gut microbiota as an environmental factor that regulates fat storage. *Proc Natl Acad Sci U S A,* 101**,** 15718-15723.

235. MASLOWSKI, K.M., VIEIRA, A.T., NG, A., KRANICH, J., SIERRO, F., YU, D., SCHILTER, H.C., ROLPH, M.S., MACKAY, F., ARTIS, D., XAVIER, R.J., TEIXEIRA, M.M. &MACKAY, C.R. 2009. Regulation of inflammatory responses by gut microbiota and chemoattractant receptor GPR43. *Nature,* 461**,** 1282-U119.

236. KIMURA, I., INOUE, D., HIRANO, K. &TSUJIMOTO, G. 2014. The SCFA Receptor GPR43 and Energy Metabolism. *Front Endocrinol (Lausanne),* 5**,** 85.

237. WONG, J.M.W., DE SOUZA, R., KENDALL, C.W.C., EMAM, A. &JENKINS, D.J.A. 2006. Colonic health: Fermentation and short chain fatty acids. *Journal of Clinical Gastroenterology,* 40**,** 235-243.

238. DECOMBAZ, J., ARNAUD, M.J., MILON, H., MOESCH, H., PHILIPPOSSIAN, G., THELIN, A.L. &HOWALD, H. 1983. Energy-Metabolism of Medium-Chain Triglycerides Versus Carbohydrates during Exercise. *European Journal of Applied Physiology and Occupational Physiology,* 52**,** 9-14.

239. OTT, A., GERMOND, J.E. &CHAINTREAU, A. 2000. Vicinal diketone formation in yogurt: (13)C precursors and effect of branched-chain amino acids. *J Agric Food Chem,* 48**,** 724-31.

240. SPECKMAN, R.A. &COLLINS, E.B. 1968. Diacetyl Biosynthesis in Streptococcus Diacetilactis and Leuconostoc Citrovorum. *J Bacteriol,* 95**,** 174-&.

241. KJELDSEN, F., CHRISTENSEN, L.P. &EDELENBOS, M. 2001. Quantitative analysis of aroma compounds in carrot (Daucus carota L.) cultivars by capillary gas chromatography using large-volume injection technique. *J Agric Food Chem,* 49**,** 4342-8.

242. GARNER, C.E., SMITH, S., COSTELLO, B.D., WHITE, P., SPENCER, R., PROBERT, C.S.J. &RATCLIFFE, N.M. 2007. Volatile organic compounds from feces and their potential for diagnosis of gastrointestinal disease. *Faseb Journal,* 21**,** 1675-1688.

243. MUSSO, A.E., TAKACS, S. J., GRIES, R. M., GRIES, G. G. 2014. New compositions and methods for attracting and stimulating feeding by mice and rats. Musso, A. E., Takacs, S. J., Gries, R. M., Gries, G. G.

244. WON, E.Y., YOON, M.K., KIM, S.W., JUNG, Y., BAE, H.W., LEE, D., PARK, S.G., LEE, C.H., HWANG, G.S. &CHI, S.W. 2013. Gender-specific metabolomic profiling of obesity in leptin-deficient ob/ob mice by 1H NMR spectroscopy. *PLoS One,* 8**,** e75998.

245. SLUPSKY, C.M., RANKIN, K.N., WAGNER, J., FU, H., CHANG, D., WELJIE, A.M., SAUDE, E.J., LIX, B., ADAMKO, D.J., SHAH, S., GREINER, R., SYKES, B.D. &MARRIE, T.J. 2007. Investigations of the effects of gender, diurnal variation, and age in human urinary metabolomic profiles. *Analytical Chemistry,* 79**,** 6995-7004.

246. DE WIT, N.J., BOSCH-VERMEULEN, H., DE GROOT, P.J., HOOIVELD, G.J., BROMHAAR, M.M., JANSEN, J., MULLER, M. &VAN DER MEER, R. 2008. The role of the small intestine in the development of dietary fat-induced obesity and insulin resistance in C57BL/6J mice. *Bmc Medical Genomics,* 1**,** 14.

247. LIN, J.H., CHIBA, M. &BAILLIE, T.A. 1999. Is the role of the small intestine in first-pass metabolism overemphasized? *Pharmacological Reviews,* 51**,** 135-157.

248. DICZFALUSY, M.A., BJORKHEM, I., EINARSSON, C., HILLEBRANT, C.G. &ALEXSON, S.E.H. 2001. Characterization of enzymes involved in formation of ethyl esters of long-chain fatty acids in humans. *Journal of Lipid Research,* 42**,** 1025-1032.

249. DAVID, L.A., MAURICE, C.F., CARMODY, R.N., GOOTENBERG, D.B., BUTTON, J.E., WOLFE, B.E., LING, A.V., DEVLIN, A.S., VARMA, Y., FISCHBACH, M.A., BIDDINGER, S.B., DUTTON, R.J. &TURNBAUGH, P.J. 2014. Diet rapidly and reproducibly alters the human gut microbiome. *Nature,* 505**,** 559-63.

250. WILLIG, S., LOSEL, D. &CLAUS, R. 2005. Effects of resistant potato starch on odor emission from feces in Swine production units. *J Agric Food Chem,* 53**,** 1173-8.

251. PALMER, C., BIK, E.M., DIGIULIO, D.B., RELMAN, D.A. &BROWN, P.O. 2007. Development of the human infant intestinal microbiota. *Plos Biology,* 5**,** 1556-1573.

252. MATSUMOTO, M., KIBE, R., OOGA, T., AIBA, Y., KURIHARA, S., SAWAKI, E., KOGA, Y. &BENNO, Y. 2012. Impact of intestinal microbiota on intestinal luminal metabolome. *Sci Rep,* 2**,** 233.

253. SCHWENDE, F.J., WIESLER, D., JORGENSON, J.W., CARMACK, M. &NOVOTNY, M. 1986. Urinary Volatile Constituents of the House Mouse, Mus-Musculus, and Their Endocrine Dependency. *Journal of Chemical Ecology,* 12**,** 277-296.

254. GUINANE, C.M. &COTTER, P.D. 2013. Role of the gut microbiota in health and chronic gastrointestinal disease: understanding a hidden metabolic organ. *Therapeutic Advances in Gastroenterology,* 6**,** 295-308.

255. NGUYEN, T.L.A., VIEIRA-SILVA, S., LISTON, A. &RAES, J. 2015. How informative is the mouse for human gut microbiota research? *Disease Models & Mechanisms,* 8**,** 1-16.

256. CASTELEYN, C., REKECKI, A., VAN DER AA, A., SIMOENS, P. &VAN DEN BROECK, W. 2010. Surface area assessment of the murine intestinal tract as a prerequisite for oral dose translation from mouse to man. *Laboratory Animals,* 44**,** 176-83.

257. TREUTING, P. &DINTZIS, S. 2012. Lower gastrointestinal tract. *Comparative Anatomy and Histology–a Mouse and Human Atlas, 1st edn (ed. Dintzis SM, Frevert CW, Liggitt HD, Montine KS, Treuting PM, editors.)*.

258. GIBBONS, D.L. &SPENCER, J. 2011. Mouse and human intestinal immunity: same ballpark, different players; different rules, same score. *Mucosal Immunol,* 4**,** 148-57.

259. SHOAIE, S., KARLSSON, F., MARDINOGLU, A., NOOKAEW, I., BORDEL, S. &NIELSEN, J. 2013. Understanding the interactions between bacteria in the human gut through metabolic modeling. *Sci Rep,* 3.

260. KALLUS, S.J. &BRANDT, L.J. 2012. The intestinal microbiota and obesity. *J Clin Gastroenterol,* 46**,** 16-24.

261. LEY, R.E., BACKHED, F., TURNBAUGH, P., LOZUPONE, C.A., KNIGHT, R.D. &GORDON, J.I. 2005. Obesity alters gut microbial ecology. *Proc Natl Acad Sci U S A,* 102**,** 11070-5.

262. LINNENBRINK, M., WANG, J., HARDOUIN, E.A., KUNZEL, S., METZLER, D. &BAINES, J.F. 2013. The role of biogeography in shaping diversity of the intestinal microbiota in house mice. *Mol Ecol,* 22**,** 1904-16.

263. BREITMAIER, E. 2006. Terpenes: Importance, General Structure, and Biosynthesis. *Terpenes.* Wiley-VCH Verlag GmbH & Co. KGaA.

264. ALI, B.H., BLUNDEN, G., TANIRA, M.O. &NEMMAR, A. 2008. Some phytochemical, pharmacological and toxicological properties of ginger (Zingiber officinale Roscoe): a review of recent research. *Food Chem Toxicol,* 46**,** 409-20.

265. XU, X., WEI, J., WEI, X., WEI, H. 2004. Herbal compositions and methods for effecting weight loss in humans. United States: XU XIURONG,WEI JING,WEI XIAN,WEI HONG.

266. CORK, A. &PARK, K.C. 1996. Identification of electrophysiologically-active compounds for the malaria mosquito, Anopheles gambiae, in human sweat extracts. *Med Vet Entomol,* 10**,** 269-76.

267. KING, R.A., MAY, B.L., DAVIES, D.A. &BIRD, A.R. 2009. Measurement of phenol and p-cresol in urine and feces using vacuum microdistillation and high-performance liquid chromatography. *Analytical Biochemistry,* 384**,** 27-33.

268. DECOMBAZ, J., ARNAUD, M.J., MILON, H., MOESCH, H., PHILIPPOSSIAN, G., THELIN, A.L. &HOWALD, H. 1983. Energy metabolism of medium-chain triglycerides versus carbohydrates during exercise. *Eur J Appl Physiol Occup Physiol,* 52**,** 9-14.

269. ANDERSEN, A. 2006. Final report on the safety assessment of benzaldehyde. *Int J Toxicol,* 1**,** 11-27.

270. SHIOTANI, A., KAMADA, T. &HARUMA, K. 2008. Low-dose aspirin-induced gastrointestinal diseases: past, present, and future. *J Gastroenterol,* 43**,** 581-8.

271. ELGAALI, H., HAMILTON-KEMP, T.R., NEWMAN, M.C., COLLINS, R.W., YU, K. &ARCHBOLD, D.D. 2002. Comparison of long-chain alcohols and other volatile compounds emitted from food-borne and related Gram positive and Gram negative bacteria. *J Basic Microbiol,* 42**,** 373-80.

272. DICZFALUSY, M.A., BJORKHEM, I., EINARSSON, C., HILLEBRANT, C.G. &ALEXSON, S.E. 2001. Characterization of enzymes involved in formation of ethyl esters of long-chain fatty acids in humans. *J Lipid Res,* 42**,** 1025-32.

273. SMITH, E.A. &MACFARLANE, G.T. 1997. Dissimilatory amino Acid metabolism in human colonic bacteria. *Anaerobe,* 3**,** 327-37.

274. AL-WAIZ, M., MIKOV, M., MITCHELL, S.C. &SMITH, R.L. 1992. The exogenous origin of trimethylamine in the mouse. *Metabolism,* 41**,** 135-6.

275. ATREYA, I., ATREYA, R. &NEURATH, M.F. 2008. NF-kappaB in inflammatory bowel disease. *J Intern Med,* 263**,** 591-6.

276. KRISTINSSON, J., ARMBRUSTER, C.H., UGSTAD, M., KRIWANEK, S., NYGAARD, K., TON, H. &FUGLERUD, P. 2001. Fecal excretion of calprotectin in colorectal cancer: relationship to tumor characteristics. *Scand J Gastroenterol,* 36**,** 202-7.

277. CARROLL, D., CORFIELD, A., SPICER, R. &CAIRNS, P. 2003. Faecal calprotectin concentrations and diagnosis of necrotising enterocolitis. *Lancet,* 361**,** 310-1.

278. JAYASENA, H., KHALID, T. &PROBERT, C.S. 2013. PTU-076 Diagnostic Potential of Volatile Organic Compounds as Faecal Biomarkers in Inflammatory Bowel Disease. *Gut,* 62**,** A75-A76.

279. WALTON, C., FOWLER, D.P., TURNER, C., JIA, W.J., WHITEHEAD, R.N., GRIFFITHS, L., DAWSON, C., WARING, R.H., RAMSDEN, D.B., COLE, J.A., CAUCHI, M., BESSANT, C. &HUNTER, J.O. 2013. Analysis of Volatile Organic Compounds of Bacterial Origin in Chronic Gastrointestinal Diseases. *Inflammatory Bowel Diseases,* 19**,** 2069-2078.

280. AHMED, I., GREENWOOD, R., COSTELLO, B.D., RATCLIFFE, N.M. &PROBERT, C.S. 2013. An Investigation of Fecal Volatile Organic Metabolites in Irritable Bowel Syndrome. *PLoS One,* 8.

281. OKAYASU, I., HATAKEYAMA, S., YAMADA, M., OHKUSA, T., INAGAKI, Y. &NAKAYA, R. 1990. A Novel Method in the Induction of Reliable Experimental Acute and Chronic Ulcerative-Colitis in Mice. *Gastroenterology,* 98**,** 694-702.

282. SHIOMI, Y., NISHIUMI, S., OOI, M., HATANO, N., SHINOHARA, M., YOSHIE, T., KONDO, Y., FURUMATSU, K., SHIOMI, H., KUTSUMI, H., AZUMA, T. &YOSHIDA, M. 2011. GCMS-based Metabolomic Study in Mice with Colitis Induced by Dextran Sulfate Sodium. *Inflammatory Bowel Diseases,* 17**,** 2261-2274.

283. HONG, Y.S., AHN, Y.T., PARK, J.C., LEE, J.H., LEE, H., HUH, C.S., KIM, D.H., RYU DO, H. &HWANG, G.S. 2010. 1H NMR-based metabonomic assessment of probiotic effects in a colitis mouse model. *Archives of Pharmacal Research,* 33**,** 1091-101.

284. SCHICHO, R., NAZYROVA, A., SHAYKHUTDINOV, R., DUGGAN, G., VOGEL, H.J. &STORR, M. 2010. Quantitative metabolomic profiling of serum and urine in DSS-induced ulcerative colitis of mice by (1)H NMR spectroscopy. *J Proteome Res,* 9**,** 6265-73.

285. DONG, F., ZHANG, L., HAO, F., TANG, H. &WANG, Y. 2013. Systemic responses of mice to dextran sulfate sodium-induced acute ulcerative colitis using 1H NMR spectroscopy. *J Proteome Res,* 12**,** 2958-66.

286. ROBERT, F.S. &RAO, J.P. *Evidence for possible involvement of guanylate cyclase in diarrhoea induced by castor oil in mice*, J Diarrhoeal Dis Res. 1996 Sep;14(3):218-9.

287. IZZO, A.A., GAGINELLA, T.S. &CAPASSO, F. 1996. The osmotic and intrinsic mechanisms of the pharmacological laxative action of oral high doses of magnesium sulphate. Importance of the release of digestive polypeptides and nitric oxide. *Magnes Res,* 9**,** 133-8.

288. SMITH, R.J. 1990. Glutamine metabolism and its physiologic importance. *JPEN J Parenter Enteral Nutr,* 14**,** 40S-44S.

289. KUSUNOKI, Y., IKARASHI, N., HAYAKAWA, Y., ISHII, M., KON, R., OCHIAI, W., MACHIDA, Y. &SUGIYAMA, K. 2014. Hepatic early inflammation induces

downregulation of hepatic cytochrome P450 expression and metabolic activity in the dextran sulfate sodium-induced murine colitis. *European Journal of Pharmaceutical Sciences,* 54**,** 17-27.

290. REEDS, P.J. &BURRIN, D.G. 2001. Glutamine and the bowel. *J Nutr,* 131**,** 2505S-8S; discussion 2523S-4S.

291. TANIDA, S., MIZOSHITA, T., MIZUSHIMA, T., SASAKI, M., SHIMURA, T., KAMIYA, T., KATAOKA, H. &JOH, T. 2011. Involvement of oxidative stress and mucosal addressin cell adhesion molecule-1 (MAdCAM-1) in inflammatory bowel disease. *J Clin Biochem Nutr,* 48**,** 112-6.

292. DAMIANI, C.R., BENETTON, C.A., STOFFEL, C., BARDINI, K.C., CARDOSO, V.H., DI GIUNTA, G., PINHO, R.A., DAL-PIZZOL, F. &STRECK, E.L. 2007. Oxidative stress and metabolism in animal model of colitis induced by dextran sulfate sodium. *J Gastroenterol Hepatol,* 22**,** 1846-51.

293. MIEKISCH, W., SCHUBERT, J.K. &NOELDGE-SCHOMBURG, G.F. 2004. Diagnostic potential of breath analysis--focus on volatile organic compounds. *Clin Chim Acta,* 347**,** 25-39.

294. KHANNA, P.V., SHIH, D.Q., HARITUNIANS, T., MCGOVERN, D.P. &TARGAN, S. 2014. Use of animal models in elucidating disease pathogenesis in IBD. *Semin Immunopathol*.

295. HANEDI, A. 2013. Physiological importance of various NFκB family members in regulating intestinal responses to injury; PhD Thesis. *University of Liverpool, UK*.

296. NEURATH, M.F., PETTERSSON, S., ZUMBUSCHENFELDE, K.H.M. &STROBER, W. 1996. Local administration of antisense phosphorothioate oligonucleotides to the p65 subunit of NF-kappa B abrogates established experimental colitis in mice. *Nature Medicine,* 2**,** 998-1004.

297. ROGLER, G., BRAND, K., VOGL, D., PAGE, S., HOFMEISTER, R., ANDUS, T., KNUECHEL, R., BAEUERLE, P.A., SCHOLMERICH, J. &GROSS, V. 1998. Nuclear factor kappaB is activated in macrophages and epithelial cells of inflamed intestinal mucosa. *Gastroenterology,* 115**,** 357-69.

298. LIU, C., ZHENG, Y., XU, W., WANG, H. &LIN, N. 2014. Rhubarb tannins extract inhibits the expression of aquaporins 2 and 3 in magnesium sulphate-induced diarrhoea model. *Biomed Res Int,* 2014**,** 619465.

299. DIELEMAN, L.A., PALMEN, M.J.H.J., AKOL, H., BLOEMENA, E., PENA, A.S., MEUWISSEN, S.G.M. &VAN REES, E.P. 1998. Chronic experimental colitis induced by

dextran sulphate sodium (DSS) is characterized by Th1 and Th2 cytokines. *Clinical and Experimental Immunology,* 114**,** 385-391.

300. HANS, W., SCHOLMERICH, J., GROSS, V. &FALK, W. 2000. The role of the resident intestinal flora in acute and chronic dextran sulfate sodium-induced colitis in mice. *Eur J Gastroenterol Hepatol,* 12**,** 267-73.

301. BARRAL, M., DOHAN, A., ALLEZ, M., BOUDIAF, M., CAMUS, M., LAURENT, V., HOEFFEL, C. &SOYER, P. Gastrointestinal cancers in inflammatory bowel disease: An update with emphasis on imaging findings. *Critical Reviews in Oncology / Hematology*.

302. BERNSTEIN, C.N., BLANCHARD, J.F., KLIEWER, E. &WAJDA, A. 2001. Cancer risk in patients with inflammatory bowel disease: a population-based study. *Cancer,* 91**,** 854-62.

303. PEPPERCORN, M.A., ODZE, R. D., . 2015. *Colorectal cancer surveillance in inflammatory bowel disease* [Online]. Available: http://www.uptodate.com/contents/colorectal-cancer-surveillance-in-inflammatory-bowel-disease 2015].

304. BARRAL, M., DOHAN, A., ALLEZ, M., BOUDIAF, M., CAMUS, M., LAURENT, V., HOEFFEL, C. &SOYER, P. 2015. Gastrointestinal cancers in inflammatory bowel disease: An update with emphasis on imaging findings. *Crit Rev Oncol Hematol,* 7**,** 30020-2.

305. CHOI, P.M., NUGENT, F.W., SCHOETZ, D.J., JR., SILVERMAN, M.L. &HAGGITT, R.C. 1993. Colonoscopic surveillance reduces mortality from colorectal cancer in ulcerative colitis. *Gastroenterology,* 105**,** 418-24.

306. ANANTHAKRISHNAN, A.N., CAGAN, A., CAI, T.X., GAINER, V.S., SHAW, S.Y., CHURCHILL, S., KARLSON, E.W., MURPHY, S.N., KOHANE, I. &LIAO, K.P. 2015. Colonoscopy Is Associated With a Reduced Risk for Colon Cancer and Mortality in Patients With Inflammatory Bowel Diseases. *Clinical Gastroenterology and Hepatology,* 13**,** 322-U163.

307. LUTGENS, M.W., OLDENBURG, B., SIERSEMA, P.D., VAN BODEGRAVEN, A.A., DIJKSTRA, G., HOMMES, D.W., DE JONG, D.J., STOKKERS, P.C., VAN DER WOUDE, C.J. &VLEGGAAR, F.P. 2009. Colonoscopic surveillance improves survival after colorectal cancer diagnosis in inflammatory bowel disease. *Br J Cancer,* 101**,** 1671-5.

308. NISHIUMI, S., KOBAYASHI, T., IKEDA, A., YOSHIE, T., KIBI, M., IZUMI, Y., OKUNO, T., HAYASHI, N., KAWANO, S., TAKENAWA, T., AZUMA, T. &YOSHIDA, M. 2012. A novel serum metabolomics-based diagnostic approach for colorectal cancer. *PLoS One,* 7**,** e40459.

309. WIRTZ, S., NEUFERT, C., WEIGMANN, B. &NEURATH, M.F. 2007. Chemically induced mouse models of intestinal inflammation. *Nat Protoc,* 2**,** 541-546.

310. SUZUI, M., MORIOKA, T. &YOSHIMI, N. 2013. Colon Preneoplastic Lesions in Animal Models. *Journal of Toxicologic Pathology,* 26**,** 335-341.

311. CALENIC, B., MIRICESCU, D., GREABU, M., KUZNETSOV ANDREY, V., TROPPMAIR, J., RUZSANYI, V. &AMANN, A. 2015. Oxidative stress and volatile organic compounds: interplay in pulmonary, cardio-vascular, digestive tract systems and cancer. *Open Chemistry.*

312. PRITCHARD, C.C. &GRADY, W.M. 2011. Colorectal Cancer Molecular Biology Moves Into Clinical Practice. *Gut,* 60**,** 116-129.

313. SCHMIDT, K. &PODMORE, I. 2015. Current Challenges in Volatile Organic Compounds Analysis as Potential Biomarkers of Cancer. *Journal of Biomarkers,* 2015**,** 16.

314. WILLIAMS, M.D., ZHANG, X., PARK, J.J., SIEMS, W.F., GANG, D.R., RESAR, L.M.S., REEVES, R. &HILL, H.H. 2015. Characterizing metabolic changes in human colorectal cancer. *Analytical and Bioanalytical Chemistry,* 407**,** 4581-4595.

315. BATTY, C.A., CAUCHI, M., LOURENCO, C., HUNTER, J.O. &TURNER, C. 2015. Use of the Analysis of the Volatile Faecal Metabolome in Screening for Colorectal Cancer. *PLoS One,* 10.

316. HOLD, G.L. &GARRETT, W.S. 2015. Gut microbiota: Microbiota organization-a key to understanding CRC development. *Nat Rev Gastroenterol Hepatol,* 12**,** 128-9.

317. ZHANG, A., SUN, H., YAN, G., WANG, P., HAN, Y. &WANG, X. 2014. Metabolomics in diagnosis and biomarker discovery of colorectal cancer. *Cancer Lett,* 345**,** 17-20.

318. SZILAGYI, A. 1998. Altered colonic environment, a possible predisposition to colorectal cancer and colonic inflammatory bowel disease: rationale of dietary manipulation with emphasis on disaccharides. *Can J Gastroenterol,* 12**,** 133-46.

319. INSTITUTE, N.-N.C. *Genetics of Colorectal Cancer–for health professionals* [Online]. Available: http://www.cancer.gov/types/colorectal/hp/colorectal-genetics-pdq [Accessed November 2015].

320. ENGLAND, P.H. *NHS bowel cancer screening (BCSP) programme* [Online]. Available: https://www.gov.uk/topic/population-screening-programmes/bowel [Accessed October 2015].

321. DENKERT, C., BUDCZIES, J., WEICHERT, W., WOHLGEMUTH, G., SCHOLZ, M., KIND, T., NIESPOREK, S., NOSKE, A., BUCKENDAHL, A., DIETEL, M. &FIEHN, O. 2008. Metabolite profiling of human colon carcinoma--deregulation of TCA cycle and amino acid turnover. *Mol Cancer,* 7**,** 72.

322. QIU, Y., CAI, G., ZHOU, B., LI, D., ZHAO, A., XIE, G., LI, H., CAI, S., XIE, D., HUANG, C., GE, W., ZHOU, Z., XU, L.X., JIA, W., ZHENG, S., YEN, Y. &JIA, W. 2014. A distinct metabolic signature of human colorectal cancer with prognostic potential. *Clin Cancer Res,* 20**,** 2136-46.

323. BACKSHALL, A., SHARMA, R., CLARKE, S.J. &KEUN, H.C. 2011. Pharmacometabonomic Profiling as a Predictor of Toxicity in Patients with Inoperable Colorectal Cancer Treated with Capecitabine. *Clinical Cancer Research,* 17**,** 3019-3028.

324. MONTROSE, D.C., ZHOU, X.K., KOPELOVICH, L., YANTISS, R.K., KAROLY, E.D., SUBBARAMAIAH, K. &DANNENBERG, A.J. 2012. Metabolic profiling, a noninvasive approach for the detection of experimental colorectal neoplasia. *Cancer Prev Res (Phila),* 5**,** 1358-67.

325. BISSAHOYO, A., PEARSALL, R.S., HANLON, K., AMANN, V., HICKS, D., GODFREY, V.L. &THREADGILL, D.W. 2005. Azoxymethane is a genetic background-dependent colorectal tumor initiator and promoter in mice: Effects of dose, route, and diet. *Toxicological Sciences,* 88**,** 340-345.

326. REDDY, B.S., WEISBURGER, J.H., NARISAWA, T. &WYNDER, E.L. 1974. Colon carcinogenesis in germ-free rats with 1,2-dimethylhydrazine and N-methyl-n'-nitro-N-nitrosoguanidine. *Cancer Research,* 34**,** 2368-72.

327. SUZUKI, R., KOHNO, H., SUGIE, S., NAKAGAMA, H. &TANAKA, T. 2006. Strain differences in the susceptibility to azoxymethane and dextran sodium sulfate-induced colon carcinogenesis in mice. *Carcinogenesis,* 27**,** 162-9.

328. WANG, C.S., LI, P., LIAN, A.L., SUN, B., WANG, X.Y., GUO, L., CHI, C.J., LIU, S.S., ZHAO, W., LUO, S.Q., GUO, Z.G., ZHANG, Y., KE, C.F., YE, G.Z., XU, G.W., ZHANG, F.M. &LI, E.Y. 2014. Blood volatile compounds as biomarkers for colorectal cancer. *Cancer Biology & Therapy,* 15**,** 200-206.

329. ALTOMARE, D.F. 2013. Exhaled volatile organic compounds identify patients with colorectal cancer (Br J Surg 2013; 100: 144-150). *British Journal of Surgery,* 100.

330. ARASARADNAM, R.P., MCFARLANE, M.J., RYAN-FISHER, C., WESTENBRINK, E., HODGES, P., THOMAS, M.G., CHAMBERS, S., O'CONNELL, N., BAILEY, C., HARMSTON, C., NWOKOLO, C.U., BARDHAN, K.D. &COVINGTON, J.A. 2014. Detection of colorectal cancer (CRC) by urinary volatile organic compound analysis. *PLoS One,* 9**,** e108750.

331. 2013. *NICE diagnostics guidance* [Online]. Available: https://www.nice.org.uk/guidance/dg11/chapter/5-Outcomes [Accessed August 2015].

332. BALFOUR SARTOR, R. 2011. Stool Markers and Clinical Microbiology in the Diagnosis and Management of Inflammatory Bowel Diseases. *In:* CHEN, C.W., CHENG, J., GINES, P., OUYANG, Q., SCHOLMERICH, J. (ed.) *Gut and Liver.* Basel: Karger Medical and Scientific Publishers.

333. TURKAY, C. &KASAPOGLU, B. *Noninvasive methods in evaluation of inflammatory bowel disease: where do we stand now? An update*, Clinics (Sao Paulo). 2010 Feb;65(2):221-31. doi:10.1590/S1807-59322010000200015.

334. SILBERER, H., KUPPERS, B., MICKISCH, O., BANIEWICZ, W., DRESCHER, M., TRABER, L., KEMPF, A. &SCHMIDT-GAYK, H. 2005. Fecal leukocyte proteins in inflammatory bowel disease and irritable bowel syndrome. *Clin Lab,* 51**,** 117-26.

335. ERBAYRAK, M., TURKAY, C., ERASLAN, E., CETINKAYA, H., KASAPOGLU, B. &BEKTAS, M. 2009. The role of fecal calprotectin in investigating inflammatory bowel diseases. *Clinics (Sao Paulo),* 64**,** 421-5.

336. SCHOEPFER, A.M., BEGLINGER, C., STRAUMANN, A., TRUMMLER, M., RENZULLI, P. &SEIBOLD, F. 2009. Ulcerative colitis: correlation of the Rachmilewitz endoscopic activity index with fecal calprotectin, clinical activity, C-reactive protein, and blood leukocytes. *Inflamm Bowel Dis,* 15**,** 1851-8.

337. GISBERT, J.P., BERMEJO, F., PEREZ-CALLE, J.L., TAXONERA, C., VERA, I., MCNICHOLL, A.G., ALGABA, A., LOPEZ, P., LOPEZ-PALACIOS, N., CALVO, M., GONZALEZ-LAMA, Y., CARNEROS, J.A., VELASCO, M. &MATE, J. 2009. Fecal calprotectin and lactoferrin for the prediction of inflammatory bowel disease relapse. *Inflamm Bowel Dis,* 15**,** 1190-8.

338. EDER, P., STAWCZYK-EDER, K., KRELA-KAZMIERCZAK, I. &LINKE, K. 2008. Clinical utility of the assessment of fecal calprotectin in Lesniowski-Crohn's disease. *Pol Arch Med Wewn,* 118**,** 622-6.

339. HILDEBRAND, F., NGUYEN, T.L.A., BRINKMAN, B., YUNTA, R.G., CAUWE, B., VANDENABEELE, P., LISTON, A. &RAES, J. 2013. Inflammation-associated enterotypes, host genotype, cage and inter-individual effects drive gut microbiota variation in common laboratory mice. *Genome Biology,* 14.

340. SORO-PAAVONEN, A., WATSON, A.M., LI, J., PAAVONEN, K., KOITKA, A., CALKIN, A.C., BARIT, D., COUGHLAN, M.T., DREW, B.G., LANCASTER, G.I., THOMAS, M., FORBES, J.M., NAWROTH, P.P., BIERHAUS, A., COOPER, M.E. &JANDELEIT-DAHM, K.A. 2008. Receptor for advanced glycation end products (RAGE) deficiency attenuates the development of atherosclerosis in diabetes. *Diabetes,* 57**,** 2461-9.

341. ELDER, G.A., SOSA, M.A.G. &DE GASPERI, R. 2010. Transgenic Mouse Models of Alzheimer's Disease. *Mount Sinai Journal of Medicine,* 77**,** 69-81.

342. YAMAMOTO, Y., HARASHIMA, A., SAITO, H., TSUNEYAMA, K., MUNESUE, S., MOTOYOSHI, S., HAN, D., WATANABE, T., ASANO, M., TAKASAWA, S., OKAMOTO, H., SHIMURA, S., KARASAWA, T., YONEKURA, H. &YAMAMOTO, H. 2011. Septic Shock Is Associated with Receptor for Advanced Glycation End Products Ligation of LPS. *J Immunol,* 186**,** 3248-3257.

343. ELLIS, D.I., DUNN, W.B., GRIFFIN, J.L., ALLWOOD, J.W. &GOODACRE, R. 2007. Metabolic fingerprinting as a diagnostic tool. *Pharmacogenomics,* 8**,** 1243-1266.

344. DE PRETER V, V.K. 2013. Metabolomics as a diagnostic tool in gastroenterology. *World J Gastrointest Pharmacol Ther.,* 4**,** 97-107.

345. SPOELSTRA, S.F. 1978. Degradation of Tyrosine in Anaerobically Stored Piggery Wastes and in Pig Feces. *Applied and Environmental Microbiology,* 36**,** 631-638.

346. GERRITSEN, J., SMIDT, H., RIJKERS, G.T. &DE VOS, W.M. 2011. Intestinal microbiota in human health and disease: the impact of probiotics. *Genes Nutr,* 6**,** 209-40.

347. WOLOWCZUK, I., VERWAERDE, C., VILTART, O., DELANOYE, A., DELACRE, M., POT, B. &GRANGETTE, C. 2008. Feeding our immune system: Impact on metabolism. *Clinical & Developmental Immunology***,** 1-19.

348. FEMIA, A.P., BENDINELLI, B., GIANNINI, A., SALVADORI, M., PINZANI, P., DOLARA, P. &CADERNI, G. 2005. Mucin-depleted foci have beta-catenin gene mutations, altered expression of its protein, and are dose- and time-dependent in the colon of 1,2-dimethylhydrazine-treated rats. *International Journal of Cancer,* 116**,** 9-15.

349. FEMIA, A.P., DOLARA, P., GIANNINI, A., SALVADORI, M., BIGGERI, A. &CADERNI, G. 2007. Frequent mutation of Apc gene in rat colon tumors and mucin-depleted foci, preneoplastic lesions in experimental colon carcinogenesis. *Cancer Research,* 67**,** 445-449.

350. KOEK, M.M., MUILWIJK, B., VAN DER WERF, M.J. &HANKEMEIER, T. 2006. Microbial metabolomics with gas chromatography/mass spectrometry. *Anal Chem,* 78**,** 1272-81.

351. KULLBERG, M.C., ROTHFUCHS, A.G., JANKOVIC, D., CASPAR, P., WYNN, T.A., GORELICK, P.L., CHEEVER, A.W. &SHER, A. 2001. Helicobacter hepaticus-induced colitis in interleukin-10-deficient mice: cytokine requirements for the induction and maintenance of intestinal inflammation. *Infect Immun,* 69**,** 4232-41.

352. CURY, D.B., MIZSPUTEN, S.J., VERSOLATO, C., MIIJI, L.O., PEREIRA, E., DELBONI, M.A., SCHOR, N. &MOSS, A.C. 2013. Serum calprotectin levels correlate with biochemical and histological markers of disease activity in TNBS colitis. *Cellular Immunology,* 282**,** 66-70.

353. TAKAO, K. &MIYAKAWA, T. 2015. Genomic responses in mouse models greatly mimic human inflammatory diseases. *Proc Natl Acad Sci U S A,* 112**,** 1167-1172.

354. WIRTZ, S., BECKER, C., BLUMBERG, R., GALLE, P.R. &NEURATH, M.F. 2002. Treatment of T cell-dependent experimental colitis in SCID mice by local administration of an adenovirus expressing IL-18 antisense mRNA. *J Immunol,* 168**,** 411-420.

Appendix 1 – Automatic (Metab) analysis vs conventional long-hand analysis

Analysis of HS-SPME-GC-MS analysis using Metab (R package) was assessed for its sensitivity, precision, false negative rate and false discover rate compared to the conventional long-hand, manual analysis. Metab was assessed using 12 chromatograms chosen at random (mixture of time points and gender) from the initial experiment to identify the healthy murine metabolome (**Chapter 3**). Each chromatogram was thoroughly manually analysed in AMDIS twice and compound found were recorded. All chromatograms included in this comparison was used to also build the library at the start of the project, and all were checked a second time prior to this method analysis. The murine specific library used had 220 compounds and was built only with murine faecal samples.

Samples were then analysed using Metab based on an AMDIS batch report using the raw data '.CDF' files using a time window of 0.5 minutes. Single reports for each chromatogram were generated and 'cleaned up' using the list of compounds found manually. The list of compounds found with Metab was then compared to the list of compounds found manually. Compounds found manually but not by Metab were labelled 'false negatives', compounds found by Metab but not manually were labelled 'false positives' and compounds found by both methods were labelled 'true positives' (**Figure A1.1**).

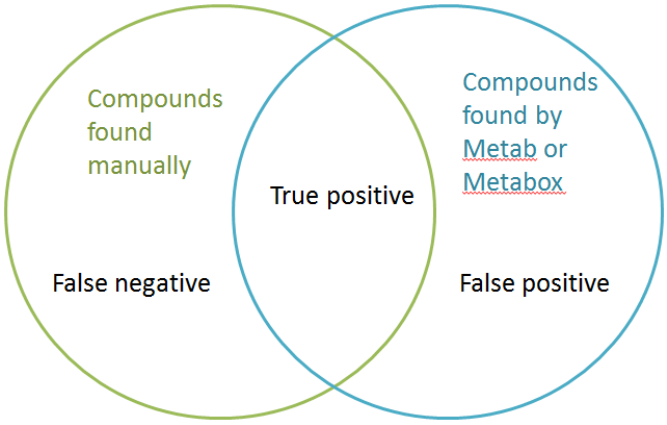

Figure A1.1 False negative, false positive and true positive definition.

Results are expressed using the sensitivity (sum true positive/sum compounds found manually), the precision (sum true positive/sum compounds found by Metab), the false negative rate (sum false negative/sum compounds found manually) and the false discovery rate (sum false positive/sum compounds found by Metab) (**Table A1.1**).

Table A1.1 Sensitivity, precision, false negative rate and false discover rate of Metab, compared to manual, long-hand analysis.

Chromatogram	Sensitivity (%)	Precision (%)	False negative rate (%)	False discovery rate (%)
1	98.25	94.92	1.75	5.08
2	100.00	94.92	0.00	5.08
3	97.62	100.00	2.38	0.00
4	95.56	97.73	2.22	0.00
5	96.08	98.00	1.96	0.00
6	96.72	100.00	3.28	0.00
7	97.37	97.37	2.63	2.63
8	100.00	100.00	0.00	0.00
9	100.00	97.22	0.00	2.78
10	100.00	97.06	0.00	2.94
11	96.97	98.46	3.03	1.54
12	98.25	100.00	1.75	0.00

Appendix 2 - T-cell transfer chronic colitis faecal VOC profile

Faecal samples donated from Dr Jim Wilson of Epistem, Manchester from an adoptive $CD4^{+}CD62L^{+}$ T cell transfer study [354]. Using the protocol by Wirtz *et al*., all mice (except untreated controls) were injected with $CD4^{+}CD62L^{+}$ T cells on day 0 and samples included in this analysis (**Figure A2.1**) were collected from the colon when mice were euthanised on day 28; confidential clinical data confirm that IgG control-treated T-cell recipient mice developed colitis.

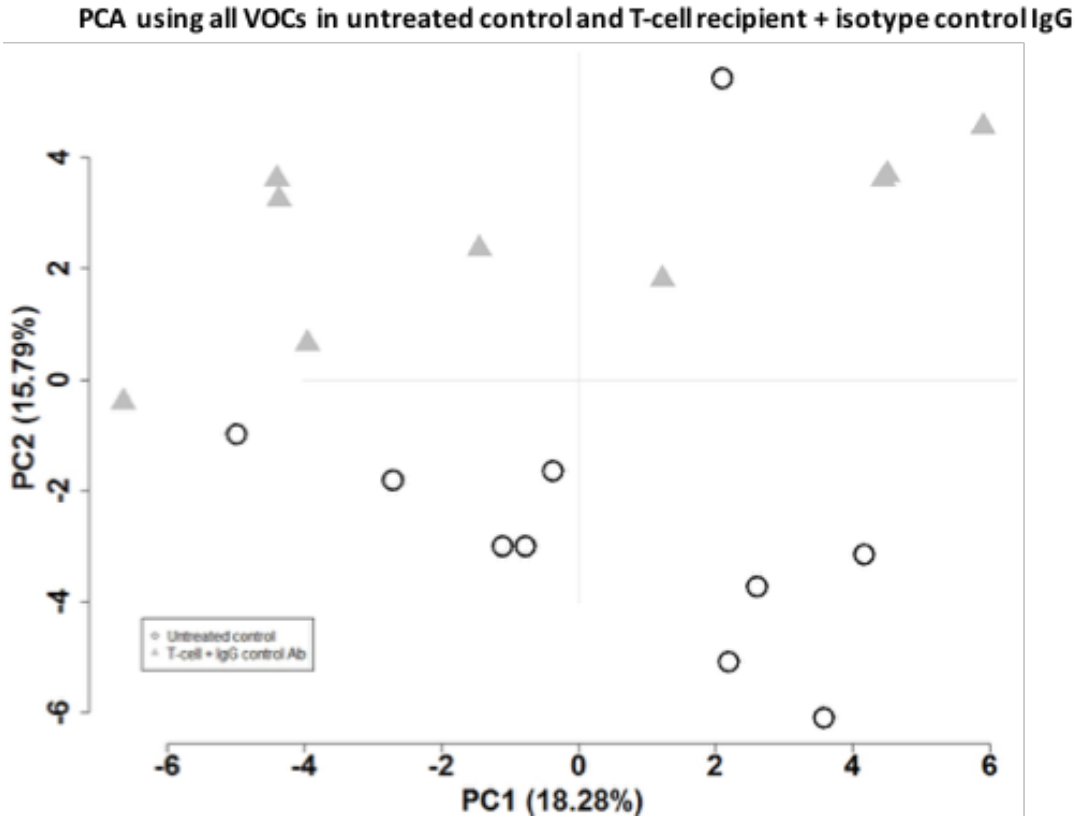

Figure A2.1 A PCA biplot for the colon content samples from untreated control and T-cell recipient mice.